Transactions

of the

ASME

NOVEMBER, 1948

VOL. 70, NO. 8

Transactions

of The American Society of Mechanical Engineers

Published on the tenth of every month, except March, June, September, and December

---

Published monthly by The American Society of Mechanical Engineers. Publication office at 20th and Northampton Streets, Easton, Pa. The editorial department is located at the headquarters of the Society, 29 West Thirty-Ninth Street, New York 18, N. Y. Cable address, "Dynamic," New York. Price $1.50 a copy, $12.00 a year; to members and affiliates, $1.00 a copy, $6.00 a year. Changes of address must be received at Society headquarters three weeks before they are to be effective on the mailing list. Please send old as well as new address. . . . By-Law: The Society shall not be responsible for statements or opinions advanced in papers or . . . printed in its publications (B13, Par. 4). . . . Entered as second-class matter March 2, 1928, at the Post Office at Easton, Pa., under the Act of August 24, 1912. . . .

Further Investigation on the Graphitization of Piping for the EEI and AEIC

By A. M. HALL[1] and S. L. HOYT,[2] COLUMBUS, OHIO

The graphitization test program initiated in 1943 at Battelle Memorial Institute by the EEI and AEIC was continued during 1947. Carbon-molybdenum, chromium-molybdenum, and vanadium-molybdenum compositions were tested at 1125 F. An effort was made to relate plastic deformation with graphitization on a laboratory basis. The high resistance of chromium-molybdenum steels was confirmed and further information was developed on the existence of an incubation period in the graphitization process.

Introduction

THE progress made from September, 1943, to November, 1946, in the investigation on the graphitization of steel piping undertaken at Battelle Memorial Institute for the Edison Electric Institute and the Association of Edison Illuminating Companies, has been summarized in three previous papers (1, 2, 3).[3] Numerous aspects of the general problem were considered, including the fundamental causes of graphitization and the mechanism of the graphitization process, the measures which may be taken to restore graphitized pipe joints, the methods which may be used to prevent graphite segregation at existing pipe joints and other kinds of steel which would have superior graphitization resistance and at the same time be suitable for high-pressure piping.

Some light has been cast on the fundamentals or mechanism of the phenomenon but much remains to be learned; the use of chemical kinetics has been helpful here. Some understanding of the effect of time and temperature on the process has been achieved, and it is known that the progress of the reaction involves growth from nuclei. However, the growth of a nucleus into a nodule is not well understood, particularly the absence of local depletion of carbon in the vicinity of a graphite nodule which may frequently be observed. Moreover, the question of nucleation itself is much in doubt; it is not positively known whether the nuclei in a steel which will graphitize are already in existence or form with time at temperature. In the former case there would be no incubation period and graphitization would start as soon as the steel reached temperature. In the latter case there would be an incubation period, during which time nuclei were forming but during which the extent of graphitization would be so small as to escape detection. A practical question is involved here. Is a steel which shows complete resistance to graphitization over a considerable period of time completely stable, or is it merely in its incubation period?

The development of other types of steel for high-pressure piping, which will be satisfactorily resistant to graphite formation, has been a fairly fruitful avenue of attack on the general problem. In particular, chromium-molybdenum steels containing $^1/_2$ per cent molybdenum with $^1/_2$ per cent or more chromium have shown themselves to be graphite-free in a variety of severe laboratory tests, and this type of steel is beginning to be used to replace old pipe as well as in new installations. There may also be other types of low-alloy ferritic steels which are satisfactorily resistant to graphitization, such as molybdenum-vanadium steel and silicon-killed carbon-molybdenum steel.

Answers to questions such as those just stated are usually given in terms of safe operating temperatures for the different steel types, particularly with reference to graphitization. Suggestions of this kind have been advanced in papers before ASME Symposiums.

This paper gives the results of further investigation of the graphitization of steel piping carried out during 1947. Additional experience with some of the more resistant types of steel was obtained as well as further information bearing on the question of the incubation period.

In addition, another effort was made to establish a relationship on a laboratory basis between the graphitization phenomenon on the one hand, and plastic deformation, such as might occur during the installation of a pipe system, on the other hand. In a previous attempt (3), plastic deformation prior to the graphitization test had been produced by compression (upsetting). In the present study, deformation was accomplished by stressing in tension. The matter is important because it bears on those disturbing special cases of severe segregated graphite formation not associated with welding but apparently related to deformation phenomena such as Lüders lines (4).

Finally, another type of continuous graphite formation is reported where the segregation did not occur in a weld-heat-affected zone.

Experimental Procedure—Materials

Previously Tested Specimens. A group of bead-welded specimens and sections of welded joints was selected for test from materials which had been on test previously at Battelle. The steels considered were those which had a past record of high resistance to graphitization. They are listed in Table 1. Included are a low-aluminum-deoxidized plain-carbon steel, two low-aluminum-deoxidized, one silicon-deoxidized, and two titanium-deoxidized carbon-molybdenum steels, two welded joints between high- and low-aluminum-deoxidized experimental chromium-molybdenum steels, two commercial chromium-molybdenum steels, and a molybdenum-vanadium cast steel.

Specimens Stressed in Tension. In the present attempt to demonstrate a relationship experimentally between deformation and graphitization, the deformation was obtained by stressing in tension using the two types of tensile specimen illustrated schematically in Fig. 1.

The rectangular specimen, Fig. 1A, was furnished in three types of steel; a high-aluminum-deoxidized plain-carbon steel, a high-aluminum-deoxidized carbon-molybdenum steel (from the original Springdale installation), both known to graphitize readily, and a high-aluminum-deoxidized chromium-molybdenum steel containing $^1/_2$ per cent chromium, considered to be relatively

[1] Metallographer in charge, Battelle Memorial Institute.

[2] Technical Adviser, Battelle Memorial Institute.

[3] Numbers in parentheses refer to the Bibliography at the end of the paper.

Contributed by the Joint ASTM-ASME Research Committee on Effect of Temperature on Properties of Metals and presented at the Annual Meeting, Atlantic City, N. J., Dec. 1–5, 1947, of The American Society of Mechanical Engineers.

 Paper No. 47—A-139.

TABLE 1 WELDED GRAPHITIZATION TEST SPECIMENS[a]

Specimen no.	Description of steel	Source	Chemical analysis C	Mn	Si	Mo	Cr	Ti	Al	V	Treatment before testing	Previous tests	Extent of graphitization
G21AW	Plain-C, low-Al deoxidation	National Tube Co.	0.27	1.11	0.21				0.01		Bead-welded	5000 hr at 1125 F	None
G210	Plain-C, low-Al deoxidation	National Tube Co.	0.27	1.11	0.21				0.01		Bead-welded and stress relieved at 1425 F	5000 hr at 1125 F	None
G18AW	C-Mo, low-Al deoxidation	National Tube Co.	0.17	0.62	0.23	0.43	0.02				Bead-welded	5000 hr at 1125 F	None
G18B1D	C-Mo, low-Al deoxidation	National Tube Co.	0.17	0.62	0.23	0.43	0.02				Bead-welded	6700 hr at 950–1150 F plus 5000 hr at 1125 F	Trace
G19Y7	C-Mo, low-Al deoxidation	National Tube Co.	0.18	0.49	0.26	0.50					Air-cooled from 2200 F, normalized at 1650 F, bead-welded	5000 hr at 1125 F	RMF[b] (20% conversion)
G31AW	C-Mo, Si-deoxidized, normal	B & W header	0.10	0.45	0.16	0.60					Bead-welded	5000 hr at 1125 F	None
G31C1D	C-Mo, Si-deoxidized, normal	B & W header	0.10	0.45	0.16	0.60					Bead-welded	6700 hr at 950–1150 F plus 5000 hr at 1125 F	None
G53	Ti-deoxidized C-Mo bar	Titanium Alloy Mfg. Co.	0.15	0.36	0.13	0.55		0.048			Bead-welded	1700 hr at 1025 F plus 5000 hr at 1125 F	None
G54	Ti-deoxidized C-Mo bar	Titanium Alloy Mfg. Co.	0.14	0.42	0.12	0.58		0.039			Bead-welded	1700 hr at 1025 F plus 5000 hr at 1125 F	None
G46-47-3AW	Welded joint between high-Al and low-Al Cr-Mo, 1/2% Cr	BMI	0.14 0.13	0.39 0.38	0.23 0.20	0.52 0.55	0.48 0.47				As-welded	5000 hr at 1125 F	None
G46-47-5AW	Welded joint between high-Al and low-Al Cr-Mo, 1% Cr	BMI	0.14 0.14	0.39 0.38	0.23 0.20	0.52 0.55	0.91 0.93				As-welded	5000 hr at 1125 F	None
G60	"Croloy"	General Electric Co.				1.00	2 1/4				Bead-welded	4000 hr at 1125 F	None
G61	Cr-Mo steel	National Tube Co.	0.11	0.50	0.34	0.51	2.18		0.003			3300 hr at 1125 F	None
G59	Mo-V cast steel	General Electric Co.	0.18	0.71	0.34	1.15				0.23	Bead-welded	4000 hr at 1125 F	None

[a] The present test was 3500 hr at 1125 F.
[b] Explanation of symbols. Type: R, random; H, segregating at the low-temperature edge of the heat-affected zone. Amount: L, little; M, moderate; G, great. Size: F, fine; I, intermediate; C, coarse.

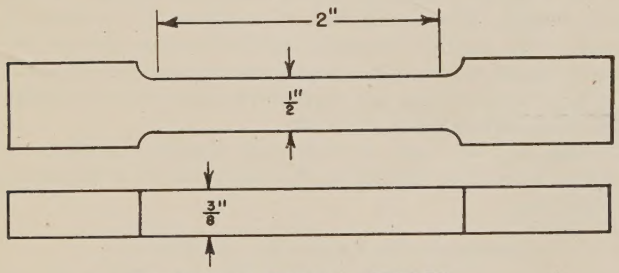

A. RECTANGULAR TENSILE SPECIMEN

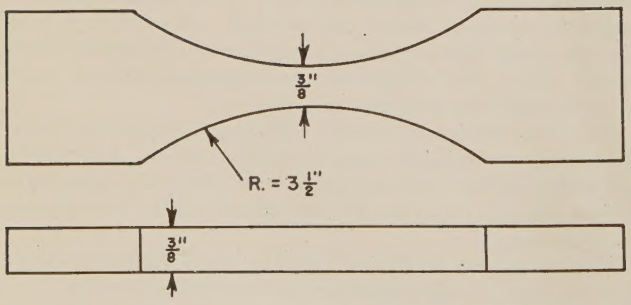

B. TENSILE SPECIMEN SHAPED WITH A LARGE RADIUS

FIG. 1 SKETCHES OF SPECIMENS USED TO STUDY THE EFFECT OF PLASTIC DEFORMATION ON THE DEVELOPMENT OF GRAPHITE

resistant to graphitization. One set of specimens of the three steels was elongated approximately 10 per cent at room temperature over a two-inch gage length. Another set was similarly elongated at 800 F. The room-temperature specimens developed very distinct Lüders lines while the 800 F specimens showed no Lüders lines.

The tensile specimen shaped with a large radius, Fig. 1B, was designed to provide a range of deformation in one test piece, varying from zero at the shoulder to a maximum at the narrowest section in the center. The high-aluminum-deoxidized carbon-molybdenum steel and the high-aluminum-deoxidized chromium-molybdenum steel containing 1/2 per cent chromium were used. One specimen of each steel was elongated 4 per cent in 2 in. at room temperature, while another specimen of each was deformed a like amount at 800 F.

All of the specimens variously stressed in tension prior to the graphitization test are listed in Table 2.

Method of Testing. As in the previous investigation (3), a single test temperature of 1125 F was used while the test period was 3500 hr. The heating equipment has been described elsewhere (3). Graphitization determinations were made with the metallographic microscope on polished specimens lightly etched with nital, using magnifications up to 1500×.

RESULTS

Previously Tested Steels. The results of examination of the various steels after they had undergone the additional 3500 hr test at 1125 F are given in Table 1 in the column headed "Extent of Graphitization." The amount of graphite found is given both in terms of the qualitative rating method originally used in this investigation as well as in the form of a quantitative estimate of the percentage of the total carbon content converted into graphite. The method of determining the latter is described elsewhere (3).

TABLE 2 STRESSED GRAPHITIZATION TEST SPECIMENS

Specimen no.	Description of steel	Source	Type of specimen	Test conditions	Extent of graphitization
G-20	Plain-C, high-Al	National Tube Co.	Rectangular bar (Fig. 1, A) stressed at room temperature	3500 hr at 1125 F	RMC[a] (complete conversion)
G-20H	Plain-C, high-Al	National Tube Co.	Rectangular bar (Fig. 1, A) stressed at 800 F	3500 hr at 1125 F	RGC (complete conversion)
G-30	C-Mo, high-Al	Springdale	Rectangular bar (Fig. 1, A) stressed at room temperature	3500 hr at 1125 F	RMC-I (50% conversion)
G-30H	C-Mo, high-Al	Springdale	Rectangular bar (Fig. 1, A) stressed at 800 F	3500 hr at 1125 F	RMC-I (50% conversion)
G-30-1	C-Mo, high-Al	Springdale	Radius specimen (Fig. 1, B) stressed at room temperature	3500 hr at 1125 F	RMI (50% conversion)
G-30-1H	C-Mo, high-Al	Springdale	Radius specimen (Fig. 1, B) stressed at 800 F	3500 hr at 1125 F	RMI (50% conversion)
G-46-3	Cr-Mo, high-Al, ½% Cr	BMI	Rectangular bar (Fig. 1, A) stressed at room temperature	3500 hr at 1125 F	None
G-46-3H	Cr-Mo, high-Al, ½% Cr	BMI	Rectangular bar (Fig. 1, A) stressed at 800 F	3500 hr at 1125 F	None
G-46-31	Cr-Mo, high-Al, ½% Cr	BMI	Radius specimen (Fig. 1, B) stressed at room temperature	3500 hr at 1125 F	None
G-46-31H	Cr-Mo, high-Al, ½% Cr	BMI	Radius specimen (Fig. 1, B) stressed at 800 F	3500 hr at 1125 F	None

[a] See note *b*, Table 1.

Plain-Carbon Low-Aluminum Steel. This steel (G-21) showed no graphite either as-welded or as-welded and postweld-stress-relieved at 1425 F after an exposure at 1125 F for a total time of 8500 hr (5000 plus 3500). This time would correspond approximately to 120,000 hr at 925 F, by applying the factor obtained by chemical kinetics.

Carbon-Molybdenum Steels. One of the low-aluminum-deoxidized carbon-molybdenum steels (G-18) showed a trace of graphite after a total time at temperature of 15,200 hr. This represented no measurable increase in extent of graphitization over the previous test of 11,700 hr. It is apparently still in the initial stages of graphite formation.

The other low-aluminum steel (G-19) showed appreciable random graphitization after 8500 hr on test; about 20 per cent of the total carbon in the material was estimated to be converted into graphite. No segregation of graphite was observed in the specimen.

In the previous test of 5000 hr at 1125 F, no graphite was found in this steel. Using this and the present result, a greatly extrapolated reaction curve for the process at 1125 F was drawn for the steel, as shown in Fig. 2. Included also is a curve for 925 F sketched in on the basis of the 15 to 1 life ratio between 925 F and 1125 F reported in a previous paper (3) for the Springdale carbon-molybdenum steel. From the scant data plotted in Fig. 2, the following highly speculative predictions can be made: The half lifetime of the graphitization process in steel G-19 is about 15,000 hr (21 months) at 1125 F and about 220,000 hr (25 yr) at 925 F.

In an effort to cast some light on why steel G-19 graphitized to a greater extent than G-18, the following spectrographic analyses were made:

Steel	Cr	Al	Ti	V
G-18	0.025	0.01	None	None
G-19	0.030	<0.01	None	None

Neither these nor the chemical analyses offer a clue to the difference in behavior between the two steels. A study was also made of initial microstructure, but here again no reason for the difference in performance was found. The two steels appeared quite similar in microstructure.

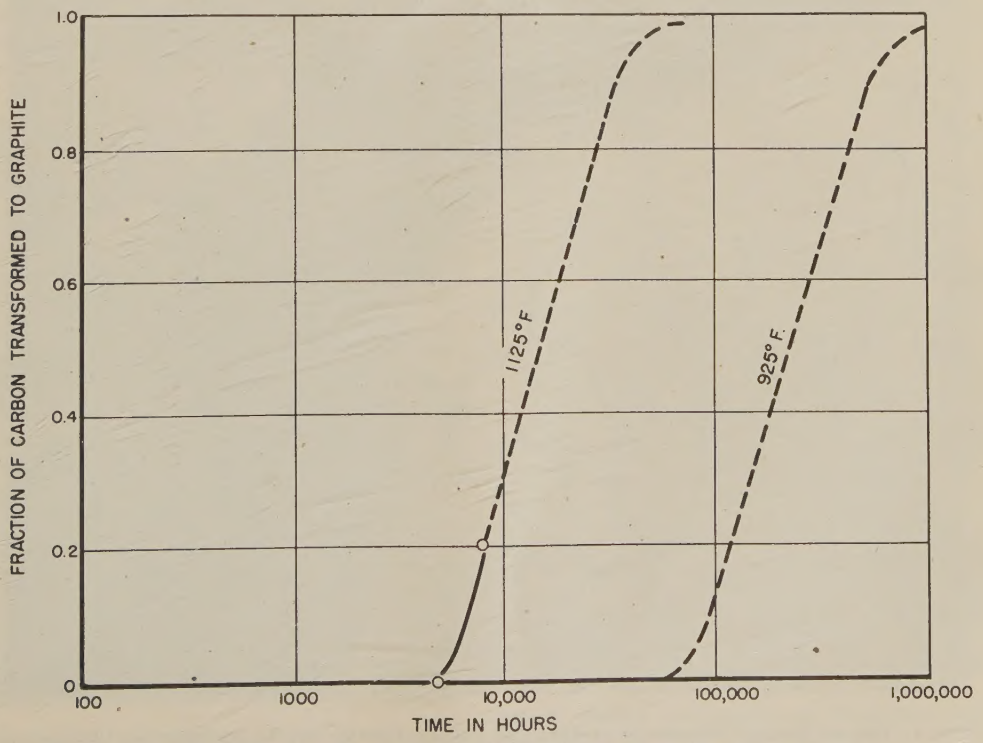

FIG. 2 GRAPHITIZATION OF CARBON-MOLYBDENUM STEEL, G-19

The silicon-deoxidized carbon-molybdenum steel used in these tests is a section from the header in the original Springdale installation. It had shown no graphite when examined after the Springdale failure in January, 1943, and after a total time of 15,200 hr of accelerated testing at 1125 F, it continues to be graphite-free.

The two experimental titanium-deoxidized carbon-molybdenum steels showed no graphite after 1700 hr at 1025 F plus 8500 hr (5000 plus 3500) at 1125 F.

Chromium-Molybdenum Steels. This group of specimens, representing chromium contents of $^1/_2$ to $2^1/_4$ per cent and molybdenum contents of $^1/_2$ to 1 per cent, continued to show no graphitization. Occasional "black spots," discussed in a previous paper (3), were again observed in some of the specimens, but they were very small and widely scattered.

Both high-aluminum and low-aluminum-deoxidized steels were included, and some of the specimens had been on test up to 8500 hr at 1125 F.

Molybdenum-Vanadium Steel. This steel, which is a cast steel containing 1.15 per cent molybdenum and 0.23 per cent vanadium, has been on test 7500 hr at 1125 F, after which it has shown no graphite formation.

Specimens Stressed in Tension. Each of these specimens was examined for graphite on the longitudinal median plane so that the effect of all variations in degree of deformation could be observed, and the stressed portion could be compared with unstressed sections back of the shoulders. The results, listed in Table 2, were negative; a correlation on a laboratory basis between graphite formation and plastic deformation was not obtained.

The two steels, G-20 and G-30, which were expected to graphitize did so in a completely random manner. The extent of graphitization appeared to be very uniform in each case over the entire specimen with respect to both nodule size and numbers of nodules. The extent of graphite formation in the stressed and in the unstressed parts of each specimen was about the same, while the specimens stressed at 800 F graphitized in about the same manner as those stressed at room temperature. Moreover, the extent of graphitization in these two steels was about what would be expected for 3500 hr at 1125 F as predicted from the reaction-rate curves for the same steels as-welded (3). This circumstance is a good indication that the deformation undergone by the materials did not influence the graphitization rate.

The chromium-molybdenum steel G-46-3, which was also tested after being deformed in tension, showed no graphite formation. Since the material contained $^1/_2$ per cent chromium, this result was expected on the basis of its performance under test as-welded.

Continuous Graphite Formation Outside a Weld-Heat-Affected Zone. In examining sections from welded joints in the steam piping system of the Iowa Power and Light Company, Des Moines, Iowa, a continuous type of graphite formation was observed in a carbon-molybdenum-steel forged fitting made to ASTM specification A-182-36. It had been in service eight years at an average temperature reported to be 925 F. The graphite was located outside, though near, the weld-heat-affected zone of the joint between the fitting and a valve. It is shown in Figs. 3, 4, 5, and 6. The formations tend to outline grains in the fitting, and appear to have nucleated in carbide areas near envelopes of free ferrite. This type of graphitization has not been encountered before in the many examinations of pipe joints and graphitization specimens made at Battelle.

Incidentally, an advanced state of graphitization existed in the weld-heat-affected zones of the fitting as well as of the pipe sections examined. Pronounced "eyebrow"-type graphite was frequently observed, and the general extent of graphitization was strongly reminiscent of the Springdale case.

Discussion

The results have raised several points of importance to the

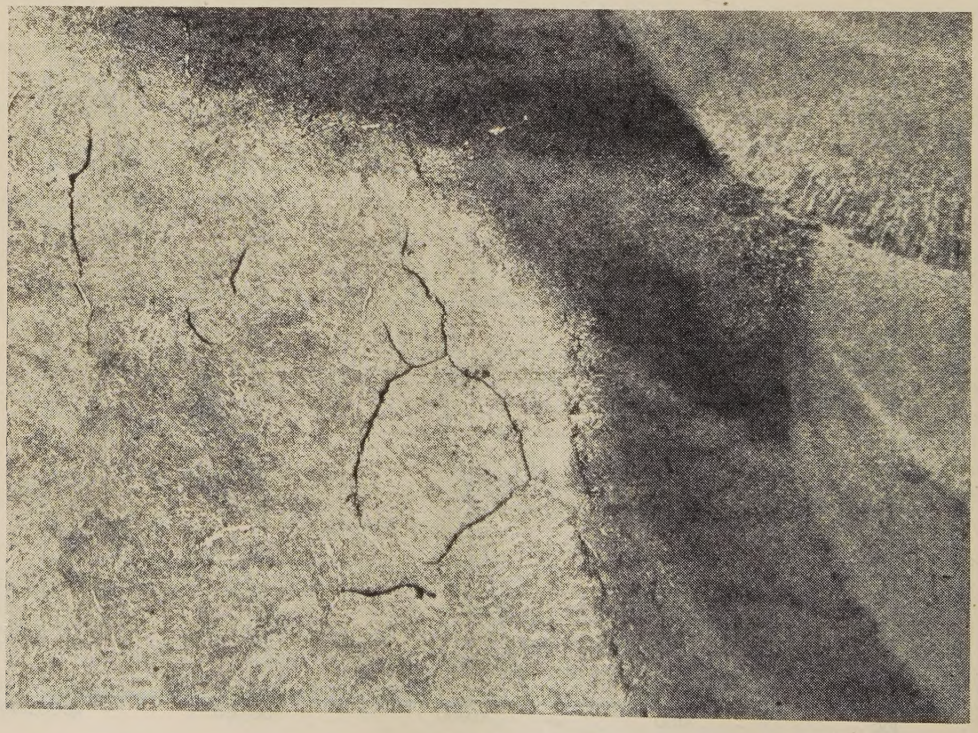

Fig. 3 Fitting Side of Welded Joint Between Forged Fitting and Valve Showing Continuous Graphite Formation Outside Weld-Heat-Affected Zone; Nital Etch, 12×

graphitization problem and serve to emphasize the limitations of our knowledge of the phenomenon.

The additional data in this paper confirm the conclusions of previous work at Battelle (3) as well as at other laboratories (5, 6) that chromium-molybdenum steel containing more than $^1/_2$ per cent chromium is satisfactorily resistant to graphitization for use as high-pressure steam piping. In fact, it is considered safe to use it at 1000 F. Moreover, the results confirm that the presence of more than $^1/_2$ per cent chromium permits the use of aluminum deoxidation in the manufacture of the steel. This point is a matter of considerable importance to both steelmaker and consumer.

In discussing chromium-molybdenum steels, reference may be made to the efforts to relate elastic strain and plastic deformation to the graphitization phenomenon. Though attempts to learn more about the development of segregated graphite in stressed or deformed regions remote from welds, through the medium of laboratory tests, have been unsuccessful, nevertheless the tests have brought out an important point. Under none of the various conditions of elastic straining or plastic deformation (by compression or tension), produced in the laboratory, has the chromium-molybdenum steel containing $^1/_2$ per cent chromium developed any graphite. In addition, the steel used for these tests was high-aluminum-deoxidized. This record serves to increase confidence in the stability of this type of steel. Perhaps it can also be expected not to show the special types of graphitization such as that associated with Lüders lines or such as that illustrated in Figs. 3, 4, 5, and 6.

The data also suggest that other compositions and types of low-alloy ferritic steel may be highly resistant to graphitization. However, experience here is extremely limited. A cast molybdenum-vanadium steel, containing 1.15 per cent molybdenum and 0.23 per cent vanadium, tested at Battelle, showed no graphite after 7500 hr at 1125 F. However, another laboratory (7) found graphite in forged $1^1/_2$ per cent molybdenum 0.16 per cent vanadium steels after 10,000 hr at 1050 F. Besides the difference in history and structure, there were differences in composition between these steels. The resistant cast steel was noticeably higher in manganese and lower in silicon than were the less resistant wrought steels. It was also higher in vanadium content.

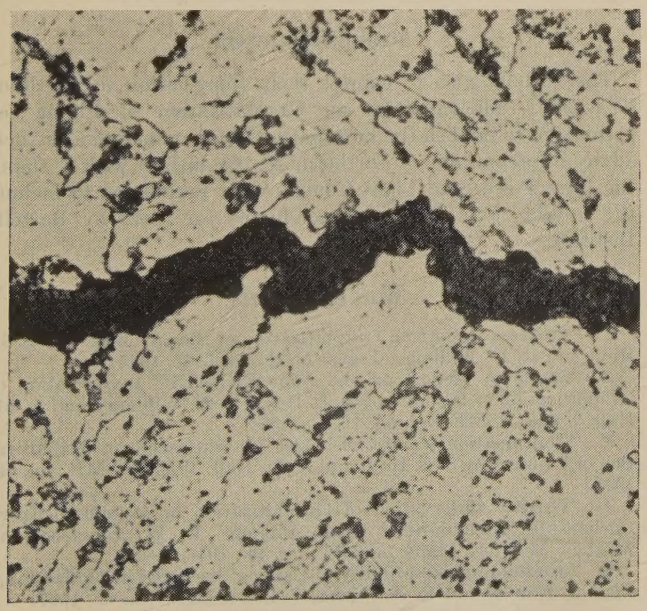

FIG. 4 PART OF THE REGION REPRESENTED IN FIG. 3, MAGNIFIED TO SHOW THE GRAPHITE FORMATION IN DETAIL; 1000×

There is room for considerable speculation on the exact effect of the three elements, vanadium, manganese, and silicon. Vanadium seems to be an inhibitor of graphite formation, but the data are insufficient to rate its effectiveness. Perhaps it must

FIG. 5 PART OF THE FORGED FITTING SHOWING CONTINUOUS GRAPHITE FORMATION AT INTERFACE BETWEEN CARBIDE-CONTAINING AREA AND FREE FERRITE; 1000×

FIG. 6 REGION OF CONTINUOUS GRAPHITE FORMATION OUTSIDE WELD-HEAT-AFFECTED ZONE IN FORGED FITTING, SIMILAR TO FIG. 5, 1000×

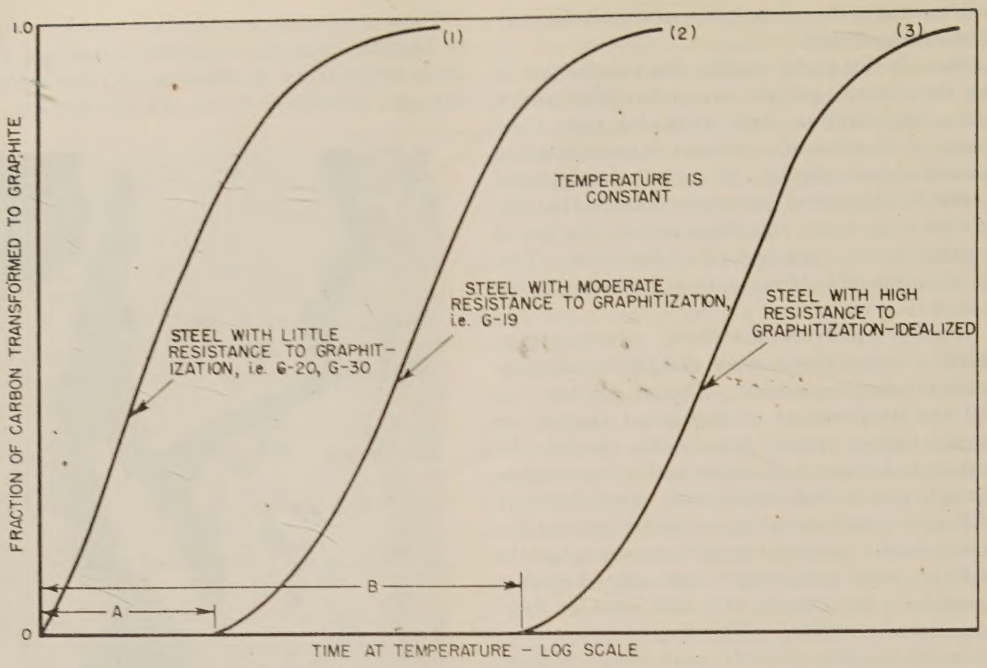

FIG. 7 RELATIONSHIP BETWEEN ORDER OF RESISTANCE TO GRAPHITIZATION AND LENGTH OF INCUBATION PERIOD
[A is the incubation period for steel (2), and B is the incubation period for steel (3).]

be present in some minimum amount which may be related to the carbon content of the steel. Again, manganese may be an important factor in the graphitization resistance of the cast molybdenum-vanadium steel. The complete freedom from graphitization shown by the plain-carbon steel, G-21, lends some support to this thought, since it was unusually high in manganese (1.11 per cent) in addition to being low-aluminum-deoxidized. Finally, the role of silicon is much in doubt. The virtue of the practice of silicon killing may not lie in the presence of silicon in the steel but in the absence of aluminum. Silicon in cast iron behaves as a graphitizer, and in larger amounts it is also a graphitizer in steel. However, the presence of considerable amounts of it, say, 0.40 per cent or more, may be required before it is effective.

Thus in addition to the chromium-molybdenum steel, a molybdenum-vanadium combination or even a manganese steel, all relatively low in silicon, might very readily meet service requirements. However, considerable further investigation would be required to develop and confirm other compositions.

The data here also throw a little more light on one aspect of the mechanism of the graphitization process, the question of whether or not there is an incubation period. This is a matter of practical importance because it bears directly on the question of whether or not a steel which does not show graphite early in service will ultimately graphitize. Can one be sure that a steel which is graphite-free over a period in service will remain so indefinitely?

The low-aluminum-deoxidized carbon-molybdenum steel, G-19, experienced a considerable period at temperature during which it did not graphitize to an observable extent; then marked graphitization began. On the other hand, plain-carbon high-aluminum-deoxidized steel, G-20, and high-aluminum-deoxidized carbon-molybdenum steel, G-30, showed virtually no incubation period (3). At least, with relatively small uncertainty, graphite formation in these steels began immediately upon reaching temperature.

These observations suggest a relationship between order of resistance to graphitization on the one hand and length of the incubation period on the other, which may be depicted schematically as in Fig. 7. The sketch shows a highly susceptible steel with little or no incubation period along with another with a pronounced incubation period which is more resistant to graphitization. An idealized steel is also shown whose incubation period is so long as to suggest permanent stability, from a practical viewpoint. This may perhaps represent the true ultimate behavior of the very resistant steels which, to date, have shown complete stability under test. Present experience has been insufficient to determine whether or not such steels actually have incubation periods. However, there is room to speculate that they do and consequently that all the common "ferritic" carbides are ultimately unstable. If this were so, the essence of graphitization resistance would lie in the incubation period.

ACKNOWLEDGMENTS

The authors wish to express their appreciation to the Joint EEI-AEIC Subcommittee on Graphitization of Piping for permission to publish the information in this paper and for their advice in preparing it. Furthermore, the authors wish to thank the Iowa Power and Light Company for permission to include the results of an inspection conducted for them by Battelle Institute.

BIBLIOGRAPHY

1 "Progress Report on Graphitization of Steam Lines," by S. L. Hoyt and R. D. Williams, Trans. ASME, vol. 67, 1945.

2 "Summary Report on the Joint EEI-AEIC Investigation of Graphitization of Piping," by S. L. Hoyt, R. D. Williams, and A. M. Hall, Trans. ASME, vol. 68, 1946, p. 571.

3 "Continuation of Joint EEI-AEIC Investigation on Graphitization of Piping," by S. L. Hoyt and A. M. Hall, Trans. ASME, vol. 69, 1947.

4 "Further Observation of Graphitization in Aluminum-Killed Carbon-Molybdenum-Steel Steam Piping," R. W. Emerson and Mathew Morrow, Trans. ASME, vol. 68, 1946, p. 597.

5 "Studies on Susceptibility of Casting Steels to Graphitization," by J. J. Kanter and E. A. Sticha, Trans. ASME, vol. 69, 1947.

6 "Graphitization Studies of Materials for High-Temperature Service in Steam Plants," by W. G. Conant and W. A. Reich, Trans. ASME, vol. 69, 1947.

7 "Graphitization of Steel at Elevated Temperatures," by A. B. Wilder and J. D. Tyson, ASM Preprint No. 14, 1947.

Discussion

W. A. Reich.[4] The Battelle Memorial Institute's graphitization reports are highly appreciated, and the authors are to be congratulated on the clarity and broad scope of their presentations. We feel that this work has been and will be of great value in making graphitization more understandable and in pointing out means of avoiding its occurrence.

It was gratifying to note that the results of these programs in many cases are paralleled by those obtained in the General Electric Company's graphitization studies. The results on molybdenum-vanadium-type steel are of special interest to us. We have examined two weld specimens representing two commercial cast heats of basic electric molybdenum-vanadium steel (1.1 per cent Mo, 0.22 V and 1.1 per cent Mo, 0.14 V) after 11000 hr at 1100 F and have found no evidence of graphitization. As noted by the authors, graphitization has been found in similar steels made by induction furnace practice. We have examined weld specimens from induction furnace heat of 1 per cent Mo, 0.20 V steel and a similar heat of pipe made by basic electric practice heat after 3000 hr at 1100 F. Graphitization was present in the induction furnace material and not in the electric furnace heat. The induction furnace heat was dirtier, but the only significant difference in chemical composition noted was in nitrogen content. The induction furnace heat measured 0.002 and the electric furnace heat 0.028 per cent nitrogen. We feel from several pieces of evidence like this that nitrogen plays an important part in graphitization. It is good to note that the Joint Committee will sponsor some work under Project 29 in the near future that promises among other things to shed more light on this subject.

The author's comments on the effect of manganese on graphitization tendency are also of interest. Int his connection, we and others have noted the tendency of this element to inhibit graphitization. For example, a sample from an induction furnace heat of plain carbon steel with a chemical composition of 0.15 C, 0.3 Si with 0.70 Mn has run in our tests 15,840 hr at 1100 F with no evidence of graphitization. A similar heat with 0.20 Si and no manganese exhibited graphitization in only 3000 hr at 1100 F.

The peculiar type of continuous graphite noted and the structures shown by the authors certainly suggest "burning" in processing of the steel. The authors' comments in this regard would be welcomed.

The authors have indicated the fact that questions of major importance remain to be answered. The question of the "incubation period" is not the least of these. We are continuing our tests in an attempt to evaluate the relative graphitization tendencies of less-familiar high-temperature steels and to add to the store of general knowledge of the subject so far accumulated.

Authors' Closure

We are very grateful to Mr. Reich for his comments on our paper, and are particularly interested in his data on the effect of vanadium on the graphitization process. Much experimental work is necessary before the role of this element can be defined. Mr. Reich's suggestion that nitrogen may possibly be very important has been noted, and this element will not be overlooked in future studies. The evidence he cited confirming our suspicion that manganese may be an effective graphitization inhibitor was gratifying. We feel that the possibilities of this element have been neglected, and it offers the attraction of being relatively inexpensive.

The continuous type of graphitization found outside the weld-heat-affected zone of a joint between a fitting and a valve, illustrated in Figs. 3, 4, 5, and 6 of our paper, is new in our experience. The structure of the fitting was certainly very coarse and could have been the result of overheating.

[4] Metallurgical Section, Schenectady Works Laboratory, General Electrical Company, Schenectady, N. Y.

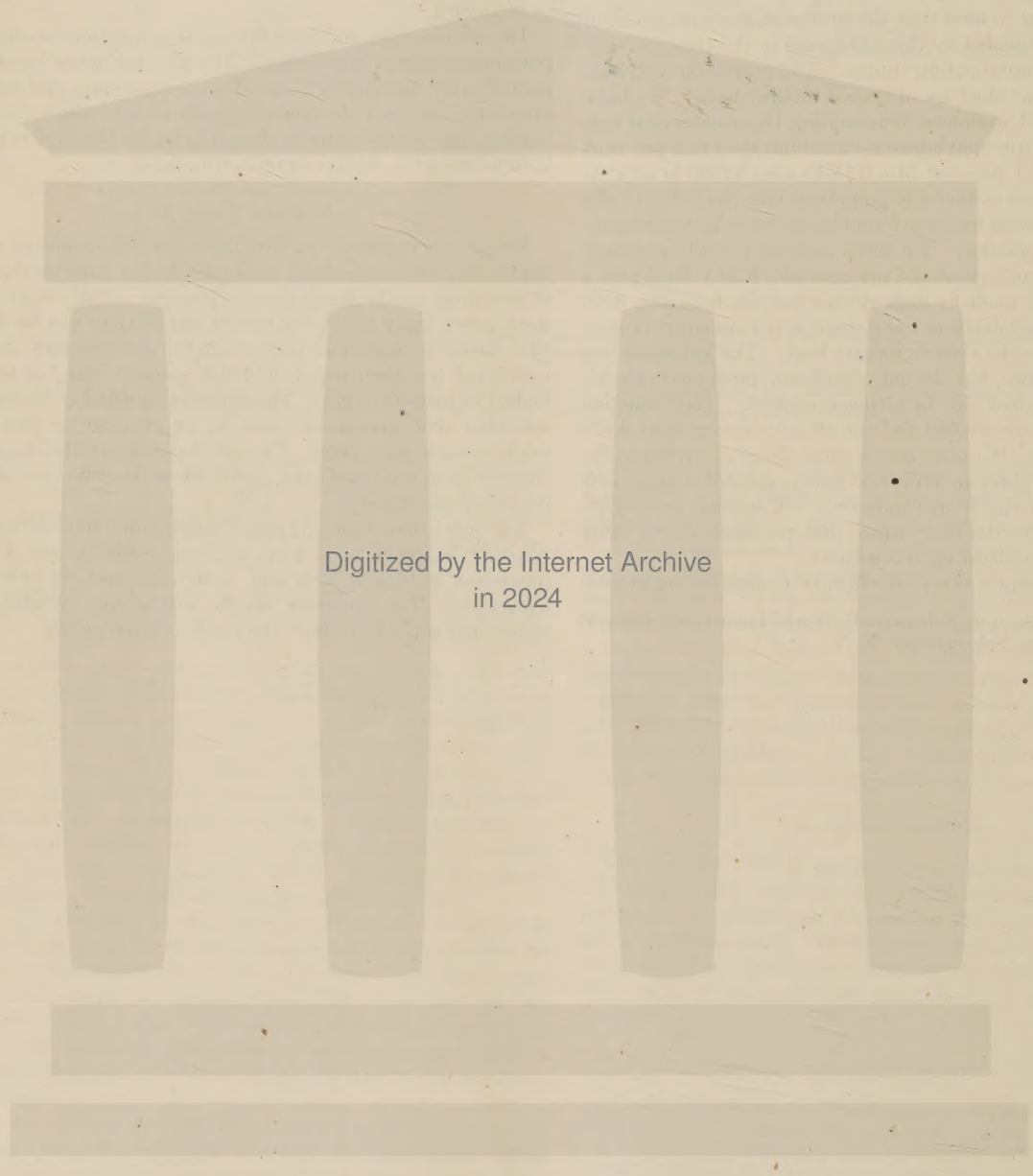

Some 1000 F Steam-Pipe Materials

By ERNEST L. ROBINSON,[1] SCHENECTADY, N. Y.

This paper presents long-time creep and rupture test results on molybdenum-vanadium pipe material in comparison with low-chromium-molybdenum compositions. The molybdenum-vanadium composition shows superior long-time strength at high temperature. Furthermore, long-time soaking of molybdenum-vanadium piping material at high temperature has so far failed to show graphite formation.

IT IS the purpose of this paper to present a number of series of test results contributing to available technical information on materials suitable for high-temperature steam piping. These series were neither planned nor run at the same time but each series was a unit in itself. The group has been selected from results mostly unpublished and presented in a form suitable for guidance in design and for a basis of comparison between different compositions currently under discussion. The author suggests that the results presented herewith should be compared with similar results obtained elsewhere.

Creep strengths are both listed and plotted for a rate of 0.01 per cent per 1000 hr. Creep strengths for a rate of 0.001 per cent per 1000 hr are listed in the tables. These strengths were determined by the General Electric "flow-rate" test which is a step-down relaxation-type test run with a total elastic-plus-plastic extension of 0.2 per cent (except in the case of Series 3). The so-called flow-rate test is usually run for 2000 to 3000 hr with one or more rates between the nominal values read from the log-log plot and tabulated.

Long-time rupture strengths are tabulated both for 10,000 hr and 100,000 hr but only the 100,000-hr strength is plotted in the diagrams. The longest test in each series is usually between 5000 and 10,000 hr although occasional specimens have run as long as 20,000 hr. The 10,000-hr figure involves little extrapolation. The 100,000-hr figure is not free from uncertainty and judgment is required in the selection of a suitable factor of safety. It must be kept in mind that breaks after a long time at high temperature are likely to be brittle in appearance with little elongation to give warning.

Series 1 presents some prewar creep-test results run on a group of compositions originally selected by A. W. Wheeler as possibly having improved high-temperature piping characteristics. The carbon content was intentionally kept low to facilitate welding but it came even lower than intended.

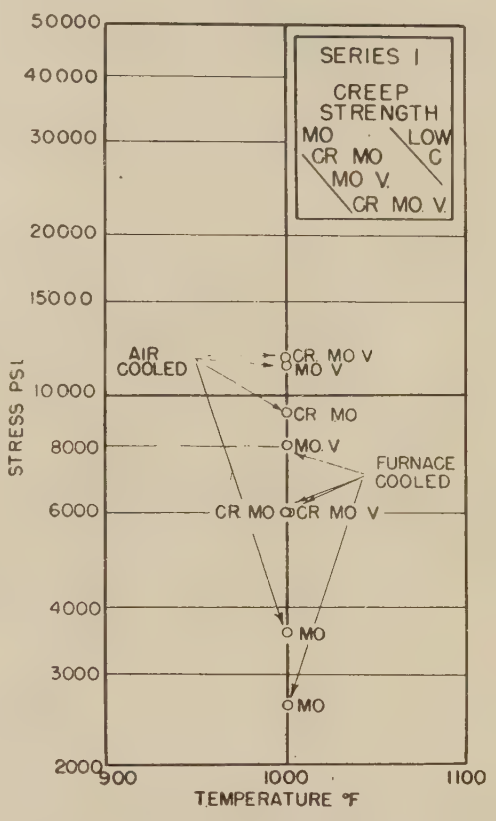

FIG. 1 CREEP STRENGTHS FOR A RATE OF 0.01 PER CENT PER 1000 HR FOR A SERIES OF LOW-CARBON STEELS CONTAINING ADDITIONS OF MOLYBDENUM, CHROMIUM AND MOLYBDENUM, MOLYBDENUM AND VANADIUM, AND ALL THREE OF THESE ELEMENTS

[Each of the four compositions was tested in the air-cooled and the furnace-cooled conditions. (Note the superiority of the air-cooled treatment and of the compositions containing vanadium).]

TABLE 1*a* SERIES 1

Item no.	Chemical composition C	Mn	Si	Cr	Mo	V	Heat-treatment Deg F	Deg F	Physical properties T.S.[c] 1000 Psi	E.L.[d] 1000 Psi	El.[e] %	R.A.[f] %
1118	0.06	0.50	0.31		0.56		1740 8 hr F.C.[a]	1290 4 hr F.C.	59.2	42.4	39.0	76.9
1119	0.06		0.31		0.56		1740 8 hr A.C.[b]	1290 4 hr F.C.	59.4	36.7	40.5	80.7
1121	0.07	0.59	0.31	0.60	0.53	0.14	1740 8 hr F.C.	1290 4 hr F.C.	62.2	43.4	41.5	77.8
1122	0.07	0.59	0.31	0.60	0.53	0.14	1740 8 hr A.C.	1290 4 hr F.C.	66.9	49.4	38.0	79.5
1124	0.07	0.59	0.30	0.57	0.55		1740 8 hr F.C.	1100 4 hr F.C.	58.9	35.2	40.0	77.0
1125	0.07	0.59	0.30	0.57	0.55		1830 8 hr A.C.	1200 4 hr F.C.	61.4	34.4	39.5	74.9
1127	0.06	0.56	0.21		0.60	0.12	1740 8 hr F.C.	1290 4 hr F.C.	59.5	40.4	40.0	80.2
1128	0.06		0.21		0.60	0.12	1740 8 hr A.C.	1290 4 hr F.C.	66.7	43.7	36.0	81.4

[a] Furnace-Cooled; [b] Air-Cooled; [c] Tensile Strength; [d] Elastic Limit; [e] Elongation; [f] Reduction of Area.

TABLE 1*b* SERIES 1

Item no.	Creep strength, psi, at 1000 F Rate 0.01%/1000 hr	Rate 0.001%/1000 hr
1118	2600	1150
1119	3600	1150
1121	6000	2650
1122	11800	7400
1124	6000	3450
1125	9400	4500
1127	8000	4700
1128	11500	8400

[1] Structural Engineer, Turbine Engineering Divisions, General Electric Company. Fellow ASME.

Contributed by the Joint ASTM-ASME Research Committee on the Effect of Temperature on the Properties of Metals and presented at the Annual Meeting, Atlantic City, N. J., Dec. 1–5, 1947, of THE AMERICAN SOCIETY OF MECHANICAL ENGINEERS.

Table 1*a* shows the chemical compositions, heat-treatments, and physical properties, and Table 1*b* gives the creep-test results at 1000 F on this series. They are also shown in Fig. 1.

A glance at these results shows the outstanding characteristics of the moly vanadium composition. While the chrome-moly-vanadium is nearly as good, it would really have to be very much superior in order to justify the greater potential difficulties in welding.

Series 2 on 0.5 per cent molybdenum steel is presented for its value as a standard background with which to compare all the other results. This well-known material has been used to pipe steam to an estimated 8,000,000 kw of steam turbines and this series, extracted from a paper (1)[2] by S. H. Weaver, gives both creep and rupture test results at both 900 F and 1000 F in two different grain sizes both of which are furnace-cooled and air-cooled.

Table 2*a* shows the chemical composition, heat-treatments, and room-temperature physical properties while Table 2*b* gives the creep and rupture test results. These are pictured in Fig. 2.

The spread between the coarse-grain air-cooled condition and the fine-grain slow-cooled condition is typical, the grain size having been obtained by the heat-treating temperature.

The "garden gate" character of this diagram may be noted. The top bar of the gate is the coarse-grain air-cooled material which is strong both at 900 and 1000 F. The bottom bar of the gate is the fine-grain slow-cooled material. The cross braces represent the fact that the coarse-grain slow-cooled material is relatively stronger at 1000 F but relatively not as strong at 900 F and that the fine-grain air-cooled material is relatively strong at 900 F but relatively not so strong at 1000 F.

This diagram does not represent the maximum spread possible with this material. No data are included for pipe "as received" in the hot-rolled condition nor for pipe in the spheroidized condition. For a complete discussion of these matters the paper by S. H. Weaver (1) should be consulted.

Series 3 presents a group of tests run a good many years ago on one of the best of the low-chromium-molybdenum compositions

[2] Numbers in parentheses refer to the Bibliography at the end of the paper.

TABLE 2*a* SERIES 2

Item no.	Chemical composition C	Mn	Si	Mo	Heat-treatment Deg F		Deg F		Physical properties T.S. 1000 Psi	E.L. 1000 Psi	El. %	R.A. %
897–909	0.17	0.88	0.20	0.42	1560	8 hr A.C.	1200	4 hr F.C.	68.1	39.0	35.5	64.4
899–911	0.17	0.88	0.20	0.42	1740	8 hr A.C.	1200	4 hr F.C.	70.9	41.0	31.5	63.2
901–905	0.17	0.88	0.20	0.42	1560	8 hr F.C.	1200	4 hr F.C.	67.1	35.0	34.5	58.0
903–907	0.17	0.88	0.20	0.42	1740	8 hr F.C.	1200	4 hr F.C.	63.6	32.0	34.0	56.9

TABLE 2*b* SERIES 2

	Creep strength, psi 0.01%/1000 hr		0.001%/1000 hr		Rupture strength, psi 10,000 hr		100,000 hr	
Item no.	900 F	1000 F	900 F	1000 F	900 F	1000 F	900 F	1000 F
897–909	20000	7200	15000	2500	46000	16000	38000	8800
899–911	24300	11000	19700	3800	52000	22000	50000	12000
901–905	14100	7600	12500	2900	32000	16000	25000	8800
903–907	13800	10800	11600	3500	34000	18000	28000	12000

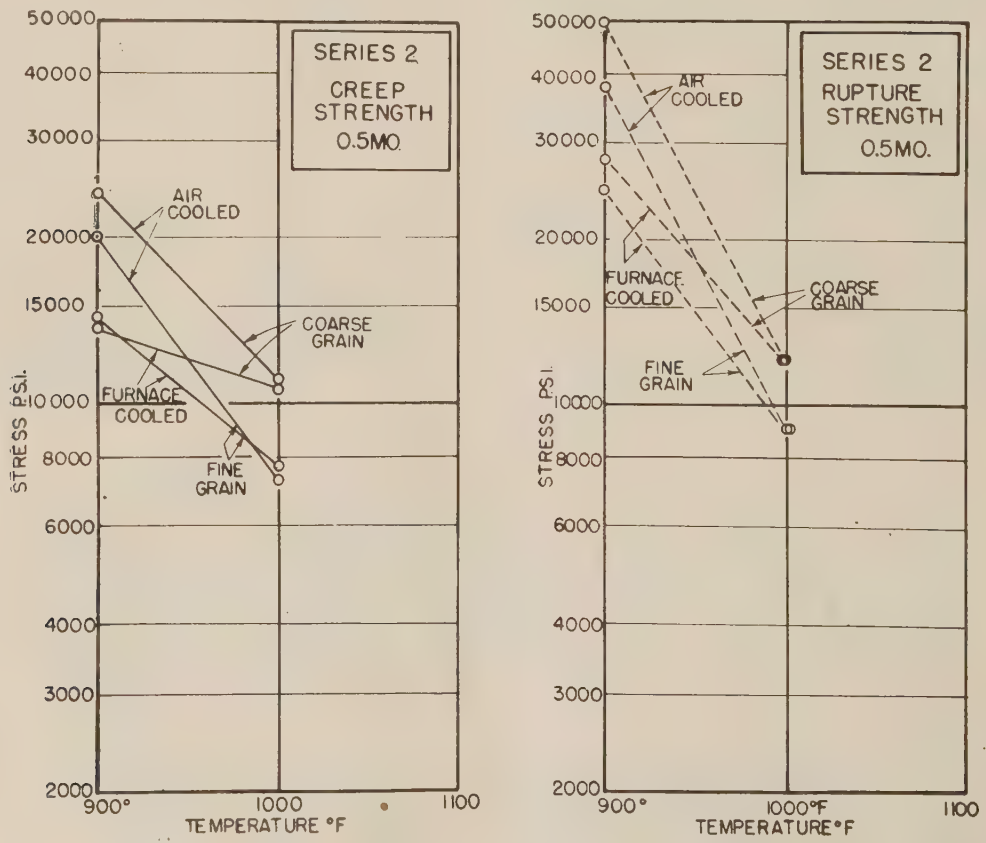

FIG. 2 CREEP STRENGTHS FOR A RATE OF 0.01 PER CENT PER 1000 HR AND 100,000-HR RUPTURE STRENGTHS OF 0.5 PER CENT MOLYBDENUM STEEL

(Note the superiority of the coarse-grain air-cooled treatment and the inferiority of the fine-grain slow-cooled treatment.)

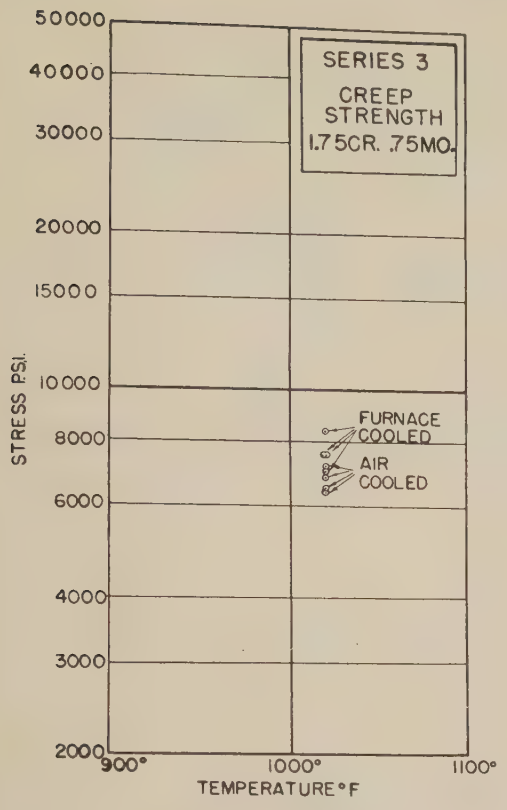

FIG. 3 CREEP STRENGTHS FOR A RATE OF 0.01 PER CENT PER 1000 HR FOR BAIN STEEL

(These tests all began with 1000 hr at 10,000 psi. Total extensions were rather less than for other materials and the results might legitimately be corrected upward an estimated 10 per cent.)

commonly called Bain steel. These tests were run as a part of a much larger series in which the test began with 10,000 psi constant stress left in the specimen for 1000 hr. Thereafter the load was stepped down to give other creep rates. This unusual type of test fitted in with the other results not here presented. The matter is mentioned only to qualify the results as not directly comparable with the others. The total extension in test was rather less than the standard 0.2 per cent. At standard extension these results might have come in the order of 10 per cent higher.

Table 3*a* shows the chemical composition, heat-treatments, and room-temperature physical properties and Table 3*b* gives the creep test results.

Early applications of this material incurred some welding difficulties and its more general use received a setback. Perhaps its introduction was somewhat ahead of its time.

Series 4 presents the results of a group of tests run in cooperation with the Consolidated Gas Electric Light and Power Company of Baltimore on two heats of 0.5 per cent chromium, 0.5 per cent molybdenum steel, one aluminum-killed and the other silicon-killed. Besides running both creep and rupture tests on these materials, results are given "as received," normalized, and also in the annealed condition.

Table 4*a* shows the chemical composition, heat-treatments, room-temperature physical properties, and Table 4*b* gives the creep test results and the rupture test results in so far as they are at present completed. Some rupture series are still incomplete. Fig. 4 pictures these results.

This diagram, like that for Series 2, also has a garden-gate pattern and the comparison is illuminating. Above the results for the specimens air-cooled for the test are the two lines representing the as-received material which may have been cooled from a still higher temperature during manufacture. As noted

TABLE 3*a* SERIES 3

Item no.	Chemical composition C	Mn	Si	Cr	Mo	Heat-treatment Deg F	Deg F	Deg F	Physical properties T.S. 1000 psi	E.L. 1000 psi	El. %	R.A. %
396	0.20	0.44	0.39	1.66	0.94	2280 6 hr F.C.	1600 5 hr A.C.	1200 3 hr F.C.	112.2	77.0	21.5	66.1
397	0.20	0.44	0.39	1.66	0.94	2280 6 hr F.C.	1740 5 hr A.C.	1200 3 hr F.C.	114.2	80.0	22.0	65.2
398	0.20	0.44	0.39	1.66	0.94	2280 6 hr F.C.	1875 5 hr A.C.	1200 3 hr F.C.	122.9	89.0	19.0	62.0
401	0.20	0.44	0.39	1.66	0.94	2280 6 hr F.C.	2280 5 hr A.C.	1200 3 hr F.C.	135.7	86.0	17.5	56.2
416	0.20	0.44	0.39	1.66	0.94	2280 6 hr F.C.	1600 5 hr F.C.	1200 3 hr F.C.	80.7	37.0	28.0	48.2
417	0.20	0.44	0.39	1.66	0.94	2280 6 hr F.C.	1740 5 hr F.C.	1200 3 hr F.C.[a]	77.7	52.0	31.5	58.3
418	0.20	0.44	0.39	1.66	0.94	2280 6 hr F.C.	1875 5 hr F.C.	1200 3 hr F.C.	81.4	29.0	27.5	46.8
419	0.20	0.44	0.39	1.66	0.94	2280 6 hr F.C.	2280 5 hr F.C.	1200 3 hr F.C.	113.8	38.0	12.0	30.8

[a] Reheat-treatment of item 417 1650 F—1 hr O.Q.—1600 F—1 hr F.C.—1200 F—1 hr F.C.

TABLE 3*b* SERIES 3

Item no.	Creep strength psi at 1022 F Rate 0.01%/1000 hr	Rate 0.001%/1000 hr
396	6500	4200
397	6400	3600
398	6800	4500
401	7100	4600
416	8400	5400
417	7500	4200
418	7500	3850
419	7000	4300

TABLE 4*b* SERIES 4

Item no.	Creep strength, psi 0.01%/1000 hr 900 F	1000 F	0.001%/1000 hr 900 F	1000 F	Rupture strength, psi 10,000 hr 900 F	1000 F	100,000 hr 900 F	1000 F
2257	26000	14800	22500	6800	40000[a]	22000[a]	30000[a]	14000[a]
2258	25500	14200	21000	6500	45000	23000	39000	14000
2259	17500	7200	13500	2300				
2260	23000	10500	19000	5000	52000		46000	
2273		6800		2000				
2264	13000	5900	10000	1800	46000[a]		45000[a]	
2265	14000	8200	11500	2900	34000[a]	29000[a]		

[a] Test still running.

TABLE 4*a* SERIES 4

Item no.	Chemical composition C	Mn	Si	Cr	Mo	Al	Al_2O_3	Heat-treatment Deg F	Deg F	Physical Properties T.S. 1000 Psi	E.L. 1000 Psi	El. %	R.A. %
2257	0.12	0.45	0.14	0.45	0.54	0.027	0.008		1200 2 hr F.C.	61.4	42.4	37.5	67.7
2258	0.13	0.50	0.22	0.48	0.56	0.003	0.002		1200 2 hr F.C.	66.9	42.7	34.5	64.4
2259	0.12	0.45	0.14	0.45	0.54	0.027	0.008	1700 2 hr A.C.	1200 2 hr F.C.	62.2	43.9	41.7	75.7
2260	0.13	0.50	0.22	0.48	0.56	0.003	0.002	1700 2 hr A.C.	1200 2 hr F.C.	71.9	51.9	34.0	65.9
2273	0.19	0.60	0.26	0.46	0.46			1600 1 hr A.C.	1250 1 hr F.C.[a]	70.4	47.4	35.5	65.6
2264	0.12	0.45	0.14	0.45	0.54	0.027	0.008	1700 2 hr F.C.	1200 2 hr F.C.	57.9	35.9	40.5	71.0
2265	0.13	0.50	0.22	0.48	0.56	0.003	0.002	1700 2 hr F.C.	1200 2 hr F.C.	61.9	39.4	37.5	64.0

[a] Item 2273 redrawn 1200 F—2 hr F.C.

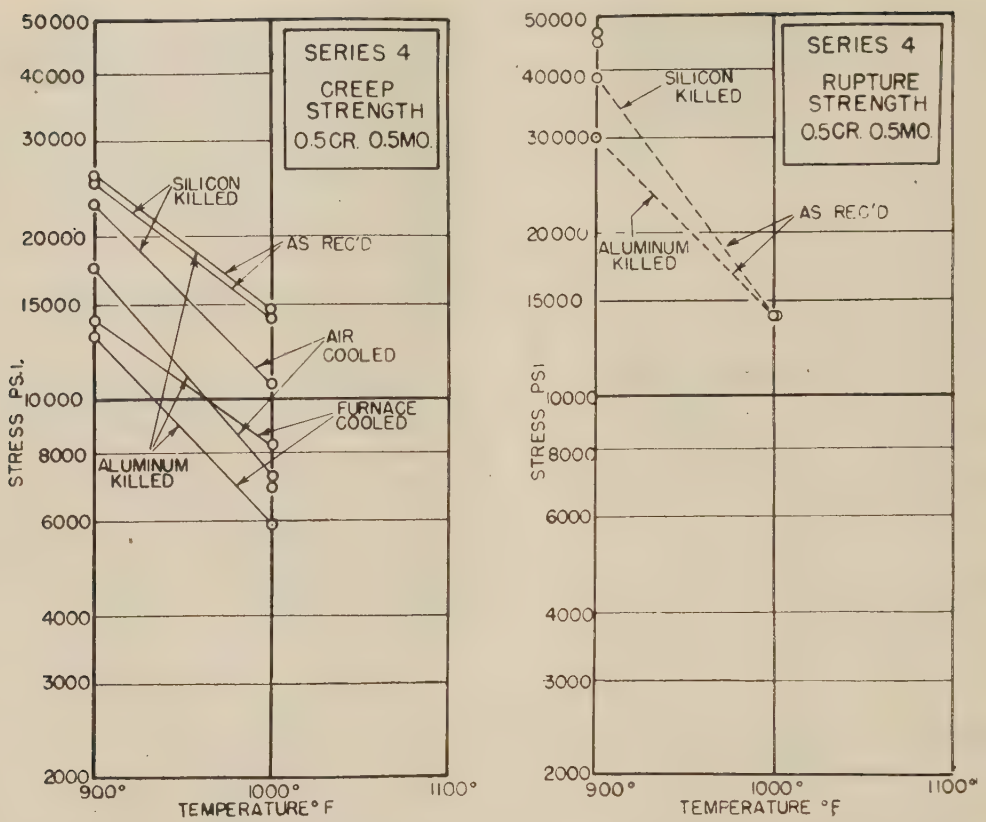

FIG. 4 CREEP STRENGTHS FOR A RATE OF 0.01 PER CENT PER 1000 HR AND 100,000-HR RUPTURE STRENGTHS FOR 0.5 PER CENT CR 0.5 PER CENT MO STEEL

(These materials were furnished by the National Tube Company and tested in co-operation with the Consolidated Gas Electric Light and Power Company of Baltimore, Md. Results may be compared with Fig. 2.)

before, corresponding results are not available for Series 2. However, the close correspondence between these results and those for plain 0.5 per cent molybdenum steel is noteworthy. The small chromium addition does not seem to have any important effect on the strength when results on similar treatments are compared.

Series 5 collects a number of scattered tests on different low-chromium-molybdenum materials that happen to be available. These include 1 per cent chromium, $^1/_2$ per cent molybdenum; 1 per cent chromium, 1 per cent molybdenum; $2^1/_4$ per cent chromium, 1 per cent molybdenum; 3 per cent chromium, 1 per cent molybdenum at temperatures at or near 1000 F.

Table 5*a* shows the chemical compositions and heat-treatments, and room-temperature physical properties, and Table 5*b* shows the creep test results which are also pictured in Fig. 5.

These scattered results are listed with some diffidence as lacking in sufficient spread to indicate the range of properties of the materials. Mostly it can be said they were tested in a condition supposed at the time to be favorable to the material.

Series 6 presents test results on low carbon-moly-vanadium steel developed largely as a consequence of the results given in Series 1. Plain molybdenum steel was falling off in strength at 1000 F and some improvement was needed which the vanadium addition seemed to afford. A similar composition had been tried for a turbine rotor and turbine wheel before the war. After the Springdale experience with graphitization the fixation of the carbon content seemed important and vanadium was thought to be a potent carbide former. Thus it appeared the logical strengthener and turbine-shell castings for 1000 F were made to this composition.

Such castings are being used on the 100,000-kw turbine for the Essex Station of the Public Service Electric and Gas Company, New Jersey, and noting the good qualities, H. Weisberg, mechanical engineer, Electric Engineering Department, inquired if piping could not be made of the same composition. Actually the composition had been originally selected with piping in mind and accordingly the turbine piping for the Essex machine has been made of molybdenum-vanadium. The composition of the piping and the castings is practically the same. However, the results show that the ordinary process of manufacture of the piping is conducive to higher strength than in the castings.

Table 6*a* shows the chemical compositions, heat-treatments, and room-temperature physical properties of this series, and Table 6*b* shows the high-temperature test results so far available. These are pictured in Fig. 6.

It will be noted that in corresponding treatments the moly-vanadium pipe material is 50 to 100 per cent stronger than the plain moly or low-chromium-moly compositions.

As regards its resistance to graphitization, neither the Conant-Reich paper (2) nor the Battelle Report (3) found any evidence of graphite formation in this material. Some small nodules have been reported as seen in samples of laboratory induction-furnace heats but none has ever been found in open-hearth or electric-furnace heats.

A word with reference to the room temperature physical properties of high-temperature materials may be appropriate. Specifications have been written for many years stating required physical properties at room temperature. These are significant for the ultimate user when the service is at room temperature. On the other hand, when the ultimate service is at high temperature, the high-temperature properties are of particular importance to the ultimate user and the room-temperature properties are

TABLE 5*a* SERIES 5

Item no.	Chemical composition C	Mn	Si	Cr	Mo	Heat-treatment Deg F	Deg F	Physical properties T.S. 1000 Psi	E.L. 1000 Psi	El. %	R.A. %
351	0.33	0.36	0.11	1.1	1.15	1830 8 hr A.C.	1200 1 hr A.C.	131.4	86.0	21.5	59.6
2160	0.14	0.40	0.42	2.79	0.92	1580 F.C. at	75 F/hr to 1200	67.4	32.7	42.7	75.6
2272	0.13	0.58	0.17	0.90	0.50		1200 2 hr F.C.	68.4	49.4	34.0	70.4
2322	0.14	0.51	0.27	2.27	1.02	1900 2 hr A.C.	1200 2 hr F.C.	119.9	69.9	15.5	68.8
2324	0.12	0.48	0.85	1.3	0.53	1700 4 hr A.C.	1200 4 hr F.C.	85.9	38.4	34.5	71.4

TABLE 5*b* SERIES 5

Item no.	Creep strength 0.01%/1000 hr 900 F	1000 F	1022 F	0.001%/1000 hr 900 F	1000 F	1022 F
351			2950			900
2160		4600			1850	
2272	27000	13500		22500	6000	
2322		10000			4900	
2324		6800			2500	

of interest only during manufacture and handling. Sometimes these may be favorable but in many cases new materials having strength at high temperature are likely to be relatively hard at room temperature and possibly lacking in the elongation that would occur at service temperature before any mishap could occur.

Series 2, 4, and 6 give both creep strength and rupture strength. A study of the creep strengths for a rate of 0.01 per cent per 1000 hr in comparison with the 100,000-hr rupture strengths shows that the rupture strength has little margin over the creep strength. This is a characteristic of all three materials as also of plain carbon steel. In other words, if a factor of safety of 3 to 1 or even 2 to 1 is taken with reference to the 100,000-hr rupture strength, the creep strength for a rate of 0.01 per cent per 1000 hr will no longer be a limitation in the case of these materials. In fact, we would welcome lower creep strength and greater elongations if such a relationship were consistent with high long-time rupture strength at high temperature. Meanwhile the room-temperature properties are whatever result in satisfactory high-temperature performance and may be definitely different from what has characterized the familiar materials of ordinary low-temperature applications. Elongations of 20 per cent sound generous and conservative but after all it is the first half of one per cent in service that irons out the stress concentrations.

This article has no new results to present in the matter of corrosion resistance. However, it appears appropriate to recall the Detroit Edison tests (4) run for 16,000 hr at 1100 F (for which

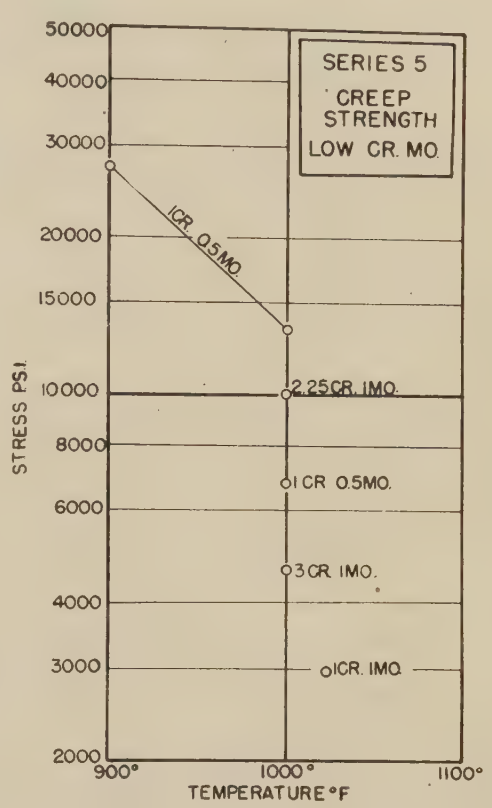

FIG. 5 CREEP STRENGTHS FOR A RATE OF 0.01 PER CENT PER 1000 HR FOR VARIOUS LOW-CHROMIUM-MOLYBDENUM STEELS
(These results fail to indicate that chromium adds to the creep strength at 1000 F.)

TABLE 6*a* SERIES 6

Item no.	Chemical composition C	Mn	Si	Mo	V	Heat-treatment Deg F	Deg F	Physical properties T.S. 1000 psi	E.L. 1000 psi	El. %	R.A. %
2250 C[a]	0.17	0.57	0.50	1.1	0.22	1920 8 hr, cool, 235 F/hr	1200 4 hr F.C.	82.9	47.4	28.5	58.8
2251 C	0.17	0.57	0.50	1.1	0.22	Note A[c]	1150 6 hr F.C.	97.1	51.6	25.0	54.6
2282 C	0.21	0.78	0.32	0.95	0.31	Note B[d]	1200 6 hr F.C.	95.6	46.9	21.5	47.5
2283 C	0.16	0.75	0.21	1.14	0.29	Note B[d]	1200 4 hr F.C.	91.4	41.4	21.0	46.9
2284 C	0.18	0.71	0.34	1.15	0.23	Note B[d]	1200 4 hr F.C.	91.9	39.9	24.0	47.8
2370 P[b]	0.20	0.58	0.26	1.04	0.21	1920 4 hr A.C.	1200 4 hr F.C.	143.9	114.9	20.5	60.1
2375 P	0.20	0.58	0.26	1.04	0.21	1920 4 hr, cool to 1740 F A.C.	1200 4 hr F.C.	139.9	109.9	21.0	62.3
2376 P	0.20	0.58	0.26	1.04	0.21	1740 8 hr A.C.	1200 4 hr F.C.	102.4	80.9	26.0	67.0

[a] C, Casting.
[b] P, Piping.
[c] 1920 F, 2 hr F.C. 1920 F, 1 hr, Cool @ 270 F/hr to 1740 F, Cool @ 1800 F/hr.
[d] 1920 F, Hold, Cool @ 450 F/hr to 930 F. 1920 F, Hold, Cool @ 180 F/hr to 930 F

TABLE 6*b* SERIES 6

Item no.	Creep strength, psi 0.01%/1000 hr 900 F	1000 F	0.001%/1000 hr 900 F	1000 F	Rupture strength, psi 10,000 hr 900 F	1000 F	1100 F	100,000 hr 900 F	1000 F	1100 F
2250		13000		4000	47000	25000	9800[a]	40000	18000	5300[a]
2251		14000		6200		30000	12000		22000	6000
2282		15500		8500		29000			20000	
2283		14000		5600		28500			18000	
2284		14500		6900						
2370		21000		12500		28500[a]			18500[a]	
2375		22000				36000[a]			23000[a]	
2376		13000		6800		33000[a]			24000[a]	

[a] Test still running.

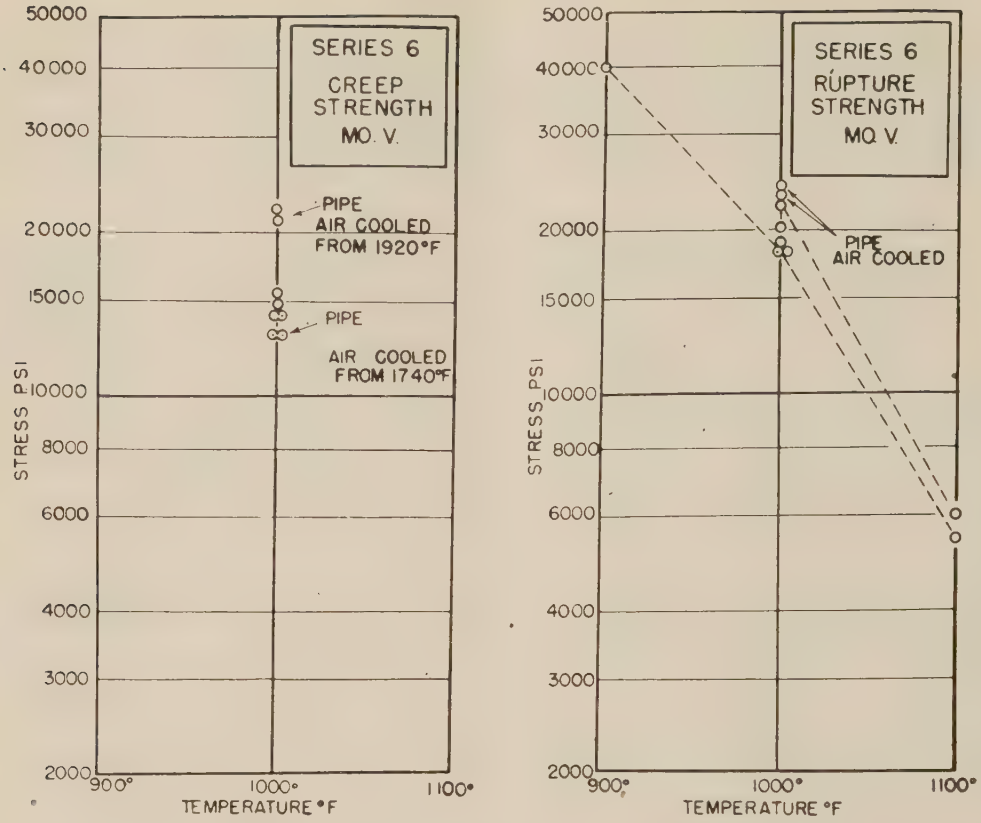

FIG. 6 CREEP STRENGTH FOR A RATE OF 0.01 PER CENT PER 1000 HR AND 100,000-HR RUPTURE STRENGTH FOR MOLYBDENUM-VANADIUM STEEL

[These tests were either made on bars cut from piping or from castings of similar composition, see Table 6. (Note the superior high-temperature strength of this composition.).]

the General Electric Company furnished a certain number of test samples). Perhaps the most striking discovery in these tests was the uncertainty of any great difference in corrosion resistance between any of the several low-chromium-molybdenum compositions and plain carbon-moly steel. While there was a considerable spread among the various low-alloy steels, they were all, as a group, with plain carbon-moly in the middle, both much better than plain carbon steel and much poorer than 12 per cent chromium steel and the high-alloy compositions.

While the object of this article is to present test results on samples of piping materials, the important question as to the relative propriety of the chromium addition seems to call for some mention of the forging and bolting materials where there does not seem to be any uncertainty. For bolts, both low-temperature strength and short-time high-temperature strength are important as well as long-time high-temperature strength and bolts are not expected to be readily weldable. Under such conditions, with a carbon content of 0.40 per cent, the triple alloy containing the chromium addition as well as the molybdenum and vanadium seems definitely appropriate. Some test results are available to show that chromium adds to the long-time rupture strength at 1000 F of a moly-vanadium rotor forging at the 0.30 per cent carbon level, which is too high for easy welding. However, at the low carbon level of piping and castings where weldability is important it seems hard to justify the use of chromium on the basis of the data at present available.

BIBLIOGRAPHY

1 "The Effect of Carbide Spheroidization Upon the Rupture Strength and Elongation of Carbon-Molybdenum Steel," by S. H. Weaver, Proceedings of the ASTM, vol. 46, 1946, p. 856.

2 "Graphitization Studies of Materials for High-Temperature Service in Steam Plants," by W. G. Conant and W. A. Reich, Trans. ASME, vol. 69, 1947.

3 "Continuation of Joint EEI-AEIC Investigations on Graphitization of Piping," by S. L. Hoyt and A. M. Hall, Trans. ASME, vol. 69, 1947.

4 "High-Temperature-Steam Corrosion Studies at Detroit," by R. M. Van Duzer, Jr., Trans. ASME, vol. 66, 1944, page 277.

Discussion

J. J. KANTER.[3] The author makes available additional creep and rupture data on steels of interest for high-temperature piping structures. This data comes as a timely and valuable contribution to those who are concerned with the specification and application of piping steels for 1000 F services.

This array of creep data, as have most previously published arrays, demonstrates that creep-strength values are apt to vary widely for a given type of material within its nominal chemical composition and for the various conditions of working and heat-treatments in which it must be utilized in structures. It would appear that if this seemingly inherent variability of creep strength is to be controlled within closer limits, more must be learned about some of the variables within manufacturing tolerance.

It is rather impressively demonstrated in the author's data that for the molybdenum-vanadium steels, a range of high-temperature strength obtains substantially above that for the molybdenum and chromium-molybdenum types. Other data corroborating this observation is to be found. Unfortunately,

[3] Materials Research Engineer, Crane Co., Chicago, Ill. Mem. ASME.

however, some evidence seems to have been found in several independent investigations that the molybdenum-vanadium steels, unless free of excess aluminum content, are quite unstable with respect to graphitization as are the aluminum-bearing molybdenum steels.

The author states that he finds it hard to justify the use of chromium in piping and castings at weldable carbon levels. On merely a basis of high-temperature strength this statement might be warranted. However, from the standpoint of high-temperature stability among the piping steels which are commercially procurable the specification of a substantial chromium content thus far seems to be the only measure which offers a thoroughly reliable safeguard against graphitization. Additions to steel, such as vanadium, molybdenum, titanium, and nickel with the presence of soluble aluminum, but without the substantial presence of chromium fail to inhibit graphitization. However, in the presence of a substantial chromium content the aluminum bearing steels with any or all of these afore-mentioned ingredients become graphitization-resistant. Thus as matters now stand, chromium is the only addition for which there is any clear-cut credit as a graphitization inhibitor in the presence of soluble aluminum. It is very well to say that if the aluminum were ruled out there would not be any graphitization problem among the high-temperature alloy steels, but until specifications can be written for procurable material thus safeguarded, we must consider chromium as the only good insurance at our disposal.

Considerable emphasis has been placed for some years past on the minimizing of carbon content in steel for welded piping structures to the end of facilitating the preparation of good welds. Now that 1000-F steampipe materials have become of vital concern, there may be a further reason for emphasizing the minimizing of carbon content, namely, good creep strength; and studying Mr. Robinson's data one may find suggestions of such a factor. While the adverse effect which high carbon content has on creep strength has received some attention in creep literature the problem has been given little systematic study. The reason for this is perhaps due to the fact that the steam-pipe-materials problem has only recently moved up into the range of temperature where the carbon effect on creep is of substantial magnitude. At 800 to 900 F, the effect of carbon on sustaining tensile and yield strengths is still of some moment. However, now that we are scrutinizing more closely the properties of steel at temperatures upward of 1000 F, the effects of carbon on the creep strength, per se, merits fuller study for all materials whether they be pipe, forgings, or castings.

C. L. Clark.[4] While we are indebted to the author for the high-temperature data he has presented on a wide variety of steels, it is believed the title of his paper may be misinterpreted by many, for on the basis of all past practices at least, the condition in which many of these steels were tested would not be considered as suitable for pipe for high-temperature service.

While none of the ASTM Specifications covering alloy-steel pipe have hardness requirements, the alloys covered are identical to those of the tubular specifications with respect to chemical composition and required room-temperature physical properties; and those tubular specifications, for the type steels considered by the author, never permit a maximum hardness in excess of 163 Brinell. Unfortunately, the author does not include hardness values but he does give room-temperature tensile strengths. By conversion the hardness of many of his steels range from 160 to 280 Brinell, which is thus way beyond the hardness ever obtained in alloy pipe.

It is known that the creep and rupture strengths of the lower alloyed steels at 1000 F are greatly influenced by heat-treatment and structure, and thus by hardness, and it is believed that the author may be testing differences in hardness rather than differences in composition. For example, tests which we now have in progress definitely indicate that when Mo-V steel is annealed to 156 Brinell its high-temperature strength is practically identical to 0.50 Mo steel annealed to even a lower hardness of the order of 137 Brinell. Likewise, the Mo-V steel (item 2250, Table 6*a*) which has room-temperature properties of the order of magnitude generally recognized as being suitable for piping has high-temperature strength characteristics very similar to many of the Cr-Mo grades now in general use.

For the same reasons as set forth in the previous paragraph it is believed that a hasty reader may get a wrong impression from Fig. 5 where the author gives only a few spot tests whereas his other charts show a range of treatments. We have results to show that the creep strength of material having a composition like Item 2324 at 1000 F may be made to vary from about 6500 to 15,000 lb depending on the structure and consequently in any comparison of this type the steel should have at least approximately the same structure or heat-treatment. Although the author apologized for not presenting a range of treatments in Fig. 5, unless his warning about this matter is heeded, a glance at the diagram only is likely to give a very false picture with respect to the influence of variations in the composition alone. As a further example, this figure shows the 3 Cr 1 Mo steel to have only about half the strength of the $2^1/_4$ Cr 1 Mo analysis. All other published results show these two analyses to have about the same strength when in the same condition of heat-treatment.

Everyone probably wishes that the author's statements with respect to the room temperature properties of steels intended for high-temperature service could be accepted but it is personally believed that considerably more experience will have to be had with these harder alloys before such can be taken for granted. If this were true, then a considerable amount of time, money, and labor have been wasted in the heat-treatment of alloy pipe and particularly on the stress relief of field welds. As another angle of approach to this question, many engineers believe that few if any failures of piping systems occur at the operating temperatures but rather during the heating and cooling periods. They further feel that these failures, when they do occur, take place at a temperature of maximum rigidity for the system which may be rather close to room temperature. If this is so, room temperature properties, or those at slightly elevated temperatures, may be of greater importance than previously assumed.

We cannot agree with the author's remarks concerning the effect of alloy additions on the oxidation and corrosion resistance of steels for it is believed the addition of chromium is necessary to insure the desired degree of surface stability at temperatures of 1000 F and higher, particularly when an extremely long service life is desired.

In closing we would like to ask the author what heat-treating cycle he recommends for stress-relieving field welds in Mo-V pipe and what hardness results?

F. Eberle.[5] The experimental data presented in this paper offer much food for thought. Without careful study the reader may be led to assume that the low chromium-molybdenum steels up to about 3 per cent chromium which have proved themselves of outstanding value in high-temperature service possess inferior creep strength, particularly when compared with the 1 per cent Mo $^1/_4$ per cent V steel developed by the General Electric Company. The paper claims that in the corresponding treatments

[4] Research Metallurgical Engineer, Timken Roller Bearing Company, Canton, Ohio. Mem. ASME.

[5] Chief Metallurgist, The Babcock & Wilcox Company, Alliance, Ohio.

the molyvanadium pipe steel is at 1000 F 50 to 100 per cent stronger than the low-chromium-moly compositions, and concludes with the statement that "at the low-carbon level of piping and castings where weldability is important it seems hard to justify the use of chromium on the basis of the data at present available." These far-reaching contentions do not seem to be adequately supported by the material offered. A careful study of the paper shows that no consideration has been paid to the melting and deoxidation practice and to the austenitizing grain size of the various steels with which the 1 per cent Mo 1/4 per cent V steel is compared. Consequently, there is more than reasonable doubt that these steels were in a comparable condition with respect to the factors which influence creep strength. These low-chromium-molybdenum steels were developed to meet certain corrosive conditions in high-temperature oil-refining operations where they have been outstandingly successful. They have also given an excellent account of themselves in superheater service. The significant fact is that they usually receive aluminum in the deoxidation practice and generally are given a full annealing treatment at moderately high temperatures, resulting in a medium- to fine-grained microstructure. Aluminum deoxidation, fine grain size, and slow furnace cooling in the final heat-treating operation do not permit these steels to attain their highest possible creep strength at such low temperatures as 1000 F. However, it must be remembered that these low-chromium-molybdenum steels are intended for service at temperatures above 1000 F, i.e., beyond the indicated application limit of the 1 per cent Mo 1/4 per cent V steel, and that they possess very satisfactory creep strength at these higher temperatures.

In so far as the 1/2 per cent Cr 1/2 per cent Mo steel is concerned which has about the same temperature range of application as the 1 per cent Mo 1/4 per cent V steel, there is evidence in the paper itself that the difference in creep strength between these two materials, on a comparative basis, is not nearly as great as the reader might be led to believe. For example, let us compare Mo-V steel No. 2376 of Series 6 which had been soaked for 8 hr at 1740 F, followed by air-cooling and drawing at 1200 F, with the 1/2 Cr 1/2 Mo steel No. 2260 of Series 4 which was annealed at 1700 F, i.e., at a lower temperature, for only two hours, followed by air-cooling and drawing at 1200 F, then we find the following relative creep-strength values for 1000 F and 0.01 per cent creep in 1000 hr:

1% Mo 1/4% V steel No. 2376	13,000 psi
1/2% Cr 1/2% Mo steel No. 2260	10,500 psi

i.e., the moly-vanadium steel shows in this case a superiority of the order of 20 per cent rather than 50 to 100 per cent as indicated in the paper.

Now let us compare Mo-V steels 2370 and 2375 in their 1920 F treated condition which should produce a rather coarse grain size favoring high creep strength, with the 1/2 per cent Cr 1/2 per cent Mo steels 2257 and 2258 in their hot-rolled condition in which they display a nonuniform medium to coarse grain size (ASTM Nos. 3–6), then we have the following creep-strength values, again for 1000 F and 0.01 per cent in 1000 hr:

1% Mo 1/4% V steels 2370 and 2375	21,000 and 22,000 psi
1/2% Cr 1/2% Mo steels 2257 and 2258	14,800 and 14,200 psi

i.e., the moly-vanadium steels have a 30 per cent superiority over the 1/2 per cent Cr 1/2 per cent Mo steel rather than 50 to 100 per cent. There is reason to believe that this difference in the creep strength of the two steels would be much smaller if they were tested in the same grain-size condition. In this connection it may be of interest to note that two other laboratories also determined the creep strength of the two 1/2 per cent Cr 1/2 per cent Mo steels 2257 and 2258 in the as-rolled and 1200 F stress-relieved condition and obtained values of 15,000 psi and 20,000 psi, respectively, for 1000 F and 0.01 per cent/1000 hr.[6]

Tapsell, Bristow, and Jenkins[7] studied the creep and creep-rupture behavior of a plain 0.5 per cent Mo steel and a 0.5 per cent Mo 0.20 per cent V steel, at temperatures ranging from 986 F to 1292 F, both steels made in an acid-lined high-frequency electric furnace and hot-rolled into 1 1/8-in-diam bars, and found "considerable similarity in the creep behavior of the two steels in the air-cooled condition." Here again, the plain molybdenum steel was at a disadvantage from a grain-size standpoint because it had been normalized at 975 C (1787 F) which produced a noticeably finer structure than that existing in the moly-vanadium steel which had been normalized at 1000 C (1832 F). Notwithstanding its more favorable microstructure, the moly-vanadium steel was found to have a margin of superiority of only about 10 C (18 F) for 0.2 per cent creep in 100,000 hr when compared on a temperature basis. The chances are that this slight superiority of the moly-vanadium steel would have been further reduced or even completely wiped out if the plain molybdenum steel had been tested in the same grain-size condition.

It therefore appears that the good showing of the 1 per cent Mo 1/4 per cent V steel described in the paper is largely dependent upon the conditioning treatment at 1920 F which is a highly undesirable temperature from a fabricating standpoint. Furthermore, one cannot help speculating on the question of what welding would do to the creep strength of this high-temperature preconditioned steel. As for welding itself, a steel which displays a room-temperature tensile strength of about 140,000 psi after air-cooling from 1900 F, would seem to possess a very high degree of weld-hardening and would seem to be crack or notch sensitive. Such a steel should be rather tender with respect to welding in the field. It would therefore be interesting to obtain information on the microstructural and mechanical properties of such moly-vanadium weldments, both as-welded and stress-relieved and before and after long-time creep testing at 1000 F. In experiments with weld metal containing 1 per cent and 2 per cent molybdenum, we observed some years ago a marked degree of secondary hardening after conventional stress-relieving treatments. Does 1 per cent Mo 1/4 per cent V metal display similar characteristics?

In conclusion, we should like to ask the author if he would recommend the 1 per cent Mo 1/4 per cent V steel, which may be of great value for applications where extreme resistance to creep is of prime importance, for temperatures above 1000 F, let us say, 1050 F, or would he then recommend the use of chromium-bearing molybdenum steels?

F. B. Foley.[8] Attention is called to what seems to be an error in the reporting of Series 1. Item 1125 has a composition (Table 1*a*) which places it in the Mo group. It has a creep strength (Table 1*b*) at 1000 F of 9400 psi for 0.01 per cent per 1000 hr creep rate. The point plotted in Fig. 1 at that load is marked Cr-Mo. If, as Table 1*a* indicates, this item has no Cr, then its high (1830 F) austenitizing temperature is probably responsible for its position high up between two Mo-V steels. This kind of strengthening is clearly indicated for 1000 F testing in Series 2.

In Series 2 rapid (air) cooling from the austenitizing tempera-

[6] "A Study of the Properties of 0.5 Per Cent Chromium 0.5 Per Cent Molybdenum Pipe Materials," by R. C. Fitzgerald, A. B. Wilder, G. V. Smith, and A. E. White. See this issue of Trans. ASME, pp. 867–878.

[7] "The Properties and Mode of Rupture of a Molybdenum and a Molybdenum-Vanadium Steel, Judged from Prolonged Creep Tests to Fracture," by H. J. Tapsell, C. Bristow, and C. H. M. Jenkins, The Institution of Mechanical Engineers—Journal and Proceedings, vol. 164, 1942, pp. 208–222.

[8] Chief Research Engineer, The Midvale Company, Philadelphia, Pa.

ture produces greater resistance to creep at 900 F than does slow (furnace) cooling. Shall we say this means that coarse ferrite and coarse carbide particles, the products of slow cooling, are contra-indicated for 900-F service? But the state of the ferrite and carbide particles have no bearing on creep resistance at 1000 F. It is the temperature of austenitizing which determines resistance to creep at 1000 F, and the higher the temperature, and therefore the coarser the austenite, the greater the resistance. Series 4 confirms these conclusions.

In Series 4, Item 2259 aluminum-killed and Item 2260 silicon-killed are both austenitized at 1700 F. Presumably the silicon-killed 2260 coarsened more than the aluminum-killed 2259 and, from what Series 2 has taught, it should have the greater resistance to creep at 1000 F, and so it has. The same should be and is true of 2264 and 2265, the former, presumably finer grained than the latter, has the lower resistance to creep. Again, the resistance to creep at 900 F is not so much a matter of austenitic grain size as it is one of ferritic and carbide crystal sizes, the air-cooled specimens being more resistant to creep, as in Series 2, than the furnace-cooled ones. It is fair to assume that the "as received" material Items 2257 and 2258 were finish-rolled at a temperature high enough to coarsen both steels and thus to produce the similar results obtained in creep testing at both 900 and 1000 F.

Confirmation of the trends noted in Series 2 and 4 can be found in Series 5. Item 2160, austenitized at only 1580 F, should give a low resistance to creep at 1000 F and does. Item 2322, austenitized at 1900 F, should have a high resistance and it has. Item 2324, austenitized at 1700 F, should be intermediate between 2160 and 2322 and it is. Item 2272, as received, was again probably finished at a high temperature, and had a coarse austenitic grain size and develops the highest resistance at 1000 F.

Series 6 has to do with castings versus wrought material and develops the anomolous result that the wrought material is the more resistant to creep. Would the values have been reversed had the castings not been grain refined but had been merely tempered? Then the "as cast" grain size might have shown to better advantage. The basis for the statement that "the Mo-V pipe material is 50 to 100 per cent stronger than the plain Mo or low Cr-Mo compositions" is not clear. The higher C, higher Mo, and higher V compositions of Series 6 are also stronger than the lower C, lower Mo, lower V steels of Series 1. The greatest gain in strength follows the pattern set by Series 1, 2, 4, and 5. Items 2370 and 2375 coarsened at 1920 F are much stronger, nearly 70 per cent, than the same composition austenitized at 1740 F as represented by Item 2376. This is not to say that the conclusion regarding the higher strength of the Mo-V steel is not correct.

The strengthening effect of a high-temperature austenite coarsening treatment against flow at 1000 F is well brought out by the data in this paper. It is also clear that the great strengthening of this type of treatment is not so important at 900 F as is the rate of cooling from the austenitizing temperature.

A. B. Wilder.[9] The creep results reported by the author for 1/2 per cent Cr 1/2 per cent Mo steel pipe, particularly in the as-rolled stress-relieved condition, indicate this type of material may be expected to have very satisfactory creep strength compared to C-1/2 per cent Mo steel. The creep results for 1 per cent Mo 1/4 V per cent pipe, however, indicate much higher creep properties compared to the 1/2 per cent Cr–1/2 per cent Mo steel. These results are particularly significant in that a steel developed for castings has been applied to seamless pipe.

The use of vanadium for seamless pipe should be explored and a considerable amount of work is being done in this field. The influence of chromium on Mo-V steels is being studied and the stability of steels of this type is being evaluated in a 10-year exposure program at elevated temperatures.

Another interesting aspect of the work which has been reported is the successful fabrication of the 1 per cent Mo 1/4 per cent V steel. This clearly demonstrates that high-strength properties at ordinary temperature or the use of special heat-treatments not involving liquid quenching may, within reasonable limits, be successfully adapted to commercial fabrication practices. In addition to evaluating the high-temperature mechanical properties of new low-alloy steels for power-plant-piping service, it is necessary to determine if a new steel has properties at high temperature which will permit the piercing of solid rounds to produce seamless pipe. Also, weldability of the material should be evaluated. No difficulty was experienced in piercing the 1 per cent Mo 1/4 per cent V steel studied in this investigation. One-half pound of aluminum per net ton of steel was used in the deoxidation practice. Physical properties of the as-rolled seamless pipe were as follows:

Yield, psi	Ultimate, psi	% Elongation in 2 in.	Brinell hardness
119,000	122,900	23	229

The high-temperature treatment applied to the 1 per cent Mo 1/4 per cent V steel should result in grain coarsening and solution of vanadium carbide. In order to compare this type of steel with 1/4 per cent Cr 1/2 per cent Mo and 1 per cent Cr 1/2 per cent Mo steels, creep properties of the latter steels should also be determined after grain coarsening. The transition temperature and impact properties of the 1 per cent Mo 1/4 per cent V steel would be of interest.

Author's Closure

Mr. Kanter recognizes the virtues of vanadium but, on the assumption that aluminum has to be present, he makes a case for adding chromium. The author's company buys pipe to a specification which limits the use of aluminum in the manufacture of moly-vanadium pipe to an addition of no more than 0.5 lb per ton and therefore finds it difficult to conclude that chromium must be used. While admitting that some evidence of small graphite nodules has been found in small induction-furnace heats of moly-vanadium, the author believes Mr. Kanter has exaggerated the possible instability of this material because no such evidence has ever been found in any of the large heats so far placed in service, either castings or piping, or in the rupture-test specimens examined after as long as 14,780 hr at 1100 F.

Dr. Clark's discussion brings out a fundamental difference in point of view about the matter of hardness which is very important. Twenty-five years ago Prof. H. F. Moore's tests showed that to improve resistance to repeated stress the most effective procedure was to increase tensile strength and hardness. There was a good correlation between fatigue strength and Brinell number. While there does not seem to be any such reliable connection between long-time high-temperature strength and room-temperature hardness, the author has always felt that the treatments that improve high-temperature creep and rupture strength were very likely to be accomplished by increased room-temperature hardness.

As Dr. Clark points out, most certainly the author is making comparisons between different compositions in different conditions. To his point of view it would be quite unfair to make any final comparison on the basis of the same condition or the same treatment. Each material should be given the advantage of the treatment from which it benefits most.

As regards the comparison between the 3 Cr 1 Mo and 2 1/4 Cr 1 Mo composition, the author expressed regret in his manuscript that he did not have a complete spread of treatments of each.

[9] Chief Metallurgist, National Tube Company, U. S. Steel Corporation Subsidiary, Pittsburgh, Pa.

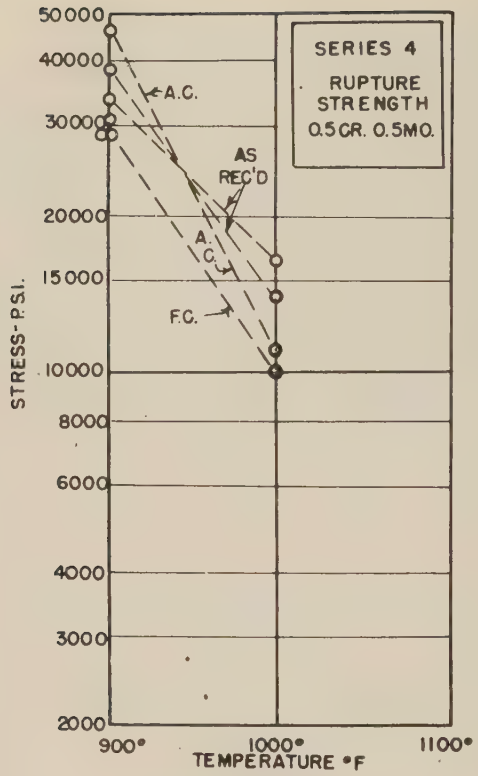

FIG. 7 100,000-HR RUPTURE STRENGTHS FOR 0.5 PER CENT CR—0.5 PER CENT MO STEEL

(This diagram plotted from Table 7 gives, as of September, 1948, the results of the tests reported 10,000 hours earlier in Table 4*b* and Fig. 4. Some are still running.)

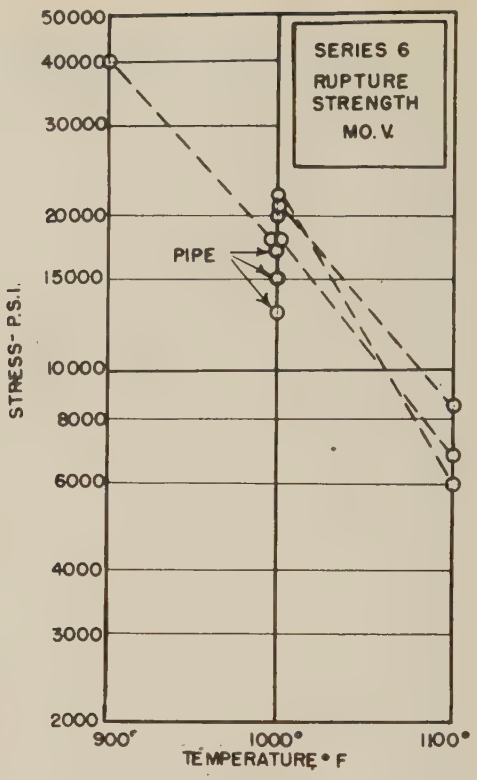

FIG. 8 100,000-HR RUPTURE STRENGTHS FOR MOLYBDENUM-VANADIUM STEEL

(This diagram plotted from Table 8 gives as of September, 1948, results of the tests reported 10000 hours earlier in Table 6*b* and Fig. 6. Some are still running.)

Mr. Foley explained the reasons for the low value on the 3 Cr 1 Mo.

It is indeed too bad if money has been wasted on the softening of power piping but the author does not believe this has always been the case. The best high-temperature strength on piping is got as it comes air-cooled from the rolls, and the author has always felt this was because it was quick-cooled from a hotter temperature than fabricators were willing to go to after bending and welding. Otherwise we would try to get the same qualities.

Ordinary stress relief of welds is not supposed to change the high-temperature properties. The relief of the localized strains about the weld ought not to soften the base material. There may be merit in the Detroit Edison proposal to normalize welds rather than just to strain-relieve them.

Mr. Eberle attributes the development of the low-chromium-molybdenum steels as suited to the corrosive conditions of high-temperature oil-refining operations, a service somewhat different from 1000 F steam lines. The author believes that steam pipes merit their own specification. Mr. Eberle cites good comparisons from the author's own figures in favor of a 20 to 30 per cent advantage for moly-vanadium steel instead of 50 to 100 per cent.

TABLE 7 SERIES 4

(Results compiled 10000 hours later than Table 4*b*)

Item no.	Rupture strength, psi 10000 Hr 900 F	10000 Hr 1000 F	100000 Hr 900 F	100000 Hr 1000 F
2257	42000	23000	34000	16500
2258	45000	23000	39000	14000
2259	38000	21000[a]	29000	
2260	52000	22000	46000	11000
2273				
2264	38000	21000[a]	31000	
2265	39000	19000	29000	10000

[a] Test still running.

In arriving at his rough estimate of this range, the author could not escape looking at the low figures sometimes obtained for the low-chromium-molybdenum steels reputed to be in proper condition. He has not found any such low values as Dr. Clark mentions in moly-vanadium samples intended for piping.

Mr. Foley's first remark calls attention to an erroneous omission of the chromium content from the composition of Item 1125 as given in the preprint of this article. The error has been corrected in this printing. The success with which Mr. Foley analyzes the relationships between treatment and creep strength is gratifying.

The eventual outcome of the investigations described by Mr. Wilder will be awaited with interest.

The author cannot help noting that every one of the discussers has commented on the creep strength while not one has mentioned the long-time rupture strength. It is the author's feeling that the long-time rupture strength is considerably more important for piping in particular and that lower rather than higher creep strength would be welcome provided it could be obtained without impairment of the long-time rupture strength.

When the manuscript for this paper was prepared in July, 1947,

TABLE 8 SERIES 6

(Results compiled 10000 hours later than Table 6*b*)

Item no.	Rupture strength, psi 10000 Hr 900 F	10000 Hr 1000 F	10000 Hr 1100 F	100000 Hr 900 F	100000 Hr 1000 F	100000 Hr 1100 F
2250	47000	25000	10800	40000	18000	6800
2251		30000	12000		22000	6000
2282		29000			20000	
2283		28500			18000	
2284		30000[a]	14000[a]		21000[a]	8500[a]
2370		24000[a]			13000[a]	
2375		31000[a]			15000[a]	
2376	58000[a]	29000[a]			17000[a]	

[a] Test still running.

a number of the long-time rupture tests in Series 4 (0.5 per cent Cr, 0.5 per cent Mo) and in Series 6 (1 per cent Mo, 0.25 per cent V) were still running and the results were marked as tentative. Now in September, 1948, 10,000 hours later, some of these tests have been completed but not all. In Table 7 and Table 8 are given the latest available figures for the tests originally reported on the right-hand side of Table 4*b* and Table 6*b* while the correspondingly revised diagrams appear in Fig. 7 and Fig. 8.

It is still necessary to mark some of these tests as "still running." The author invites study of these longer and therefore more valid results. In both Series 4 and Series 6, there was a tendency for the 100,000-hr rupture strength to drop somewhat as the longer-time test points came in. However, that tendency appears to have stopped in the case of the moly-vanadium tests for which the existing predictions are now based on unbroken bars still running. Thus any further revision of these results should be upward.

In conclusion the author notes that all discussers with the exception of Dr. Clark find the moly-vanadium composition advantageous, the principal argument having to do with the percentage amount. From an over-all viewpoint, it appears to the author that Dr. Clark's reservations are predicated on code rules which the author believes should be changed. New conditions of service ought to be recognized by new rules. The author does not advocate greater hardness for its own sake but is willing to tolerate it because it seems to accompany both long-time high-temperature strength and low-temperature cyclic strength.

It so happens that all the moot points of discussion relate to the creep-strength figures which were final when the manuscript was first prepared and are unchanged now. However, the author feels he cannot conscientiously close this discussion without including the later figures for long-time rupture strength which have had to be definitely revised downward. On the other hand any further breaks in the still unbroken bars can only improve these results which still show a marked superiority of moly-vanadium over the low-chromium-molybdenum compositions.

A Study of the Properties of 0.5 Per Cent Chromium—0.5 Per Cent Molybdenum Pipe Steel

By R. C. FITZGERALD,[1] A. B. WILDER,[2] G. V. SMITH,[3] AND A. E. WHITE[4]

Study of the mechanical properties, including creep, and of the welding and fabrication characteristics of steel containing 0.5 per cent chromium and 0.5 per cent molybdenum, designed for elevated-temperature service, has shown this grade to be essentially similar to 0.5 per cent molybdenum steel without chromium. However, elevated-temperature exposure tests have shown the steel whether deoxidized with aluminum or not, to be resistant to graphitization in butt-welded pipe as well as bead-weld tests lasting up to 15,000 hr at 1025 F and 12,000 hr at 1100 F. Scaling tests and hardness and notch-impact tests before and after air exposure at elevated temperature have indicated that only slight oxidation and little or no embrittlement may be anticipated during service of this grade of steel.

Introduction and Summary

Since the occurrence, early in 1943, of severe local graphitization and failure of a welded joint of molybdenum steel in a high-pressure steam line at the Springdale Station of the West Penn Power Company, considerable effort has been expended by metallurgists and engineers in attempting, on one hand, to gain an insight into the fundamental factors involved in the reversion of carbide to graphite, and on the other, to develop alloys and manufacturing practices which will inhibit the formation of graphite during commercial usage.

Of the several changes proposed to minimize or prevent graphitization, that involving the alloying addition of chromium has generally been considered to be the most efficacious means of accomplishing this end. The co-operative study reported here was undertaken to test this possibility. An arbitrary chromium addition of 0.5 per cent to the 0.5 per cent molybdenum level commonly used for steam pipe, was selected. Since this investigation was started in July, 1944, ASTM Specification A280-46aT relating to Seamless Chromium-Molybdenum Alloy Steel Pipe for Service at High Temperatures has been introduced. The chemical analysis of the steels studied lies within the scope of this specification.

Two heats of commercial size, which cannot always be approximated by small experimental or laboratory heats, were employed for the tests. These were rolled into $10^3/_4$-in-OD × 1.125-in-wall seamless pipe. The two heats were nominally identical except for the deoxidation practice employed, one being made to coarse-grained, the other to fine-grained practice. The coarse-grained heat was deoxidized with silicon only, i.e., no aluminum, while the fine-grained heat was deoxidized with $1^1/_4$ lb of aluminum per ton of steel in addition to a prior silicon addition. Study of the influence of deoxidation practice was dictated by the important roles which aluminum plays in the service of steel at elevated temperature. A large aluminum addition results in fine grain size which, though beneficial to toughness and freedom from embrittlement, is generally considered detrimental to creep strength. In recent years a large aluminum addition has been clearly proved to contribute to susceptibility to graphitization. Yet the use of at least some aluminum is quite desirable from the purely mechanical aspects of steel processing to obtain desirable surface quality and thus economy of manufacture. Thus a compromise must be made in the aluminum addition to properly balance its good and bad effects.

The two steels have been extensively studied in most all respects that are of interest in the contemplated use of the material, and the results are described in detail in the following sections prepared by the different co-operators. The statements in the individual sections do not necessarily represent the opinions of the remaining authors. The results may be summarized briefly as follows:

1 The mechanical properties of this material at ordinary temperature, Table 1, are at a slightly higher level than in the plain molybdenum steel.

2 Satisfactory flattening and etch tests of the pipe may be expected.

3 Welding electrodes have been developed which will satisfactorily deposit 0.5 per cent Mo weld metal containing either of two levels of chromium content, 0.35 and 0.5 per cent, with properties similar to the base metal.

4 Satisfactory procedures are available for welding this material under commercial conditions. These involve preheating at 500 F as well as postheating at 1300 F.

5 Bending and upsetting tests indicate that this material may be fabricated as readily as other pipe material.

6 The results of residual-stress measurement are presented.

7 The material possesses adequate scaling resistance for the contemplated service range of temperature, Table 3.

8 Hardness and notch-impact tests before and after exposure at elevated temperature indicate that no deleterious embrittlement may be expected during the use of this material, Table 3.

9 Extensive studies have failed to show graphitization in this material, however deoxidized or initially or posttreated, when exposed up to 15,000 hr at 1025 F or 12,000 hr at 1100 F.

10 The creep strength of this grade of steel is comparable to some of the low-chromium low-molybdenum types of steel.

11 In the as-rolled and stress-relieved condition, heat X11647, to which was added 1.25 lb of aluminum per ton of

[1] Senior Engineer, Consolidated Gas Electric Light and Power Company of Baltimore, Baltimore, Md.

[2] Chief Metallurgist, National Tube Company, Pittsburgh, Pa.

[3] Research Metallurgist, U. S. Steel Corporation, Research Laboratory, Kearny, N. J.

[4] Director, Engineering Research Institute and Professor of Metallurgical Engineering, University of Michigan, Ann Arbor, Mich. Fellow ASME.

Contributed by the Joint ASTM-ASME Research Committee on Effect of Temperature on Properties of Metals and presented at the Annual Meeting, Atlantic City, N. J., December 1–5, 1947, of The American Society of Mechanical Engineers.

Note: Statements and opinions advanced in papers are to be understood as individual expressions of their authors and not those of the Society. Paper No. 47—A-173.

steel, had the higher creep strength, while in the normalized and stress-relieved condition, heat X11648, to which no aluminum was added, had the higher creep strength.

MATERIALS

Prepared by A. B. Wilder[2]

The $10^3/_4$-in-OD × 1.125-in-wall seamless pipe used in this investigation was made from electric-furnace steel to applicable parts of ASTM Specification A206-44T for plain 0.5 per cent molybdenum steel pipe. All of the requirements in ASTM Specification A280-46aT, which had not been issued at the time the pipe was manufactured, were also met with the exception of the carburized austenitic grain size in the heat made to fine-grain deoxidation practice. Recently, Specification A280 has been changed from 0.40/0.60 per cent chromium to 0.50/0.70 per cent chromium. The chromium content of the steels investigated was 0.45/0.48 per cent chromium.

The 0.5 per cent chromium—0.5 per cent molybdenum steel used in this investigation is essentially similar to the plain 0.5 per cent molybdenum steel from a specification point of view. The strength requirements of the chromium bearing steel are identical with those of the plain 0.5 per cent molybdenum steel, and in Specification A280, a carburized austenitic grain size of 1 to 5 is specified while in A206 a structural grain size of 3 to 6 may be and generally has been specified.

Chemical Analysis and Mechanical Properties. The chemical and mechanical properties of the 0.5 per cent chromium—0.5 per cent molybdenum steels tested are shown in Table 1. Tests were conducted on as-rolled and heat-treated material removed from pipe wall. Heat-treatments were made of full pipe sections; the specification procedures employed are included in Table 1. Standard 0.505-in-round tensile test specimens were used. Photomicrographs corresponding to the five conditions of heat-treatment studied in graphitization tests are presented in Figs. 2 and 3 for the two heats, and discussed in the corresponding section.

Although no aluminum was added to the coarse-grain heat, steel of this type is frequently made with aluminum additions in the ladle not exceeding 0.5 lb per net ton of steel. The use of aluminum in addition to silicon helps to insure a satisfactory etch test in the finished pipe. Although no aluminum was added to the coarse-grain heat studied, it contained a very slight amount of aluminum, most probably being introduced in the ferroalloy additions. The carbon and chromium contents of both heats were on the low side of the range. The silicon-aluminum-killed heat contained sufficient aluminum to insure a fine austenitic grain size after carburizing and a high coarsening temperature.

Stress relieving at 1200 F increased the longitudinal and decreased the transverse yield strength of both types of steel compared with the as-rolled condition. The transverse yield strength of all the steels tested in different heat-treated conditions exceeded the longitudinal yield strength, particularly in the coarse-grain material. This condition may be associated with residual stresses in the pipe material.

The 1950 F air-cool treatment increased the yield and tensile strength of the coarse-grain steel, but did not appreciably affect the fine-grain steel. The 1950 F furnace-cool treatment had, in general, the lowest mechanical properties of the material tested. The properties of 1650 F and 1450 F air-cooled materials were, in general, similar. Material annealed at 1350 F had lower mechanical properties compared to similar material stress-relieved at 1200 F.

The tensile requirements of specification A280 (for as-rolled stress-relieved material) are met by either of the two heats examined. The strength characteristics are on a slightly higher level than for the plain 0.5 per cent molybdenum steel.

In addition to the chemical and mechanical properties shown in Table 1, satisfactory flattening and etch tests were obtained.

Grain Size and Normality. Austenitic-grain-size determinations in the carburized region shown in Fig. 1 were made after carburizing samples of the stress-relieved pipe material for 8 hr at 1700 F and slow cooling in the furnace. The steel with no aluminum addition was coarse-grained, ASTM 1 to 3, and the hypereutectoid case was normal, i.e., contained no free ferrite. The aluminum-killed steel was fine-grained, ASTM 6 to 8, and the metallographic structure was slightly abnormal. The grain size

TABLE 1 CHEMICAL ANALYSIS AND MECHANICAL PROPERTIES OF 0.5 PER CENT Cr—0.5 PER CENT Mo STEELS

Heat no.	Al added lb/net ton	C	Mn	P	S	Si	Cr	Mo	Al	Al_2O_3
X11648	None	0.13	0.50	0.009	0.019	0.22	0.48	0.56	0.003	0.002
X11647	1¼	0.12	0.45	0.012	0.019	0.14	0.45	0.54	0.027	0.008

	As-rolled	1200 F Stress-relieved	1350 F Anneal	1950 F Air-cool	1950 F Furnace-cool	1650 F Air-cool	1450 F Air-cool
Heat no. X11648—No aluminum							
Longitudinal							
Yield strength (1000 psi)	40	47	41	51	30	35	36
Tensile strength (1000 psi)	71	68	63	79	61	69	69
Elongation % in 2 in.	32	33	37	27	35	35	36
Transverse							
Yield strength (1000 psi)	56	53	48	72	38	52	51
Tensile strength (1000 psi)	75	71	66	88	61	73	72
Elongation % in 2 in.	25	27	32	21	34	27	32
Brinell hardness	143	124	124	163	112	131	131
Heat no. X11647—1¼ lb aluminum/net ton							
Longitudinal							
Yield strength (1000 psi)	38	49	41	38	34	39	33
Tensile strength (1000 psi)	66	67	63	63	57	61	62
Elongation % in 2 in.	34	33	37	39	40	40	38
Transverse							
Yield strength (1000 psi)	53	50	45	42	38	43	44
Tensile strength (1000 psi)	70	67	62	65	58	63	64
Elongation % in 2 in.	28	29	34	30	37	36	35
Brinell hardness	143	131	118	131	116	126	126

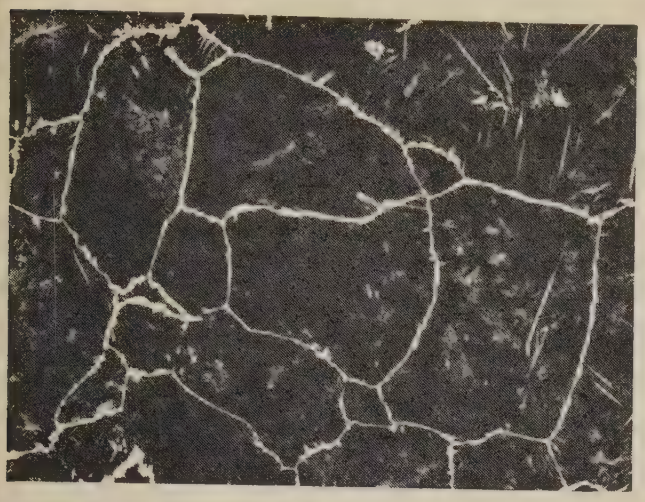

×100

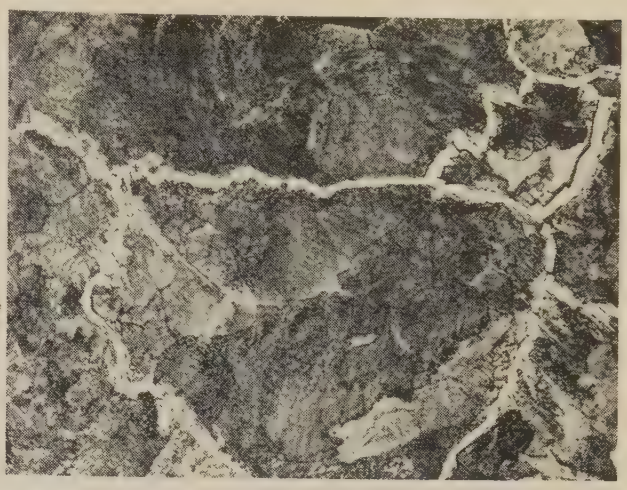

×500

HEAT X11648, NO ALUMINUM

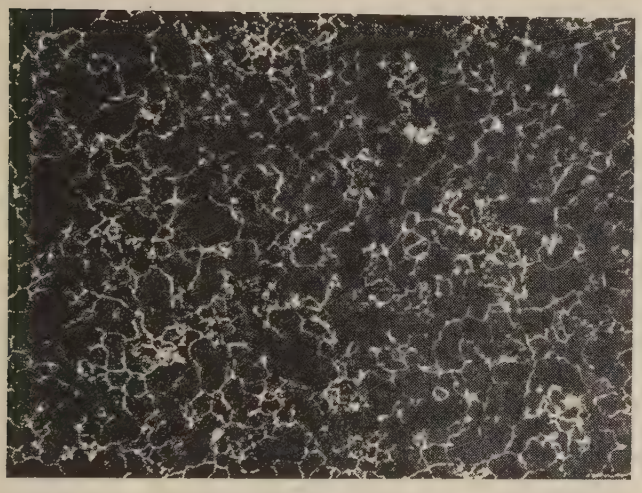

×100

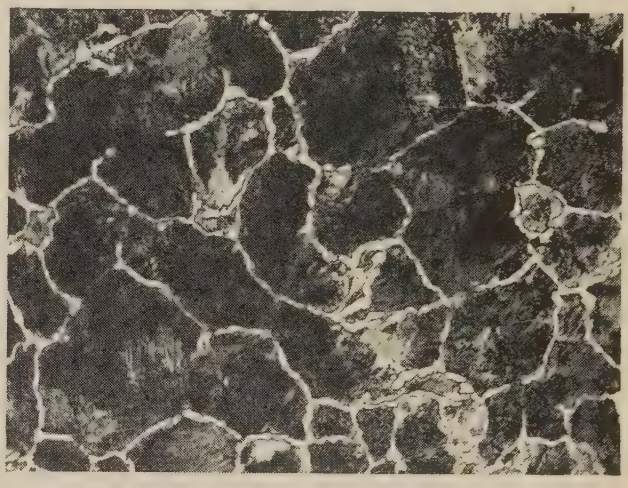

×500

HEAT X11647, 1¼ LB PER TON ALUMINUM

FIG. 1 AUSTENITIC GRAIN SIZE AND NORMALITY REVEALED IN CARBURIZED SPECIMENS; NITAL ETCH

characteristics of the pipe samples were similar to the results obtained on $10^1/_2$-in-diam rounds from which the pipe was made.

Plain 0.5 per cent molybdenum steel was originally made to fine-grain practice, but coarse-grain practice was later optionally specified. This change in steelmaking practice was based on creep-strength data, but the change in practice also resulted in greater resistance to graphitization although this latter was not recognized at the time. The coarse and fine-grain steels used in this investigation are therefore similar with reference to grain-size characteristics, to the plain 0.5 per cent molybdenum steel which is in power-plant service today.

FABRICATION TESTS

PREPARED BY R. C. FITZGERALD[1]

Electrode Acceptance Tests. Up to the time of this testing program no cases of graphitization have been reported in weld metal. However, because of the possibilities of graphitization appearing later, it was considered desirable to stabilize the weld metal as well as the pipe material by a suitable chromium addition. A number of electrode manufacturers were requested to develop electrodes which would deposit weld metal similar in analysis to the pipe materials. Such electrodes were submitted by three manufacturers.[5]

Electrodes submitted were of two types, E7010 and E7011, and were supplied in two chromium ranges. The electrodes were tested comparatively for ease of handling, soundness of deposited metal, and mechanical properties. Typical chemical analyses and mechanical properties of the weld metal deposited with 300 F preheat and a stress-relieving of 1150 F are shown in Table 2. Standard 0.505-in. tensile specimens were used.

In preliminary welding tests it was found that the type E7011 electrodes were superior from the standpoint of ease of handling. Tensile fractures of these electrode deposits also showed fewer "fisheyes" compared to type E7010 electrodes, although there was little difference in mechanical properties. The type E7011 electrodes were selected for all subsequent testing. For purposes

[5] Arcos Corporation, Philadelphia, Pa., Arcrods Corporation, Sparrows Point, Md., and Metal and Thermit Corporation, New York, N. Y.

TABLE 2 TYPICAL CHEMICAL ANALYSIS AND MECHANICAL PROPERTIES OF WELD METAL

A.W.S. type	C	Mn	P	Si	Mo	Cr	Yield strength 1000 psi	Tensile strength 1000 psi	% Elong. 2 in.	% Red. area
E 7010	0.08	0.39	0.017	0.21	0.67	0.27	66	80	27	60
E 7010	0.08	0.44	0.018	0.26	0.66	0.55	73	87	25	61
E 7011	0.10	0.43	0.017	0.19	0.59	0.35	70	83	25	63
E 7011	0.12	0.43	0.017	0.16	0.56	0.50	72	84	24	65

of this testing program it was necessary to select a single analysis for the deposited metal. All electrode tests had shown that the 0.35 per cent chromium and the 0.5 per cent chromium electrodes of the type E7011 were equally good. The 0.35 per cent chromium electrode was arbitrarily chosen for the procedure-qualification test, and all other tests involving welding.

Welding Procedure. The development of a procedure for welding the chromium-molybdenum pipe materials involved an application of the practices developed for welding low-alloy steels. Preliminary work was conducted to determine a suitable preheat temperature and, subsequent to the development and qualification of the procedure, residual-stress measurements were made on full-sized butt welds to confirm stress-relieving practices.

Weld-bead hardness tests indicated a maximum hardness of 297 Brinell, with a base-metal temperature of 70 F, and 210 Brinell hardness with 500 F preheat. These values were determined by Rockwell A hardness traverse in the coarse-grained steel. The maximum hardness occurred in the pipe material close to the fusion line. In similar tests with the fine-grained steel, the values were 245 Brinell and 200 Brinell, respectively. On the basis of these tests, a minimum preheat temperature of 500 F was chosen.

The joint design and general welding procedure used in this investigation were similar to those used in the installation of approximately 250,000 kw of generating capacity with plain molybdenum steels. The minimum preheat and the stress-relieving temperatures were the principal points of difference. The welding groove is a modified U-type groove machined so that the butting edges may be readily joined by a small oxyacetylene root weld which takes the place of the customary backing ring. After the root bead weld is made, the remainder of the groove is filled by metallic-arc welding in the conventional manner. The procedure specification is as follows:

Base Metal. ASTM Specification A280-46 AT (with exception of carburized grain size in the fine-grained heat).

Filler Metal. (1) Oxyacetylene welding rod: ASTM Specification A251-46T, Class GA-60, 1/8 in. diam. (2) Welding electrodes: ASTM Specification A-233-45T, 1/8 in. and 5/32 in. diam. Type E7011.

Position. Welding shall be done in the horizontal and vertical fixed positions.

Welding Technique. Oxyacetylene weld: The first bead or oxyacetylene root bead shall be deposited in the backhand manner with a neutral flame. Metallic-arc weld: In horizontal joints, beads of welding shall be deposited by weaving across the width of the welding groove. Vertical joints shall be welded by means of fillet-type welds deposited in layers in the welding groove.

Preheating. The region of the joint shall be preheated to 500 F minimum. This temperature shall be maintained until the welding is completed and stress-relief treatment is applied.

Stress-Relieving. Stress-relieving shall consist of heating the welded joint by 60-cycle induction heating to the stress-relieving temperature of 1300 F at a rate not to exceed 500 F per hour. After the stress-relieving temperature is reached it shall be maintained without interruption for a period of time equivalent to two hours per inch of pipe wall.

A heated band at least four times the maximum width of the welding groove shall be maintained at stress-relieving temperature during the soaking period.

The cooling rate shall not exceed the heating rate.

Bending and Upsetting Tests. These tests were made on full-size pipe from both heats of steel.[6] The purpose of performing full-size fabrication operations of this kind was to determine if the addition of chromium to the molybdenum steel would in any way increase the difficulties of the pipe fabricators or necessitate any modification of common practices.

One hot bend in pipe in each heat of steel was fabricated by practices employed with plain molybdenum pipe. The pipe sections were filled with sand, heated to 1700 to 1800 F, and pulled on a bending table to a curve of radius of four pipe diameters or approximately 40 in. As each section was bent true with a template it was quenched with a stream of water to hold its shape while the hotter sections were being pulled to shape. The quenching action was mitigated by the heat in the filling sand which quickly reheated the pipe to 1200 to 1400 F. After bending, the pipe showed no cracks or other defects. Ring sections cut out of the bends at points of drastic quench were tested for hardness. The maximum hardness observed was 215 Brinell (by conversion from Rockwell B).

The coarse-grained pipe was heated to 1900 F for upsetting. A Van Stone machine was used to upset the heated end an amount equivalent to 50 per cent of the original wall thickness. The material showed no hot shortness, and the maximum hardness after this operation was 163 Brinell (by conversion from Rockwell B).

The bending and upsetting tests indicated that the 0.5 per cent chromium—0.5 per cent molybdenum materials may be fabricated as readily as other pipe materials.

Residual-Stress Measurements. Residual-stress measurements were made by the Welding Laboratory of the U. S. Naval Engineering Experiment Station on four welded joints in the fine-grained steel. Eighteen-inch lengths of pipe were joined with butt welds in accordance with the procedure already described, except that two joints were stress-relieved at 1275 F while the remaining two were stress-relieved at the specified temperature of 1300 F.

The residual-stress determinations were made by the method of direct relaxation. This method of residual-stress determination is based on the relaxation of elements of the pipe by machining. Stress is calculated from observation of strain produced by the relaxation operation. The results are as follows:

1 Average circumferential stress at the periphery of the pipe, 8700 psi (tension).

2 Average circumferential stress at the bore of the pipe (internal surface), 6050 psi (compression).

3 Distribution of this stress in the three-foot sections (weld at center) were as follows: (*a*) Weld zone, negligible (1000 to 2000 psi) (*b*) unheat-treated ends of three-foot sections—8150 psi to 10,500 psi.

To explain the high values of residual stress at the ends of the

[6] The Pittsburgh Pipe and Equipment Company, Pittsburgh, Pa., made the bending tests. W. K. Mitchell and Company, Philadelphia, Pa., made the upsetting tests.

locally stress-relieved joints one joint was re-stress-relieved at 1275 F and the residual stresses measured by the relaxation method. The stress values in the region of the weld and stress-relief band were negligible, while the stresses in the unheated pipe ends ranged up to 15,000 psi.

EXPOSURE TESTS

Prepared by G. V. Smith[3]

In the use of metals at elevated temperature, as in steam lines, several characteristics of the metal at the service temperature are of interest. The most important of these is of course the ability to support a stress which involves the measurement of creep strength; such determinations are reported in the next section. In addition to suitable creep strength, however, the metal must possess adequate resistance to scaling or other corrosive attack, as well as resistance to the deterioration in strength or toughness resulting from what is generally termed structural instability. Accordingly, this aspect of the suitability of 0.5 per cent chromium—0.5 per cent molybdenum steels has been examined by means of measurement of the loss in metal weight resulting from scaling, as well as of the change in hardness and notch-impact strength at atmospheric temperature, after exposure at elevated temperatures. In addition, quite extensive studies were made to determine the susceptibility of the steels to graphitization. These results were obtained by experiments conducted by the National Tube Company, the Consolidated Gas Electric Light and Power Company of Baltimore, and the Research Laboratory, United States Steel Corporation.

Hardness, Notch-Impact Strength, and Scaling. Brinell hardness determinations (by conversion from Rockwell B) are reported in Table 3 for the two heats of steel in the heat-treated condition. These measurements were made on one-inch-square bars before and after exposure at 900, 1050, and 1100 F. The aluminum-deoxidized steel was studied in the normalized, annealed, and quenched and tempered conditions to determine the effect of exposure on widely different microstructures. Exposure at 900 and 1050 F had little effect on the hardness, but exposure at 1200 F resulted in a marked decrease in this property.

The results of the standard Charpy keyhole notch-impact tests are also listed in Table 3. These tests were made on different portions of the same bars used for the hardness tests. A marked increase in notch-impact strength occurred on exposure for 10,000 hr at 1200 F, whereas the changes at the lower temperatures were of much less magnitude and in either direction depending upon the temperature, deoxidation practice, and initial heat-treatment. The notch-impact strength of the silicon-deoxidized steel was notably inferior to that deoxidized with both silicon and aluminum. These data indicate that no harmful embrittlement is to be expected during the service of these materials.

The metal loss from scaling in air was also determined on the 1-in-sq × 20-in-long bars after 10,000 hr exposure. The results are reported in Table 3 in terms of per cent loss in metal weight, determined after removal of the scale by the sodium-hydride technique. The numbers given apply only to the shape tested, but may be employed for other shapes by conversion to weight loss per unit surface area. Oxidation was slight at 900 and 1050 F, but considerable at 1200 F. The results were not influenced by differences in initial heat-treatment. In the range of temperature for which this steel has been recommended, 950 F maximum, entirely adequate scaling resistance is indicated by the results. Although no comparative data are at present available for other materials, it may be expected that these steels are slightly superior in this regard to plain molybdenum steel, but inferior to steels containing higher chromium (or/and silicon).

Graphitization Susceptibility. The microstructural stability at elevated temperature, with particular reference to the resistance to graphitization of the two heats of chromium-molybdenum steel, was studied quite extensively by metallographic techniques in several series of tests.

Sections From Full-Size Welded Joints. In the most extensive series of tests, lengths of $10^3/_4$-in-OD × 1.125-in-wall pipe were welded together and sections from these joints exposed for extended periods at 1025 F, then examined with the microscope. Five different initial conditions of the pipe of each heat were employed as follows:

Initial Conditions of Pipe Sections Prior to Welding

Heat X11647 $1^1/_4$ lb of Al designation	Heat X11648 no Al designation	Treatment
A	F	As-rolled, stress-relieved at 1200 F
B	H	1950 F, air-cooled
C	J	1950 F, furnace-cooled
D	K	1650 F, air-cooled
E	L	1450 F, air-cooled

Photomicrographs of each of these conditions are shown in Figs. 2 and 3 for the fine and coarse-grained steels, respectively. There is little or no difference between the two heats for the as-rolled and stress-relieved and the 1450 F air-cooled conditions. In the photomicrographs representing this latter treatment, the partial transformation of the as-rolled structure to austenite is apparent. Complete transformation to austenite occurred in the 1650 F and 1950 F treatments and the difference in deoxidation practice may be observed in the size of the ferrite-pearlite or ferrite-Widmanstätten regions resulting from subsequent re-transformation, particularly for the 1950 F treatments. The difference in rate of cooling from 1950 F has produced a striking difference in microstructure for the coarse-grained steel, the faster cooling rate resulting in Widmanstätten, the slower in pearlitic, carbide regions. In the fine-grained steel the two cooling rates from 1950 F resulted in similar microstructure except for banding in the furnace-cooled sample.

Five full-size joints were made, corresponding to the five initial conditions, in each case a 2-ft section of the fine-grained steel pipe being welded to a similar length of the coarse-grained steel pipe of the same initial heat-treatment. The welds were made by personnel experienced in welding steam pipe. The specific conditions of welding are described in an earlier section on welding procedure under the general section, "Fabrication Tests." Fig. 4*a* shows a polished and etched cross section of one of the welded joints.

Subsequent to welding, three sections approximately 3 × 3 ×

TABLE 3 EFFECT OF 10,000-HR EXPOSURE AT 900, 1050, AND 1200 F ON HARDNESS, NOTCH IMPACT STRENGTH, AND SCALING OF 1-IN-SQ BARS OF 0.5 Cr—0.5 Mo STEEL

Sample no.	Al added lb/net ton	Heat-treatment prior to exposure	Hardness-Brinell				Charpy impact ft-lb, keyhole notch				Metal loss—due to scaling of 1-in-sq bars; % loss in weight		
			As heat-treated	Exposed 10,000 hr 900 F	Exposed 10,000 hr 1050 F	Exposed 10,000 hr 1200 F	As heat-treated	Exposed 10,000 hr 900 F	Exposed 10,000 hr 1050 F	Exposed 10,000 hr 1200 F	Exposed 10,000 hr 900 F	Exposed 10,000 hr 1050 F	Exposed 10,000 hr 1200 F
12B	0	1650 F—Norm.	143	143	134	98	35.3	33.0	43.7	62.3	0.8	1.6	24.0
12DX	$1^1/_4$	1650 F—Norm.	126	126	121	..	68.9	73.9	54.4	..	0.7	1.8	..
12DY	$1^1/_4$	1650 F—Anneal	118	112	112	98	62.9	58.0	51.0	98.0	1.0	1.8	22.9
12DZ	$1^1/_4$	1650 F—Water quench, 1200 F—Draw	183	187	159	95	66.9	69.5	76.4	94.3	0.9	1.7	24.2

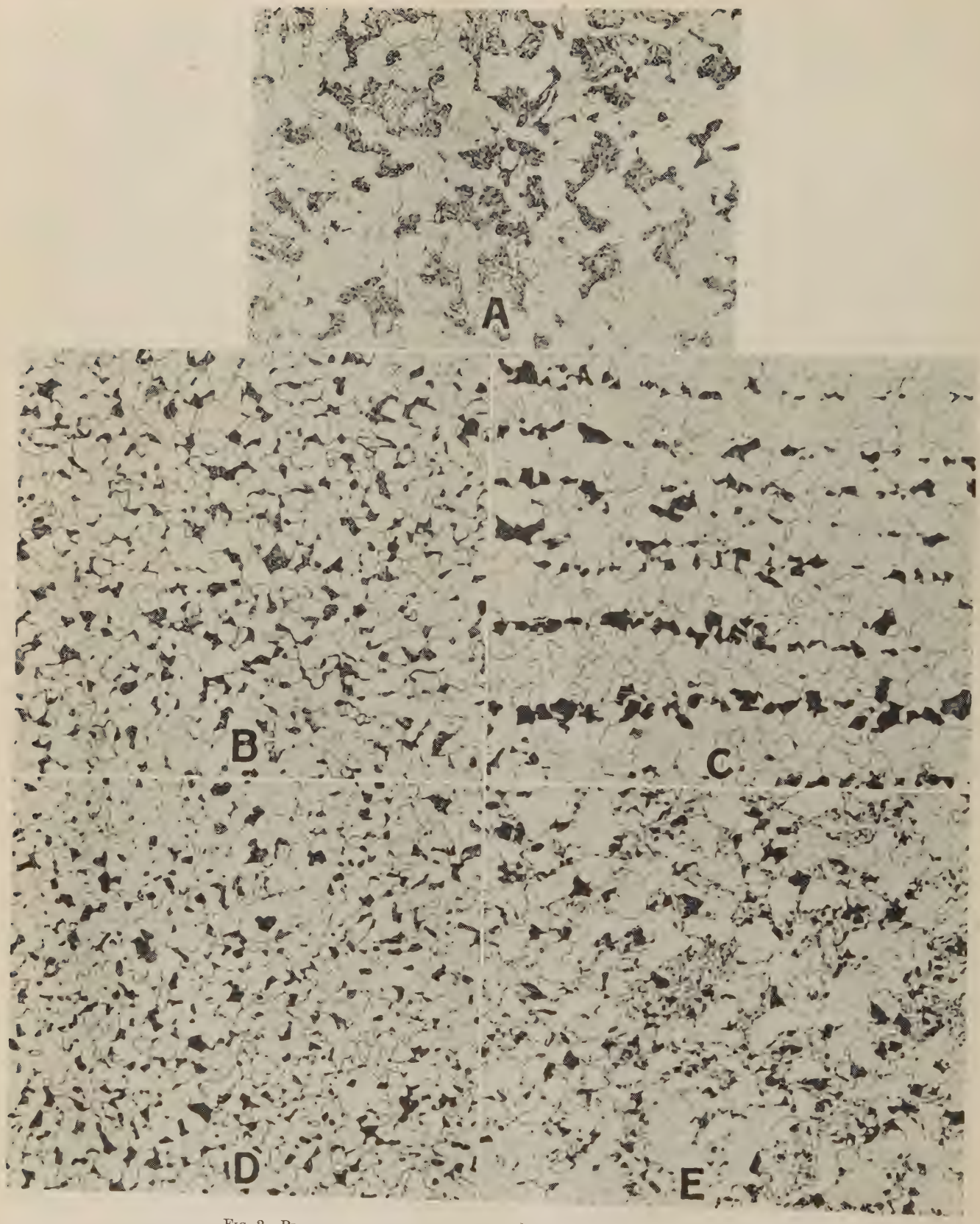

FIG. 2 PHOTOMICROGRAPHS OF FINE-GRAINED STEEL. NITAL ETCH, ×100
(A, as-rolled, stress-relieved 1200 F; B, 1950 F, air-cooled; C, 1950 F, furnace-cooled; D, 1650 F, air-cooled; E, 1450 F, air-cooled.)

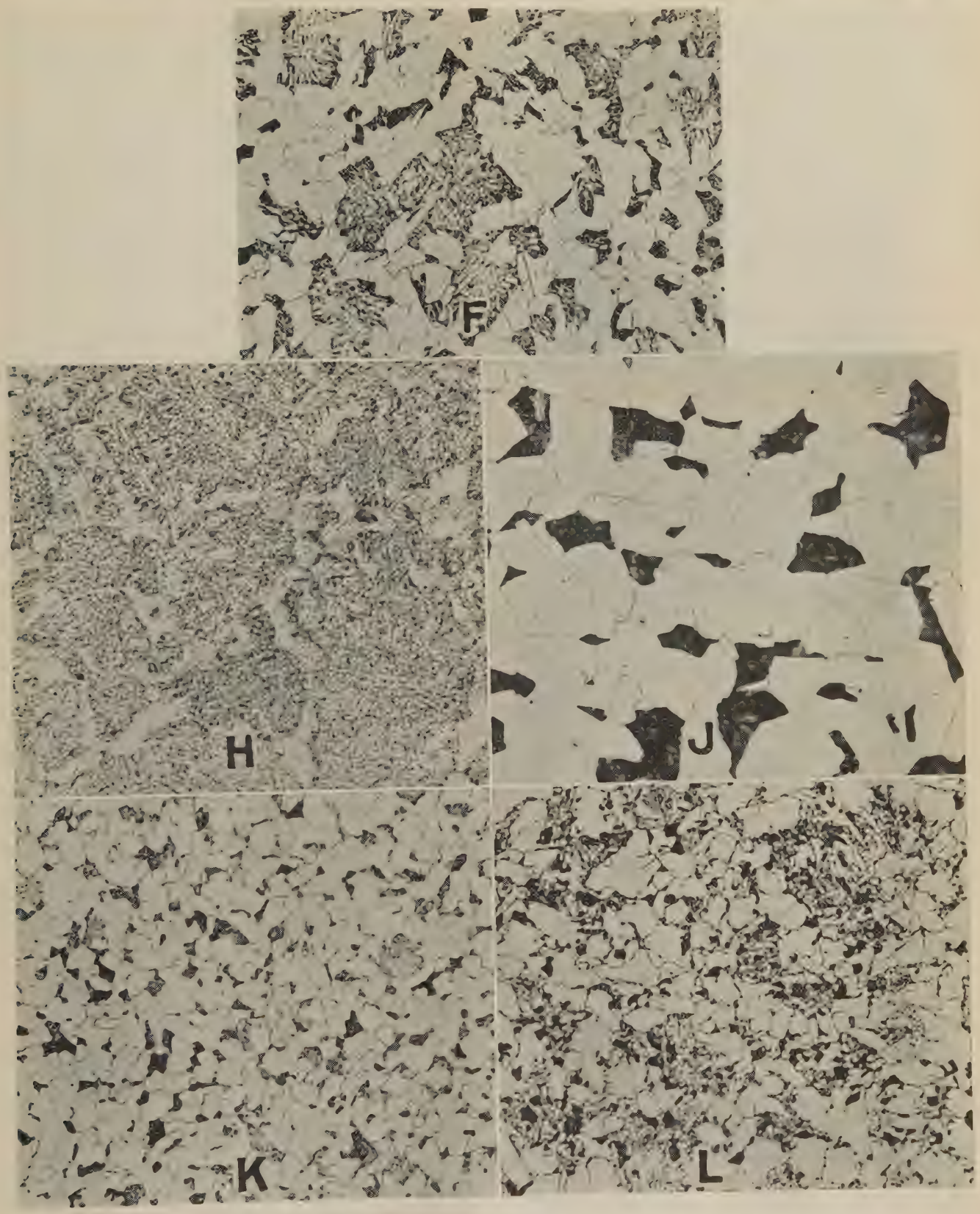

FIG. 3 PHOTOMICROGRAPHS OF COARSE-GRAINED STEEL. NITAL ETCH, ×100
(F, as-rolled, stress-relieved 1200 F; H, 1950 F, air-cooled; J, 1950 F, furnace-cooled; K, 1650 F, air-cooled; L, 1450 F, air-cooled.)

$1^1/_8$ in. were taken from each of the five joints to include the weld and a portion of the base metal on either side, as in Fig. 4*a*. One from each joint was stress-relieved at 1300 F for 4 hr, another was stress-relieved at 1200 F for $2^1/_4$ hr (this corresponds to commercial practice for plain molybdenum steel), and the third was not subjected to any postweld stress-relieving treatment.

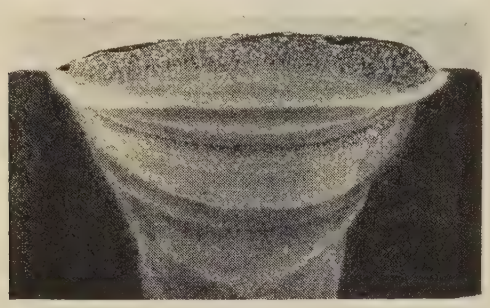

FIG. 4*a* CROSS SECTION THROUGH WELDED JOINT; PICRAL-NITAL ETCH, ×1

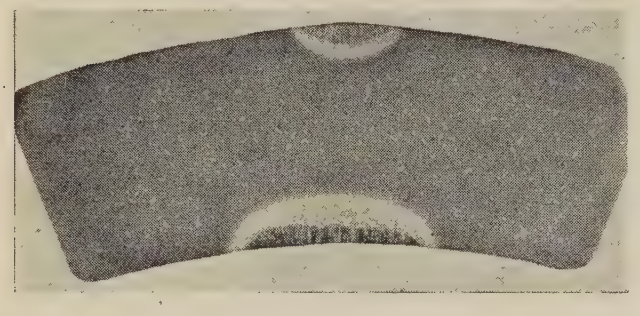

FIG. 4*b* CROSS SECTION THROUGH SINGLE-BEAD WELD TEST SPECIMEN; PICRAL-NITAL ETCH, ×1

All 15 samples were then introduced into muffle-type furnaces at 1025 F for extended exposure. At periodic intervals the samples were removed from the furnaces, a section removed for microscopic examination, and the remainder reheated to 1025 F for further exposure. Exposure was continued to a total of 12,000 hr (1.4 yr) for all the samples, while those initially air-cooled from 1650 or from 1450 F were exposed for 15,000 hr (1.7 yr).

In addition to the samples just described, another set of two sections were taken from each of the five joints for exposure at 1100 F. One of these was stress-relieved $2^1/_4$ hr at 1200 F, the other 4 hr at 1400 F, prior to exposure. The total exposure of these samples was 12,000 hr at 1100 F.

None of the samples whether of coarse- or fine-grained deoxidation practice and regardless of the preheat- or postheat-treatment or of the exposure temperature showed any graphite during the exposure, in any portion of the sample—weld metal, heat-affected region, or unaffected base metal. The photomicrographs of Fig. 5 illustrate, before-and-after exposure of 15,000 hr, the microstructure at low and high magnification in the region of the heat-affected zone in which localized (segregated) graphite is encountered when it occurs, and clearly show the absence of graphite. Some spheroidization may be detected as well as the occurrence of a fine precipitate characteristic of plain molybdenum and low-chromium-molybdenum steels. The photomicrographs of Fig. 5 are for the steel of fine-grained deoxidation practice, initially air-cooled from 1650 F, and not post-treated after welding, but except for differences attributable to initial or postheat-treatment (i.e. in size of ferrite-carbide patches, etc.), they are characteristic of all samples.

Control specimens of plain molybdenum steel of fine-grained deoxidation practice field-normalized after welding were included in one of the two 1025 F furnaces and in the 1100 F furnace. In both instances considerable random graphitization occurred on exposure for 12,000 hr.

Steam-Line Exposure. In addition to the sections from full-size welded joints described, a similar joint was made between a section of the fine-grained and one of the coarse-grained heat, each in the as-rolled and stress-relieved condition, and this joint welded into a regular steam line operating at 900 F and 1250 psi steam temperature and pressure. This joint has now been in service for 10,000 hr, but in view of the results of the longer time exposure at 1025 F, has not yet been examined. It is planned to continue this joint in service indefinitely and to make periodic examination for graphite.

Single-Bead Weld Tests. Since it has often been observed that the severity of localized or segregated graphite is inversely proportional to the width of the weld-heat-affected region and, in fact, that graphite may sometimes occur in a narrow heat-affected region and not at all in a wide heat-affected zone, single-bead welds with a rather narrow heat-affected region were made on sections of pipe approximately $4 \times 3 \times 1^1/_8$ in. of both the fine-grained and coarse-grained chromium-molybdenum steel in the same five initial conditions described earlier. On the opposite faces, of each section a weld bead with a somewhat wider heat-affected region was laid down. Fig. 4*b* shows the appearance of a transverse section through one of the specimens.

The specific weld conditions employed in this series of tests are summarized as follows:

Test Conditions for Single-Bead Weld Tests

Preheat, none
Postheat, none
Electrode, Type E7020
Weld type, bead weld deposited in flat position

	Narrow bead	Wide bead
Current, amp	200	285
Arc voltage	28	30
Speed, in./min	9	3
Heat input, Btu/in.	35	162

These specimens were exposed for a total of 10,000 hr, with microscopic examination at intervals of 2000, 5000, and 10,000 hr. In no case did graphite form. The microstructures observed before and after exposure are similar to those shown in Fig. 5.

Unwelded Bars. The bars of coarse and fine-grained steels exposed for 10,000 hr at 900, 1050, and 1200 F for the hardness, notch-impact, and scaling determinations summarized in Table 3 were also examined for graphite. None was observed.

CREEP STRENGTH OF 0.50 Cr—0.50 Mo STEEL

PREPARED BY A. E. WHITE[4]

Creep tests were made at 950 and 1000 F on samples cut from the as-rolled and stress-relieved pipe from both heats. Normalized and drawn samples were also tested at 950 F. The tests were of approximately 1000 hr duration and were selected to establish the stress for a creep rate of 0.01 per cent per 1000 hr or 1 per cent per 100,000 hr.

In view of the unexpected results from the tests on the as-rolled samples, verifying tests were conducted at two other laboratories. The major portion of the testing was concentrated on samples cut from as-rolled and stress-relieved pipe because that is the condition in which it is most widely used. Most of the tests were made at 950 F as that was, in general, the upper operating temperature for which this particular composition was intended.

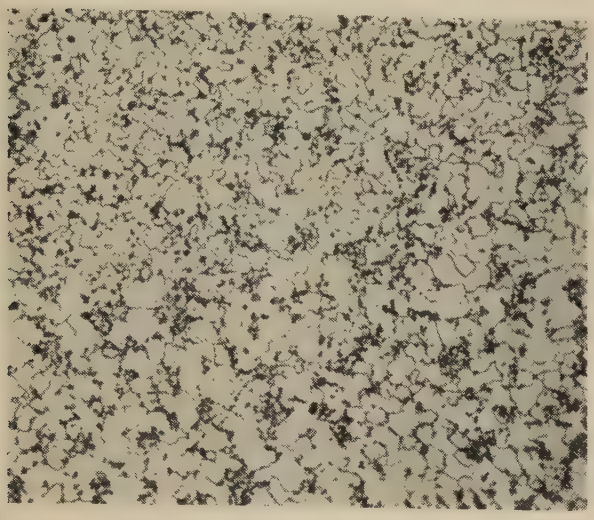

×100 Before Exposure

×100 After Exposure

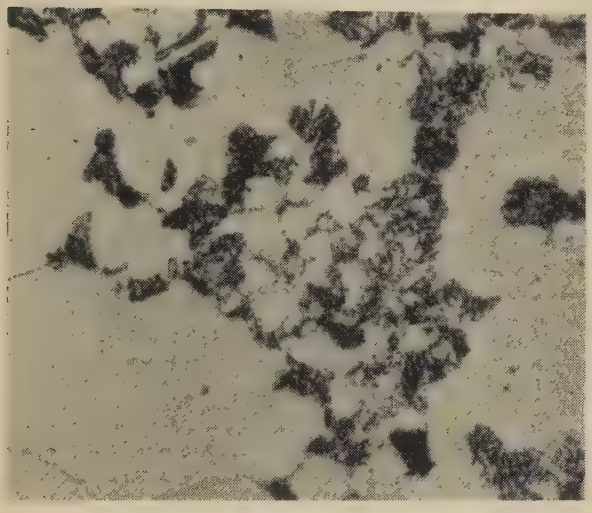

×1000 Before Exposure

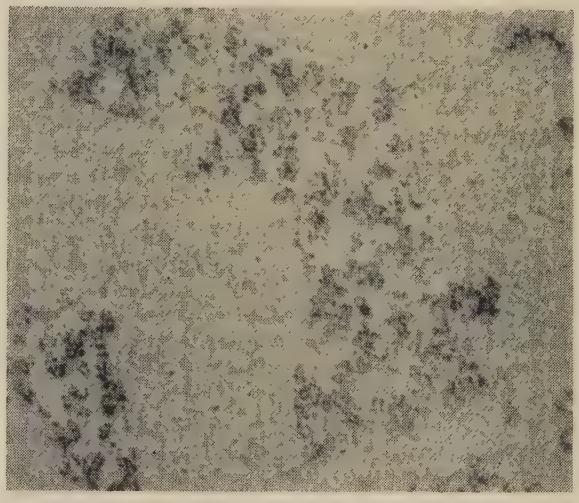

×1000 After Exposure

Fig. 5 Structure in Weld Heat-Affected Zone Before and After 15,000 Hr Exposure at 1025 F of Fine-Grained Steel Initially Air-Cooled From 1650 F and Not Posttreated After Welding; Nital-Picral Etch

Material Tested

The material tested was classified as first, second, and third samples, as follows:

1 Test bars cut from the as-rolled and stress-relieved pipes from heats X11647 and X11648 described by Mr. Wilder in the first section of the paper. (Designated as first samples.)

2 Similar test bars cut at random from another section of the as-rolled and stress-relieved pipe from heat X11648 and submitted at a later date. (Designated as second samples.)

3 Bars from the first samples normalized at 1650 F for one hour and air-cooled and then stress relieved at 1200 F for one hour. These heat-treatments were carried out in small laboratory furnaces.

The as-rolled and stress-relieved samples were tested at both 950 and 1000 F. The normalized and stress-relieved samples were tested only at 950 F. A duplicate test on an as-rolled and stress-relieved sample from heat X11647 was conducted at 1000 F by Crane Company. Duplicate tests on the second lot of samples from heat X11648 were made at 950 F at both the United States Steel Research Laboratory and the University of Michigan. An additional test was conducted on this material at 1000 F by the University. All creep tests were of approximately 1000 hr duration.

The effect of creep testing on the properties of the steel was checked by means of tensile, impact, and hardness tests, and by metallographic examination of the specimens after completion of the creep tests.

Results

The results from the creep tests are shown by logarithmic curves of stress versus creep rate in Figs. 6 and 7. The creep strengths shown by these curves are summarized in Table 4. The significant results from these tests were as follows:

1 Both heats of the 0.50 Cr—0.50 Mo steel had excellent creep strength. The stress for a rate of 0.01 per cent per 1000 hr (1 per cent per 100,000 hr) at 950 F ranged from 10,500 to 25,500 psi. The as-rolled and stress-relieved samples gave strengths of 15,000 and 20,000 psi at 1000 F.

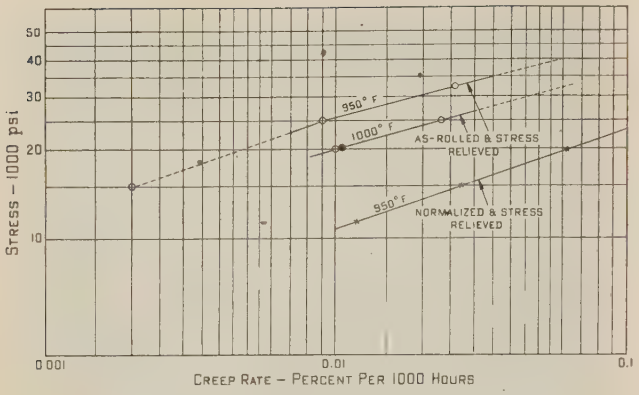

FIG. 6 CREEP-TEST RESULTS

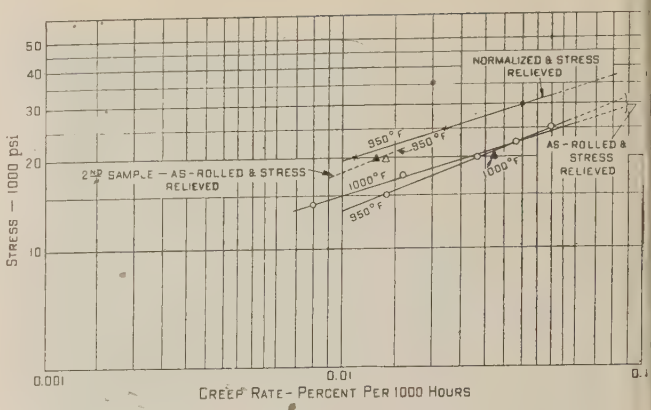

FIG. 7 CREEP-TEST RESULTS

TABLE 4 CREEP STRENGTHS AT 950 AND 1000 F FOR 0.50 Cr—0.50 Mo STEEL

Heat no.	Aluminum added (lb/ton)	Sample	Treatment	Brinell hardness	Test temp. (deg F)	Stress for a creep rate of 0.01%/1000 hr (psi)	Testing laboratory
X11647	1.25	1st	As-rolled pipe stress relieved at 1200 F	131	950	25,500	U of M
X11648	None	1st	As-rolled pipe stress relieved at 1200 F	124	950	13,500	U of M
X11648	None	2nd	As-rolled pipe stress relieved at 1200 F	..	950	18,000	U of M
X11648	None	2nd	As-rolled pipe stress relieved at 1200 F	..	950	18,000	U. S. Steel
X11647	1.25	1st	Bars cut from pipe, then normalized 1 hr at 1650 F and stress relieved 1 hr at 1200 F	121	950	10,500	U of M
X11648	None	1st	Bars cut from pipe, then normalized 1 hr at 1650 F and stress relieved 1 hr at 1200 F	156	950	20,000	U of M
X11647	1.25	1st	As-rolled pipe stress relieved at 1200 F	131	1000	20,000	U of M
X11647	1.25	1st	As-rolled pipe stress relieved at 1200 F	131	1000	20,000	Crane Co.
X11648	None	1st	As-rolled pipe stress relieved at 1200 F	124	1000	15,000	U of M
X11648	None	2nd	As-rolled pipe stress relieved at 1200 F	..	1000	15,000	U of M

2 In the as-rolled and stress-relieved condition, the heat to which aluminum was added (heat X11647) had the higher creep strength at both 950 and 1000 F.

3 In the normalized and drawn condition, the silicon-deoxidized heat (heat X11648) had the higher creep strength.

4 The agreement between duplicate tests at different laboratories leads one to believe that testing techniques were not responsible for the unusual creep characteristics observed.

5 Creep testing at 950 and 1000 F had no appreciable effect on the physical properties of 0.50 Cr—0.50 Mo steel at room temperature, as is shown by the data in Tables 5 and 6. Microscopic examination did not show any detectable structural alteration as a result of creep testing.

6 The tests show that these steels appear to have creep strengths comparable to some of the low-chromium, low-molybdenum types of steel.

Discussion of Creep Properties

The creep strengths observed for the 0.50 Cr-0.50 Mo steels in this investigation indicate that they have good high-temperature properties. Like all steels, however, they may have a wide range in creep strengths, depending on the steelmaking practice, the conditions of fabrication, heat-treatment, and other possible factors. The work reported by no means covers all of the possible variables.

The results of the tests on the normalized and drawn samples were in the usually accepted order. That is, the steel to which no aluminum was added had a higher creep strength than the steel with the aluminum addition.

In the tests at 950 F on the pipe steel in the as-rolled and stress-relieved condition, the steel with the aluminum addition had a higher creep strength than the steel to which no aluminum was added. The creep strength of the steel with no aluminum addition appeared to be lower than would normally be expected. However, since the three tests that were run to obtain the stress for a creep rate of 1 per cent per 100,000 hr all fell on the same straight line, the test procedure is therefore assumed to be accurate.

This feeling is confirmed by the close agreement resulting from check tests with the U. S. Steel Corporation, though in this case higher stress values resulted, and with Crane Company, though in this latter case the test was made at 1000 F.

Whether the value should be 13,500 or 18,000 psi, or some other value, is left to the reader's judgment.

Again, it is interesting to note that at 1000 F in the as-rolled and stress-relieved condition the steel with the aluminum addition had a higher creep strength than the steel to which no aluminum was added.

Attention is also called to the similarity in creep strength at 950 and 1000 F for the first lot of as-rolled and stress-relieved samples from heat X11648 (no aluminum added). What is surprising is that the test at 1000 F showed a higher creep strength than the test at 950 F. The check tests showed results which are believed to be in the normal order, i.e., the creep strength at 950 F is higher than the creep strength at 1000 F. Had the first set of tests at 950 F been run for a longer time period than 1000 hr, the results might have been different, though all of these tests were run for 1000 hr as that is the normally accepted time period to determine the creep rate for a given stress.

A further interesting matter is the widely differing creep strengths from the two heats, with apparently identical microstructures as shown in Figs. 2*a* and 3*f* when in the as-rolled and stress-relieved condition. The explanation must be that there are other factors than grain size and carbide structure contributing to creep strength.

It is important to note, however, that both heats had very good creep strengths, even though the results did not follow the expected trends when the tests were made on samples in the as-rolled and stress-relieved condition.

Conclusions

The 0.50 Cr-0.50 Mo steels were found to have excellent creep strengths at 950 and 1000 F. No evidence of detrimental

TABLE 5 COMPARATIVE TENSILE PROPERTIES AT ROOM TEMPERATURE FOR 0.50 Cr + 0.50 Mo STEELS BEFORE AND AFTER CREEP TESTING

Material	Treatment	Creep-testing conditions: Temp. (deg F)	Stress (psi)	Time of test (hr)	Tensile strength (psi)	Offset yield stress (psi): (0.1%)	(0.2%)	Proportional limit (psi)	Elongation in 2 in. (%)	Reduction of area (%)
Heat no. X11647 1.25 lb per ton of aluminum added	As-rolled pipe stress relieved at 1200 F		Original		66,200	43,500	45,500	25,000	32.0	63.0
		950	15,000	1025	68,000	43,500	46,800	27,500	30.0	68.3
			25,000	1025	67,500	45,800	47,300	30,000	32.5	68.5
		1000	20,000	1295	67,200	44,700	47,000	30,000	32.5	67.0
	Bars cut from pipe then normalized 1 hr at 1650 F and stress relieved 1 hr at 1200 F		Original		65,125	43,500	45,000	25,000	37	78.5
		950	11,500	1107	63,000	42,000	43,500	25,000	36.5	78.5
			15,000	1105	63,750	42,800	44,800	28,500	38	78.5
Heat no. X11648 No aluminum added	As-rolled pipe stress relieved at 1200 F		Original		66,800	43,000	43,800	27,500	33	66.5
		950	15,000	1025	67,750	40,000	43,000	27,500	35	69.7
			20,000	1005	67,700	44,500	46,500	27,500	34.5	68.5
		1000	14,000	1295	70,000	42,800	45,700	22,500	32.0	66.0
			17,500	1105	69,200	43,500	46,500	22,500	31.0	65.3
	Bars cut from pipe then normalized 1 hr at 1650 F and stress relieved 1 hr at 1200 F		Original		72,500	52,500	54,000	47,500	30.0	70.0
		950	20,000	1007	75,000	53,000	55,000	37,000	32.5	69.0

TABLE 6 COMPARATIVE IMPACT AND HARDNESS PROPERTIES AT ROOM TEMPERATURE FOR 0.50 Cr + 0.50 Mo STEELS BEFORE AND AFTER CREEP TESTING

Material	Treatment	Creep-test conditions: Temp. (deg F)	Stress (psi)	Time of test (hr)	Modified Izod impact strength (ft-lb)[a]	Vickers hardness number
Heat no. X11647	As-rolled pipe stress relieved at 1200 F		Original		86	156
		950	32,500	1005	86, 91	162
1.25 lb per ton of aluminum added	Bars cut from pipe then normalized 1 hour at 1650 F and stress relieved 1 hour at 1200 F	1000	25,000	1012	93, 92	159
			Original		82, 91	136
		950	20,000	1005	90, 95	136
Heat no. X11648	As-rolled pipe stress relieved at 1200 F		Original		20	147
		950	25,000	1005	13, 10	155
		1000	22,500	1205	14, 20	156
No aluminum added	Bars cut from pipe then normalized 1 hour at 1650 F and stress relieved 1 hour at 1200 F		Original		56, 61	162
		950	30,000	1105	60, 78	165

[a] 0.365-in-sq specimens with 0.050-in-deep V-notch.

changes in physical properties or structural alteration was observed during creep testing.

In the as-rolled and stress-relieved condition, heat X11647, to which 1.25 lb per ton of aluminum were added during deoxidization, had the higher creep strength.

When normalized and stress relieved, heat X11648, to which no aluminum was added, had the higher creep strength.

Acknowledgment

The author wishes to express his appreciation for the assistance of Dr. J. W. Freeman in preparing this section of the paper.

The Structural Stability of Several Cast Low-Alloy Steels at Elevated Temperatures

By V. T. MALCOLM[1] and S. LOW,[2] INDIAN ORCHARD, MASS.

The effect of temperature on several cast low-alloy steels has been investigated in the laboratories of The Chapman Valve Manufacturing Company. ASTM A217-46T Grade WC1, and modifications of this composition, were surveyed thoroughly. The following variables were investigated with respect to structural stability: (1) The effect of aluminum on a cast carbon-molybdenum steel; (2) the effect of furnace practice on a cast carbon-molybdenum vanadium steel; (3) the effect of chromium on a cast carbon-molybdenum steel; (4) the effect of vanadium on a cast carbon-molybdenum steel; (5) the effect of various combinations of chromium, vanadium, and titanium on a cast carbon-molybdenum steel; and (6) the effect of chromium, nickel, and high molybdenum on a cast carbon-molybdenum steel.

The physical properties of the alloys investigated are given in detail. Data are presented on the results of McQuaid-Ehn, tensile, Jominy hardenability, creep, and weldability tests. Photomicrographs are used to illustrate structural stability after various aging cycles. New work is presented to illustrate the effect of aging at elevated temperature on static bend bars and V-notch Charpy bars.

THE discovery of a most deleterious type of segregated graphite in the carbon-molybdenum steel steam lines in the Springdale Station of the West Penn Power Company early in 1943, instituted numerous investigations as to the cause, effect, and prevention of similar occurrences in steam lines in operation and others in the process of construction and design.

Since the company with which the authors are associated produces steel valves for high-temperature steam service, it became necessary to carry out extensive co-operative and independent research programs in its laboratory to investigate graphitization in alloy-steel castings. A careful study of the available literature, together with the results of our investigations, has led us to believe that graphitization of the segregated chain type, as observed in Springdale piping, does not occur in castings. Graphite in cast-alloy steels is generally found to be of the nodular type, rather randomly distributed, even in the low-temperature heat-affected zones of weldments.

At the time of the Springdale failure, manufacturers were furnishing valves to ASTM A217-46T Grade WC1 specifications for high-temperature steam service. As a general rule, most of these castings were poured in green-sand molds, and the steel "killed" with $1\frac{1}{2}$ to 3 lb of aluminum per ton. It has been our practice, since 1937, to furnish castings for this service to the chemical specifications of ASTM A217-46T Grade WC1 with the following additions: Cr, 0.25 to 0.30 per cent; V, 0.06 to 0.10 per cent; Ti, 0.02 to 0.04 per cent. This steel, known as CMCVT, meets the chemistry of A217-46T WC1, and possesses superior creep properties and greater stability at elevated temperatures.

In order to investigate the problem logically, with respect to castings, the following types of cast alloy steels were investigated:

1 ASTM A217-46T Grade WC1. (*a*) Killed with 0.35 to to 0.45 per cent Si, (*b*) killed with 2 lb Al per ton.

2 ASTM A217-46T Grade WC1 + 0.08 to 0.12 per cent. (*a*) Induction furnace heat, (*b*) basic electric-arc furnace heat.

3 ASTM A217-46T Grade WC3.

4 ASTM A217-46T Grade WC3 + 0.08 to 0.12 per cent V + 0.05 to 0.07 per cent Ti (Chapman CMCVT).

5 ASTM A217-46T Grade WC1 + 0.90 to 1.10 per cent Cr + 0.08 to 0.12 per cent V.

6 ASTM A217-46T Grade WC1 + 1.25 to 1.50 per cent Cr + 0.20 to 0.25 per cent V + 0.70 to 0.90 per cent Mo (total).

7 ASTM A217-46T Grade WC4 + 1.00 per cent Mo (total).

The chemistry, heat-treatment, tensile properties, and McQuaid-Ehn test results for the various heats investigated are shown in Table 1.

Weld beads were laid on sample coupons utilizing the method proposed by Battelle Memorial Institute (1).[3] All specimens were stress-relieved after welding at temperatures shown in Table 1.

At the beginning of the investigation it was felt that microscopic examination of samples alone, while showing conclusive evidence of the graphitization resistance of a steel, nevertheless left much in doubt. Chain-type graphite, when segregated in a manner similar to the Springdale findings, undoubtedly markedly affects the physical properties of the steel; but how deleterious is one nodule of graphite viewed in a 100× microscope field?

Careful consideration of the problem seemed to indicate that a physical test for static ductility, coupled with a physical test for impact resistance before and after aging at 1025 F, might indicate the effect of temperature on the alloy steels tested. It was decided to use a bend-test and a V-notch Charpy impact bar as test specimens. Fig. 1 illustrates an etched cross section of a welded test coupon with the location of the test bars shown. A standard-size Charpy bar and a $\frac{1}{8} \times \frac{3}{16} \times$ 3-in. bend bar were used. The V-notch on the Charpy bar was located so that the low-temperature heat-affected zone in the base metal was at the root of the notch. The bend bar was located (and subsequently bent) in such a manner that the low-temperature heat-affected zone of the base metal was in tension. Table 2 contains the results of the bend and impact tests before and after aging.

At the time of the instigation of this investigation, it was felt that the optimum aging temperature was 1025 F; since that time, however, Hoyt, Williams, and Hall (2) have shown the maximum rate of graphitization occurs at a somewhat higher temperature. Test results reported in this paper were obtained from specimens aged at 1025 F. Fig. 2 illustrates the muffle furnaces in The Chapman Valve Manufacturing Co. laboratory used for aging.

---

[1] Director of Research, The Chapman Valve Manufacturing Company.

[2] Research Engineer, The Chapman Valve Manufacturing Company. Jun. ASME.

Contributed by the Joint ASTM-ASME Research Committee on Effect of Temperature on Properties of Metals, and presented at the Annual Meeting, Atlantic City, N. J., December 1–5, 1947, of The American Society of Mechanical Engineers.

Note: Statements and opinions advanced in papers are to be understood as individual expressions of their authors and not those of the Society. Paper No. 47—A-174.

[3] Numbers in parentheses refer to the Bibliography at the end of the paper.

TABLE 1 CHEMISTRY, HEAT-TREATMENT, PROPERTIES, AND McQUAID-EHN TEST RESULTS FOR VARIOUS HEATS INVESTIGATED

Mark	ASTM A217-46T material	Chemical composition, per cent C	Mn	Si	P	S	Ni	Cr	V	Total Al	Acid soluble Al	Mo	Cu	Ti	T.S. psi	Y.S. (0.2% offset) psi	El in 2 in. per cent	R.A. per cent	McQuaid-Ehn test Austenitic grain size	Normality	Heat-treatment
S-1	WCl-o.Al	0.23	0.62	0.32	0.030	0.006	0.29	0.28	0.02	0.029	0.010	0.55	0.09	0	92,500	70,000	16.5	25.0	5-6	I-II	N, [e] 1750 F; D, 1200 F; SR, [g] 1200 F
S-2	WCl-2 lb Al/T	0.23	0.62	0.32	0.030	0.006	0.29	0.28	0.02	0.050	0.025	0.55	0.09	0	81,000	61,000	25.0	45.0	8-9	II	N, 1750 F; D, 1200 F; SR, 1200 F
S-3*a*	WCl[a]	0.22	0.49	0.36	0.025	0.012	0.30	0.22	0.02	0.052	0.027	0.51	0.11	0.03	82,000	61,000	30.0	47.0	7-8	II-III	N, 1800-1600-1650 F; D, 1200 F; SR, 1200 F
S-3*b*	WCl[b]	0.22	0.49	0.36	0.025	0.012	0.30	0.22	0.02	0.052	0.027	0.51	0.11	0.03	81,000	60,000	30.0	48.0	6-8	II-III	N, 1800-1600-1650 F; D, 1200 F; SR, 1200 F
S-4[c]	WCl + 0.10% V	0.24	0.69	0.46	0.032	0.026	0.26	0.34	0.16	0.065	0.030	0.54	0.10	0	82,000	55,000	24.0	37.0	6-7	II	N, 1750 F; D, 1200 F; SR, 1200 F
S-5[d]	WCl + 0.10% V	0.23	0.62	0.32	0.030	0.006	0.29	0.28	0.14	0.065	0.030	0.55	0.09	0	85,000	65,000	23.0	51.0	6-7	II	N, 1750 F; D, 1200 F; SR, 1200 F
S-6	WC3	0.19	0.70	0.32	0.020	0.032	0.30	0.55	0.05	0.050	0.024	0.49	0.11	0	82,000	64,000	28.0	62.0	8-9	II	N, 1750 F; D, 1200 F; SR 1200 F
S-7	WC3 + 0.12% V + 0.03Ti	0.22	0.47	0.53	0.026	0.010	0.42	0.61	0.10	0.022	0.010	0.45	0.11	0.07	82,000	54,000	29.0	54.0	4-6	II	N, 1800-1600-1650 F; D 1325 F; SR, 1325 F
S-8	WCl + 1.00% Cr + 0.10% V	0.18	0.43	0.46	0.020	0.003	0.28	1.00	0.08	0.05	0.020	0.59	0.10	0.03	93,000	60,000	22.0	46.0	5-7	I-II	H, [h] 1750 F; N, 1600 F; D 1325 F; SR, 1325 F
S-9	WCl + 1.35% Cr + 0.25% V	0.22	0.45	0.40	0.026	0.005	0.28	1.43	0.23	0.052	0.030	0.84	0.08	0.03	127,000	90,000	17.0	33.0	5-7	I-II	H, 1750 F; N, 1600 F; D, 1325 F; SR, 1325 F
S-10	WC4 + 1.00% Mo (Total)	0.20	0.54	0.53	0.029	0.012	1.11	0.89	0.01	0.048	0.022	0.98	0.10	0.02	115,000	69,000	22.0	43.0	1-8	I-II	N 1900-1600-1650 F; D, 1400 F

[f] S-3*a*, Casting shaken out of sand at 2000 F and water-quenched; [b] S-3*b*, casting cooled in sand; [c] S-4, induction furnace heat; [d] S-5, basic electric-furnace heat; [e] N, normalize; [f] D, draw; [g] SR, stress relieve (after welding); [h] H, homogenize.

TABLE 2 RESULTS OF BEND AND IMPACT TESTS BEFORE AND AFTER AGING

Mark	Hours specimens aged 1025 F	Free bend — Before aging (deg)	Free bend — After aging (deg)	V-Notch Charpy impact — Before aging (ft-lb)	V-Notch Charpy impact — After aging (ft-lb)
S-1	20,000	180	180	20.0	7.5
S-2	20,000	180	180	19.0	7.0
S-3*a*	9,000	180	180	12.0	10.5
S-3*b*	9,000	180	180	12.5	10.0
S-4	20,000	180	180	5.0	3.5
S-5	20,000	180	180	6.0	3.0
S-6	20,000	180	180	13.5	8.0
S-7	20,000	180	180	23.0	19.5
S-8	9,000	180	180	4.0	3.0
S-9	9,000	180	180	4.5	3.0
S-10	9,000	180	180	17.0	5.5

FIG. 1 SECTIONED TEST COUPON SHOWING LOCATION OF CHARPY IMPACT AND BEND BARS; ×2, AMMONIUM-PERSULPHATE ETCH

FIG. 2 BATTERY OF ELECTRICALLY HEATED MUFFLE FURNACES USED IN VARIOUS STRUCTURAL-STABILITY TESTS

Figs. 3 to 13 illustrate the structures of the low-temperature heat-affected zones of the several alloy steels after aging at 1025 F for the times noted.

The effect of aluminum additions may be noted in Figs. 3 and 4. Since Messrs. Kerr and Eberle (3) first reported the effect of normality on graphitization, there has been a great deal of interest shown in steels containing no aluminum. Some purchasers have attempted to procure castings killed with silicon only, on the premise that these castings would possess a coarse-grained, normal structure as shown by the McQuaid-Ehn test. While

steel S-1 is relatively coarse-grained and of Type I and II normality, nevertheless, it graphitized, although not so severely as steel S-2. The aluminum reported in the chemical composition of steel S-1 is of the order of magnitude usually encountered in straight silicon-killed cast steels. Unfortunately, or fortunately, aluminum is not altogether without its good points. It is imperative that steel be deoxidized with aluminum if sound ductile castings are to be secured from green-sand molds.

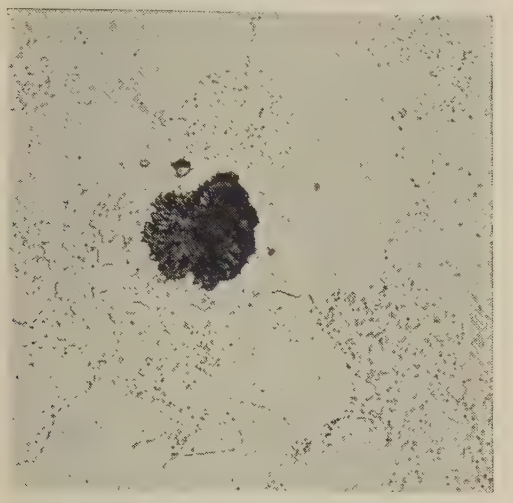

FIG. 3 STEEL S-1, LOW-TEMPERATURE HEAT-AFFECTED ZONE; ×500, NITAL-PICRAL ETCH, AGED 20,000 HR AT 1025 F

FIG. 4 STEEL S-2, LOW-TEMPERATURE HEAT-AFFECTED ZONE; ×500, NITAL-PICRAL ETCH, AGED 20,000 HR AT 1025 F

The deleterious effects of aluminum may be mitigated by using $1^1/_4$ to $1^3/_4$ lb of aluminum per ton added in the form of shot. In our practice, we add the aluminum shot in small quantities to the ladle as the furnace is being tapped. This practice insures that the major portion of the aluminum will combine with the oxygen in the steel and be brought to the surface because of the violent agitation in the ladle during tapping. The acid-soluble aluminum remaining in the steel is then a minimum and the steel is more normal as shown by the McQuaid-Ehn test than a steel deoxidized with aluminum ingot.

Since there have been some thoughts advanced that graphitization may be controlled by manipulation of the initial rate of austenite transformation when a casting cools in the sand mold, a heat of ASTM A217-46T Grade WC1 steel was cast to investigate this theory. One set of test bars were removed from the sand at 2000 F and water-quenched, the second set were allowed to cool in the sand mold to room temperature. Both sets were subsequently heat-treated in accordance with Table 1. If the theory that graphitization proceeds at a higher rate in castings cooled slowly, because of a concentration of carbon in regions high in alloy content, thereby producing relatively stable lakes of austenite which will ultimately transform to an unstable carbide and hence to graphite, is correct, it would be reasonable to assume that steel S-3*a* would be more stable than steel S-3*b*. Experimental results to date do not tend to conclusively substantiate or refute the theory. Figs. 5 and 6 illustrate these steels.

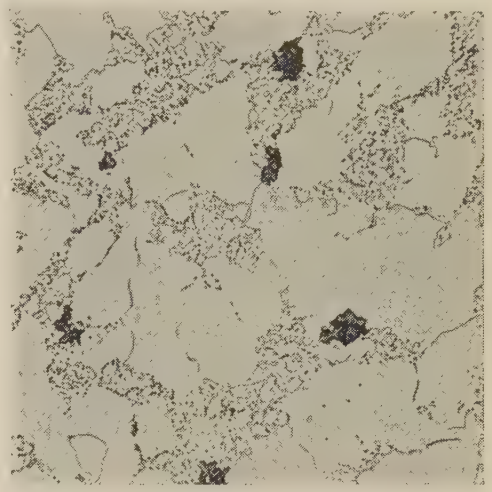

FIG. 5 STEEL S-3*a*, LOW-TEMPERATURE HEAT-AFFECTED ZONE; ×500, NITAL-PICRAL ETCH, AGED 9000 HR AT 1025 F

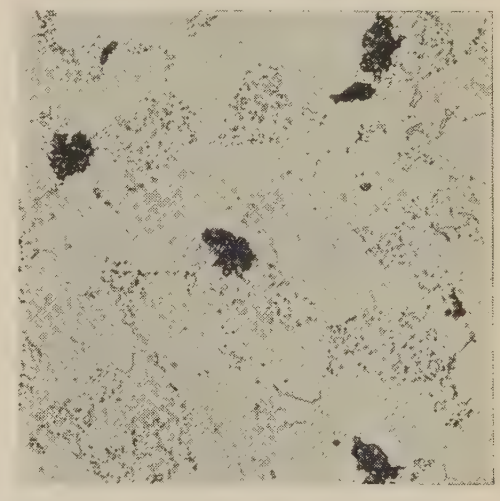

FIG. 6 STEEL S-3*b*, LOW-TEMPERATURE HEAT-AFFECTED ZONE; ×500, NITAL-PICRAL ETCH, AGED 9000 HR AT 1025 F

A rather important variable in the production of cast alloy steels is the method of melting. Steels S-4 and S-5 were made almost identical in chemical composition. S-4 was melted in an induction furnace while S-5 was melted in a basic electric-arc furnace. Approximately 0.10 per cent vanadium was added to the base chemical composition of ASTM A217-46T Grade WC1 (S-4 and S-5) in an effort to increase the stability of the carbides. Figs. 7 and 8 illustrate the aged structure of the low-temperature

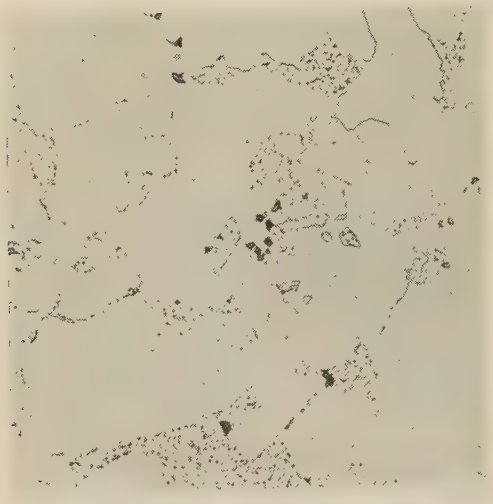

FIG. 7 STEEL S-4, LOW-TEMPERATURE HEAT-AFFECTED ZONE; ×500, NITAL-PICRAL ETCH, AGED 20,000 HR AT 1025 F

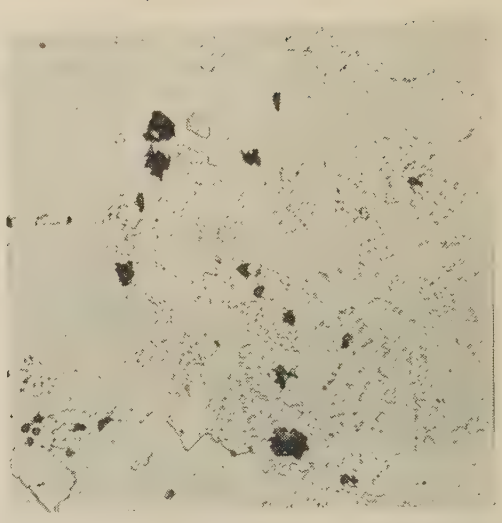

FIG. 9 STEEL S-6, LOW-TEMPERATURE HEAT-AFFECTED ZONE; ×500, NITAL-PICRAL ETCH, AGED 20,000 HR AT 1025 F

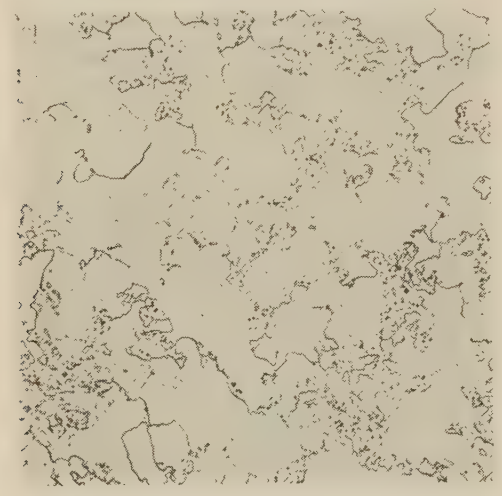

FIG. 8 STEEL S-5, LOW-TEMPERATURE HEAT-AFFECTED ZONE; ×500, NITAL-PICRAL ETCH, AGED 20,000 HR AT 1025 F

FIG. 10 STEEL S-7, LOW-TEMPERATURE HEAT-AFFECTED ZONE; ×500, NITAL-PICRAL ETCH, AGED 20,000 HR AT 1025 F

heat-affected zone. The difference in the rate at which graphitization occurs may be readily noted. It is also obvious that the addition of 0.10 per cent vanadium alone to ASTM A217-46T Grade WC1 is not sufficient to insure carbide stability.

Fig. 9 illustrates the structure of the low-temperature heat-affected zone of steel S-6. Steels S-7 (CMCVT), S-8, and S-9 are modifications of S-6 containing more alloy content. Steel S-7 (CMCVT), as previously noted, was originally developed in 1937 to increase the creep strength on Grade WC1. At the time this steel was developed, the alloy content of WC1 was increased judiciously so that superior creep properties could be obtained at a low cost, the chromium content being 0.25 to 0.30 per cent, vanadium 0.06 to 0.10 per cent, and titanium 0.02 to 0.04 per cent. Power plants using this particular steel for valves have run up to 10 years at temperatures as high as 930 F without any evidence of graphitization. Fig. 10 illustrates the structure of the low-temperature heat-affected zone of this steel after aging.

In the light of the knowledge gained in the last four years, the alloy content has been increased in this steel so that the chromium is now 0.60 to 0.80 per cent, vanadium 0.10 to 0.15 per cent, titanium 0.02 to 0.05 per cent. This steel is basically a welding grade and experimental work has shown its suitability for both field and shop welding including the weld-joining to higher-chromium-content steel piping.

Steels S-8, S-9, and S-10 were made to investigate the properties of materials containing more alloy content than ASTM A217-46T Grades WC3 and WC4. Figs. 11, 12, and 13 illustrate the structure of the low-temperature heat-affected zones after aging.

Since all of the steels are intended for welding in both the shop and field, Jominy hardenability tests and Battelle weldability tests (4) were conducted. The Jominy bars were quenched from 2100 F to insure complete carbide solubility and to simulate welding temperature. Table 3 shows the results of these tests.

The creep strengths of the various alloys have been determined and are shown in Table 4.

In conclusion it may be stated that a sufficiently high chromium content, or the proper combination of chromium, vanadium, and titanium added to ASTM A217-46T Grade WC1 cast alloy steel will insure carbide stability as shown by laboratory tests extending to a total of 20,000 hr at 1025 F. The Chapman Valve Manufacturing Co. cast alloy, known as CMCVT, has been proved stable in installations operating up to 930 F for times extending to 10 years. All the steels investigated are readily weldable, providing certain proper precautions are taken.

TABLE 3 HARDENABILITY AND WELDABILITY TEST RESULTS

Jominy hardenability test																		Battelle weldability test	
S-1		S-2		S-3 *a* and *b*		S-4		S-5		S-6		S-7		S-7		S-8		S-9			
D[a]	RC[b]	D	RC	D	RC	D	RC	D	RC	D	RC	D	RC	D	RC	D	RC	D	RC	Mark	Crack length in mm
1	46	1	45	1	46	1	27	1	40	1	35	1	43.5	1	45	1	48	1	50	S-1	0
4	42.5	4	43	4	39	4	22	4	37	4	25	4	40	4	42	4	46	4	50	S-2	0
8	30.5	8	32.5	8	32	8	18	8	26	8	24	8	31	8	36	8	41.5	8	50	S-3*a*	0
12	26	12	28	12	27	12	17	12	25	12	22	12	26	12	33.5	12	39.5	12	49	S-3*b*	0
16	24	16	24	16	23.5	16	15	16	22.5	16	21	16	23	16	32	16	38	16	46	S-4	0
20	22	20	23	20	21.5	20	15	20	22	20	19.5	20	20	20	31	20	36.5	20	43	S-5	0
24	21.5	24	21	24	20	24	15	24	20	24	18	24	19.5	24	30	24	35.5	24	40	S-6	0
28	19.5	28	20	28	20	28	12.5	28	19.5	28	17	28	18.5	28	29.5	28	34.5	28	37.5	S-7	0
32	18	32	19	32	19.5	32	10	32	16	32	15	32	18	32	29	32	33.5	32	35.5	S-8	0
																				S-9	0.10
																				S-10	0.20

[a] Distance from quenched end of specimen. 1/16 in.; [b] Rockwell hardness, C-scale.
Note: Jominy tests are reported in this form to conserve space.

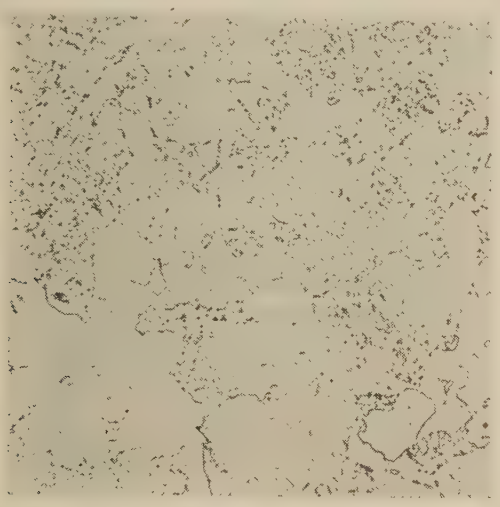

FIG. 11 STEEL S-8, LOW-TEMPERATURE HEAT-AFFECTED ZONE ×500, NITAL-PICRAL ETCH, AGED 9000 HR AT 1025 F

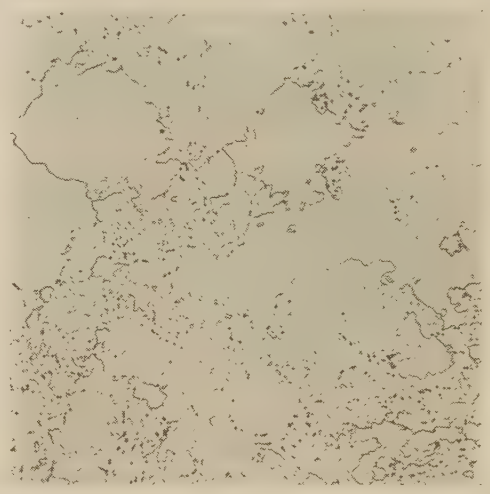

FIG. 12 STEEL S-9, LOW-TEMPERATURE HEAT-AFFECTED ZONE ×500 NITAL-PICRAL ETCH, AGED 9000 HR AT 1025 F

Experiments, not reported in this paper, have proved that heat-treatment is related to the graphitization rate and steels should be "drawn" at as high a temperature as commensurate with the required physical properties, if maximum carbide stability is desired.

Aluminum must be used to deoxidize steel castings, but it is preferable to use silicon as a killing agent prior to the aluminum deoxidation. Alloys such as vanadium and titanium should be added in a manner that insures they will combine with carbon rather than oxygen.

TABLE 4 CREEP STRENGTHS OF VARIOUS ALLOYS

Mark	Temperature (deg F)	Creep strengths, psi, 1%/10,000 hr	1%/100,000 hr
S-1, S-2, S-3*a*, S-3*b*	900	27,000	16,000
	1000	12,000	8,000
S-4, S-5	900	29,000	17,800
	1000	14,200	9,200
S-6	950	30,000	18,000
	1000	16,000	10,000
S-7	900	33,000	20,000
	1000	27,000	13,200
S-8	950	30,000	18,200
	1000	17,500	12,000
S-9	950	33,000	19,600
	1000	23,000	13,400
S-10	950	26,000	15,300
	1000	12,000	7,200

BIBLIOGRAPHY

1 "Studies on Susceptibility of Casting Steels to Graphitization," by J. J. Kanter, Trans. ASME, vol. 68, 1946, pp. 581–587.

2 "Summary Report on the Joint EEI-AEIC Investigation of Graphitization of Piping," by S. L. Hoyt, R. D. Williams, and A. M. Hall, Trans. ASME, vol. 68, 1946, pp. 571–580.

3 "Graphitization of Low-Carbon and Low-Carbon-Molybdenum Steels," by H. J. Kerr and F. Eberle, *Welding Journal*, vol. 24, 1945, pp. 86-*s* to 122-*s*.

FIG. 13 STEEL S-10, LOW-TEMPERATURE HEAT-AFFECTED ZONE; ×500 NITAL-PICRAL ETCH, AGED 9000 HR AT 1025 F

4 "Effect of Recent Research on the Weldability and Control of the Production of Steel Aircraft Tubing," by A. J. Williamson, *Welding Journal*, vol. 24, 1945, pp. 485-*s* to 496-*s*.

Discussion

A. B. WILDER.[4] The authors have presented interesting and worth-while information concerning the properties of low-alloy

[4] Chief Metallurgist, National Tube Company, U. S. Steel Corporation Subsidiary, Pittsburgh, Pa.

cast steels for power-plant service. Reference is made to the use of aluminum in the deoxidation of steels for sound castings. The practice used in the deoxidation of 1/2 Cr, 1/2 Mo and 1 Cr, 1/2 Mo steel for seamless pipe results in a coarse carburized austenitic grain size of 1–5 while most of the castings examined were fine-grain steel. In the melting of coarse-grain steel for seamless pipe less than 1/2 lb per ton of aluminum is used, and this practice should not be overlooked in a comparison of the properties of seamless pipe with steel castings.

An appreciable amount of chromium and nickel was present in the cast steels investigated. Although it is recognized that chromium inhibits graphitization, experimental data have indicated that nickel, when present in a sufficient amount, will increase the rate of graphitization. Graphitization was observed in some of the cast steels with 1/4 per cent chromium. This has also been observed in seamless pipe and technical information to date indicates that at least 1/2 per cent chromium should be present in 1/2 per cent molybdenum steels for resistance to graphitization.

The occurrence of graphitization in cast vanadium bearing steels should be noted. Graphite has also been observed in several Mo-V induction-furnace heats with and without the use of aluminum in the deoxidation practice. However, the behavior of small induction-furnace heats may differ from steel melted under commercial conditions in an electric-arc furnace. This is illustrated in the hardenability data reported in Table 3 of steel S-4 which appears to be low compared to the other steel investigated. The behavior of small induction-furnace heat may frequently be associated with the cleanliness of the steel.

The stabilizing influence of titanium with reference to graphitization is under investigation in the laboratories of National Tube Company. A steel of this type should be compared with chromium bearing steels. Additional data will be required before the stabilizing influence of titanium will be generally recognized in the manufacture of seamless pipe. Further, the piercing properties of such a steel would require evaluation.

Although graphitization of the segregated chain type has seldom been observed in castings and seamless pipe, the occurrence of nodular graphite is not desirable. All types of graphitization should be avoided in the development of steels for power-plant use as carbide stability is one of the desired objectives.

Authors' Closure

The authors wish to thank Dr. Wilder for his information relating the behavior of cast and wrought steels. Both the deoxidation practice and the tramp elements present in the steels investigated, reflect normal commercial practice.

The authors agree with Dr. Wilder that the behavior of an electric-arc-furnace heat cannot be predicated on the behavior of a small induction-furnace heat; although an "ored" induction heat will behave somewhat similiar to an electric-arc-furnace heat.

Theory and Practice of the Crush-Dressing Operation on Grinding Wheels

By E. C. HELFRICH,[1] CINCINNATI, OHIO

This paper presents a qualitative analysis of the crush-dressing process based upon experimental evidence. The theory developed herein accounts for the forces involved, power requirements, rate of wheel removal, the effect of wheel and crusher diameters, and surface speed on the crushing process. The equations and data presented will enable the designer to engineer crush-dressing applications more intelligently, and will contribute to a clearer understanding of the process by all who may be interested in applying it. The advantages and disadvantages of crush-dressing versus diamond-truing are discussed with reference to the physical properties of crystals.

Nomenclature

The following nomenclature is used in the paper:

- R = radius of grinding wheel
- r = radius of crush dresser
- L = length of arc of contact, BD in Fig. 1
- θ = angle subtended by arc of contact at center of crush dresser
- F = resultant force between grinding wheel and crush dresser
- $\theta/2$ = angle between F, and center line of wheel.
- h = penetration of crusher into grinding wheel. It will also be referred to as penetration per revolution, or thickness of ring of material removed each time a crush dresser traverses the circumference of wheel
- b = width of contact between crusher and wheel
- $A = bL = br \sin \theta$ = projected area of contact between crusher and wheel
- $p = F/A$ = pressure (stress) existing at the area of contact between crush dresser and grinding wheel
- T = torque necessary to crush-dress
- W = rate of wheel removal

Introduction

Within the past decade the ancient art of crush-dressing grinding wheels has been improved and applied to a variety of precision-grinding operations in the modern machine shop. At present crush-dressing is rapidly finding its place as a valuable tool in industry; however, diamond-truing has not been replaced by any means. Most authors on this subject agree that, while diamond-dressing may produce a more accurate surface of revolution, and a somewhat better finish on the work, crush-dressing has often proved itself to be the most economical process. Crush-dressing, moreover, has the advantages of providing cooler grinding and less normal force, plus its adaptability to the process of dressing intricate forms in the wheel surface. Vitrified grinding wheels lend themselves most readily to crush-dressing, and are, in fact, the only type to which this process has yet been applied successfully in commercial practice.

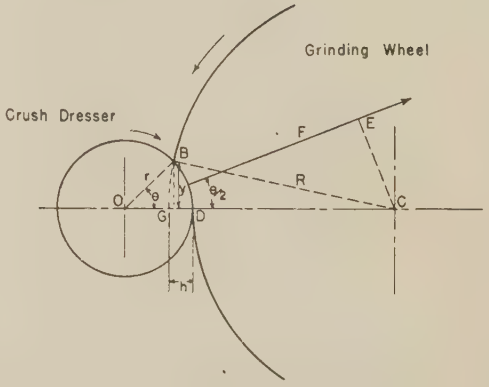

Fig. 1 Geometry of Crush Dressing

Theory of Crush-Dressing

The abrasive grains in a grinding wheel are arranged in much the same manner as the atoms in a crystalline material. These grains are held in place by the bond which may be compared to the forces holding the atoms in place in a crystalline solid. Between the grains are voids which might be compared to the empty space existing between atoms in a crystal.

In the manufacture of grinding wheels, the grains (excluding special mixtures) are maintained approximately equal in size by screening. The strength of the bond between grains is determined by the ratio of bond material to grit material, and is maintained as uniform as possible by a thorough mixing of ingredients. The voids are produced by putting particles of an organic material into the mix which burns out when the wheel is fired. The extent to which a grinding wheel measures up to the ideal, i.e., grains uniform, bonds of equal strength, and uniform spacing, depends upon the excellence of the manufacturing process.

In view of this analogy, one might suspect that the material of which a vitrified grinding wheel is composed will have many of the properties of a crystalline solid. This leads at once to the fundamental assumption of the theory of crush-dressing, namely, that a definite pressure (force per unit area) must be applied to the grinding wheel by the crush dresser to overcome the resistance to penetration, i.e., the grinding-wheel structure exhibits a definite "crushing pressure." In other words, if the voids have sufficient volume to accommodate the grains as they are pushed inward, and the average force to dislodge each individual grain is constant throughout a given grinding wheel, the ultimate pressure that the wheel will support is equal to the product of that force times the number of grains per unit area. Assuming the structure to be uniform throughout, this ultimate crushing pressure may be considered to be a constant for a given wheel. Actually, this has been found by experiment to be the case; the pressure (force per unit area of contact) between crush

[1] Research Engineer, Research Department, The Cincinnati Milling Machine Company. Jun. ASME.

Contributed by the Special Research Committee on Metal Cutting Data and Bibliography, and Production Engineering Division, and presented at the Semi-Annual Meeting, Milwaukee, Wis., May 30–June 5, 1948, of The American Society of Mechanical Engineers.

Note: Statements and opinions advanced in papers are to be understood as individual expressions of their authors and not those of the Society. Paper No. 48—SA-42.

dresser and wheel has been found to be essentially a constant for a given wheel.

In crush-dressing, the force is normal to the wheel surface and consequently the grains are pushed inward as they are detached from the wheel. As they are pushed inward they must have some place to go, that is, the voids must be large enough to accommodate the grains until the crusher passes by, at which time the coolant should wash the detached grains from the wheel surface. If the voids are too small, many grains undoubtedly will be wedged tightly into the wheel structure. Experiment indicates that this is the case, particularly for larger values of penetration of the crush dresser into the wheel, which causes the grains to be pushed inward greater distances. If the voids are filled in the manner described, the crushing pressure will be increased because the individual grains encounter greater resistance to movement when detached from the wheel structure.

The way in which the system adjusts itself to this constant pressure is readily appreciated if it is borne in mind that the arc of contact increases as the penetration of the crush dresser into the grinding wheel increases. When a certain force is applied to the dresser, the penetration increases until the area of contact is large enough so that the pressure is equal to the "crushing pressure," i.e., the maximum pressure that the wheel will support without further penetration. Therefore, during crush-dressing, the stress existing between the crush dresser and grinding wheel remains equal to the crushing pressure of the given grinding wheel.

In order to make use of this principle, it is of course necessary to know the area of contact A, between crush dresser and wheel. Referring to Fig. 1, we see that the arc of contact L, of the crush dresser with the wheel extends from B to D. Since the angle subtended by the arc of contact is small, (generally from 0 to 2 deg), BD and BG are approximately equal to the half-chord whose length is denoted by y. The penetration h, of the crusher into the wheel may be divided into sagittal distances, h_1 and h_2, such that

$$h = h_1 + h_2$$

Then by the sagittal theorem of geometry (see Appendix), since h is small compared with R and r, and L is approximately equal to y

$$h = \frac{y^2}{2r} + \frac{y^2}{2R}$$

where r is the radius of the crush dresser, and R is the radius of the grinding wheel. Hence

$$L = y = \sqrt{\frac{2hRr}{(r + R)}} \quad \ldots\ldots [1]$$

and

$$A = bL = b\sqrt{\frac{2hRr}{(r + R)}} \quad \ldots\ldots [2]$$

where b is the linear width of contact, and A is the projected area of contact. The projected area of contact is defined to be the actual area of contact projected on a plane perpendicular to the center line of the grinding wheel and crush dresser, i.e., perpendicular to the line of action of the normal crushing force. Since we are interested in the normal crushing force, it is necessary to use the projected area of contact. If an element of area A, on the crush dresser be inclined at an angle ϕ, to the axis of the crush dresser, then the element of normal force F, corresponding to this area is

$$F = p\Delta A \cos \phi$$

where $A \cos \phi$ is the projected area of contact. If the crush dresser is a right circular cylinder, the projected area of contact is very nearly the same as the actual contact area, whereas in form dressing it is not.

As already pointed out, the pressure on the projected area of contact in crush-dressing has been found to be a constant for a given wheel. Thus the resultant force F, between crush dresser and grinding wheel is equal to this pressure times the projected area of contact. Therefore we may write

$$F = pA = pb\sqrt{\frac{2hRr}{(r + R)}} \quad \ldots\ldots [3]$$

where F denotes the resultant crush-dressing force, and p denotes the crushing pressure. Since this force is assumed to be equally distributed over the area of contact, the line of action of the force F, will bisect the arc of contact, and consequently will be inclined to the center line of the wheel at a very small angle ($\theta/2$ in Fig. 1). Because this angle is small, (from 0 to 1 deg), F is approximately equal to the radial or normal crushing force.

However, because $\theta/2$ is not zero, F has a tangential component and therefore the torque necessary to drive the grinding wheel in crush dressing is equal to the product of this component and the radius R. This is the same, however, as the product of the force F, and the moment arm EC, in Fig. 1. By using the sagittal-arc theorem, similar triangles, and simplifying, we get

$$EC = \sqrt{\frac{hR\ (r + R)}{2r}}$$

and using Equation [3] and simplifying

$$T = F(EC) = pbhR \quad \ldots\ldots [4]$$

where T denotes the torque required.

The penetration h, of the crush dresser into the wheel may be thought of as the radial feed per revolution, therefore

$$W = h \text{ (rpm)} \quad \ldots\ldots [5]$$

where, if h is in inches, W will be the rate of wheel removal in inches off the radius per minute.

Having selected a rate of wheel removal and a satisfactory surface speed, the penetration h, is thereby determined, Equation [5]. Given also the crushing pressure p, for a given wheel, the radii (R and r) of grinding wheel and crush dresser, and the width of wheel b, to be crush-dressed; then the radial force F, and the torque T, necessary to crush-dress may be computed by means of Equations [3] and [4]. Thus the quantities which are of greatest importance from an engineering standpoint can be calculated from the crushing pressure p, and the readily obtainable quantities h, R, r, and b.

Method of Obtaining Data

The theory presented in this paper was arrived at as a result of an attempt to explain a considerable quantity of data taken with a crush-dressing setup in the research laboratories of the author's company. Data are presented herein to demonstrate that the theory is valid if certain limitations are kept in mind.

The apparatus used, Fig. 2, consisted of a 2-in-diam solid cylindrical crush dresser made of high-strength steel hardened to Rockwell C-64. The dresser was mounted on the outside of sealed precison ball bearings which in turn, were fitted on a shaft. The dresser and assembly were mounted as an integral part of a hydraulic piston. A mating cylinder and mounting fixture were securely fixed to the table of a cylindrical grinder in such a manner that the center line of the crusher roll and piston were at the same height as the center line of the grinding wheel. Force

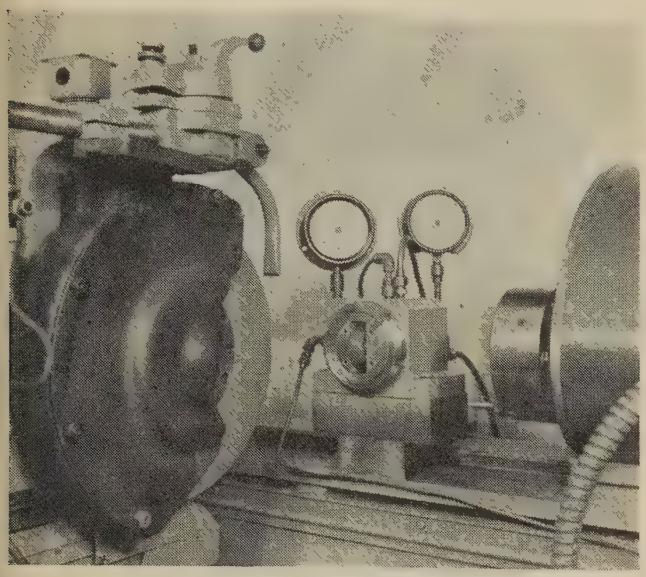

FIG. 2 EXPERIMENTAL CRUSH DRESSER MOUNTED ON TABLE OF CENTER-TYPE GRINDER

was applied to the crusher roll hydraulically by means of the cylinder and piston. A hydraulic circuit was provided containing a special pressure-reducing valve, which made it possible to control the pressure over wide limits, and therefore vary the radial force on the dresser over rather wide limits. This valve also served to maintain the pressure at a constant value throughout a test. A square-shouldered throttle valve built into the cylindrical surface of the piston and the cylinder wall was used to position the piston and crush dresser very accurately (to ± 0.0001 in.). High-pressure oil was applied to the intake port on the throttle, while the exhaust port was connected to the reservoir. The incoming and outgoing resistances (square shoulders on piston and ports on cylinder) were functions of the relative position of the piston in the cylinder. Thus the hydraulic pressure in the central chamber of the valve was a function of the position of the piston in the cylinder.

The object of the test was to measure the penetration per revolution of a given grinding wheel over a wide range of normal crushing forces. The force was maintained at a constant value during a determination, and the time necessary for the crush dresser to penetrate 0.005 in. was measured with a stop watch. The grinding wheel was powered with a direct-current motor and control unit which maintained the speed of the wheel constant at 25 rpm (92 fpm). The crushing pressure for the wheel was then computed by means of Equation [3] (solving for p).

A big problem in earlier tests was the elimination of the effect of machine deflection in measuring the penetration of the dresser into the wheel. This was overcome by the use of the throttle valve on the piston. The load was adjusted to that used in the test (wheel stationary) and the piston and dresser position adjusted by means of the grinder infeed until the pressure between the ports of the throttle valve was zeroed at about one-half pump pressure. The wheel was then moved in 0.005 in. by means of a 0.0001 dial indicator. With the piston and wheel in this position at the start of a test run, the dresser had penetrated 0.005 in. when the piston and valve returned to the zero position.

After a penetration of 0.005 in. was reached, the wheel surface was found to contain slight hills and valleys arising from nonuniformity of wheel structure. The throttle valve served to integrate this unevenness and give an average value for the final penetration.

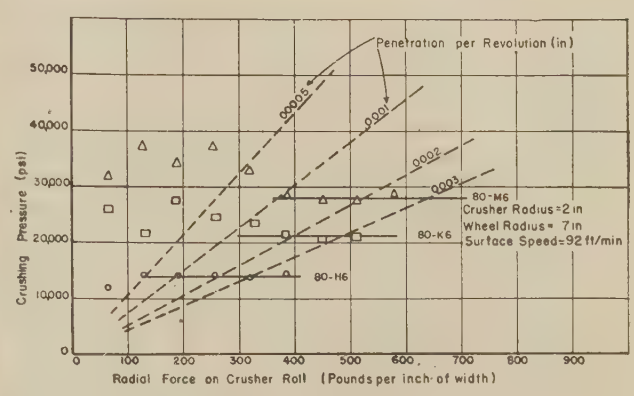

FIG. 3 CRUSHING PRESSURE VERSUS RADIAL FORCE ON CRUSHER ROLL FOR THREE 80-GRAIN-SIZE GRINDING WHEELS, GRADED H6, K6, and M6

DISCUSSION OF DATA

Fig. 3 is a plot of the crushing pressure versus the normal force on the crush dresser for three 80-grit wheels, graded H, K, and M by the manufacturer. Superimposed on these curves are the dotted constant-penetration lines, showing the variation in the penetration per revolution. It can be seen at a glance that the crushing pressure fulfills the theoretical assumption in that it appears to have a constant value between a range in penetration of from 0.0001 in. to 0.0003 in. per revolution of the grinding wheel. It develops that for values of the penetration less than 0.0001 in. per revolution, the length of the arc of contact is equal to or less than the average spacing between the grains in these wheels. In view of this, the fact that the crushing pressure is somewhat erratic in this range is not hard to understand. It would undoubtedly be advantageous to control the penetration or the crushing force during a crush-dressing operation so as to remain in the range where the crushing pressure is constant. We might conclude, therefore, that for the purpose of engineering calculations, the crushing pressure is constant in the useful range for these wheels.

Since wheels of fine grain size are usually recommended for crush-dressing applications, a 120-K and a 180-I wheel were tested. These data are presented in Fig. 4. The value of the crushing pressure appears to increase gradually throughout a range of penetration of from 0.000025 to 0.00015 in. per revolution for the 120-K wheel. For the 180-I wheel, the pressure appears to increase slowly from 0.000025 to 0.0001 in. penetration per revolution. If an average value is taken for the crushing pressure between these ranges and for these wheels, we could assume it to be a constant without introducing an error larger

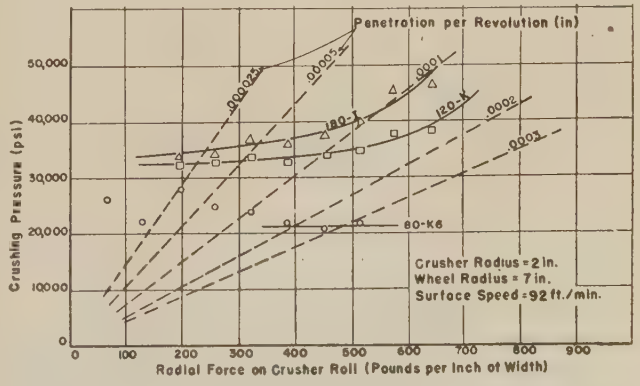

FIG. 4 CRUSHING PRESSURE VERSUS RADIAL FORCE ON CRUSHER ROLL FOR 80-K6, 120-K, AND 180-I GRINDING WHEEL

than 5 per cent. For penetrations larger than 0.00015 in. for the 120 wheel, and 0.0001 in. per revolution for the 180 wheel, the crushing pressure increases at a greater rate. Thus it appears that if we exceed a certain rate of crush-dressing for a given wheel, the voids are too small to accommodate the material removed until it has a chance to be washed away by the coolant. It also would be expected that, as the penetration and the amount of material removed increase, a portion of the crushed material is wedged into the voids so tightly that it is not removed by the coolant after the crusher has passed by. This would be undesirable from the standpoint of grinding practice, and therefore it would be advisable not to exceed those rates of penetration for which the crushing pressure approximates a constant. When a Brinell hardness test is performed on the side of one of these grinding wheels, the mean pressure supporting the ball is found to be from 1.5 to 3 times the crushing pressure as determined in these tests. Examining the spherical seat it is found that the crushed material has been pushed ahead of the ball, and pressed into the voids, thus forming a solid supporting surface. However, when crush-dressing, the penetration per revolution of the crusher into the wheel is of the order of 0.0001 in., whereas in a Brinell hardness test (500 kg load), the total penetration is in the neighborhood of 0.030 in., 300 times that incurred in crush-dressing. In removing 0.030 in. off the radius of the grinding wheel by crush-dressing, the wheel would make 300 revolutions and the crushed bond and grit material would be removed between each successive pass of the dresser over the same portion of the grinding-wheel surface.

It is not surprising to find that consistent values of the crushing pressure are obtained at smaller rates of penetration for the 120- and 180-grit wheels than for the 80-grit wheels, since the number of grains per unit area has been increased, and the distances between grains and size of voids have been correspondingly decreased in going from the larger to the smaller grain sizes.

Results of Tests as Applied to Crush-Dressing Practice

A number of grinding-wheel faults were observed during the author's experience with crush-dressing. Wheels are often found to be harder and stronger in some parts than in others. For example, a wheel may be harder on one side than on the other, resulting in an unequal force distribution across the face of the crush dresser and an unwanted taper in the crush-dressed surface due to deflection. A more general fault is the variation in hardness from point to point around the periphery of the wheel. All wheels tested seemed to have this fault to some extent, although, in general, the finer-grit wheels seem to be of a more uniform structure than the coarse wheels. This fault produces an out-of-roundness which is objectionable as it will cause chatter and poor finish. Thus the general application of the crush-dressing process for precision grinding would seem to be limited in part by lack of homogeneity in grinding-wheel structure. These results may be due in part to the author's use of resilient loading of the crush dresser (in order to permit measurements of force and penetration) plus a low wheel speed, which allowed the dresser to "follow" the wheel surface. A more rigid dresser mounting should minimize the effects resulting from nonuniformity of wheel structure.

The structure of a crush-dressed wheel is more open than a diamond-trued wheel, with larger voids (and consequently a smaller number of grains) in prominence (see Figs. 5 and 6). This can be observed by eye or by making Faxfilm impressions of the wheel surface, which can be studied with a microscope. A special technique was employed in making the Faxfilm (plastic) impressions illustrated in Figs. 5 and 6. Instead of the usual procedure of applying the solvent to the surface which is to be studied, and pressing the Faxfilm down with thumb or roller,

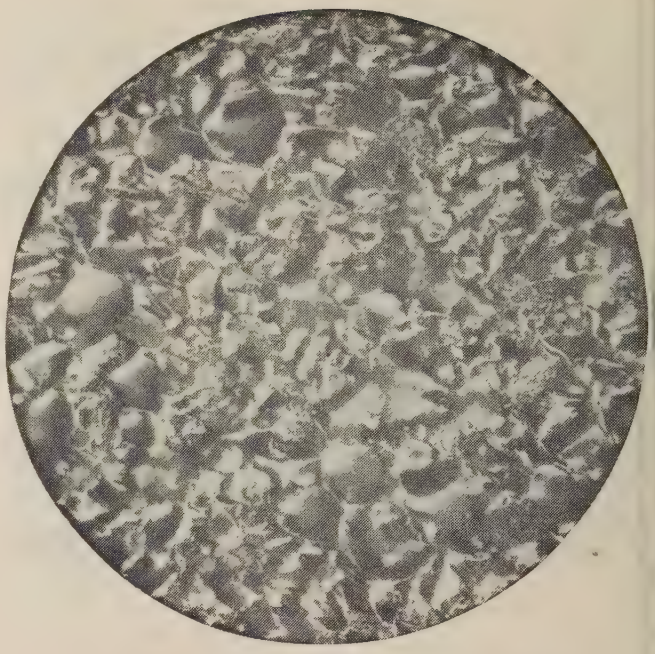

Fig. 5 Photomicrograph of Typical Faxfilm Replica of 180-I Grinding-Wheel Surface When Diamond-Trued; ×64

Fig. 6 Photomicrograph of Typical Faxfilm Replica of 180-I Grinding-Wheel Surface When Crush-Dressed; ×64

the solvent in this case was placed on the plastic ribbon which was held against the wheel surface with a flexible strip. This procedure was used so that only the high spots in the wheel surface (grains that would normally contact the work when grinding) would contribute to the impression. Microscopic examination of the Faxfilm impressions also showed that a considerable number of grains were loosened (without being removed) by the crush-dressing process, whereas in diamond-dressing very few grains were loosened without being completely removed.

There is considerable evidence that crush-dressing produces sharp edges on the grains whereas diamond-truing produces

many flats parallel to the wheel surface. These conclusions can be interpreted scientifically if we think of the grains being split along cleavage planes, just as in the "cutting" of gems. For example, the ruby has the same composition and crystal structure as aluminum-oxide abrasive grains, with the exception of impurities which determine the color. Aluminum oxide (corundum) crystals are hexagonal and are described as having almost perfect cleavage parallel to the base and faces of the unit rhombohedron. Thus there are eight directions in which aluminum-oxide crystals may cleave or split. Therefore, if a thrust is applied to the tip of an abrasive grain embedded in a grinding wheel, a portion of the grain may be split off along that cleavage plane which is subjected to the maximum unit stress. Since the thrust is approximately normal to the surface in crush-dressing, the new surfaces produced on the grains will be inclined at a considerable angle to the wheel surface.

In diamond-truing, the force that the diamond exerts on the abrasive grains at impact is approximately tangential; thus the new surfaces produced when the grains are cut will be along that cleavage plane which is most nearly parallel to the wheel surface, thereby producing a "duller" wheel. These considerations lead us to the conclusion that diamond-truing tends to produce relatively dull grains, whereas crush-dressing tends to produce sharper grains.

Two advantages of crush-dressing that can be demonstrated are cooler grinding and less normal force for a given rate of metal removal. Cooler grinding depends on the larger voids, increased chip clearance, and better application of the coolant; plus the elimination of rubbing between work and flank of tool (abrasive grain), which undoubtedly would be present with tangential flats on the tips of the grains. Therefore crush-dressing may be used as a means for eliminating overheating of the work surface during grinding. Less normal force is understandable because of the sharper grains which, by virtue of their sharpness, require less force to penetrate the workpiece. Therefore crush dressing is helpful when grinding a fragile workpiece between centers; normally in such a case the deflection produced by a dull wheel may result in chatter and lack of straightness. Previous tests made by the author, in which the ratio of tangential to normal grinding force was studied, revealed that, in general, higher ratios of tangential to normal force were obtained (during grinding) with a crush-dressed wheel as compared to a wheel that had been trued with a diamond. A high ratio of tangential to normal grinding force was found to be indicative of more efficient metal removal and less heating of the work during grinding.

Recommendations made in recent articles (1, 2, 3, 4)[2] on crush-dressing, differ in detail, but, in general, agree on many recommended practices. Regular-grain grinding wheels are preferred to those containing special mixtures. Grinding-wheel surface speeds up to 300–350 fpm are recommended for crush-dressing. Where the machine is equipped for the use of a cutting fluid this is generally used during crush-dressing, whereas compressed air is used on machines, such as surface grinders, when no cutting-fluid system is provided. The principal function of the fluid is the removal of detached grits, although certain other factors also appear to be involved. Helical gashes, unequally spaced, are sometimes machined into the crusher roll to facilitate the removal of detached grits when a deep form is being dressed into the wheel.

Crusher rolls are usually made of hardened high-speed steel, although other materials are frequently used. In the author's experience crusher-roll wear was not appreciable when the grinding wheel was allowed to drive the roll; however, noticeable wear was encountered (especially in starting) when the crusher roll was made to drive the grinding wheel.

[2] Numbers in parentheses refer to the Bibliography at the end of the paper.

Conclusions

In developing the theory presented in this paper, only the most general case of crush-dressing was considered, i.e., external grinding, vitrified wheels, and crusher rolls with solid surfaces of revolution. No special cases, such as the use of star wheels, Ross dressers, conical cutters, and the like, were considered.

Some power readings were taken during this investigation of crush-dressing, and after proper elimination of frictional and electrical losses, the measurements were in close agreement with the theory. These data, however, have not been presented in this paper for the sake of brevity. All of the readings were taken with a grinding-wheel surface speed of approximately 100 fpm, and no attempt was made to investigate the accuracy of the theory at higher speeds.

At present the process of crush-dressing is an art. To do satisfactory work the machine operator must be thoroughly familiar with the limitations of his machine, and also have an insight into the nature of crush-dressing. To the author's knowledge, very little information has been published concerning the basic principles of the crush-dressing process. It is hoped that this paper will serve to stimulate interest in crush-dressing and serve as a basis for further development of the subject.

Acknowledgments

The author wishes to express his appreciation to Mr. Hans Ernst, Research Director; Mr. Albert Dall, Assistant Research Director; and Dr. M. Eugene Merchant, Research Physicist of The Research Department, Cincinnati Milling Machine Company, for their helpful comments and suggestions.

Bibliography

1 "Crushed Wheel Grinding," by J. C. Wilson, *Tool Engineer*, vol. 17, December, 1946, pp. 35–39.

2 "Dressing Grinding Wheels," by W. F. Aller, *Mechanical Engineering*, vol. 66, 1944, pp. 779–782.

3 "Crush Dressing of Grinding Wheels," by R. Y. Moss, *Mechanical Engineering*, vol. 68, 1946, pp. 885–888.

4 "Comparison of Crush Dressing and Diamond Dressing," by E. V. Flanders, *Mechanical Engineering*, vol. 69, 1947, pp. 123–127.

Appendix

Sagittal-Arc Theorem

In Fig. 7, R is the radius of curvature of the arc AC, BC is the sagitta, and AB is the half-chord. Let $BC = s$, and $AB = y$; then from the right triangle AOB it follows that

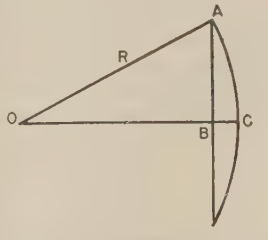

Fig. 7 Sagittal-Arc Diagram

$$R^2 = y^2 + (R - s)^2$$

$$y^2 = 2Rs - s^2$$

If R is much larger than s, we may neglect s^2 and obtain the sagittal theorem

$$s = \frac{y^2}{2R}$$

Discussion

E. V. Flanders.[3] This paper presents a clear analysis of the

[3] Chief Engineer, Thread Grinder Division, Jones & Lamson Machine Company, Springfield, Vt.

theory of crush-dressing, and the work done by the author in developing formulas for determining the various quantities which are of importance in the art, should be of help in the design of crush-dressing equipment.

Because of the long experience we have had in thread and form-grinding, it was natural that we should have made a careful study of crush-dressing as applied to our equipment. As a result of these studies, we became convinced that the crushing of grinding wheels was best accomplished by hydraulic rather than by manual or more conventional forms of power-feed devices. As a result we now have hydraulic crusher devices at work both in our own plant and in the field. A simple description of the operation of this device is as follows:

The operator must stop rotation of grinding wheel (manually).

Pull lever which feeds crusher roll required amount for crushing of wheel (manually). This lever also actuates the limit switch which starts the hydraulic pump in the truing device.

Oil is forced under pressure against piston which pushes roll-carrying ram forward until it engages wheel.

Once contact between roll and wheel is positive, wheel automatically starts rotating at crushing speed of approximately 130 sfpm, driving the crusher roll.

Crusher roll advances into the wheel until stopped positively by predetermined adjustment on truing device. This actuates a synchronized timer which allows a predetermined "crush out" of wheel to smooth out irregularities. This interval may be anywhere from 10 to 40 sec, after which the wheel stops automatically.

The crusher roll is withdrawn and the grinding wheel starts rotating at grinding speed, both automatically.

Wheel wear is compensated for automatically in this design.

The author states, "the process of crush-dressing is an art." We agree with that statement. We know of no way to tell just how a wheel is going to respond to the crushing action if we have had no previous experience with it or the form to be crushed. An intelligent guess can be made, however, which can then be changed to improve the action as observed by the operator, thanks to the flexibility of hydraulic control. Once satisfactory conditions have been established, a record can be made of crusher pressure, crush-out time, and the like, which will enable the operator to repeat crushing performance as long as the same conditions are maintained. We believe that the automatic control of crushing increases crusher life and the number of pieces which can be ground per roll.

We were much interested in checking penetration per revolution on our dresser against figures given by the author. In making this comparison, it should be borne in mind that examples given are not laboratory tests but records of jobs which are or have been running in production. We find, for instance, that in some cases we show a higher rate of penetration for somewhat similar wheel ratings. We have learned also that the shape of the form to be crushed affects the rate of crushing. Great care, for instance, must be exercised where there are wide diameter variations in the crusher-roll form.

Table 1 of this discussion shows that in many cases it is possible successfully to form the wheel with feed per revolution which exceeds the 0.0002 or 0.0003 which has been set up as a tentative penetration figure by the paper under discussion. Tests Nos. 1, 2, and 3 show a record of the crushing of 40-deg-included-angle form with three different wheels. The first was a 150-hard fine-grain wheel. This was crushed at the rate of 0.0005 in. per revolution. The second time the job was run, a 120-J wheel was used with a No. 7 structure. Here again we had the same rate of penetration, even though the grit size was somewhat coarser, with the probability of greater space area for the loosened grains. A third test was made on the same form using a 220 wheel. This wheel though harder was less dense than the others, so we were still able to crush at the rate of 0.0006 in. per revolution. On the other hand, on some of the fine-pitch forms which were crushed we found it necessary to drop the feed back to about 0.0003 in. per revolution in order to obtain the best form with the very fine-grit wheel which worked best on that particular job.

As the author states, it is important that the loose particles be washed away as rapidly as they are separated from the main body of the wheel. Although we have not proved this point, we have the feeling that where oil is used as a cooling agent, there is less tendency for the particles to become permanently embedded in the body of the wheel.

One of the effects of extreme pressure between crusher roll and wheel is to upset the wheel structure so thoroughly as to loosen or break off portions of the wheel as much as 0.010 to 0.015 in. below the contact point of the roll with the wheel. This is most easily observed when crushing acme or worm forms where a fairly wide flat root makes the flushing action of the coolant a little more difficult. However, it should be kept clearly in mind that the condition mentioned is obtained only when too great crusher pressure has been used.

We have listed in the few examples given the diameter of the crusher roll and radial thrust on the crusher, with such other items of information as seem of interest.

R. S. Moore.[4] In view of the author's statement that all of his work was done with a so-called "water-soluble oil," it is suggested that he investigate the use of other fundamentally different media in order to establish more completely the limits of performance in crush-dressing. For example, the use of a homogeneous medium such as a solution of suitable additives in a light-petroleum-oil base or a solution in water of suitable wetting agents, detergents, film strength additives, and rust preventives, often shows an improvement in crushing over the use of an heterogeneous medium such as a water emulsion of an oil, fat, or wax, etc. This homo-

[4] Quaker Chemical Products Corporation, Detroit, Mich.

TABLE 1 WHEEL-CRUSHING DATA

Job	Diam of crusher roll	Crushing speed, fpm	Wheel specifications				Crushing pressure, per sq in.	Total time for crushing, min-sec	Crush out or recrush cycle, sec	Depth crush, in.	Feed per rev, in.	Radial thrust on crusher, lb
			Grain	Grade	Structure	Width in.						
40-deg incl. 2 rib lead 0.2244	4	130	150	N	T	.240	60	7–0	30	.090	.00051	376.8
40-deg incl. 2 rib lead 0.2244	4	130	120	J	7	.240	60	7–0	20	.090	.00051	376.8
40-deg incl. 2 rib lead 0.2244	4	130	220	M	10	.240	75	5–30	25	.087	.00063	471.0
40-deg incl. 12 rib lead 0.0797	4	130	120	K	5	2.000	150	10–0	25	.100	.0004	942.0
27 P. pipe 3/4 Tpr. lead 0.037	3.875	130	320	I	13	.964	100	4–0	20	.030	.0003	628.0
27 P. pipe 3/4 Tpr. lead 0.037	3.875	130	320	K	13	.964	120	4–40	20	.033	.00028	753.6
Seaming roll	3.687	118	220	K	9	.3125	50	4–35	20	.070	.0006	314.0
Seaming roll	3.687	115	220	K	9	.3125	50	4–10	20	.070	.00067	314.0

geneity of the medium plays an important part in reducing the loading of the wheel and, possibly, by this means, crushing pressures.

H. W. Wagner.[5] The writer is in general agreement with the statements made in this paper, after comparison of those statements with findings in the laboratory of his company. The author has been wise in employing the device of geometrical analysis to correlate theory with experiment, which leads to substantial guidance for practice.

Discussion involves the temptation of offering amplifications, and an excursion into crush-dress-grinding which is not included in the subject. A few thoughts are offered in brief form.

One of the author's reasons for the success of grinding after the wheel face is crush-dressed should be emphasized. That reason is sharpness. Crush-dressing shatters the face, leaving it armed with sharp jagged abrasive points, which penetrate and grind the work with generation of less heat and with less pressure built up between wheel and work than exist when the wheel is diamond-trued as in average practice. The lower pressure permits the wheel face to hold its accurate form for a longer duration of grinding.

Another important reason for success in grinding is that a grinding oil is generally used. The abrasive points remain sharp much longer with oil than with a mixture of water and compound.

In a laboratory comparison an experimental form, 2 in. wide and of a maximum depth of $^1/_8$ in., was ground cylindrically in 2-in-diameter hard steel with a crush-dressed wheel face. With grinding oil, 10 cuts per dressing were made without serious loss of form. With a 1:50 mixture of soluble oil and water, the form was lost after 3 cuts per dressing. The power required to drive the wheel was much higher, and the Profilometer reading was much higher under the second condition. The wheel and time per cut were the same for both grinding fluids.

Ratio of "tangential to normal grinding force" is mentioned in the paper. It is believed this ratio is what is called "coefficient of grinding friction." A high ratio (or coefficient) is desirable (provided a very fine finish is not required) when it is due to sharpness, as from crush-dressing, and as pointed out by the author. However, a high coefficient may also be caused by a loaded wheel face, in which case it is not desirable and results in more heat generated per unit of stock removal. The safe criterion is to maintain sharpness of wheel face.

The paper mentions a method of producing voids in the grinding-wheel structure, which method is employed for a comparatively new type of wheel called "open structure." In the long-established type of vitrified structure, the voids are natural. A volume of sand, even under heavy compression, contains a material percentage of voids. Abrasive, being less rounded, contains a still higher percentage of natural voids.

[5] Research Engineer, Research Laboratories, Mechanical Section, Norton Company, Worcester, Mass.

Author's Closure

The author appreciates the very informative discussion presented by Mr. Flanders and finds the remarks in good agreement with the author's findings. The data presented by Mr. Flanders show higher values for the penetration per revolution in some cases than those investigated by the author. Crushing pressures computed from these data give values less than the upward trend of the curves given in the paper for a 120 and a 180 grit wheel would indicate. It appears that the wheels tested by Mr. Flanders were of a more open structure than those covered in the paper. Recent data taken by the author indicate that the more open the structure the smaller the crushing pressure becomes—all other factors remaining the same. In view of the ideas presented in the paper it seems reasonable to expect that a more open structure would minimize the tendency for the crushing pressure to increase for higher values of the penetration per revolution.

Mr. Moore suggests the use of a light petroleum oil or a solution in water of suitable wetting agents, detergents, film strength additives, and rust preventatives. The author feels that a test comparing the crushing process under the action of various coolants such as air, oil, and various types of soluble coolants would be timely, and give much valuable information.

The author agrees with the points contained in the discussion of Mr. Wagner and appreciates the clarification of points and additional information contaned therein.

An Evaluation of Cylindrical-Grinding Performance

By R. E. McKEE,[1] R. S. MOORE,[2] and O. W. BOSTON[3]

This paper, the third in a series on cylindrical grinding,[4] presents some of the results of an investigation of the grinding process with particular reference to the influence of certain variables, such as, wheel grain, grade, and velocity, table-traverse feed, depth of cut, and type of material.

Testing Conditions

THE machine used in this investigation was a standard Cincinnati No. 2 cylindrical grinder powered with direct-current motors driving the wheel spindle, work spindle, and, table-traverse mechanism. Each of the direct-current motors was controlled with a field-type rheostat, so that conditions of machine operation for each test might be kept constant. Details of the machine operating conditions and motor controls were given in the first paper of the series.[5]

The results given in this paper were obtained when grinding the following materials.

SAE 1020 steel (hot-rolled), 131 Bhn.
SAE 1045 steel (heat-treated), 260 Bhn.
SAE 52100 steel (heat-treated), 653 Bhn.
Cast iron, 187 Bhn, 20,000 psi.
Cast iron, 229 Bhn, 40,000 psi.

In determining the influence of any variable of the grinding process, all other operating conditions were kept constant for each of several values of the variable. The conditions of testing were described in the first paper,[5] and are listed on each figure. The type, volume, and temperature of the grinding compound were kept constant in all tests. It was a clear water-soluble synthetic grinding compound of the emulsion type containing no mineral oil or fat. It was mixed with water at a 5 per cent by volume concentration. It is one of the best compounds used in former evaluation tests.

All of the wheels used in this investigation were produced in the laboratory of the Carborundum Company, Niagara Falls, N. Y.

Definition of Terms

The terms used in this paper were defined in the first two papers[4,5] with the exception of the following.

"Grinding rating," by which is meant the quotient of the volume of metal removed per unit of wheel wear, all in cubic inches, divided by the product of the unit net horsepower (hp_n per cu in. per min), and the surface finish (microinches, rms). This quantity serves to summarize the performance of given conditions of grinding in terms of volume ratio, unit horsepower, and surface finish; thus

$$\text{Grinding rating} = \frac{V_m/V_w}{(hp_n/\text{cu in. per min}) \times (\text{surface finish})}$$

$$= \frac{V_R}{hp_n \times \text{sf}}$$

Production in industry demands a high value of metal removal in a given unit of time, the best surface finish, a low rms value, consistent with a given practice, and a low unit net horsepower. Hence this rating value should be high and should aid in the evaluation of the grinding process by the analysis of a given grinding performance.

Specifications of Materials

The specifications and heat-treatment of the SAE 52100 steel specimens were given in the first paper.[5]

SAE 1020 Steel. This material was obtained in 2-in-diam round bars in a hot-rolled condition and machined to our standard size and shape specifications.[5] The analysis indicates a carbon range of 0.18–0.23 per cent, manganese 0.30–0.60 per cent, maximum phosphorus 0.040 per cent, and maximum sulphur 0.050 per cent. It is highly ductile and generally used in low-stressed parts.

SAE 1045 Steel. This material represents a medium-carbon class of steel, used extensively for highly stressed working parts of machinery, such as spindles, piston rods, gear blanks, crankshafts, etc. It has a carbon range of 0.43–0.50 per cent, manganese 0.60–0.90 per cent, maximum phosphorus 0.040 per cent, and maximum sulphur 0.050 per cent. This material, also purchased in 2-in-diam round hot-rolled bars, was machined to proper specifications,[5] and heat-treated by quenching in water from 1500 F, and tempering at 950 F, to a hardness of 260 Bhn.

20,000-Psi Cast Iron. This material represents a commonly used, relatively soft grade of gray iron which has free-machining characteristics and general damping capacity. It might be used in such parts as machine-tool bases, etc. The analysis of this material gives 3.50 per cent total carbon, 2.50 per cent silicon, 0.70 per cent manganese, 0.010 per cent sulphur, and 0.30 per cent phosphorus. The structure of this material consists of a coarse graphite with a matrix of pearlite and ferrite.

40,000-Psi Cast Iron. This high-nickel cast iron is a type of material used commonly in cylinder blocks, machine housings, Diesel crankshafts, refrigerator crankshafts, etc. The analysis gives 3.25 per cent total carbon, 2.25 per cent silicon, 0.70 per cent manganese, 0.08 per cent sulphur, 0.18 per cent phosphorus, 1.50 per cent nickel, and 0.50 per cent chromium. The structure of this material is a fine graphite with a pearlite matrix.

[1] Assistant Professor of Metal Processing, University of Michigan, Ann Arbor, Mich.

[2] Manager, Detroit Branch, Quaker Chemical Products Corporation, Conshohocken, Pa.

[3] Professor of Metal Processing and Chairman of the Department of Metal Processing, University of Michigan, Ann Arbor, Mich. Fellow ASME.

[4] "Experimental Study of Cylindrical Grinding," by R. E. McKee, R. S. Moore, and O. W. Boston, Trans. ASME, vol. 69, 1947, pp. 891–896.

[5] "An Investigation of the Removal of Metal by the Process of Grinding," by R. E. McKee, R. S. Moore, and O. W. Boston, Trans. ASME, vol. 69, 1947, pp. 125–129.

Contributed by the Special Research Committee on Metal Cutting Data and Bibliography and presented at the Semi-Annual Meeting, Milwaukee, Wis., May 30–June 5, 1948, of The American Society of Mechanical Engineers.

Note: Statements and opinions advanced in papers are to be understood as individual expressions of their authors and not those of the Society. Paper No. 48—SA-9.

Effect of Wheel Velocity on Grinding Performance

Fig. 1 indicates the effect of change in wheel velocity on the evaluative criteria volume ratio, net horsepower, grinding characteristic, and unit horsepower (hp_n per cu in. per min). Three velocities for each of several grades of wheels are used as abscissas.

The wheels used in these tests were type A-abrasive, No. 6-structure, and vitrified bonded. The grain-size and grade specifications of each wheel are indicated on each curve.

At 4500 and 5500 surface ft per min (sfpm), the volume ratios metal removal per unit of wheel wear) follows a similar pattern. In each case the 150-P and 150-Q wheels seem to be more efficient than the 150-O wheel. At 6500 sfpm, the volume ratios of the 150-M, P, and Q wheels remain the same as at the lower speeds, but the 150-O wheel shows much better performance with a volume ratio of 70. Net-horsepower requirements show little variation with a change in peripheral velocity, but there is an indication of an increase in power with an increase in grade of hardness. This indicates that the actual tangential grinding force is reduced as the grinding speed is increased.

In terms of grinding characteristic (volume ratio divided by net

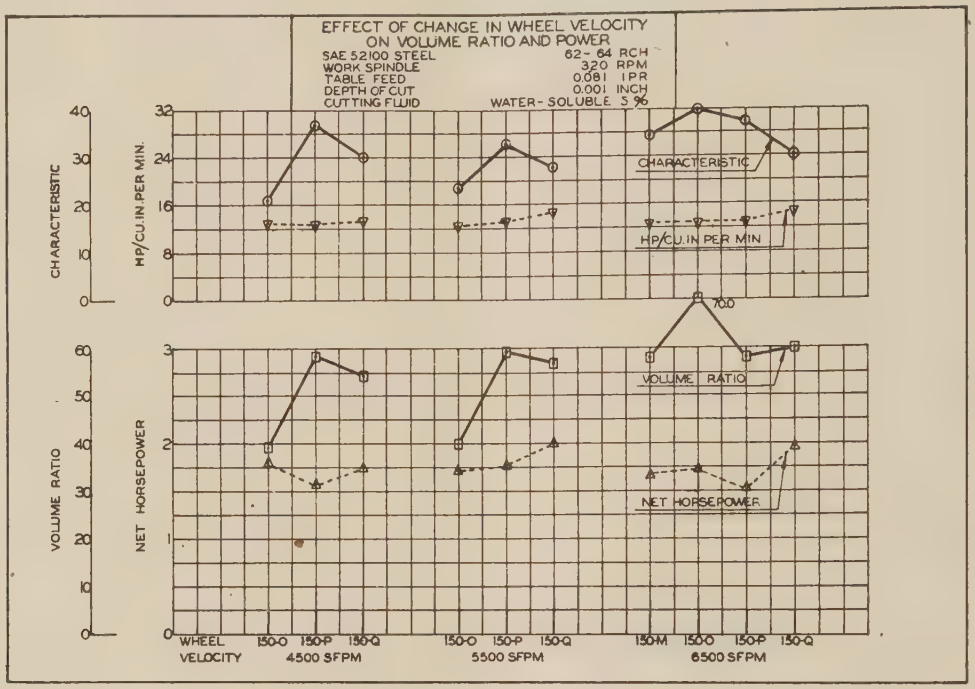

Fig. 1

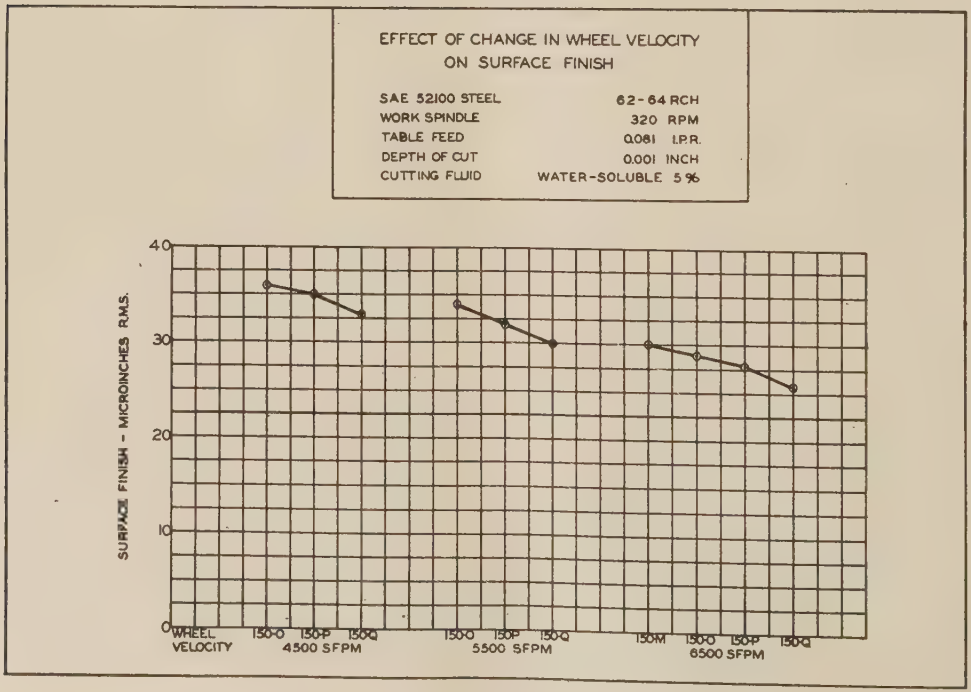

Fig. 2

power) the 150-O, P, and Q wheels seem to function as well at 4500 sfpm as they do at 6500. The 150-O wheel shows an outstanding performance of 6500 sfpm due to the high volume ratio and low power shown in the lower half of the figure. The net horsepower per cubic inch per minute remains practically constant at 13 for all conditions.

In Fig. 2 the value of surface finish in microinches, rms, is plotted as ordinate over the wheel grade and velocity. These readings were made longitudinally on the periphery of the work specimens. There is a definite indication of an improvement in surface finish (lower rms value) as a result of an increase in wheel velocity and a change in grade from O to Q at each velocity. The poorest finish is 36 for the 150-O wheel at 4500 sfpm, and best at 26 for the 150-Q wheel at 6500 sfpm.

Fig. 3 provides a summary of the data given in the preceding figures. The units used as ordinates range from 0.083 (poorest performance) to 0.194 (highest performance). This rating provides an index to high volume ratio, low unit horsepower, and best surface finish.

The peripheral velocity of 6500 sfpm, is better for all grades of

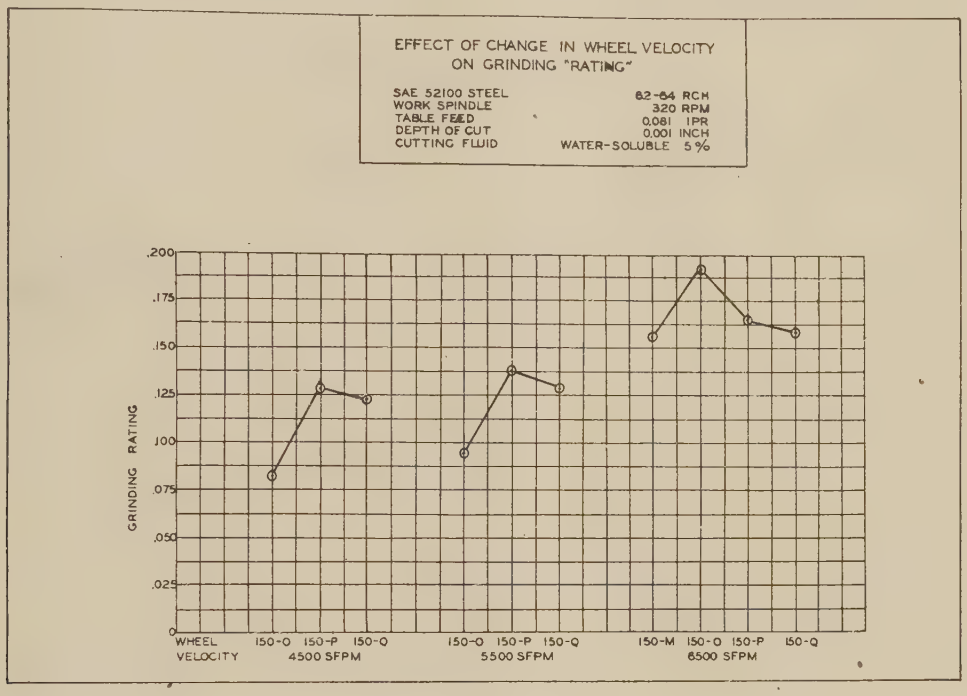

Fig. 3

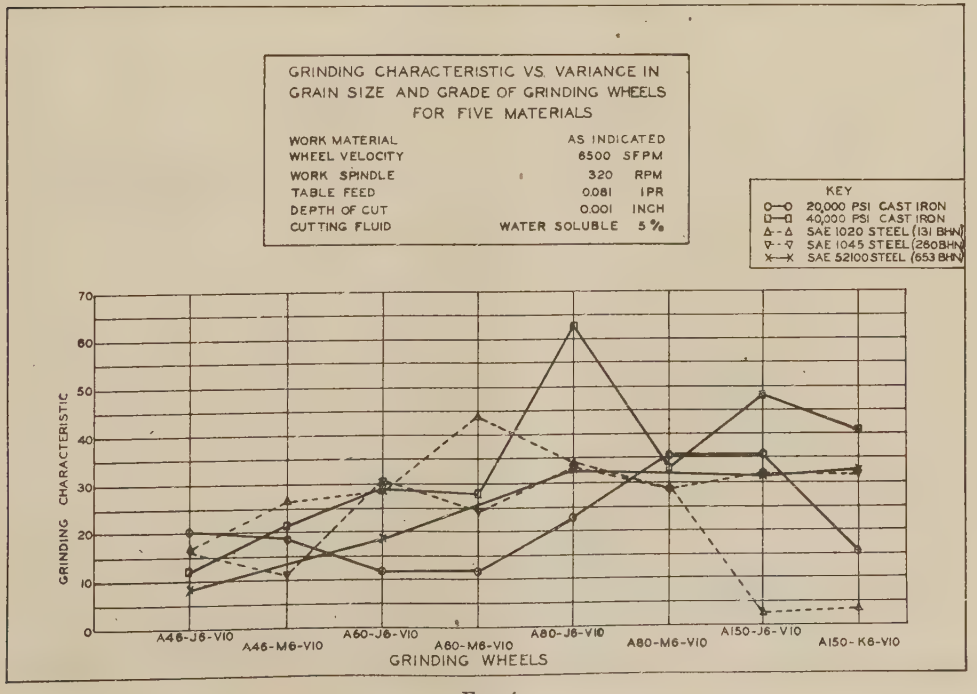

Fig. 4

wheels shown than the lower velocities. Thus for the conditions of grinding shown in this figure, the 150-O wheel operating at 6500 sfpm gives the outstanding performance with the rating of 0.194.

Effects of Variance in Grain Size and Grade of Grinding Wheels as Applied to Five Different Materials

The effect of variance in grain size and grade of grinding wheels on the grinding characteristic (V_R/hp_n) as applied to the grinding of five materials is shown in Fig. 4. The data points on the figure are connected by lines to show relative performances and trends rather than to show the development of curves.

At the table feed and depth of cut shown in the heading, the 46-grain wheels are poor in all cases, the 60-grain wheels give fair performance (except when grinding the 20,000-psi cast iron), the 80-grain wheels are relatively high for all materials, and the 150-grain wheels show good performance on the hard materials, but relatively poor performance on the soft ductile steel (SAE 1020).

In Fig. 5 there is an indication that unit horsepower (hp_n/cu in. per min) may be reduced by a decrease in the grain size of the grinding wheel. This applies to the set of conditions shown in

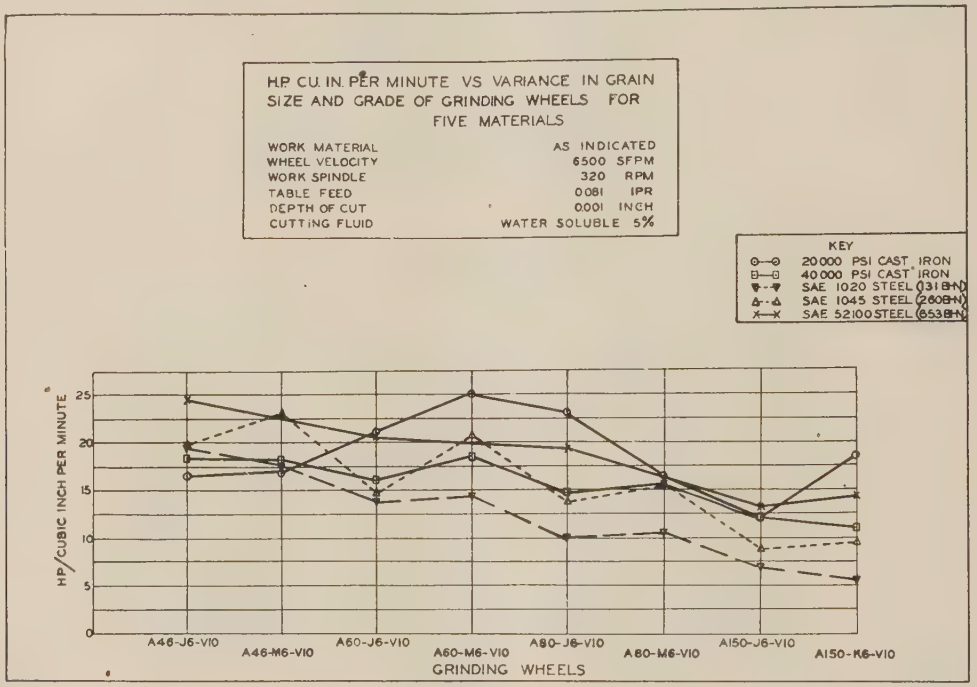

Fig. 5

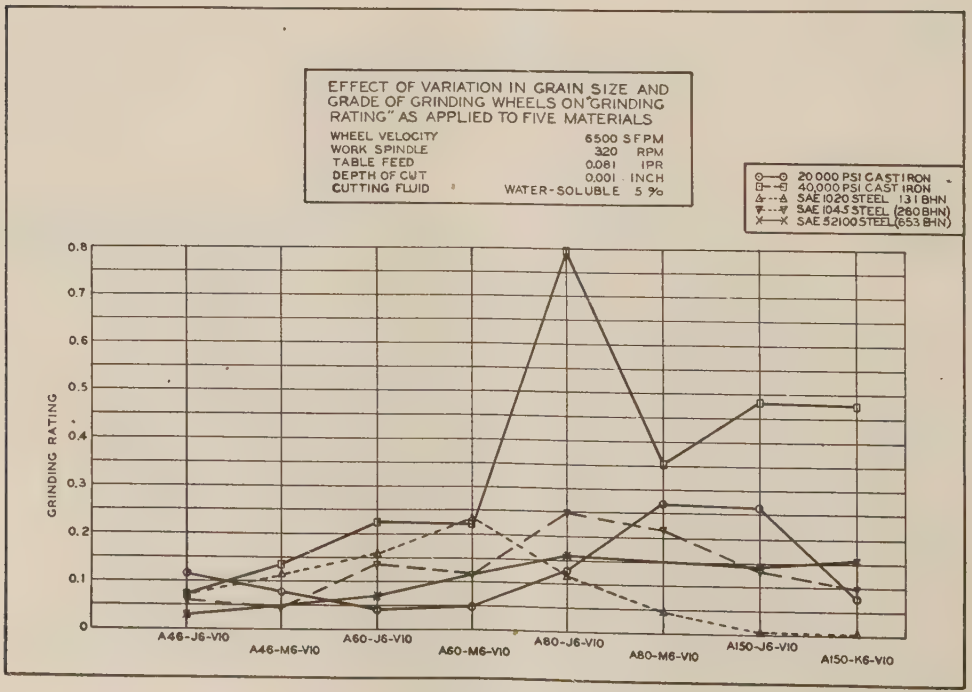

Fig. 6

the heading and would not be representative of more severe conditions of testing with higher table feed or greater depth of cut.

Except for the 20,000-psi cast iron, the unit-horsepower patterns are quite similar for all metals as the wheels are varied. The values increase slightly as the grade becomes harder, but it decreases as the grain size is reduced.

Fig. 6 represents the final "rating" for eight wheels used on five materials with a given table feed and depth of cut. The highest rating indicates the best performance in terms of high volume ratio, low unit horsepower, and low value of surface finish.

For good general grinding conditions, it seems desirable to maintain a volume ratio of at least 50.0 (50 times as much metal removal as wheel wear), a unit horsepower factor of not more than 13.0, and a surface finish of not more than 25 microinches, rms, with no sparkout. For these desirable conditions a "rating" of 0.154 is obtained. In Fig. 6 about 50 per cent of the ratings are above this 0.15 level. Those below seem to be unsatisfactory.

Effect of Variation in Table Feed and/or Depth of Cut

In Figs. 7 to 12, inclusive, various combinations of table feed and depth of cut are used as abscissas when grinding the two steels and two cast irons with the A80-M6-V10 wheel. This is done, primarily, to show the effect of change in either one or both of the factors used as ordinates and to compare the performances for these various combinations. Assuming the depth of cut of 0.001 in. as unity, the data are plotted for 1, 3, 6, and 10X. Again, assuming the table feed 0.081 in. per revolution (ipr) to be unity, the data are plotted 1 and 2X.

In Fig. 7 the SAE 1020 and 1045 steels show similar patterns in the decrease in volume ratio with a 2X table feed and/or a 3X depth of cut. The volume ratio falls off sharply as the size of cut is increased and approaches 0 for the heaviest cut of 2X feed and 3X depth.

The performance of the 80-M grinding wheel on the 20,000-psi cast iron shows a decrease in volume ratio with a 2X table feed, but a sharp increase with a 3X depth of cut. This material also shows excellent performance at 2X table feed and 3X depth of cut.

The 40,000-psi cast iron shows an improvement in performance with the 2X table feed and the 3X depth of cut.

Fig. 8 indicates the sharp increase in net horsepower consumption with an increase of feed, depth, or both. The SAE 1020 and 1045 steels could not be tested satisfactorily beyond 3X depth of cut and 2X table feed as the heavy cuts overloaded the motor. The heavier cuts are more efficient, however, than the light cuts.

The power requirements for the 20,000- and 40,000-psi cast irons level off at the 3X depth of cut and 2X table feed, due to the rapid breakdown of the grinding wheel, with the resultant loss in performance because of lowered speeds at overloaded power.

Fig. 9 is similar to Fig. 7 in the general pattern. It may be noted, in comparing the two figures, that the results on the 40,000-psi cast iron show the severity of increase in power consumption at the 2X table feed with a resultant decrease in grinding characteristic, since net horsepower is placed in the denominator of this quantity.

The unit-horsepower factor is reduced sharply as a result of variation in table feed and/or depth of cut, as shown in Fig. 10. This results from an increase in the volume of metal removed per minute without a proportional increase in the net-horsepower requirement. An increase in table feed or depth of cut will proportionally increase the volume of metal removal per minute and thus increase the mechanical efficiency of the operation, provided that other conditions such as surface finish have not been affected.

A range of 16.5 for the light cuts to 4.0 hp per cu in per min for the heaviest cut is shown in this figure.

Fig. 11 shows the effect of varying the table feed and/or depth of cut on surface finish in microinches, rms. These surface-finish readings represent actual cut conditions with no allowance for sparkout. Readings of 100 microinches and above would not be satisfactory for cylindrical grinding and thus certain conditions and materials (such as the SAE 1020 steel) are completely eliminated when used with the A80-M6-V10 wheel. Surface

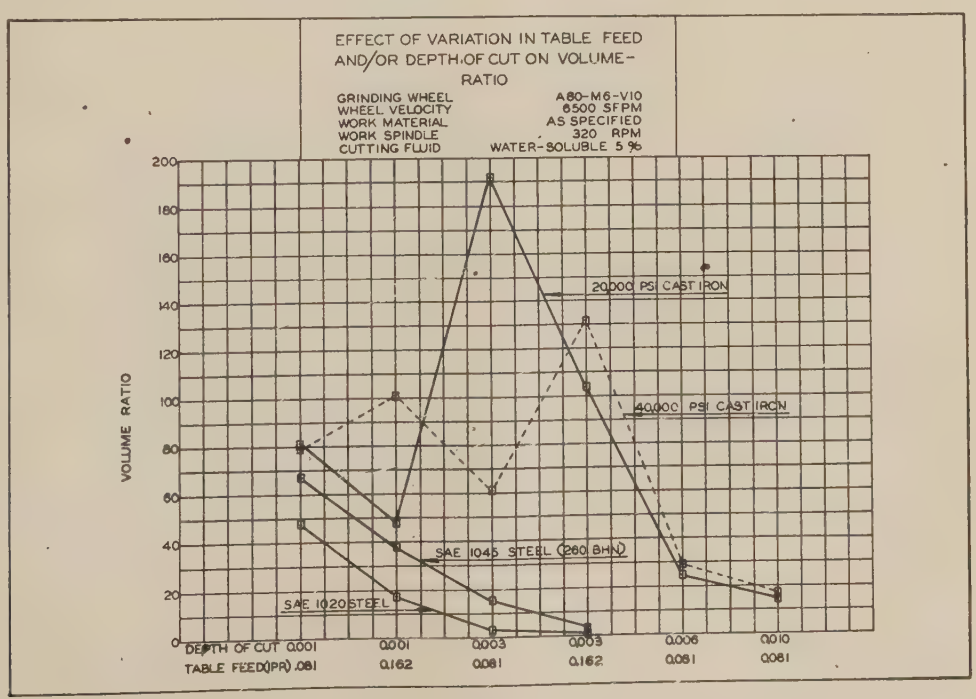

Fig. 7

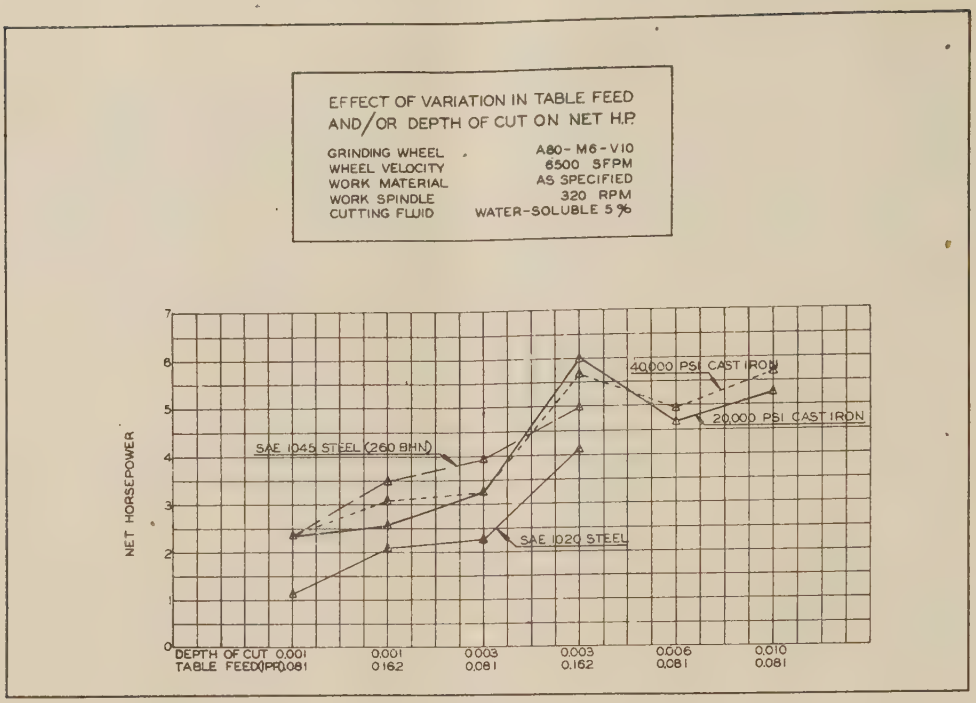
EFFECT OF VARIATION IN TABLE FEED AND/OR DEPTH OF CUT ON NET H.P.
GRINDING WHEEL A80-M6-V10
WHEEL VELOCITY 6500 SFPM
WORK MATERIAL AS SPECIFIED
WORK SPINDLE 320 RPM
CUTTING FLUID WATER-SOLUBLE 5%
NET HORSEPOWER
40,000 PSI CAST IRON
20,000 PSI CAST IRON
SAE 1045 STEEL (260 BHN)
SAE 1020 STEEL
DEPTH OF CUT 0.001 0.001 0.003 0.003 0.006 0.010
TABLE FEED(IPR) 0.081 0.162 0.081 0.162 0.081 0.081

FIG. 8

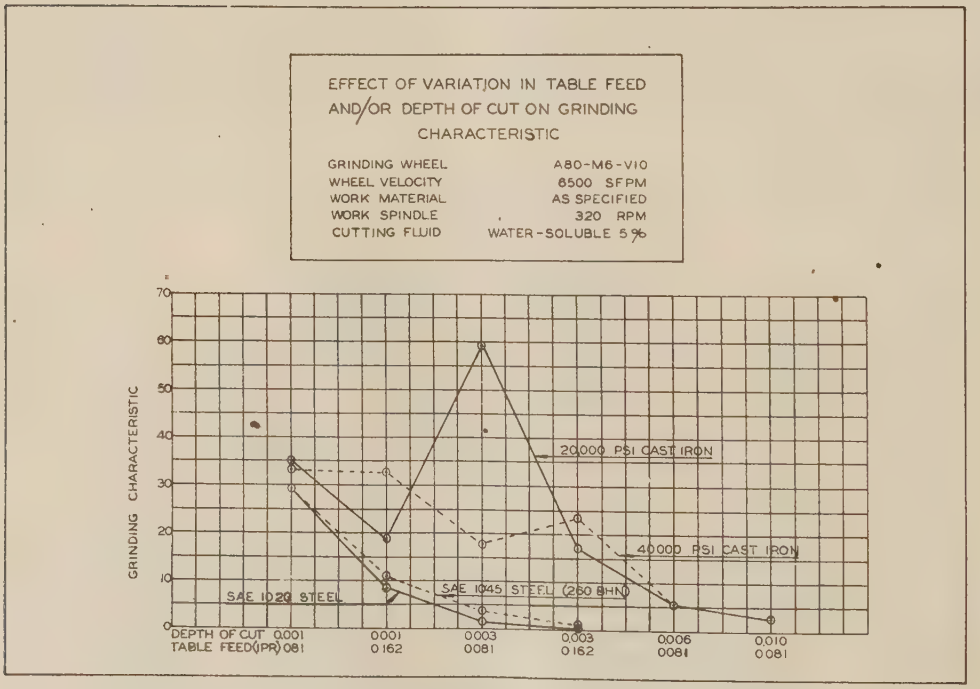
EFFECT OF VARIATION IN TABLE FEED AND/OR DEPTH OF CUT ON GRINDING CHARACTERISTIC
GRINDING WHEEL A80-M6-V10
WHEEL VELOCITY 6500 SFPM
WORK MATERIAL AS SPECIFIED
WORK SPINDLE 320 RPM
CUTTING FLUID WATER-SOLUBLE 5%
GRINDING CHARACTERISTIC
20,000 PSI CAST IRON
40,000 PSI CAST IRON
SAE 1020 STEEL
SAE 1045 STEEL (260 BHN)
DEPTH OF CUT 0.001 0.001 0.003 0.003 0.006 0.010
TABLE FEED(IPR) 0.081 0.162 0.081 0.162 0.081 0.081

FIG. 9

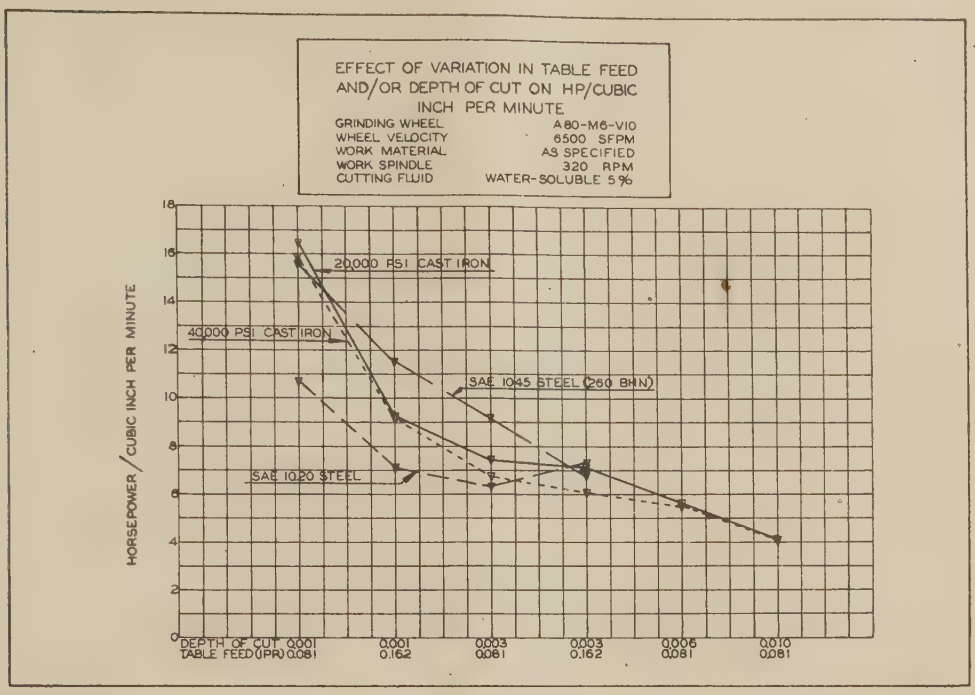
EFFECT OF VARIATION IN TABLE FEED AND/OR DEPTH OF CUT ON HP/CUBIC INCH PER MINUTE
GRINDING WHEEL A80-M6-V10
WHEEL VELOCITY 6500 SFPM
WORK MATERIAL AS SPECIFIED
WORK SPINDLE 320 RPM
CUTTING FLUID WATER-SOLUBLE 5%
HORSEPOWER / CUBIC INCH PER MINUTE
20,000 PSI CAST IRON
40,000 PSI CAST IRON
SAE 1045 STEEL (260 BHN)
SAE 1020 STEEL
DEPTH OF CUT 0.001 0.001 0.003 0.003 0.006 0.010
TABLE FEED (IPR) 0.081 0.162 0.081 0.162 0.081 0.081

FIG. 10

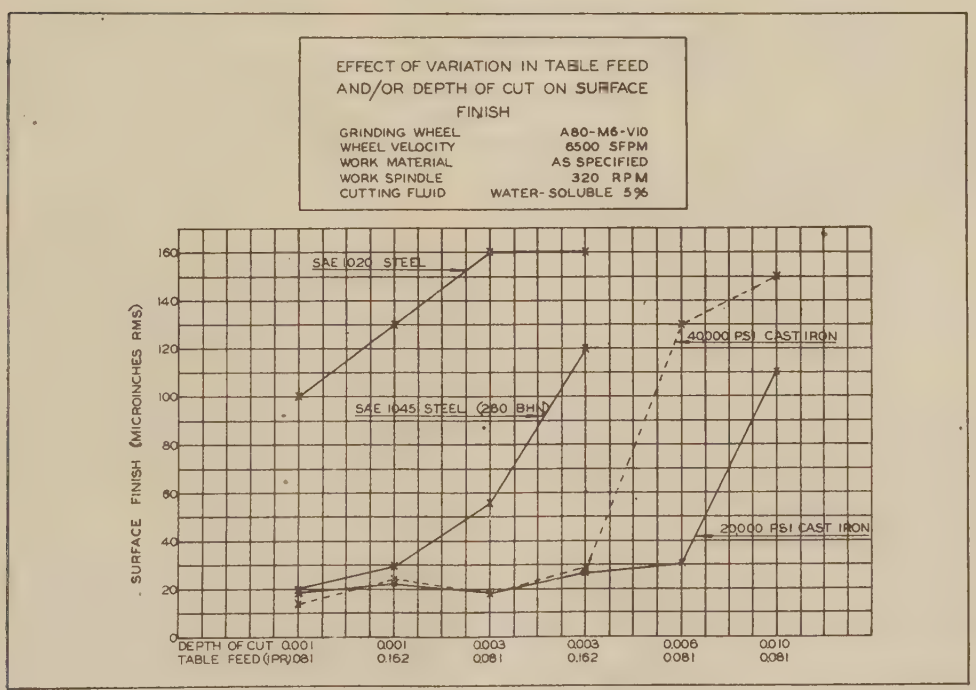
EFFECT OF VARIATION IN TABLE FEED AND/OR DEPTH OF CUT ON SURFACE FINISH
GRINDING WHEEL A80-M6-V10
WHEEL VELOCITY 6500 SFPM
WORK MATERIAL AS SPECIFIED
WORK SPINDLE 320 RPM
CUTTING FLUID WATER-SOLUBLE 5%
SURFACE FINISH (MICROINCHES RMS)
SAE 1020 STEEL
40,000 PSI CAST IRON
SAE 1045 STEEL (280 BHN)
20,000 PSI CAST IRON
DEPTH OF CUT 0.001 0.001 0.003 0.003 0.006 0.010
TABLE FEED (IPR) 081 0.162 0.081 0.162 0.081 0.081

FIG. 11

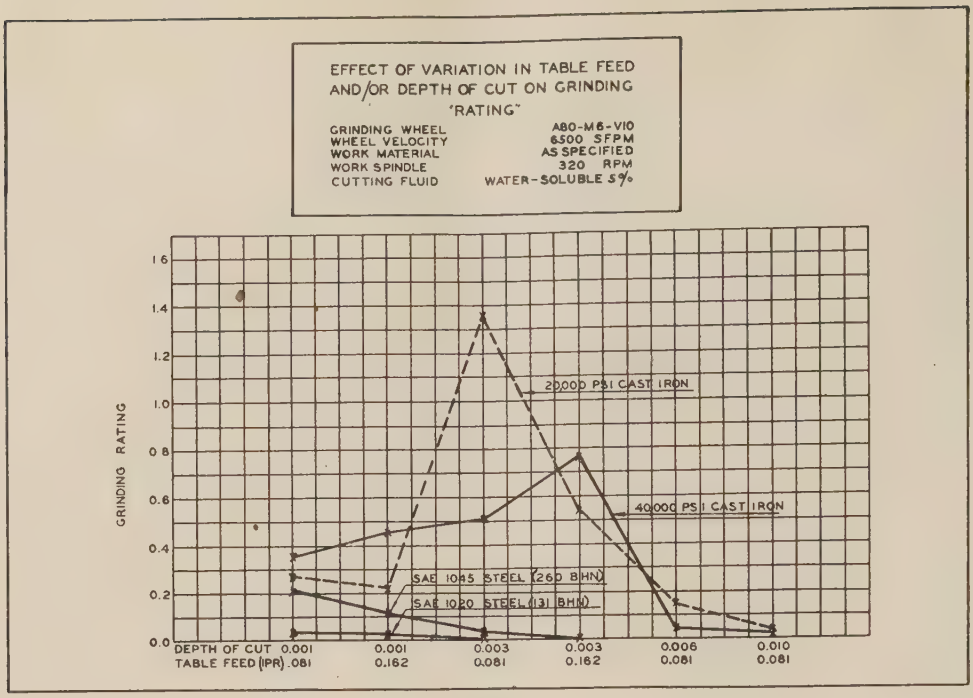

FIG. 12

finishes of 20 microinches may be considered excellent for this type of grinding with no allowance for sparkout.

Fig. 12 gives the final ratings of the four materials ground with the A80-M6-V10 wheel under each of several conditions of table feed and depth of cut.

A rating of less than 0.15 might be considered poor for steel, and those above this rating generally acceptable. The SAE 1020 and 1045 steels are eliminated on the basis of poor performance, with the exception of the latter steel at 0.001 depth of cut and 0.081 ipr table feed.

A higher minimum rating of 0.20 for cast iron might be acceptable, as most of the points for cast iron are above 0.20 on this figure. The 20,000 and 40,000-psi cast irons give excellent performance with the 80-M wheel at a 3X depth of cut and a 2X table feed.

The greater depths of cut, i.e., 6X and 10X, are eliminated for all materials ground with the 80-M wheel.

Summary

1 A change in the peripheral velocity of a grinding wheel will affect its relative performance in terms of (1) volume ratio (metal removal per unit wheel wear), (2) unit net horsepower, and (3) surface finish. The data submitted in this paper support the use of 6500 sfpm as the proper peripheral velocity for a grinding wheel used in external cylindrical grinding.

2 With a set of conditions of 0.001 in. depth of cut and 0.081 ipr table feed, the unit net-horsepower requirement may be reduced appreciably by a decrease in grain size, but slightly increased with the use of harder grades for a given grain size.

3 A grinding rating of at least 0.154 might indicate favorable conditions, such as, a volume ratio of 50.0, a unit net horsepower of 13.0, and a surface finish of 25 microinches.

4 An increase in table feed and/or depth of cut will reduce the volume ratio, increase the net power requirement, and give a poorer surface finish as applied to the grinding of steel.

5 An increase in table feed and/or depth of cut may increase the volume ratio, decrease the unit net power requirement, and give a poorer surface finish in the grinding of the cast irons.

6 Cast iron may be ground satisfactorily with aluminous-oxide grinding wheels, and a volume ratio up to 192 times as much metal removal as wheel wear has been recorded in this operation.

Acknowledgment

This work was done as an Engineering Research Project in the Department of Metal Processing, University of Michigan. The program was initiated and sponsored by the Quaker Chemical Products Corporation of Conshohocken, Pa.

Discussion

J. S. KOZACKA.[6] This paper, together with other papers presented by the authors on this subject, is a step forward in taking the art of removal of metal by grinding into the field of science. Test results obtained so far are of value to the users of grinding wheels as well as to the manufacturers who are striving to develop better products.

Of general value are the terms volume ratio, horsepower, characteristic, horsepower per cubic inch per minute, and percentage increase in horsepower, as they give methods of evaluating the qualities of the grinding wheels, in general, and the self-dressing qualities in particular.

The wheels used in the tests, were of uniform grit size, and uniformity in performance may be expected from such wheels. On the other hand, had the tests been run long enough, over the entire life of the grinding wheels, the results presented by the investigators might have been somewhat different, for as the wheel wears, even at constant speed, other conditions remaining the same, the wear may become a function of the size of the wheel.

It would be of general interest if a standardized procedure of testing grinding wheels for hardness was developed in connection with the performance tests. This hardness-testing procedure

[6] Associate Professor of Mechanical Engineering and Director of Shop Laboratory, University of Illinois, Chicago Branch, Chicago, Ill. Mem. ASME.

should be applicable to wheels of different density structure and to the wheels possessing porous structure. Uniformity of wheel hardness over its entire surface might be indicative of its ability to perform consistently. Standardized marking of grinding wheels is a great help in their selection. However, the hardness of grinding wheels so designated varies quite widely, so much so, that a grinding wheel marked A 150 J 6V10 by one maker, may be harder than a grinding wheel made and marked the same way by another maker.

In surface-grinding tests of grinding wheels on tungsten-carbide cutting tools conducted under the writer's direction at Vascoloy-Ramet Corporation, for the purpose of determining the best silicon-carbide grinding wheels for the job, it has been found that the self-dressing qualities of the wheels vary from wheel to wheel, and even within the wheel itself when it is run at a constant peripheral speed, other conditions remaining the same. One hundred commercial-type silicon-carbide wheels of different make, hardness, density, porosity, and grit sizes 80, 100, and 120 were tested under actual shop operating conditions over the entire life of the wheels. Results obtained indicated lower temperature for the finer-grit-size wheels, resulting in less loss of carbide tools because of cracks, and more cubic inches of carbide removed per wheel life, that is, higher volume ratio. All wheels were soft enough to possess the self-dressing feature so necessary in the economical production of tungsten-carbide tools. In these tests it was found that some grinding wheels, identified with the same marking, used by the same operator, on the same machine, and all conditions of grinding remaining constant, gave a volume ratio which varied up to 100 per cent.

Of interest too would be the data on grinding-wheel performance running at cutting speeds 3000, 4000, 5000, and 6000 fpm.

Authors' Closure

We appreciate Professor Kozacka's discussion of this paper and agree wholeheartedly with his comments regarding the availability of wheels of a specific grade of hardness which are uniform throughout. This has been the desire of industry for years to obtain exact duplications of wheels uniform throughout and meeting the same specifications of wheels formerly used.

We, too, found that as the wheels wear, their hardness or grade varies along the radius but perhaps of greater significance is the variation found along the face of the wheel, or on opposite diameters. This caused differences in grinding between the two sides of the wheel, as the work traversed from right to left and from left to right. In our work to overcome the variation in grade along the radius, we first found it necessary to dress off some of the periphery, after which the wheel wear was kept small. That is, in any single series of tests, we wore the wheel from approximately $13^1/_2$ inches to not less than 12 inches in diameter.

The authors have developed and used a test of their own for selecting wheels for each series of tests to eliminate the variations in wheels. This, we believe, is in accordance with the suggestion of Professor Kozacka. The variation in wheels, however, is the greatest uncontrolled variable in the grinding process.

Heat Transfer Through Thick Insulation on Cylindrical Enclosures

By T. S. NICKERSON[1] and G. M. DUSINBERRE[2]

A graph is presented for finding the heat transfer through relatively thick insulation applied to an enclosure having the form of a short cylinder such as a tank. Incorrect treatment of the corner effect in this case may lead to serious error. The "relaxation" method of calculation was used.

Nomenclature

The following nomenclature is used in the paper:

L = length of uninsulated cylinder
D = diameter of uninsulated cylinder
x = thickness of insulation
A_i = inner area of insulation
A_o = outer area of insulation
A_m = effective area for heat transfer
Δt = temperature difference
k = thermal conductivity
q = heat transfer per unit time
f = area ratio

Any consistent units may be used.

Method of Estimating

It is often required to estimate the heat transfer through insulation applied to an enclosure of specified shape. The following assumptions are frequently justified:

(*a*) The insulation is homogeneous and the variation of its conductivity with temperature is negligible.

(*b*) The insulation is applied in slabs or shapes so as to have a constant thickness.

(*c*) The inner surface of the insulation is isothermal at a given temperature, and the outer surface is isothermal at another given temperature.

Under these conditions it is convenient to take the thickness of the insulation as an effective length of path for heat flow, and to find an effective area of path such that the heat transfer can be calculated by the usual equation for a flat slab

$$q = A_m \frac{k}{x} \Delta t \quad [1]$$

In general, A_m will have some mean value between the inside and outside areas, A_i and A_o; A_i will generally be fixed, while A_o will depend upon the selected thickness of insulation. It will be convenient to set up an area ratio

$$f = \frac{A_m}{A_i} \quad [2]$$

so that

$$q = f A_i \frac{k}{x} \Delta t \quad [3]$$

and f will depend only upon the geometry of the system.

For enclosures of any shape, provided x is small in comparison with any other dimension of the system, it is most convenient and quite satisfactory to take the effective area as the arithmetic mean of the inner and outer areas, or

$$f = \frac{A_i + A_o}{2A_i} \quad [4]$$

This is because the special effect of curvature and of corners will become negligible. This calculation may properly be used for walls of buildings, large furnaces or ovens, and the like. There may even be no great error in assuming $f = 1$.

When the enclosure is a long cylinder, such as a pipe, with axial heat flow negligible, it is readily shown that the effective area is the logarithmic mean of the inner and outer areas, and

$$f = \frac{A_o - A_i}{A_i \ln (A_o/A_i)} \quad [5]$$

For a spherical enclosure the geometric mean is appropriate. In these cases if the insulation is thick the use of the arithmetic mean would cause appreciable error.

When the enclosure is rectangular the analytical solution is extremely difficult and, to the authors' knowledge, has not been accomplished. However, for this case we have the studies and experiments of Langmuir[3] and others, expressed in the form of equations, and found most readily in the text by McAdams.[4]

A common form of enclosure in engineering practice is the tank, which may be approximated as a short cylinder with flat ends. The analytical solution of this case is also not known to have been obtained. However, a numerical solution is possible, has been undertaken, and the results are presented in Fig. 1.[5]

The shape of any right circular cylinder can be expressed as the ratio of diameter to length, D/L. The shape of the insulation can be expressed in terms of this ratio and the ratio of insulation thickness to cylinder diameter, x/D. Fig. 1 gives the area ratio f in terms of these parameters for a range of values commonly encountered. The method of determining these curves is outlined in the Appendix.

As the work reported here is purely mathematical, the question of accuracy pertains to the relation between the initial assumptions and the final conclusions. Just as the accuracy of a series solution depends upon the number of terms calculated, so the accuracy of a numerical solution depends upon the scale of subdivision used. In simpler cases where a comparison is possible,

---

[1] Engineer, E. I. du Pont de Nemours and Company, Belle, W. Va. Jun. ASME.

[2] Department of Mechanical Engineering, University of Delaware, Newark, Del. Mem. ASME.

Contributed by the Heat Transfer Division and presented at the Annual Meeting, Atlantic City, N.J., December 1–5, 1947, of The American Society of Mechanical Engineers.

Note: Statements and opinions advanced in papers are to be understood as individual expressions of their authors and not those of the Society. Paper No. 47—A-63.

[3] "Flow of Heat Through Furnace Walls; the Shape Factor," by Irving Langmuir, E. Q. Adams, and G. S. Meikle, Trans. American Electrochemical Society, vol. 24, 1913, p. 53.

[4] "Heat Transmission," by W. H. McAdams, second edition, McGraw-Hill Book Company, Inc., New York, N.Y., 1942, p. 13.

[5] The details of this work constitute a thesis submitted by T. S. Nickerson in partial fulfillment of the requirements for the degree of master of science at Virginia Polytechnic Institute.

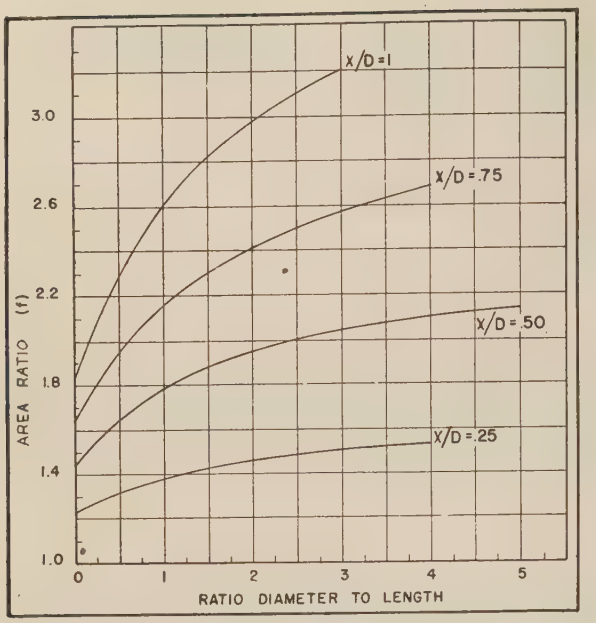

FIG. 1

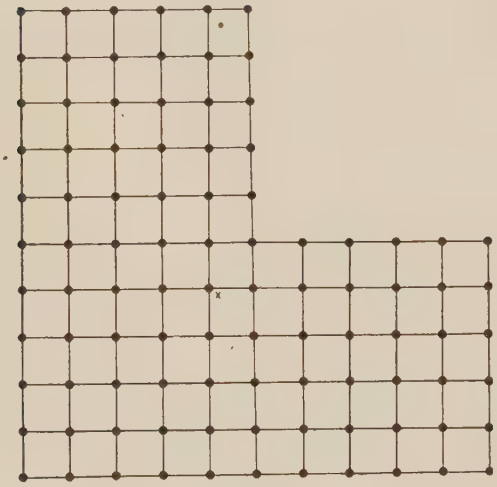

FIG. 2

the authors find that a numerical solution on the present scale will agree with the analytical solution within 3 per cent, and that may be taken as an estimate of the accuracy of the present work.

EXAMPLE

A tank 2 ft in diameter and 4 ft long is insulated with 1 ft of cork having a conductivity of 0.025 Btu/(hr)(sq ft)(deg F/ft). The temperature of the inner surface of the insulation will be —30 F and of the outer surface, 70 F. Estimate the heat flow.

Solution:

$\Delta t = 70 - (-30) = 100$ F
$D/L = 2/4 = 0.5$
$x/D = 1/2 = 0.5$

From Fig. 1

$f = 1.65$

$$A_i = 2 \times \frac{\pi}{4} \times 2^2 + \pi \times 2 \times 4 = 31.4 \text{ sq ft}$$

TABLE 1 TEMPERATURE DISTRIBUTION CORRESPONDING TO FIG. 2

0	30	63	101	146	200	...	...	...	...	...
0	30	63	101	146	200	...	...	...	...	...
0	29	62	100	145	200	...	...	...	...	...
0	28	60	97	143	200	...	...	...	...	...
0	26	56	92	139	200	...	...	...	...	...
0	23	50	83	128	200	200	200	200	200	200
0	19	41	67	98	132	146	152	155	156	156
0	14	31	50	70	89	101	108	112	114	114
0	10	21	33	45	56	64	70	73	74	74
0	5	10	16	22	27	31	34	36	37	37
0	0	0	0	0	0	0	0	0	0	0

TABLE 2 AREA RATIOS CALCULATED BY RELAXATION

x/D	D/L	F	x/D	D/L	f	x/D	D/L	f	x/D	D/L	f
1/4	8/5	1.43	1/2	1	1.79	3/4	4/9	1.92	1	1/3	2.15
	2	1.46		5/3	1.90		4/5	2.08		1	2.59
	8/3	1.49		5/2	2.00		4/3	2.26		3	3.19
	4	1.53		5	2.13		4	2.68		...	..

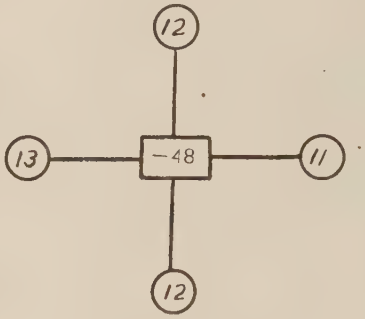

FIG. 3

By Equation [3]

$$q = 1.65 \times 31.4 \times \frac{0.025}{1} \times 100 = 129.6 \text{ Btu per hr}$$

The use of Equation [4] for this system, would give $f = 2.10$, an error over 27 per cent. Equation [5] would give $f = 1.89$, an error over 14 per cent. If conduction had been assumed negligible in the corners between flat and cylindrical surfaces, then $f = 1.36$, an error over 17 per cent.

Appendix

The method of calculation is that outlined by Emmons.[6] By considerations of symmetry the problem is reduced to the two-dimensional treatment of an L-shaped portion of the cylinder and its base. A uniform rectangular spacing of reference points was chosen and the conductance between points was made proportional to the radius.

A typical system (for $D/L = 1$ and $x/D = 0.5$) is shown in Fig. 2. A point such as x has the "relaxation pattern"[7] shown in Fig. 3. The calculated temperature distribution for this system is shown in Table 1. Temperatures were assumed 0 deg F at the outer surface and 200 F at the inner surface. Calculations were carried out to the nearest unit, and were continued until the residuals were small and evenly distributed, and the heat transfer at the outer and inner surfaces agreed within 4 per cent or better. The average of these was used to calculate f. Values found by relaxation of such systems are shown in Table 2.

As L becomes very large, the system degenerates to that of the infinite cylinder, and values can be calculated by Equation [5] for $D/L = 0$. These values were also used to interpolate beyond the point where temperatures at the mid-plane were found to differ negligibly from those in the infinite cylinder.

Points obtained in all these ways were plotted and the curves of Fig 1 were drawn through them.

---

[6] "The Numerical Solution of Heat-Conduction Problems," by H. W. Emmons, Trans. ASME, vol. 65, 1943, p. 607.

[7] The term "relaxation pattern" is used here in the same sense as by Emmons[6] and should not be confused with temperature distribution as shown in Table 1.

Discussion

H. G. Elrod, Jr.[8] By means of fifteen calculations with the numerical method, the authors have provided solutions for a triply infinite class of heat-conduction problems. Their success points the way to further applications of the same method and warrants the following consideration of the conditions under which the method will be useful:

The authors' method (numerical solution plus two-dimensional graph) is applicable to a series of solids describable by two shape parameters, composed of a single isotropic substance, and bounded by (A) surfaces at constant source temperature T_i, (b) surfaces at constant sink temperature T_0, and (C) surfaces across which no heat transfer occurs ($\partial T/\partial n = 0$). The conductivity of the solid material may be any physically possible function of temperature. The heat transfer is found by computing the flow appropriate to an assumed constant conductivity K_c and multiplying by the factor

$$\frac{1}{k_c}\int_{T_0}^{T_i}\frac{kdT}{T_i - T_0}$$

Although well known to mathematicians, the following proof of the foregoing statements does not appear in standard heat-transfer texts:

The exact differential equation for steady-state heat transfer in isotropic solids is

$$\nabla \cdot K\nabla T = 0 \quad \ldots\ldots [6]$$

Since

$$K > 0, \quad L \equiv \int^T K dT$$

has a one-to-one correspondence with temperature. Hence Equation [6] becomes

$$\nabla^2 L = 0 = (L_i - L_0)\nabla^2\left(\frac{L - L_0}{L_i - L_0}\right) \equiv (L_i - L_0)\nabla^2\psi \quad \ldots [7]$$

The function ψ has the value unity on surfaces (A), the value zero on surfaces (B), and its normal derivative vanishes on surfaces (C). Hence ψ is unique.

The heat transfer across surfaces (A) is given by

$$Q = \int_{S_A}\int K\nabla T \cdot d\vec{S} = \left(\frac{L_i - L_0}{T_i - T_0}\right)\left\{\int_{S_A}\int \nabla\psi \cdot d\vec{S}\right\}(T_i - T_0) \quad \ldots [8]$$

For constant conductivity

$$\frac{L_i - L_0}{T_i - T_0} = K_c$$

so that

$$Q_c = K_c\left\{\int_{S_A}\int \nabla\psi_c \cdot d\vec{S}\right\}(T_i - T_0) \quad \ldots [9]$$

But

$$\psi_c = \frac{T - T_0}{T_i - T_0} = \psi$$

by the preceding uniqueness requirement.

Hence

$$Q = \frac{Q}{Q_c}\cdot Q_c = \frac{1}{K_c}\left(\frac{L_i - L_0}{T_i - T_0}\right)Q_c = \frac{1}{K_c}\frac{\int_{T_0}^{T_i} K dT}{(T_i - T_0)}Q_c \quad \ldots [10]$$

[8] Student. Harvard University, Cambridge, Mass. Jun. ASME.

Now if D is some characteristic length of a series of solids of the same shape, then we may define

$$X' \equiv \frac{X}{D};\ Y' \equiv \frac{Y}{D};\ z' \equiv \frac{z}{D};\ \nabla\psi = \frac{1}{D}\nabla'\psi \quad \ldots\ldots [11]$$

Hence if Q_1 is the heat flow corresponding to $D = 1$

$$Q_D = \left(\frac{L_i - L_0}{T_i - T_0}\right)\left\{\int_{S_A}\int \frac{1}{D}\nabla'\psi \cdot D^2 d\vec{S'}\right\}$$

$$(T_i - T_0) = DQ_1 \quad \ldots\ldots [12]$$

Thus a single point on a chart such as the authors' Fig. 1 can provide the solution for all solids of a given shape and of widely different conductivity properties. Since the chart has two degrees of freedom, results for two shape parameters can conveniently be represented.

C. M. Fowler.[9] The authors of this paper have brought forward a point in favor of numerical solutions to heat-flow problems that is frequently overlooked.

Most people working in this field concede the utility of numerical methods for working specific problems, but are apt to criticize the method for its lack of parameterization when compared to analytic solutions when they can be found.

The authors, however, have furnished a very convincing counter-example to this criticism by obtaining a relatively small number of solutions to the finite, insulated, enclosed cylinder, and parameterizing their data to treat the general case for this cylinder.

The writer's only question concerns the accuracy of their tabulated data. Although the function f, approaches the correct limit as $D/L \to 0$, the writer would like to know if the authors checked some of their data using finer space increments than those shown in Fig. 2, for larger values of f.

To the writer's knowledge, the only exact solution by perfect relaxation is that for the one-dimensional slab. For example, the cylinder with negligible end effects when the relaxation has been carried to the limit, has the solution

$$T_r = \frac{T_a - T_b}{\psi(a) - \psi(b)}\cdot\psi(r) + \frac{T_b\psi(a) - T_a\psi(b)}{\psi(a) - \psi(b)}$$

with

$$\psi(r) = \sum_{k=0}^{k=n}\frac{1}{k + 1/2}$$

Here, T_a and T_b are the temperatures on the inner and outer walls.

On the other hand the analytical solution has the $\psi(r)$ function replaced by the logarithm of the same arguments in the foregoing equation.

If the number of subdivisions is very small, the two solutions may be considerably different, although it is possible that the numerical solution may give engineering accuracy, in spite of this.

Victor Paschkis.[10] The problem dealt with by the authors is one of considerable interest and importance, and the development of charts for the solution of the problem is desirable. Therefore the authors have earned the thanks of people having to solve such problems continuously.

However, the value of the chart, Fig. 1, is greatly reduced by the assumption (C), of an isothermal surface of the insulation. In

[9] Physics Department, University of Michigan, Ann Arbor, Mich.

[10] Technical Division, Heat and Mass Flow Analyzer Laboratory, Columbia University, New York, N. Y. Mem. ASME.

most practical cases the boundary conductance h, at least on the cold surface, cannot be neglected, and it would be desirable to have charts including different h values. Moreover, the curves in Fig. 1 are too widely spaced for comfortable interpolation.

In the example, the authors try to show the necessity of a more accurate calculation than hitherto customary by comparing their result with those obtained by using Equation [4] or [5], respectively.

The writer has always contended that the geometric mean gives a better approximation than the arithmetic mean. In the case of the present example, the geometric mean would lead to a value of $f = 1.79$ or an error of only 8.5 per cent.

The magnitude of error in the example is very large and larger than for most practical cases for two reasons: (a) the authors selected an unusual value of x/D; and (b) they neglect the h value, as just stated. Insulation of more practical thickness (resulting in a smaller x/D), and the introduction of the h value would reduce materially the error; for most practical cases it is sufficiently accurate to base work on the geometric mean.

Authors' Closure

The authors wish to thank Messrs. Elrod, Fowler, and Paschkis for the interest shown in this paper. Mr. Elrod's extension of the applicability of the results is a valuable contribution. In answer to Mr. Fowler's question pertaining to the accuracy of the results, the case of $D/L = 3$, $x/D = 1$, with $f = 3.19$ was relaxed using a network half again as fine as the one originally used. The change of the factor f was less than one per cent.

The purpose of this paper is to present a convenient method of solving the heat transferred through unusually thick insulation applied to cylindrical enclosures having a high D/L ratio. The authors have calculated the error resulting from the use of the geometric-mean area for each of the networks reported in Table 2. Curves have been drawn of per cent error against D/L ratio for the ranges covered by Fig. 1. The work is too long to be reported here; however, for the 13 networks reported in Table 2 the minimum error is 10.5 per cent and the maximum is 17.9 per cent. In general, the error increases with both x/D and D/L. The authors feel that the curves offer an appreciable advantage over the use of the geometric-mean area.

The paper is limited to the case of infinite surface coefficients. The magnitude of the error introduced by this assumption may be calculated in the case of infinitely long cylinders by the equation

$$\text{Per cent error} = 1 - \frac{fkh_oA_o + xh_ih_oA_o + h_iA_ifk}{xh_ih_oA_o}$$

where h_i and h_o are inside and outside surface coefficients, respectively. It is suggested that this equation be used to indicate the order of magnitude of the error in the case of cylinders of finite length. The error will always be negative. If the indicated error is too large it becomes necessary to solve the problem by relaxation.

Condensation on Six Finned Tubes in a Vertical Row

BY D. L. KATZ[1] AND J. M. GEIST,[2] ANN ARBOR, MICH.

Condensing heat-transfer coefficients for Freon-12, *n*-butane, acetone, and water were obtained for six horizontal finned tubes in a vertical row. The over-all heat-transfer coefficients were measured for each tube at a series of water velocities and were plotted by the method of Wilson to obtain the condensing coefficients. The differences between experimental and predicted coefficients for the top tube were less than 14 per cent, and the average condensing coefficient for the six tubes was less than 10 per cent below that for the top tube. The finned surface was entirely effective for condensation even for organic liquids having a tendency to be retained by the fins under static conditions.

Nomenclature

The following nomenclature is used in the paper:

A_{eq} = total effective outside surface finned tubes, sq ft
A_t = horizontal surface finned tubes, sq ft
A_f = area of fins, sq ft
D_{eq} = equivalent diameter of finned tube for use in Nusselt's equation, in. or ft
D_2 = diameter over fins, in. or cm
D = root diameter finned tubes, in. or cm
g = acceleration due to gravity, ft/hr²
h = condensing film coefficient, calculated from Nusselt's equation for single tube, Btu/(hr)(deg F)(sq ft)
k = thermal conductivity of condensing vapor at average film temperature, Btu/(hr)(deg F)(ft)
L = equivalent vertical height of finned tube, in.
n = number of tubes in vertical row
q = heat transferred, Btu per hr
T_1 = average cooling-water temperature for runs with Freon-12, deg F
T_2 = average cooling-water temperature for runs with other material, deg F
U_0 = over-all heat-transfer coefficient based upon outside surfaces, Btu/(hr)(deg. F)(sq ft)
ΔT = mean temperature difference between cooling water and condensing vapor, deg F
V = cooling water velocity, fps
Δt = mean temperature difference between metal and condensing vapor, deg F
λ = latent heat of vaporization of condensate, Btu per lb
ρ = density of condensate at average film temperature, lb per cu ft
μ = viscosity of condensate at average film temperature, lb per ft per hr
b = factor to be supplied to (n) for finned tubes in a vertical row
γ = surface tension of liquid adhering to fins, dynes/cm
s = spacing between fins, cm

Introduction

This research was conducted to determine if heat-transfer coefficients for liquids of high surface tension would follow the prediction of Nusselt (1)[3] when condensing on a vertical row of horizontal finned tubes.

Condensation coefficients for heat transfer depend on the thickness and properties of the liquid film on the surface. Increases in the rate of condensation increase the film thickness and hence the condensation coefficients are diminished. The dripping of liquid from one tube to lower tubes in a multitube condenser increases the film thickness on the lower tubes, and reduces the coefficients for the lower tubes, as compared with the top tube. Measurements on a bank of plain tubes (2) indicated that the effect of the number of tubes in a vertical row is less than that predicted by Nusselt's theory (1).

For film-type condensation of a saturated vapor outside a vertical row of n horizontal tubes, Equation [1] has been derived by assuming viscous flow of liquid from the tubes, transfer of heat through the liquid film by conduction, and idealized boundary conditions (1)

$$h_{\text{mean}} = 0.725 \left(\frac{k^3 \rho^2 g \lambda}{n D \Delta t \mu} \right)^{1/4} = \frac{h_{\text{single tube}}}{n^{0.25}} \quad \ldots\ldots\ldots [1]$$

This equation, modified for single finned tubes (3, 4), has been shown to apply to the vertical surface of the fins and the horizontal tube surface. Measurements on a commercial condenser, having an average of 3.2 finned tubes per row (5), indicated that Equation [1] would apply to Freon-12 for multitube condensers.

In translating data for condensing refrigerants on finned tubes into expected performance for petroleum or organic chemicals, differences in physical properties should be considered. Static tests to determine the liquid retention on finned tubes indicated that liquids of high surface tension and low density adhered to the bottom of the finned tubes and increased the film thickness (see Appendix 1). Any retention of liquid under dynamic conditions would be most significant for the lower tubes in a vertical row.

Equipment and Procedure

The experimental work was conducted on a condenser having six horizontal finned tubes in a vertical row. A reboiler supplied the vapors to be condensed. Fig. 1 shows the equipment, and Fig. 2 is a line diagram of material flow.

The condenser shell was constructed from a 10-in. pipe, 3 ft long, with tube sheets $1^1/_2$ in. thick welded on each end. Fig. 3 gives the tube-sheet layout. Three sight glasses were installed in the shell of the condenser for visual observation of the condensation. The condenser, reboiler, and lines were insulated.

Copper integral finned tubes with $^5/_8$ in. root diam were used. The tubes had 15 actual fins per in., but are listed as nominal 16 fins per in. The dimensions of the tubes are given in Table 1,

---

[1] Professor. Chemical Engineering, University of Michigan. Mem. ASME.

[2] Graduate Student, University of Michigan.

Contributed by the Heat Transfer Division and presented at the Annual Meeting, Atlantic City, N. J., December 1–5, 1947, of The American Society of Mechanical Engineers.

 Paper No. 47—A-96.

[3] Numbers in parentheses refer to the Bibliography at the end of the paper.

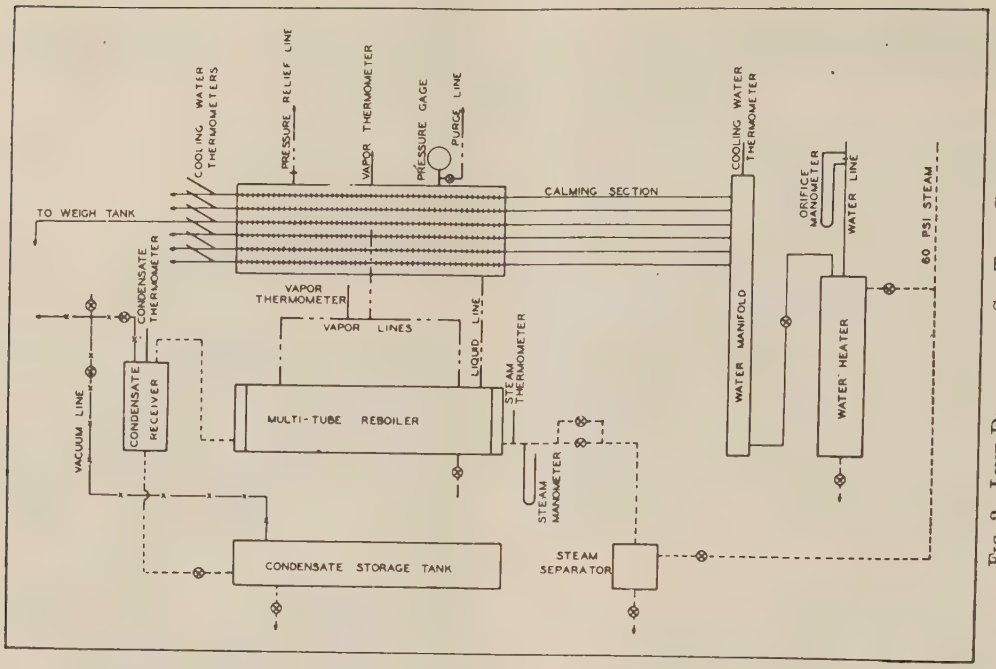

FIG. 2 LINE DIAGRAM OF SIX-TUBE CONDENSER

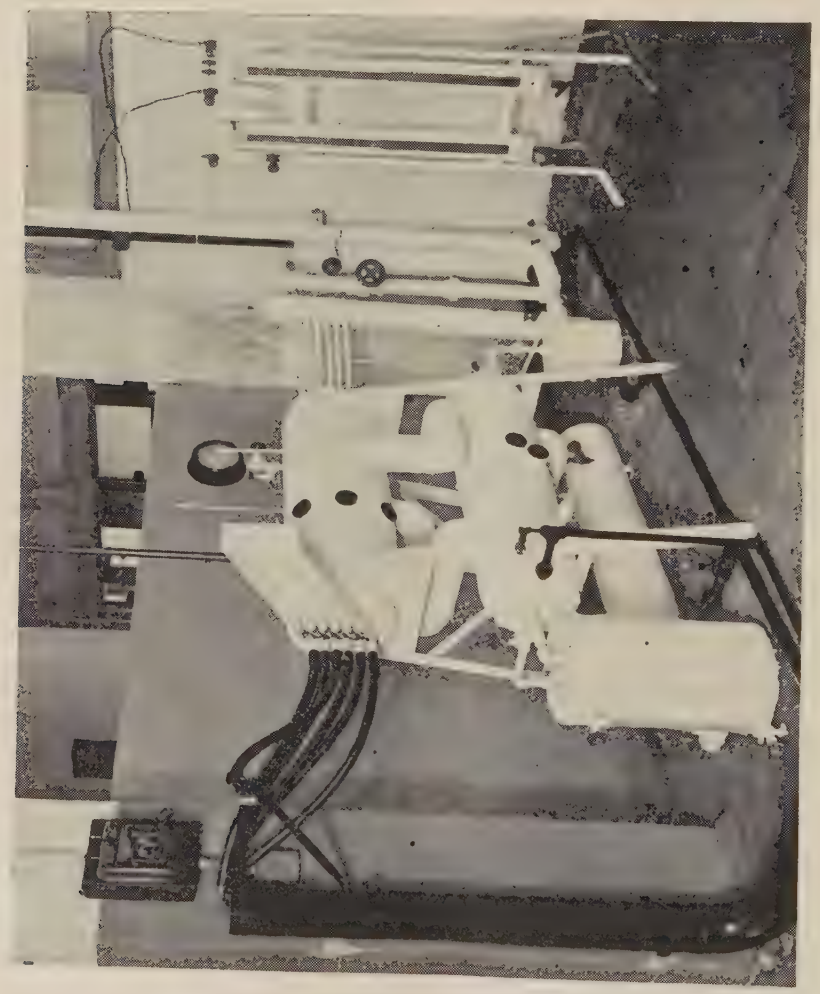

FIG. 1 TEST APPARATUS

TABLE 1 PHYSICAL DIMENSIONS OF TUBES FOR CONDENSER

Distance between tube sheets = 35⁷/₈ in.
Integral, spiral-finned, copper tubes, nominal 16 fins per in.

Tube No.	Root Dia. D ins.	Dia. Over Fins D_2 ins.	Dia. of Plain Ends ins.	Nominal Inside Dia. ins.	Actual Number Fins/in.	Length of Finned Section ins.	Actual Outside Area sq.ft.	Equivalent Dia. for Nusselt Eq. D_{eq} ins.	Ratio of Outside Area to Outside Area of 3/4-inch Plain Tube
1	0.621	0.746	0.750	0.555	15.0	34-3/8	1.452	0.116	2.46
2	0.621	0.747	0.750	0.555	15.0	34 1/4	1.457	0.116	2.46
3	0.621	0.745	0.750	0.555	15.0	34-3/8	1.444	0.116	2.46
4	0.621	0.747	0.750	0.555	15.0	34-3/8	1.462	0.116	2.46
5	0.621	0.745	0.750	0.555	15.0	34-1/4	1.440	0.116	2.46
6	0.621	0.746	0.750	0.555	15.0	34-1/4	1.449	0.116	2.46

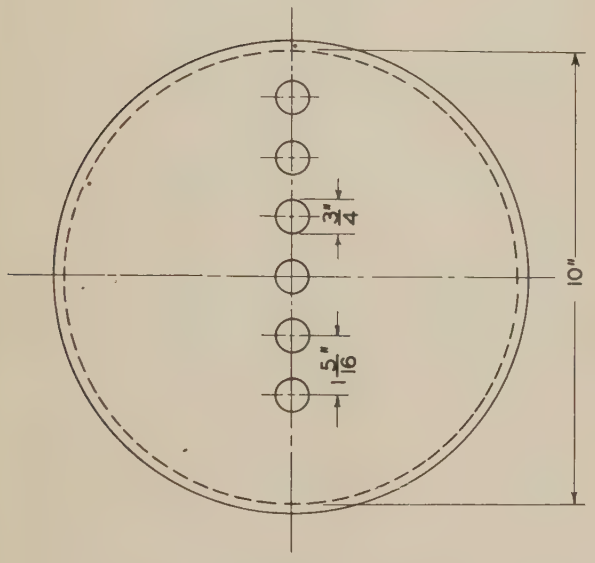

FIG. 3 END VIEW OF CONDENSER, INDICATING SPACING OF FINNED TUBES

and a typical fin profile, as measured with an optical micrometer, is given in Fig. 4. The tubes were rolled into the tube sheets. The tubes were smooth on the inside.

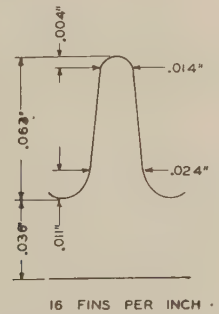

FIG. 4 PROFILE OF FIN CROSS SECTION AS MEASURED WITH AN OPTICAL MICROMETER
(Copper tubes, integral fins, ⅝ in. root diam.)

A heat exchanger was used for preheating the cooling water to the desired temperatures before the water entered the manifold which fed the tubes. Approximate water rates were measured with an orifice manometer; a weigh tank was used for measuring actual water rates. Before obtaining the heat-transfer data, the relative rates of flow between tube 3 and the remainder of the tubes were determined by simultaneous measurements in two weigh tanks at a series of water rates. When taking the heat-transfer data, only the water from tube 3 was collected and weighed. The rates of water flow for the other tubes were obtained from the calibration curves, and the maximum variation between tubes was 5 per cent.

Calibrated thermometers with 0.1 deg F graduations were installed for measuring the entering cooling-water temperature and the temperature of the cooling water leaving each tube. For measuring the temperatures of the vapor line and the saturated vapor, thermometers with 0.5-deg F graduations were installed. A calibrated pressure gage gave the pressure in the condenser. A calibrated condensate receiver for the steam from the reboiler was used to obtain data for heat balances.

Before charging the heat-transfer fluid, the condenser and reboiler were evacuated to less than 1 mm Hg abs pressure. After the materials were charged, the system was purged to a vent line several times. Because the pressure of the system during the water runs was below atmospheric, it was necessary to purge from the system into an evacuated tank.

Since the condensing film coefficients were to be determined from modified "Wilson" plots (3, 6), measurements for each material were made at five condenser water rates. Preliminary observations were made with cooling-water velocities of 4.5 and 12.5 fps to determine the range of temperatures and pressure over which satisfactory measurements were possible. The temperature and pressure of the system were then set at values which could be maintained over the range of velocities.

For the first run, the cooling-water rate was set at about 4.5 fps and kept constant by reducing the fluctuations of the water-orifice manometer to a minimum. The rate was measured by recording the time necessary for collecting 300 to 400 lb of cooling water. The temperature of the condensing vapor was maintained constant by manual control of the steam to the reboiler. The temperatures of the entering and leaving cooling water, the temperature and pressure of the condensing vapor, and the temperature of the vapor in the transfer line were recorded at about ½-min intervals. The temperature and pressure of the steam to the reboiler, the temperature of the condensate, and the rate of accumulation of the steam condensate were also recorded.

Subsequent runs at higher water rates were similarly performed with one exception. The cooling water was preheated so that the average cooling-water temperature in the top tube, and the mean temperature difference between the condensing vapor and the cooling water in the top tube were maintained at a constant value for all the runs with the same material. Duplicate runs were made at each water velocity, after purging for 1 min, to determine

TABLE 2 SUMMARY OF MEASURED AND CALCULATED DATA

Material	Run No.	Average Bulk Water Temp. °F - Tube No. 1	Average Saturated Vapor Temp. °F	Average Mean Temp. Difference °F.	Average Water Velocity Ft. Per Sec.	U_o - Heat Transfer Coefficient Btu / (Hr.) (°F) (Sq. Ft. Outside Surface)							Water Rate - Pounds Per Hour						Temperature Rise of Water Degrees					
						Tube 1	Tube 2	Tube 3	Tube 4	Tube 5	Tube 6	Average	Tube 1	Tube 2	Tube 3	Tube 4	Tube 5	Tube 6	Tube 1	Tube 2	Tube 3	Tube 4	Tube 5	Tube 6
Freon - 12	28	67.66	107.70	40.04	4.56	191.1	175.6	185.2	168.6	169.0	162.7	175.4	1693	1716	1735	1693	1777	1686	6.56	6.01	6.20	5.88	5.55	5.66
	29	67.73	107.70	39.97	4.58	191.3	176.0	185.4	169.4	169.3	162.7	175.7	1700	1723	1742	1700	1784	1693	6.53	5.99	6.17	5.87	5.53	5.63
	30	67.71	107.77	40.06	6.42	210.2	195.7	201.9	191.1	187.7	182.3	194.8	2388	2415	2437	2388	2495	2381	5.12	4.75	4.80	4.71	4.38	4.48
	31	67.83	107.70	39.87	6.39	209.0	194.0	202.0	189.5	191.2	181.5	194.5	2377	2404	2428	2377	2484	2370	5.09	4.71	4.81	4.67	4.36	4.46
	32	67.77	107.68	39.91	8.59	223.8	210.4	217.4	207.9	203.9	198.0	210.2	3202	3231	3254	3202	3332	3189	4.06	3.80	3.86	3.80	3.54	3.61
	33	67.83	107.69	39.86	8.60	226.0	212.6	219.0	207.7	204.3	198.9	211.4	3205	3234	3257	3205	3335	3192	4.08	3.83	3.88	3.79	3.53	3.62
	34	67.75	107.70	39.95	10.71	233.3	220.5	226.7	218.9	211.1	206.4	219.5	3992	4033	4057	3992	4154	3976	3.39	3.19	3.23	3.21	2.94	3.02
	35	67.77	107.71	39.94	10.71	235.4	222.6	228.2	220.3	213.1	209.3	221.5	3982	4033	4057	3992	4154	3976	3.42	3.22	3.25	3.23	2.97	3.06
	36	67.71	107.69	39.98	12.44	242.7	230.5	234.5	224.1	222.7	217.5	228.7	4635	4686	4710	4635	4823	4616	3.04	2.87	2.88	2.87	2.67	2.74
	37	67.64	107.70	40.06	12.45	237.7	227.8	232.4	222.9	218.3	215.8	225.8	4639	4690	4714	4639	4827	4620	2.98	2.84	2.84	2.82	2.62	2.72
N - Butane	38	68.35	148.53	80.18	4.50	212.8	205.6	213.2	195.3	197.1	190.3	202.4	1672	1694	1713	1672	1754	1665	14.82	14.23	14.44	13.78	13.11	13.40
	39	68.27	148.52	80.25	4.51	212.5	206.1	212.7	195.0	196.5	189.6	202.1	1677	1699	1718	1677	1759	1670	14.77	14.23	14.38	13.73	13.05	13.32
	40	68.57	148.54	79.97	6.34	234.0	228.1	237.9	221.7	221.3	213.5	226.1	2357	2383	2405	2357	2463	2350	11.53	11.18	11.43	11.03	10.42	10.59
	41	68.51	148.50	79.99	6.34	233.4	229.7	238.3	222.1	222.4	215.4	226.9	2359	2385	2407	2359	2465	2352	11.49	11.24	11.44	11.04	10.46	10.67
	42	68.47	148.55	80.08	8.57	255.4	251.5	262.4	246.6	243.7	235.2	249.1	3196	3225	3248	3196	3326	3183	9.29	9.11	9.34	9.05	8.49	8.60
	43	68.41	148.61	80.20	8.57	253.2	249.1	260.0	244.9	242.1	233.7	247.2	3195	3224	3247	3195	3325	3182	9.23	9.04	9.27	9.00	8.45	8.57
	44	68.43	148.50	80.07	10.67	264.1	260.5	272.5	256.3	253.2	244.4	258.5	3978	4019	4043	3978	4140	3962	7.72	7.57	7.79	7.55	7.08	7.18
	45	68.45	148.50	80.05	10.68	263.6	261.1	273.4	257.9	254.1	246.0	259.4	3979	4030	4044	3979	4141	3963	7.70	7.58	7.81	7.59	7.10	7.22
	46	68.44	148.50	80.06	12.39	268.6	266.4	277.5	263.5	258.5	249.6	264.0	4619	4670	4694	4619	4807	4600	7.76	6.66	6.83	6.68	6.22	6.31
	47	68.53	148.57	80.04	12.35	270.1	268.4	279.4	264.2	260.1	251.5	265.6	4603	4655	4678	4603	4790	4584	6.82	6.73	6.90	6.72	6.28	6.38
Acetone	48	74.01	153.92	79.91	4.60	254.5	244.8	249.0	228.7	227.4	221.8	237.7	1709	1732	1751	1709	1793	1702	17.28	16.53	16.49	15.78	14.82	15.28
	50	73.90	153.99	80.09	4.61	254.5	245.8	251.5	231.1	230.1	223.0	239.4	1713	1736	1755	1713	1797	1706	17.28	16.59	16.64	15.93	14.98	15.35
	51	73.84	154.00	80.16	6.43	289.6	280.9	289.8	269.4	265.1	258.1	275.5	2394	2421	2445	2394	2502	2387	14.08	13.59	13.76	13.25	12.36	12.67
	52	73.92	154.00	80.08	6.43	290.4	282.3	290.5	269.6	264.7	256.9	275.7	2391	2418	2440	2391	2499	2384	14.12	13.66	13.80	13.27	12.35	12.62
	53	73.87	153.92	80.05	8.60	324.3	313.7	324.4	303.6	296.2	287.9	308.4	3208	3237	3260	3208	3338	3195	11.75	11.33	11.52	11.12	10.32	10.53
	54	73.93	154.00	80.07	8.60	323.8	313.7	324.2	304.9	296.1	288.0	308.4	3204	3233	3256	3204	3334	3191	11.75	11.35	11.54	11.18	10.33	10.55
	55	74.05	153.95	79.90	10.68	349.1	337.8	348.8	326.8	318.0	308.9	331.6	3982	4023	4047	3982	4144	3966	10.17	9.80	9.96	9.62	8.80	9.08
	56	74.03	153.98	79.95	10.68	350.1	338.2	348.5	327.0	318.1	310.4	332.0	3981	4022	4046	3981	4143	3965	10.21	9.82	9.96	9.63	8.91	9.13
	57	73.87	153.96	80.09	12.40	367.5	355.5	363.9	340.4	332.6	323.8	347.3	4620	4672	4695	4620	4808	4601	9.25	8.90	8.98	8.66	8.04	8.22
	58	73.94	153.91	79.97	12.38	367.9	354.9	365.2	344.6	335.3	327.9	349.3	4613	4665	4688	4613	4801	4594	9.26	8.88	9.01	8.76	8.10	8.32
Water	59	68.13	145.10	76.97	8.60	452.8	451.5	476.3	465.5	477.1	457.7	463.5	3207	3256	3259	3207	3337	3194	15.78	15.66	16.20	16.28	15.84	16.03
	60	68.36	144.95	76.84	10.76	506.9	506.8	535.7	515.9	520.3	499.2	514.1	4011	4052	4076	4011	4174	3994	14.10	14.01	14.54	14.42	13.82	13.93
	61	67.99	144.91	76.92	12.43	539.9	540.0	568.4	549.3	545.3	523.7	544.4	4632	4683	4707	4632	4820	4613	13.02	12.93	13.38	13.31	12.57	12.68

if noncondensable gases were affecting the measurements. Because of the limitations of the reboiler, condensing-steam coefficients were measured at only the three highest cooling-water rates.

Freon-12, *n*-butane, acetone, and water were selected as test fluids to give a wide range of ratios of surface tension to density (see Appendix 1). Satisfactory performances for Freon-12, *n*-butane, and acetone on a vertical bank of finned tubes should indicate that finned-tube condensers would be effective for most organic materials.

The Freon-12 was the commercially available refrigerant purchased from Kinetic Chemicals, Inc., the *n*-butane was purchased as 99 per cent pure from the Phillips Petroleum Company, the acetone was purchased as C.P. from the Commercial Solvents Corporation, and the water was laboratory distilled.

Visual Observations

Visual observations were made (through the sight glasses) of the condensate dripping from the tubes. The description of condensate flow applies to the runs for Freon-12, *n*-butane, and acetone. The rate of condensation of water vapor was so small that the amount of condensate flowing from tube to tube was also very small. Despite prolonged periods of operation, the condensation of water appeared to be predominantly dropwise rather than filmwise.

At low cooling-water rates, the amount of condensate dripping from tube 2 appeared to be about twice the amount dripping from tube 1. Tube 3 was slightly bowed as a result of the rolling operation, and a portion of the liquid from tube 2 did not appear to drip on tube 3. Equal amounts of condensate appeared to be dripping from tubes 3, 4, 5, and 6. Some of the condensate did not fall to the tubes below but splashed to the sides owing to the motions imparted in draining from the fins. At increasing rates of condensation (higher cooling-water rates), the fraction of condensate splashing to the sides, rather than impinging on the tubes below, increased.

At low rates of condensation, the condensate fell from the tubes in drops; at high rates of condensation, continuous streams of condensate flowed from the tubes at intervals of about 3 in. The points from which the dripping or streaming took place seemed to oscillate. This was probably due to the spiral motion imparted by the fins.

Calculation of Results

From the observed data, the over-all coefficients of heat transfer in Btu per hour per degree F per square foot outside surface, and the water velocities in feet per second, were calculated as given in Table 2, and indicated in Fig. 6. A modified Wilson plot (6) was made in order to obtain the condensing film coefficients at infinite water velocity. The Wilson plot consists of the reciprocal of the over-all coefficient versus the reciprocal of the 0.8 power of the water rate. The intercept is equal to the resistance of the condensing vapor, the metal wall, and any fouling. The slope depends upon the physical properties of the cooling water and the condenser tubing. One modification consisted of a correction factor to include the effect of temperature on the physical properties of cooling water (3). By the use of the correction factor $(1 + 0.011T_1)/(1 + 0.011T_2)$ on the velocity term, the same slope was used for a given tube, independent of the material. Because of slight variations in the dimensions of the tubing, there were variations in the slopes of the Wilson plots for a given material, for each of the six tubes.

It has been shown that although the original Wilson plot requires a constant temperature difference between the tube wall and the condensing vapor, a satisfactory plot will result if a constant temperature difference between cooling water and condensing vapor is maintained (3). Fig. 5 is the Wilson plot for acetone condensing on the copper tubes with 16 (nominal) fins per in. An example calculation required to obtain condensing coefficients is given in Appendix 2.

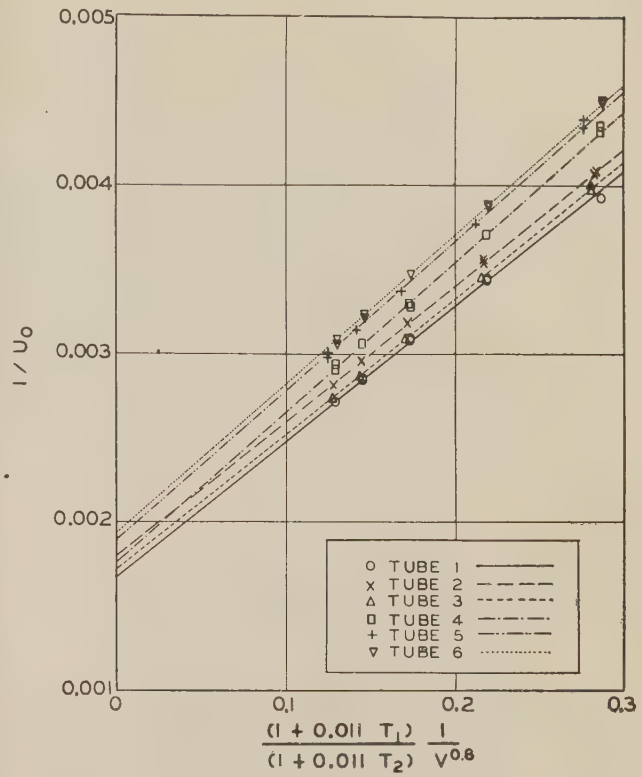

Fig. 5 Wilson Plot for Acetone
(Horizontal finned-tube condenser, six tubes in a vertical row, 5/8 in. root diam, 16 fins per in.)

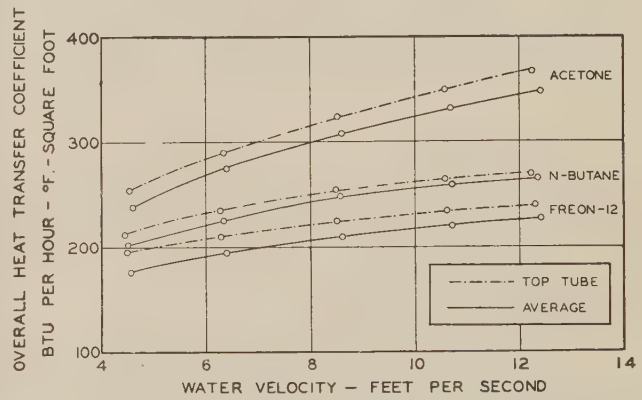

Fig. 6 Comparison of Over-All Heat-Transfer Coefficients for Top Tube and Average of Six Tubes in a Row
(Horizontal condenser; copper tubes, 16 fins per in., 5/8 in. root diam.)

Tables 3 and 4 list the experimentally determined condensing film coefficients and compare the coefficients with those calculated from the Nusselt equation. Rather than applying the equations for the horizontal and vertical surfaces to relative areas represented, Equation [1] is used with the following definitions of the equivalent diameter (3) based upon the fraction horizontal and the fraction vertical surface

$$\frac{1}{D_{eq}^{1/4}} = \frac{0.943}{0.725}\frac{A_f}{A_{eq}L^{1/4}} + \frac{A_t}{A_{eq}D^{1/4}} \quad \ldots\ldots\ldots [2]$$

TABLE 3 CONDENSING FILM COEFFICIENTS
Copper tubes, 16 fins per in., 5/8 in. root diam

	Freon - 12 Condensing Temp. 107.7°F 40°F ΔT (overall)				n - Butane Condensing Temp. 148.5°F 80°F ΔT (overall)				Acetone Condensing Temp. 154.0°F 80°F ΔT (overall)				Water Condensing Temp. 145.0°F 77°F ΔT (overall)			
Tube No.	Intercept on Wilson Plot	Experimental Coefficient *	Coefficient Calculated From Nusselt Equation	Ratio of Experimental to Calculated Coefficient	Intercept on Wilson Plot	Experimental Coefficient *	Coefficient Calculated From Nusselt Equation	Ratio of Experimental to Calculated Coefficient	Intercept on Wilson Plot	Experimental Coefficient *	Coefficient Calculated From Nusselt Equation	Ratio of Experimental to Calculated Coefficient	Intercept on Wilson Plot	Experimental Coefficient *	Coefficient Calculated From Nusselt Equation	Ratio of Experimental to Calculated Coefficient
1 (top)	0.00304	332	387	0.86	0.00256	395	420	0.94	0.00167	610	581	1.05	0.00070	1490	1920	0.78
2	0.00330	306	264	1.16	0.00262	386	286	1.35	0.00180	565	397	1.42	0.00070	1490	1310	1.14
3	0.00317	318	232	1.37	0.00246	411	251	1.64	0.00171	595	348	1.71	0.00070	1490	1148	1.30
4	0.00326	309	212	1.46	0.00256	395	230	1.72	0.00176	578	318	1.82	0.00070	1490	1052	1.42
5	0.00338	299	200	1.50	0.00262	386	217	1.78	0.00190	535	301	1.78	0.00070	1490	993	1.50
6	0.00346	292	189	1.55	0.00273	370	204	1.82	0.00194	523	283	1.85	0.00070	1490	935	1.60
Average		309	247	1.25		390	268	1.46		568	371	1.53		1490	1226	1.21

*Condensing film Coefficients in Btu/(hr.)(°F)(sq. ft. outside surface)

TABLE 4 COMPARISON OF CONDENSING FILM COEFFICIENTS FOR TOP TUBE AND AVERAGE OF SIX TUBES

Copper tubes, 16 fins per in., 5/8 in. root diam

Material	Experimental coefficient for tube 1, h_1	Average experimental coefficient for six tubes, h_m	Ratio of coefficient for tube 1 to average coefficient, (h_1/h_m)	b*
Nusselt's Theory	h_1	h_m	1.565	1.0
Freon-12	332	309	1.073	0.22
Butane	395	391	1.010	0.017
Acetone	610	568	1.073	0.22
Water	1490	1490	1.000	0.0

* b in equation $h_m = \frac{h_1}{(bn)^{0.25}}$.
Coefficients in Btu/(hr) (deg F) (sq ft outside surface).

where

D_{eq} = equivalent diameter of horizontal finned tube, ft
A_f = area of fins, sq ft
A_t = area of horizontal tube having diameter equal to root diameter, sq ft
$A_{eq} = A_t + A_f \times$ fin efficiency, sq ft
D = root diameter, ft
L = average height of finned area, ft

The fin efficiency was greater than 0.95 for all conditions and was used as 100 per cent in this paper, as indicated in the example calculation in Appendix 3.

The coefficient calculated by Nusselt's equation for tube 2 was obtained from the coefficient for tube 1 by the following relation, as derived from Equation [1]

$$h_2 = [n^{0.75} - (n-1)^{0.75}]h_1 = 0.683h_1 \quad [3]$$

A similar calculation was made for the lower tubes.

The deviation between the experimental and predicted coefficients for the top tube (tube 1) for organic liquids is less than 14 per cent and is as close as that previously found (3, 4). The data indicate that the decrease in condensing coefficients for tubes below the top tube is much less than that predicted by Nusselt. This is not surprising since the liquid dripping from one tube may not strike the tube below, nor does it necessarily increase the film thickness over the entire heat-transfer area. Also, the effect of turbulent flow of the liquid would tend to increase the coefficients over the calculated values for the lower tubes in the row. The values of b, given in Table 4, multiplied by n give an indication of the effective number of finned tubes in a vertical row when following the Nusselt theory.

Conclusions

The 5 per cent difference between the experimental and predicted coefficient for acetone condensing on the top tube of a bank of copper finned tubes indicates that high static liquid retention does not decrease condensing coefficients under dynamic heat-transfer conditions. Organic liquids, having a ratio of surface tension to density, high as compared with refrigerants, may be condensed on the outside of copper integral-finned tubes with all the fin surface effective and without interference by liquid retention between the fins. The experiments also indicate that the decrease in condensing film coefficients with the number of tubes in a vertical row is much less for finned tubes than would be predicted by the application of Nusselt's theory. For a bank of six tubes in a vertical row, the average condensing heat-transfer coefficient was only 10 per cent below that of the top tube. For design purposes Nusselt's theory, applied to a bank of horizontal finned tubes, may be expected to give condensing heat-transfer coefficients below the experimental values.

Acknowledgment

The experimental data were obtained on a project in the Department of Engineering Research, sponsored by the Wolverine Tube Division of Calumet and Hecla Consolidated Copper Company. Permission to publish the data is gratefully acknowledged. R. E. Hope and S. C. Datsko constructed the equipment used in the investigation, and obtained the experimental data on static liquid retention by finned tubes. J. O. Copeland and D. B. Robinson assisted in obtaining the heat-transfer data.

BIBLIOGRAPHY

1 "Über slächenkondensation des Vasserdamft," by W. Nusselt, *Zeitschrift des Vereines deutscher Ingenieure*, vol. 60, 1916, pp. 541–546 and 569–575.

2 "Condensation of Saturated Freon-12 Vapor on a Bank of Horizontal Tubes," by F. L. Young and W. J. Wohlenberg, Trans. ASME, vol. 64, 1942, pp. 787–794.

3 "Condensation of Vapors on Finned Tubes," by K. O. Beatty, Jr., *Chemical Engineering Progress*, vol. 44, 1948, p. 55.

4 "Condensation of Freon-12 With Finned Tubes, Part 1—Single Horizontal Tubes," by D. L. Katz, R. E. Hope, S. C. Datsko, and D. B. Robinson, *Refrigerating Engineering*, vol. 33, March, 1947, pp. 211–217.

5 "Condensation of Freon-12 With Finned Tubes, Part 2—Multi-Tube Condensers," by D. L. Katz, R. E. Hope, S. C. Datsko, and D. B. Robinson, *Refrigerating Engineering*, vol. 33, April, 1947, pp. 315–319 and 352–354.

6 "Basis for Rational Design of Heat-Transfer Apparatus," by E. E. Wilson, Trans. ASME, vol. 37, 1915, pp. 47–70 and 70–82.

7 "Heat Transmission," by W. H. McAdams, McGraw-Hill Book Company, Inc., New York, N. Y., 1942, second edition.

Appendix 1

Retention of Liquids by Fins Under Static Conditions

The retention of liquids by finned tubes was investigated under static conditions. A formula was derived to give the liquid retained between the fins in terms of the properties of the fluid and the dimensions of the tube. This formula shows that the angle subtended by the liquid retained between the fins is a function of the ratio of the surface tension to the density of the liquid

$$\frac{\phi/360}{\sin \phi/2} = \frac{\gamma}{g\rho}\left[\frac{(4D_2 - 2D + 2s)}{\frac{\pi}{4}(D_2^2 - D^2)s}\right] = \frac{\gamma}{g\rho} \times C_T$$

where

ϕ = angle subtended by liquid retained in space between fins, deg

$\phi/360$ = fraction of heat-transfer surface covered by retained liquid

γ = surface tension of liquid, dynes per cm

ρ = density of liquid, g per cc

D_2 = diameter over fins, cm

D = root diameter, cm

s = spacing between fins, cm

g = local acceleration due to gravity, approximately 980 cm/sec²

C_T = constant for given finned tube

Fig. 7 is a plot of the surface covered by retained liquid under static conditions as measured on ten different finned-tube sections using acetone, carbon tetrachloride, aniline, and water as liquids. The liquid retained was weighed, and the angle subtended by this quantity of liquid was computed.

Because of the simplified mechanism for liquid retention by fins, postulated in deriving the foregoing formula, agreement between the formula and experimental data would be fortuitous. However, the formula does indicate that the dimensions of the finned tube and the properties of the retained liquid given in the formula provide suitable variables for correlating the data.

Fig. 7 for static conditions indicates that liquids having surface tensions considerably above that of refrigerants might be retained to an extent that they would interfere with the condensation process. The heat-transfer experiments on

$$\text{Acetone}\left[\frac{\gamma}{\rho} = 24\ \frac{(\text{dynes})\ (\text{cc})}{(\text{cm})\ (\text{g})}\right]$$

$$\text{Butane}\left[\frac{\gamma}{\rho} = 14\right]$$

$$\text{Freon-12}\left[\frac{\gamma}{\rho} = 6\right]$$

indicate that the increased liquid retained by acetone under static conditions is not reflected in any decrease in heat transfer. Experimental data on acetone compare as favorably with calculated heat-transfer coefficients as the experimental data on Freon-12 compare with its calculated data. From this it is concluded that static liquid retention is no criterion for judging performace under condensing conditions and therefore the details of the static-liquid-retention research are omitted. This brief note and Fig. 7 have been included to dispel any apprehensions which others may have as to the performance of finned surfaces when condensing liquids which are retained on finned tubes under static conditions.

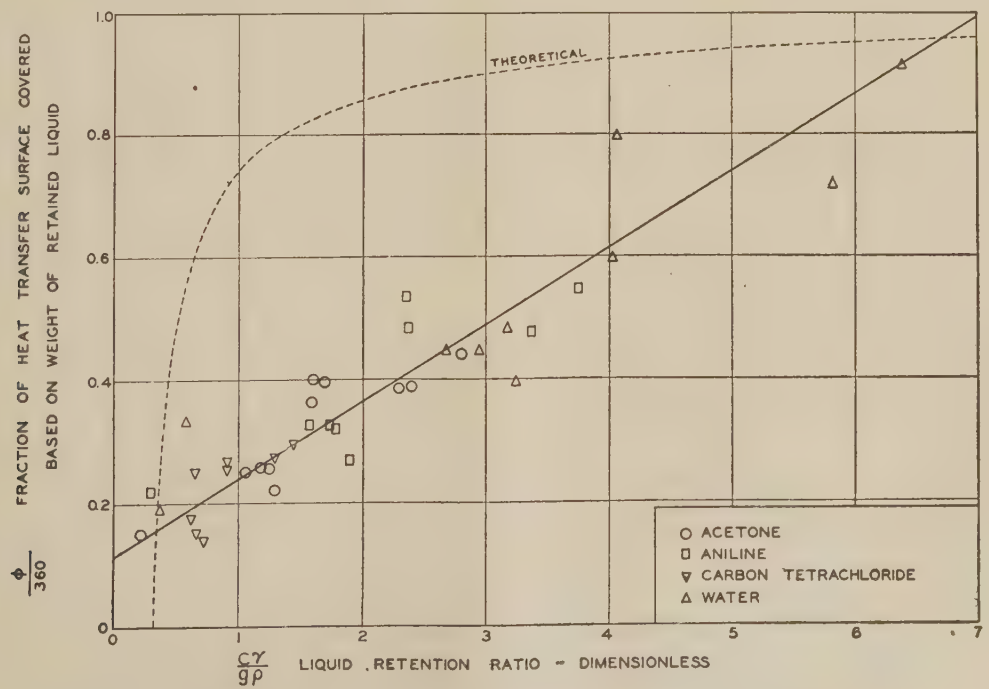

Fig. 7 Liquid Retention by Finned Tubes Under Static Conditions

Appendix 2

EXAMPLE CALCULATION OF DATA FOR WILSON PLOT

Run No. 48—Acetone
Tube No. 1–1.452 sq ft outside area
Cooling-water rate = 1709 lb per hr
Cooling-water temperature rise = 17.28 F
Average cooling-water temperature = 74.01 F
Average cooling-water temperature for Freon-12 = 67.7 F
Average condensing-vapor temperature = 153.92 F
Heat transfer = (1709)(1)(17.28) = 29,530 Btu per hr

$$U_0 = \frac{q}{A_{eq}\Delta T} = \frac{29{,}530}{(1.452)(153.92 - 74.01)} =$$

254.5 Btu/(hr)(deg F)(sq ft)

$$V = \frac{(1709\text{ lb})}{3600\text{ sec}}(0.01605\text{ ft}^3/\text{lb})\left(\frac{144}{\frac{\pi}{4}(0.555)^2\text{ ft}^2}\right) = 4.54\text{ fps}$$

$$\frac{1}{U_0} = \frac{1}{254.5} = 0.003929\text{ (ordinate)}$$

$$\left(\frac{1 + 0.011\,T_1}{1 + 0.011\,T_2}\right)\frac{1}{V^{0.8}} = \left(\frac{1 + 0.011 \times 67.7}{1 + 0.011 \times 74.0}\right) \times \frac{1}{4.54^{0.8}} = 0.287\text{ (abscissa)}$$

Appendix 3

EXAMPLE CALCULATION OF EQUIVALENT DIAMETER FOR FINNED TUBE FOR USE IN NUSSELT EQUATION

$$\frac{1}{(D_{eq})^{1/4}} = \frac{0.943}{0.723}\frac{A_f}{A_{eq}L^{1/4}} + \frac{A_t}{A_{eq}D^{1/4}}$$

For tubes with nominal 16 fins per inch—actual 15 fins per inch:
Root diameter = 0.621 in.
Fin diameter = 0.746 in.

$$L = \frac{\pi}{4}\frac{(0.746)^2 - (0.621)^2}{0.746} = 0.180\text{ in.}$$

$$A_f\text{ per foot of tube} = \frac{\pi}{4}\frac{(0.746)^2 - (0.621)^2}{144} \times 2 \times 15 \times 12 = 0.3356\text{ sq ft}$$

$$A_t = \pi \times \frac{0.621}{12} = 0.1626\text{ sq ft per ft of tube}$$

$$A_{eq} = 0.3356 \times 1.00 + 0.1626 = 0.4982\text{ sq ft per ft of tube}$$

$$\frac{1}{(D_{eq})^{1/4}} = \frac{0.943}{0.725} \times \frac{0.3356}{0.4982} \times \frac{1}{(0.180)^{1/4}} + \frac{0.1626}{0.4982} \times \frac{1}{(0.621)^{1/4}}$$

$D_{eq} = 0.1163$ in., assuming 100 per cent efficiency for the low fin copper tube.

Discussion

D. S. CRYDER.[4] No explanation is offered for the discrepancy between the experimental average coefficient and the average coefficient predicted by Nusselt. According to the data, the former is about 46 per cent greater (for freon and acetone) than the Nusselt coefficient. Deviations from ideal streamline flow, due to splashing, diversion of condensate to side walls of enclosure, etc., may account for the difference but at least these differences should be pointed out.

It would also have been interesting to have extended the work to cover more viscous liquids such as light petroleum fractions. It is conceivable that such liquids might conform more closely to the Nusselt theory.

The writer would like to see this work continued to cover various finned dimensions and a wider range of fluids so that we have a sound basis for changing the Nusselt exponent, if necessary.

[4] Professor, Chemical Engineering, The Pennsylvania State College, State College, Pa.

Stability of SR-4 Electric Strain Gages and Methods for Their Waterproofing and Protection in Field Service

By A. BOODBERG[1], E. D. HOWE,[2] AND B. YORK[3]

Tests were conducted to determine the effects of time in service, changes in temperature, humidity, methods of mounting, and of several waterproofing agents upon the stability of SR-4 electric strain gages, and also to determine the protecting qualities and durability of waterproofing agents and coverings that could be conveniently applied under field conditions. Most tests were conducted on steel blocks not subjected to loads, but a few tests were also made on gages applied to bars and plates which were subjected to repeated loadings. The results have been reassuring and demonstrate that the gages are reliable if properly used.

Introduction

TESTS of stability of SR-4 electric strain gages at the University of California were undertaken as preliminary and supplementary studies to an investigation instituted by the Office of Scientific Research and Development into the history of residual stresses in welded ships in February, 1944.[4] The tests were started to determine the protective qualities and durability of waterproofing agents that could be applied conveniently to SR-4 gages which were to be installed on the decks of the ships used in the investigation. The effects of changes in temperature, humidity, and methods of mounting were also studied and, as the test progressed, it was decided to check the stability of certain SR-4 gages for a longer period of time.

Most of the tests were conducted under static conditions on ship-plate blocks that were not subjected to loads, readings on the gages being taken daily during the first months of the investigation and at less frequent intervals later. Some results were obtained from bars equipped with SR-4 gages and subjected to various tensile and compressive loads at different times throughout the test period of over 30 months. The results have demonstrated that the SR-4 electric strain gages, if properly waterproofed and well protected from mechanical damage, are reliable for a considerable length of time even under the most severe type of usage.

Scope of Tests

SR-4 gages of the following types were used in the tests: A-1, A-5, AX-5, A-7, A-11, and AR-1. The gages used in static stability tests were mounted on small pieces of ship plate (about $^5/_8$ in. × 2 in. × 6 in.), some of which were carefully annealed to prevent creep within the test specimen from affecting the readings of the gages; as an extra precaution a few of the gages were mounted on the sides of a 4-in. Hoke gage block. Readings were taken daily on Baldwin-Southwark SR-4 portable strain indicators for the first few months; later the readings were taken at less frequent intervals. To test the effectiveness of waterproofing, specimens covered with several waterproofing agents were given prolonged exposure in various environments. These waterproofing tests were conducted as a guide in the selection of a waterproofing agent, or combination of agents, which would provide adequate protection and also would be easy to apply under field conditions. No attempt was made to test all available agents nor to exhaust the possible conditions or methods of application of those that were tested.

Gages used in the dynamic tests were mounted on several pieces of steel which were subjected to several loading cycles within the elastic limit of the material during a period of about 30 months.

Compensators or "dummies" used in this series of tests, as well as those used in the main investigation of residual stresses in ships, were made by mounting various gages on small pieces of annealed ship plate. The stability of these dummy gages was carefully checked by obtaining readings on an SR-4 strain meter using one leg of a rosette gage of the dummies as the active gage and the other leg of the same rosette gage as the dummy gage, as well as by reading one dummy gage against another dummy at frequent intervals during the period of test which lasted well over 3 years.

Procedure

Gages were mounted on test pieces of ship plate of convenient dimensions. These were prepared by wire-brushing the surface of the plate free of scale and rust, then smoothing with emery cloth. Oil and dirt were removed by washing with acetone. The gages were cemented in place with quick-drying celluloid cement (made by dissolving 25 grams of celluloid in 1 lb of ethyl acetate) and were held in place by pressing lightly until set. Some gages were allowed to dry at room temperature and others were heated by infrared lamps to as high as 140 F to accelerate and facilitate the drying. Insulated single-strand wires were soldered to the gage lead wires and then stapled securely to the small wood blocks that were bolted to the specimen plate. Waterproofing agents, listed in Table 1, were applied after allowing at least 24-hr drying time, except in the case of one set of gages which was prepared especially to determine the effect of applying waterproofing to gages that had dried for short periods. The waterproofing agents were applied in copious quantities to both the gage and the plate and extended $^1/_2$ in. or more beyond the edge of the gage. When one agent was applied over another, the second was extended $^1/_2$ in. or more beyond the edge of the first. The lead wires of the gages were coated with the waterproofing agent up to the insulation of the connecting wires. Specimens were then subjected to varying degrees of humidity and different temperatures and

---

[1] Associate Professor of Mechanical Engineering, University of California, Berkeley, Calif.

[2] Assistant Dean, College of Engineering, University of California. Mem. ASME.

[3] Assistant Professor of Mining, University of California.

[4] "History of Residual Stresses in Welded Ships," OSRD Report No. 6359, Serial No. N-586, Nov. 28, 1945.

Contributed by the Industrial Instruments and Regulators Division and presented at the Annual Meeting, Atlantic City, N. J., December 1–5, 1947, of THE AMERICAN SOCIETY OF MECHANICAL ENGINEERS.

NOTE: Statements and opinions advanced in papers are to be understood as individual expressions of their authors and not those of the Society. Paper No. 47—A-120.

some were placed in glass vessels containing fresh or salt water, and Diesel or fuel oils. A wax-protected gage on a test block and one undergoing an immersion test are shown in Fig. 1.

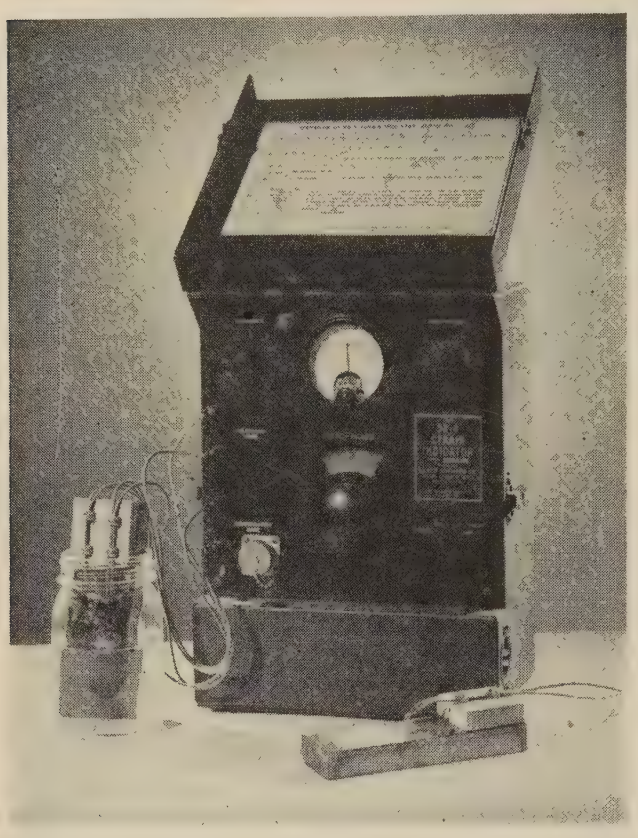

FIG. 1 METHOD OF SECURING LEAD WIRES TO GAGE BLOCK AND SPECIMEN UNDERGOING IMMERSION TEST

The tests were conducted under controlled conditions, wherever practicable, in order to determine the effect of each influencing factor separately. Care was taken to assure good connections at the indicator and to have the indicator, specimens, and dummy at equal temperature, except when testing for the effect of a cold indicator. Cross-comparisons of gages and dummies were made regularly so that the deviation of individual specimens would be apparent. Electrical resistance between the gage wire and plate was carefully checked throughout the test period.

Tests in which the gages were subjected to tensile and compressive loads were made by mounting gages on a piece of spring steel, $^1/_4$ in. × 2 in. × 20 in., a piece of hot-rolled mild steel, 1 in. × 1 in. × 60 in., and a piece of ship plate $^3/_4$ in. × 8 in. × 30 in. The spring steel and the square hot-rolled stock bars were used as cantilever beams during the test period and the ship-plate specimen was stressed in a universal testing machine. Stresses as high as 25,000 psi in tension and compression were reached in the test pieces several times during the test period of $2^1/_2$ years, and accurate records of the gage readings at various load levels were kept.

Several means of mechanical protection were devised for guarding gages on board ship from damage. The sturdy cover shown in Fig. 2 was used on the decks of two ships that were equipped with strain gages and were in regular service for a period of about 6 months. Fig. 3 shows the installation on the underside of the deck. Some of the other types of covers shown in Fig. 4 were used to protect SR-4 gages on ships that were tested during the construction period.

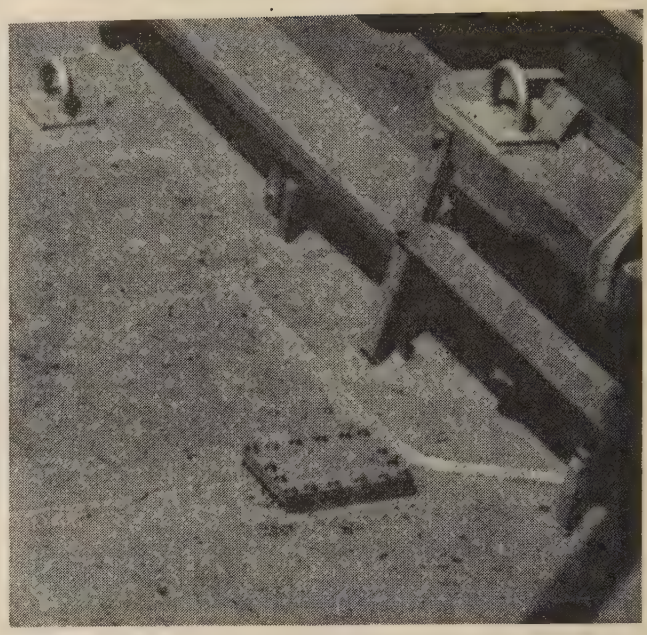

FIG. 2 HEAVY-DUTY STRAIN-GAGE COVER INSTALLED ON MAIN DECK OF LIBERTY-TYPE SHIP

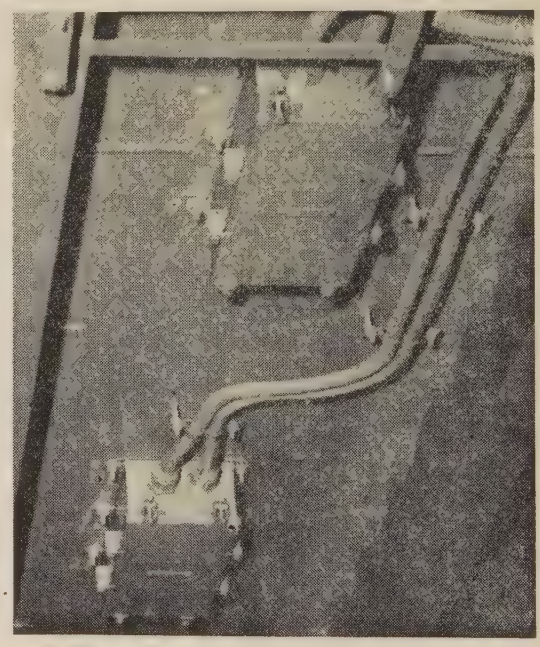

FIG. 3 STRAIN-GAGE COVER USED ON UNDERSIDE OF DECK
(Wires connect individual gage stations to central panel.)

RESULTS OF TESTS

Comparison of Gages by Type. The tests disclosed no apparent difference in stability of gages by types. When well protected, all types of gages showed good stability both in the static time tests and the tests where loads were applied to specimens. The multiple layers of wire and paper in the AR-1 rosette and AX-5 type gages had no measurable effect on stability.

Effect of Time. Some specimens were under observation for over 40 months, others for a shorter period, with good results when adequately protected from moisture. Though it is difficult to isolate the effect of time from that of temperature, moisture, etc., it is apparent that time alone causes only minor de-

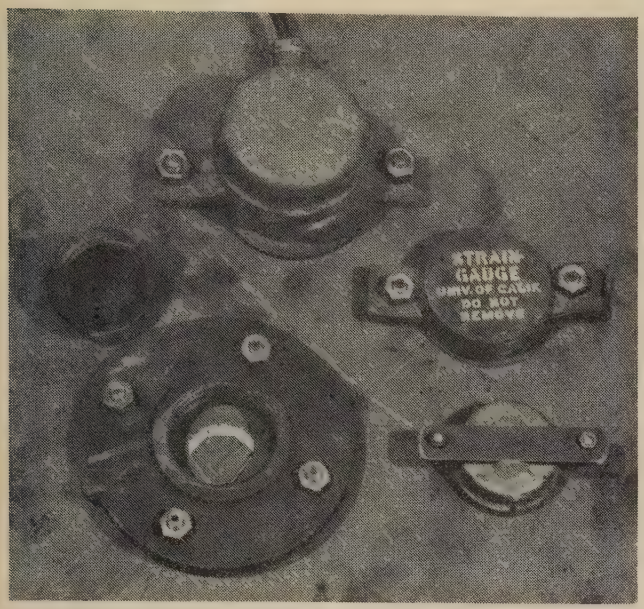

FIG. 4 VARIOUS TYPES OF STRAIN-GAGE COVERS USED ABOARD SHIP

viations, or drift, if any, from the original reading. Table 2 shows the deviations for some of the pairs chosen as representative from among adequately waterproofed specimens. It also shows deviations of gages used in the dynamic tests. Table 3 shows dummy check readings with differences from their median for a period of 43 months. These dummies were used as compensating gages in obtaining most of the strain readings taken by Project NRC-74 in study of stresses in welded ship hulls,[4] and during the test period were often subjected to temperatures ranging from 30 F to 100 F as well as rain, fog, and salt-water spray. These dummy check readings show only minor fluctuations, but no drift trend during the period of these observations.

Effect of Temperature. Variations in temperature within a moderate range, as they were in these tests, have no appreciable effect on the rate of drift. This is shown by a comparison of the drift rates of specimens kept in a controlled-temperature room with those that were subjected to temperature variations between 55 and 85 F.

Temperature apparently has no effect on constancy and accuracy of reading, provided the gage and dummy are selected from the same wire lot and that the temperatures of the gage and dummy are equal, as has been demonstrated by the dummy check readings taken at various temperatures (see Table 3).

Varying the temperature of the indicator while that of the gage and dummy remained constant gave fluctuations of small magnitude (± 10 microinches).

Effect of Humidity. Ordinary room humidity has no apparent effect on stability of SR-4 gages, even unprotected ones. However, gages that are to serve in damp conditions must be waterproofed to avoid damage. This need is shown by the curves in Fig. 6. It was not apparent on visual examination that the gages were damaged by moisture, but it was at once apparent from the decrease in electrical resistance between the gage wires and the plate (a drop from nearly infinity to below 5 megohms for some of the specimens).

Effect of Time of Drying of Mounting Cement Before Waterproofing. Gages that were dried for only 13 min prior to heating in preparation for waterproofing showed as good a stability under

TABLE 1 EFFECT ON STABILITY OF SR-4 GAGES OF DRYING TIME ALLOWED BEFORE WATERPROOFING

Specimen	Gage type	Protection used	Total drying time	Temperature at application of waterproofing, deg F	Length of observation, months	Maximum deviation from original reading, microinches per in.
20D	A-11	Petrosene A wax applied to hot plate	90 min	125	24	+10 −15
21D	A-11	Petrosene A wax applied to cold plate	24 hr	65	24	0 −25
22D	A-11	Petrosene A wax applied to hot plate	13 min	125	24	+10 −15
23D	A-11	Petrosene A wax applied to hot plate	85 min	105	24	+10 −20
Star below dummy	AR-1	Ozite B over Petrosene A wax applied to hot plate	45 min	125	30	+20 −20
Star top dummy	AR-1	Ozite B over Petrosene A wax applied to hot plate	45 min	125	30	+20 −15
Port below dummy	AR-1	Ozite B over Petrosene A wax applied to hot plate	45 min	125	30	+15 −10
Port top dummy	AR-1	Ozite B over Petrosene A wax applied to hot plate	45 min	125	30	+20 −15
Star dummy	AX-5	Ozite B over Petrosene A wax applied to hot plate	30 min	140	20	+10 −10
Dummy No. 1	AR-1	Ozite B over Petrosene A wax applied to hot plate	20 min	140	18	+15 −20

LIST OF WATERPROOFING AGENTS USED IN TESTS

Sauereisen Nos. 30 and 78....Saureisen Cement Company, Pittsburgh, Pa.
Glyptal.....General Electric Company, Schenectady, N. Y.
Bakelite Varnish, B#61.....Bakelite Corporation, Bound Brook, N. J.
Americoat No. 33.....
....American Pipe and Construction Company, South Gate, Calif.
Petrosene A wax.....General Petroleum Corporation, San Francisco, Calif.
Ozite B.....General Cable Corporation, San Francisco, Calif.

TABLE 2 DEVIATION OF GAGE READINGS WITH TIME

SPECIMEN	ACTIVE GAGE		DUMMY GAGE		ENVIRONMENT AND TYPE OF TEST	LENGTH OF OBSERVATION	DEVIATION FROM ORIGINAL READING MICRO-INCHES/INCH
	TYPE	PROTECTION	TYPE	PROTECTION			
4	A-11	PETROSENE A WAX ON HOT PLATE	A-11	PETROSENE A WAX ON HOT PLATE	HIGH HUMIDITY (100% RH) VARIABLE TEMPERATURE	40 MONTHS	+ 50 TO - 20
O	A-11	OZITE B OVER PETROSENE A WAX ON HOT PLATE	A-11	"	IMMERSED IN SEA WATER	39 MONTHS	+ 20 TO - 15
M	A-11	"	A-11	"	" "	"	+ 30 TO - 10
GH	A-1	PETROSENE A WAX ON HOT PLATE	A-1	PETROSENE A WAX ON HOT PLATE	LOW HUMIDITY (50% RH) CONSTANT TEMPERATURE 70°F.	38 MONTHS	+ 15 TO - 10
GH	A-5	"	A-1	"	" "	"	+ 10 TO - 15
U	A-1	OZITE B OVER PETROSENE A WAX ON HOT PLATE	A-1	OZITE B OVER PETROSENE A WAX ON HOT PLATE	HIGH HUMIDITY (100% RH) VARIABLE TEMPERATURE	35 MONTHS	+ 25 TO - 15
U	A-1	"	A-11	PETROSENE A WAX ON HOT PLATE	" "	"	+ 10 TO - 20
Q1	AR-1	"	AR-1	OZITE B OVER PETROSENE A WAX ON HOT PLATE	" "	"	+ 10 TO - 15
Q1	AR-1	"	A-11	PETROSENE A WAX ON HOT PLATE	" "	"	+ 30 TO - 20
B1	AX-5	PETROSENE A WAX ON HOT PLATE	AX-5	OZITE B OVER PETROSENE A WAX ON HOT PLATE	SUBJECTED TO VARIOUS LOADS VARIABLE TEMPERATURES AND HUMIDITY	30 MONTHS	+ 20 TO - 25
B1	A-7	"	A-7	PETROSENE A WAX ON HOT PLATE	" " "	"	+ 15 TO - 20
B2	AR-1	"	AR-1	OZITE B OVER PETROSENE A WAX ON HOT PLATE	" " "	"	+ 10 TO - 15
B2	AR-1	"	AR-1	"	" " "	"	+ 15 TO - 15
B3	A-1	"	AR-1	"	" " "	"	+ 15 TO - 20
B3	A-1	"	AR-1	"	" " "	"	+ 15 TO - 25

TABLE 3 COMPARISON OF DUMMY CHECK READINGS

(Air temperature variations 30 F to 105 F. Active and dummy gage mounted on same annealed steel block. All values are in microinches per inch.)

IDENTIFICATION OF DUMMY	PORT BELOW		STAR BELOW		PORT TOP		STAR TOP	
DATE	READING	DIFFERENCE FROM MEDIAN	READING	DIFFERENCE FROM MEDIAN	READING	DIFFERENCE FROM MEDIAN	READING	DIFFERENCE FROM MEDIAN
3-17-44	2-979	- 14						
3-18-44	2-965	0						
3-21-44	2-970	+ 5	3-927	+ 9	3-1645	+ 10	4-1425	- 5
3-23-44	2-975	- 10	3-935	+ 17	3-1630	- 5	4-1420	0
3-24-44	2-970	+ 5	3-923	+ 5	3-1635	0	4-1415	+ 5
3-25-44	2-970	+ 5	3-925	+ 7	3-1645	+ 10	4-1420	0
3-27-44	2-978	+ 13	3-925	+ 7	3-1625	- 10	4-1425	+ 5
3-30-44	2-968	+ 3	3-925	+ 7	3-1635	0	4-1420	0
3-31-44			3-925	+ 7			4-1428	+ 8
4- 3-44	2-969	+ 4	3-920	+ 2	3-1630	- 5	4-1439	+ 19
4- 4-44	2-962	- 3	3-918	0	3-1620	- 15	4-1430	+ 10
4-10-44	2-975	+ 10	3-920	+ 2	3-1630	- 5	4-1420	0
4-12-44	2-961	- 4	3-914	- 4	3-1645	+ 10	4-1430	+ 10
4-19-44	2-963	- 2	3-915	- 3	3-1645	+ 10	4-1430	+ 10
4-25-44	2-970	+ 5			3-1638	+ 3		
4-28-44	2-965	0	3-915	- 3	3-1631	- 4	4-1420	0
5- 2-44	2-965	0	3-920	+ 2	3-1630	- 5	4-1410	- 10
5- 3-44	2-960	- 5	3-922	+ 4	3-1630	- 5	4-1415	- 5
5- 4-44	2-960	- 5	3-920	+ 2	3-1630	- 5	4-1420	0
5- 5-44	2-960	- 5	3-925	+ 7	3-1635	0	4-1420	0
5- 7-44	2-955	- 10	3-910	- 8	3-1630	- 5	4-1415	- 5
5- 8-44	2-955	- 10	3-905	- 13	3-1630	- 5	4-1420	0
5-21-44	2-965	0	3-915	- 3	3-1635	0	4-1410	- 10
6-21-44	2-970	+ 5	3-907	- 11				
6-22-44	2-955	- 10	3-915	- 3	3-1645	+ 10	4-1432	+ 12
7- 1-44	2-978	+ 13	3-905	- 13	3-1640	+ 5	4-1425	- 5
8-10-44	2-975	+ 10	3-905	- 13	3-1650	+ 15	4-1405	- 15
8-15-44	2-970	+ 5	3-915	- 3	3-1645	+ 10	4-1410	- 10
8-29-44	2-965	0	3-910	- 8	3-1650	+ 15	4-1420	0
9- 1-44	2-960	- 5	3-900	- 18	3-1625	- 10	4-1405	- 15
9- 5-44	2-965	0	3-910	- 8	3-1620	- 15	4-1410	- 10
11-15-44	2-960	- 5	3-910	- 8	3-1630	- 5	4-1420	0
2-27-45	2-960	- 5	3-915	- 3	3-1630	- 5	4-1420	0
4-15-45	2-970	+ 5	3-920	+ 2	3-1635	0	4-1430	+ 10
6- 5-45	2-960	- 5	3-905	- 13	3-1630	- 5	4-1410	- 10
8-14-46	2-965	0	3-915	- 3	3-1625	- 10	4-1410	- 10
9-14-46	2-960	- 5	3-910	- 8	3-1630	- 5	4-1415	- 5
10-18-46	2-960	- 5	3-920	+ 2	3-1620	- 15	4-1410	- 10
1-13-47	2-965	0	3-910	- 8	3-1630	- 5	4-1425	+ 5
10-20-47	2-960	- 5	3-920	+ 2	3-1645	+ 10	4-1430	+ 10
MEDIAN	2-965		3-918		3-1635		4-1420	
MAXIMUM		+ 14		+ 17		+ 16		+ 19
DEVIATIONS		- 10		- 18		- 15		- 15

static conditions as gages that were dried for a period of 24 hr. The deviation of each as read against a wax-covered dummy gage is shown in Table 1. None of the waterproofing agents used in the tests and listed in Table 1 showed detrimental effects on gage stability.

Results of Tests of Waterproofing Agents. Results of readings taken on specimens variously waterproofed while immersed in fresh or sea water are shown in Fig. 5. The covering found most suitable in protective quality and ease of application was a combination of Ozite B over Petrosene A wax applied to a heated plate. Each of these applied alone to the heated plate, and a combination of them applied to the cold plate failed to give adequate protection against prolonged immersion. Other agents and combination of agents tested failed after a relatively short time.

Petrosene A wax applied to heated plate provided adequate protection for specimens exposed to a moisture-saturated atmosphere. However, dynamic tests of gages mounted on bars used as cantilever beams showed that the wax had a tendency to crack when the bars were stressed at temperatures below 40 F. Ozite B surface did not show any such cracks at 30 F, and it may be assumed that it would retain its waterproof qualities down to that temperature.

None of the waterproofing agents tested withstood prolonged immersion in Diesel or heavy fuel oil.

Petrosene A wax and Ozite B each provided some degree of mechanical protection, particularly against tearing out of the slender lead wires of the SR-4 gages.

Detailed data of the behavior of SR-4 gages subjected to various conditions can be found in the OSRD report mentioned.[4]

Conclusions

1 SR-4 gages showed no indication of drift with time when well protected from moisture.

2 Of the several waterproofing agents tested, a combination of Petrosene A wax and Ozite B applied on the heated plate performed best over a long period of time.

Acknowledgment

This paper is one of the series covering the work done at the University of California under contract with the Office of Scientific Research and Development; Contract OEMsr-1217. The official title of the work was "History of Residual Stresses in Welded Ships" and was designated as NRC-74. The complete report of this project is covered in the following OSRD reports:

OSRD No. 4866, Serial No. M-445, March 19, 1945.
OSRD No. 5262, Serial No. M-494, July 2, 1945.
OSRD No. 6359, Serial No. M-586, November 28, 1945.
OSRD No. 6388, Serial No. M-609, December 5, 1945.
OSRD No. 6587, Serial No. M-623, February 25, 1946.
OSRD No. 6588, Serial No. M-624, February 25, 1946.
OSRD No. 6589, Serial No. M-625, February 25, 1946.
OSRD No. 6590, Serial No. M-630, February 25, 1946.

Discussion

D. M. Nielsen.[5] This paper offers much data on the actual performance of SR-4 strain gages under adverse installation conditions. Information in this field has previously existed only in

[5] Vice-President, Nielsen & Fryer, Inc., Chicago, Ill. Jun. ASME.

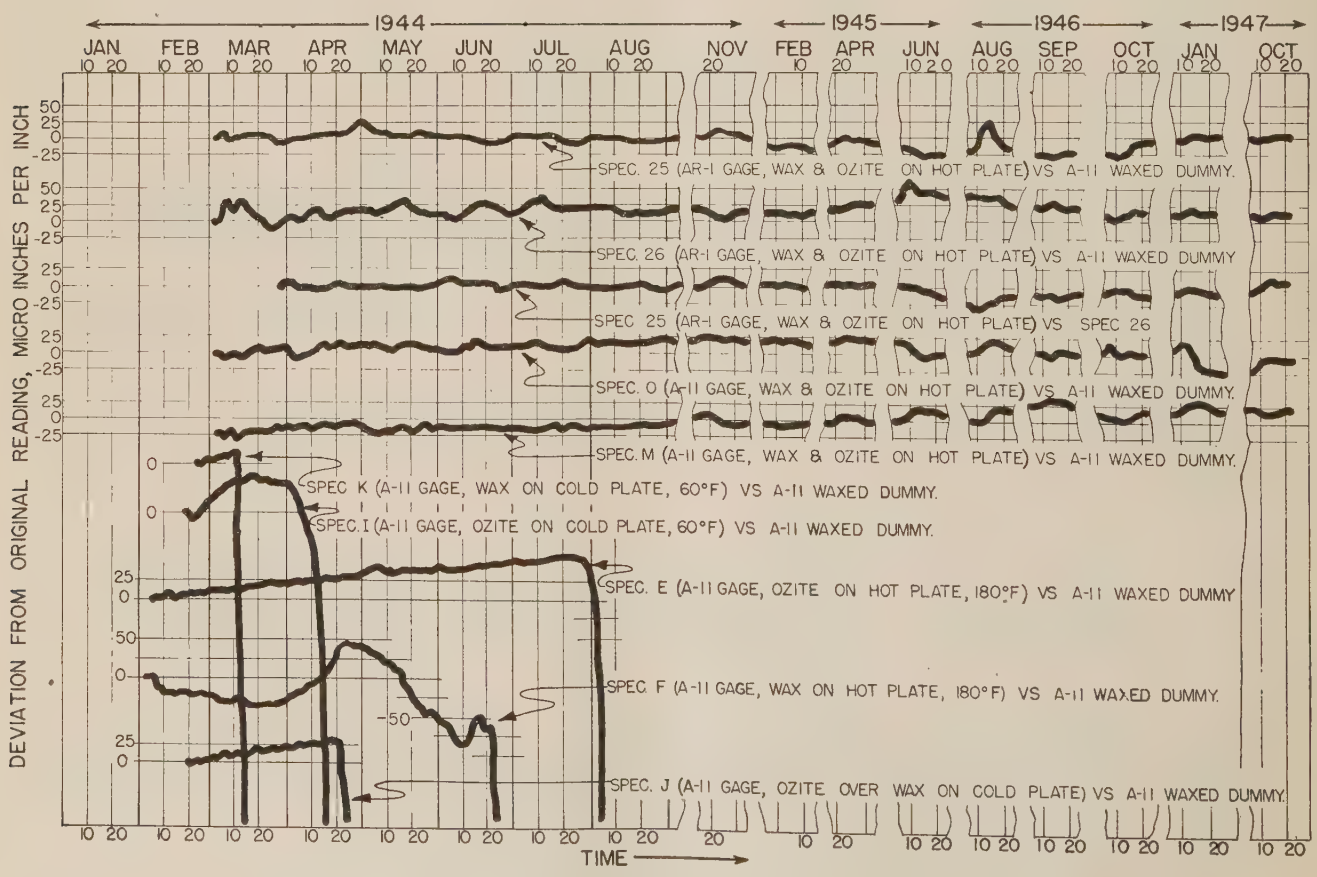

Fig. 5 Deviation From Original Reading With Time for Gages Immersed in Sea Water

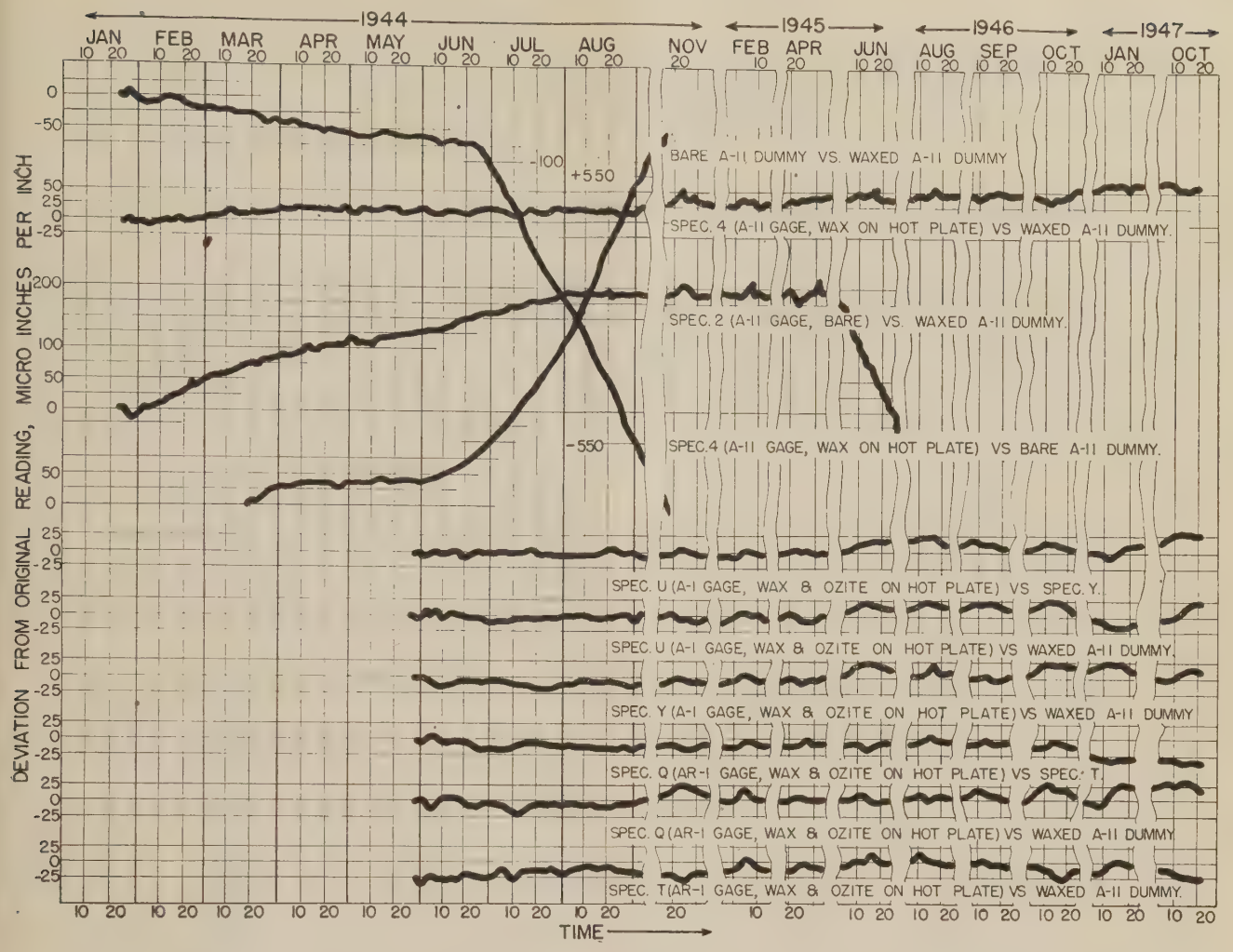

FIG. 6 DEVIATION FROM ORIGINAL READING WITH TIME FOR GAGES TESTED UNDER CONDITIONS OF HIGH HUMIDITY—RELATIVE HUMIDITY 100 PER CENT—AND 65 TO 75 F

scattered form in various publications, and has been based on far less complete investigations. This paper now gives the structural designer and stress analyst a valuable guide to desirable practice in installing strain gages, and the order of measuring accuracy possible to obtain.

The general experimental method is the cross-comparison of gages installed on sample specimens against dummy gages. No reference is made to any checks against resistance standards. This appears to be a valid technique for studying the effect of temperature, humidity, moistureproofing, and other ambient conditions under no-load conditions.

Much of the data in the tables given show deviations considerably smaller in magnitude than the error reasonably to be expected in the SR-4 indicator readings over a period of months under field operating conditions. The first reaction is to question the accuracy of the deviation figures given. However, if the same instrument were used on all tests, then the random nature of deviation values given in Figs. 5 and 6, and the absence of any consistent drift in all gages for readings on the same date indicate that the instrument introduced no significant error. Analysis of the detailed data behind these tables should provide further light on this point.

It does seem doubtful that accuracies of the order given in this paper will be generally obtainable. A more reasonable order of accuracy to expect is the instrument error guaranteed by the manufacturer plus gage errors of the magnitude given in this paper.

The purpose of the general investigation, of which this paper is a part, was the study of residual stresses in welded ships. For such applications a basic question is the stability of gage zero and strain-sensitivity factor over a long period of maintained stress, during which there is no chance to remove the strain and check gage zero. There must be some question as to whether the tests given in this work of stability at zero stress are valid for maintained stress conditions.

Some work was done using gages on loaded specimens, as mentioned in the text, and in the data on the last 6 gages in Table 2. It would be helpful to give in more detail the readings on the dynamic tests, including the stress values, lengths of time over which the load was maintained, gage deviations under constant maintained stress, and deviations of gage zero in successive returns to zero stress conditions. Such data would reveal the existence and magnitude of any gage drift or hysteresis to be expected in residual-stress measurements.

Data of this same sort would have additional value for the applications where strain gages are used as conversion elements in sensitive units for the detection and measurement of fluid pressure, torque, weight, etc. For such applications the need for permanent stability of gage characteristics is obvious. General practice on applications of this type has been to use bakelite

gages rather than the paper-backed type used in the ship experiments. Also, in some cases the gages have been built in place to obtain a better bond between the gage and the mounting surface. Data of the type described in the preceding paragraph might indicate whether refinements are generally essential.

S. B. Spracklen.[6] It is specifically stated in the abstract that both static and dynamic tests were made, but there is no statistical table in this report covering any of the dynamic tests. It is regrettable that a thorough coverage of dynamic tests on the SR-4 strain gages is not included in this report. While this omission of data reduces the value of the report, the authors should be commended for their thoroughness on that part of the report dealing with the waterproofing and protection of strain gages in service, and the static tests which were run for the verification of those waterproofing tests.

If statistical information is available on the dynamic testing of strain gages, it is suggested that such data be included in the report.

Authors' Closure

Discussion brought out several points which require further elaboration of the test results. One such item has to do with the small tolerance on repeated readings over long periods of time. These tolerances are given in Tables 1 and 3, and refer to gages used as "dummies." Therefore they are not comparable to service gages subjected to loads. The readings tabulated refer to the comparison of two strain gages mounted on the same piece of unstressed annealed plate, the whole assembly being carefully guarded from mechanical damage and thoroughly waterproofed. This is also true for the deviations shown in Figs. 5 and 6.

The introduction of load had little effect on the stability as has been demonstrated by the consistency in readings of some gages which were repeatedly loaded to as high as 20,000 psi in tension and 20,000 psi in compression. Most of the gages used in load tests were mounted on pieces of steel which were used as cantilever beams. No drift was shown by any of the gages for a period of over 30 months, although in many cases the gages would not return exactly to zero after a cycle of loading, especially when loads were maintained for a considerable time. This deviation of gage zero due to loading was not included in the tabulated values as the deviations shown in the tables were limited only to the effect of time on the gage readings. Errors in the gage zero due to loading varied considerably from gage to gage but in no case did they exceed 35 microinches per in. throughout the test period.

Additional checks on the performance of the SR-4 gages and their stability were obtained during a later phase of the NRC-74 research program when plugs were trepanned from decks of Victory ships and C-4 troop transports. Several gage spots on the decks of these ships were provided with SR-4 rosette gages and were also marked for $2^1/_2$-in-gage-length mechanical gages. These gages were placed on the deck plates while the ships were under construction and were left on for the sea trials of the vessels. Thus they were subjected to various loads for a considerable length of time. At the end of the sea trials the gages were trepanned from the decks and the relaxation stresses were thus measured. Total change of strains during construction as well as the relaxation strain, as measured by the mechanical and the SR-4 electrical gage, were in excellent agreement; a typical example is shown in Table 4 of this closure.

TABLE 4 CHANGES OF STRAIN DURING CONSTRUCTION AND RELAXATION STRAINS

	Gage no.	Side of plate	Mechanical gage, $2^1/_2$ in. gage length	SR-4 rosette
Relaxation strain measured in deck plate Hull No. 732	1 fore and aft	Top	— 160	— 180
		Bottom	— 100	— 50
		Average	— 130	— 115
Relaxation strain measured in deck plate Hull No. 732	1 athwartship	Top	— 100	— 70
		Bottom	— 75	— 55
		Average	— 87	— 63
Relaxation strain measured in deck plate Hull No. 732	2 fore and aft	Top	— 300	— 270
		Bottom	100	55
		Average	— 100	108
Relaxation strain measured in deck plate Hull No. 732	2 athwartship	Top	— 300	— 250
		Bottom	50	35
		Average	— 125	— 108
Relaxation strains along weld in deck plates	1	Top	1500	1485
		Bottom	1175	1215
		Average	1337	1350

[6] Special Instrumentation Department, Instrument Division, Carbide and Carbon Chemicals Corporation, So. Charleston, W. Va.

Oscillating-Piston Meters for Fuel Consumption in Aircraft

By C. S. HAZARD,[1] NEW YORK, N. Y.

The amount of fuel remaining in the tanks of an airplane in flight may be determined in two ways: (*a*) by measuring the liquid levels in the tanks; or (*b*) by measuring the fuel as it is consumed and subtracting from the amount on board at take-off. The oscillating-piston type of displacement meter has been used successfully in the latter system. This paper describes two such meters, and gives data on the accuracy of this method of fuel measurement.

Introduction

AN URGENT problem in aircraft instrumentation is the apparently simple one of telling the pilot how much fuel is left in his tanks, since that determines how much longer he can remain aloft. The problem has become more urgent with the advent of jet propulsion, because of the comparatively high rate of fuel consumption in this type of power plant.

For many years pilots have relied principally on float-operated liquid-level gages installed in the fuel tanks. The limitations of this type of gage were recently summarized by A. J. Snyder (1).[2] He reached the conclusion that, unless the accuracy of this method could be greatly increased, the commercial airlines would be forced to revert to the laborious method of computing the fuel consumed from periodic readings of the rate-of-flow meter.

Since the early days of the war, several instrument manufacturers, in order to overcome the mechanical difficulties of the float-type gage, have been developing tank gages which depend upon the difference in electrical capacitance between air and gasoline (2, 3, 4, 5). These gages respond to the change in capacity of a two-plate condenser suspended in the fuel tank. While this system eliminates all moving parts from the tank, and has the valuable feature of measuring mass instead of volume, it is still subject to the following limitations:

1 The depth of the liquid in the wing tank of an airplane is small compared to the horizontal cross-sectional area of the tank, so that a slight change in liquid level corresponds to a relatively large change in volume. This severely limits the accuracy of measurement.

2 The gallonage corresponding to a particular liquid level may vary with the flight attitude of the airplane.

3 The capacity of a fuel cell may be altered by temporary displacement of the walls of the cell.

4 When a large number of wing fuel cells are used, each requiring its own gage, the installation becomes complicated.

Another solution, along the lines proposed by Snyder (1), is described by D. W. Moore (6). He accurately measures the rate of fuel consumption, and then integrates this rate electronically to determine the total consumption.

Working on this problem in 1937, the engineers of a major airline reasoned that the best way to measure volume would be to use a volumetric meter, rather than to integrate the readings of a rate meter. In addition to using reciprocating-piston meters in regular service, they installed an oscillating-piston meter in the engine fuel line on one of their transoceanic flying boats, and ran extensive flight tests. The readings of this instrument proved considerably more accurate and reliable than their tank gages. On the basis of these and other tests, a meter of this type was developed during the war for the U. S. Army Air Forces. Two versions of this meter have been cleared for publication by the Air Materiel Command.

Description of Instrument

Fig. 1 shows a cutaway view of the AAF Class 30 fuel flowmeter, which is standard equipment on one of our jet-powered fighters. Plan views of the measuring chamber, showing the operation of the piston, are given in Fig. 2. With the piston in the position shown in Fig. 2(*a*), liquid enters the space 2 through the inlet port 1, and leaves the space 6 through the outlet port 5, moving the piston 3 progressively through the positions shown in Fig. 2(*b*, *c*, *d*), and back to that shown in Fig. 2(*a*). A similar cycle occurs in the inner chamber formed between the piston and the center ring.

The piston is guided in its motion by contact of its spindle 7 with the center roller 8, which holds the piston continuously in contact with both the inner and outer walls of the chamber. The radial clearance between piston and cylinder wall is closely held at 0.0015 in., which allows for capillary seal. Vertical clearance is 0.0020 in., which allows for two capillary seals, one above and one below. The result is a true piston action.

The measuring element drives the transmitting cam through reduction gearing. This cam closes a switch once for each gallon, actuating a three-digit solenoid counter on the instrument panel. A knurled wheel is provided on the counter for setting the reading manually to the gallons on hand at take-off. Each impulse from the meter subtracts 1 gal from the reading of the counter and thus shows at all times the gallons remaining. The counter is wound for 24 volts direct current.

The Class 30 fuel flowmeter has a maximum operating pressure of 35 psi, and is installed on the low-pressure side of the fuel system. The meter weighs 6.06 lb, the counter 0.48 lb.

Fig. 3 shows another meter of the same type, the AAF type H-1. This meter is designed for operation on the high-pressure side of the fuel system, at a maximum working pressure of 600 psi, and weighs 13.6 lb. The packed stuffing-box which was satisfactory for the low-pressure meter, is impractical at high pressure, and the magnetic clutch, shown in Figs. 3 and 4, accordingly is used. It consists of a pair of 6-pole rotating permanent magnets, of Alnico No. 2, separated by a bronze shell 0.051 in. thick, which retains the liquid pressure. The pull-out torque of this clutch is 6.5 in.-oz, which is about 5 times the maximum torque imposed by the transmitting cam.

In order to insure a supply of fuel to the engine, even if the measuring unit should jam, there is a spring-loaded by-pass valve

---

[1] Director of Research, Neptune Meter Company; formerly Commander, S (A), USNR. Mem. ASME.

[2] Numbers in parentheses refer to the Bibliography at the end of the paper.

Contributed by the ASME Research Committee on Fluid Meters and presented at the Annual Meeting, Atlantic City, N. J., December 1–5, 1947, of The American Society of Mechanical Engineers.

Note: Statements and opinions advanced in papers are to be understood as individual expressions of their authors and not those of the Society. Paper No. 47—A-54.

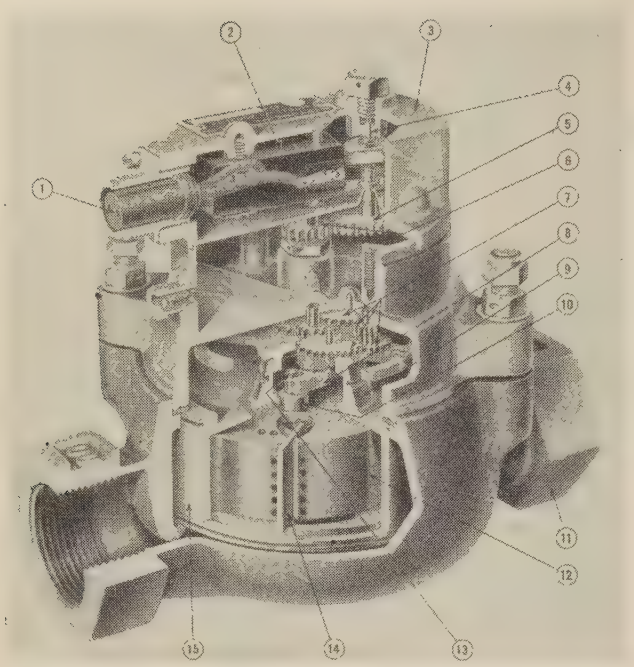

1 Electrical receptacle
2 Switch
3 Switch housing
4 Test hand spindle
5 Change gear
6 Change gear
7 Gear train
8 Driving crank
9 Upper cylinder head
10 Piston hub
11 Inlet
12 Piston
13 Piston spindle
14 Diaphragm
15 Measuring chamber

FIG. 1 CUTAWAY VIEW OF LOW-PRESSURE FUEL METER

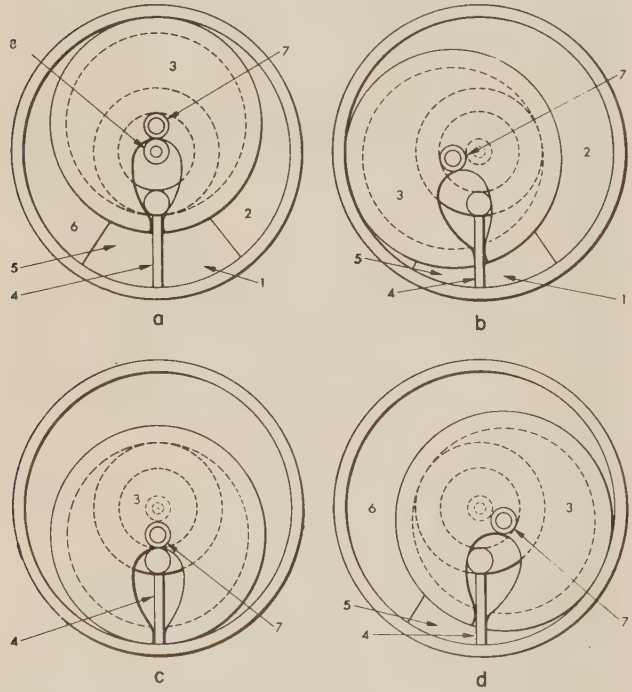

1 Inlet port
2 Incoming liquid space
3 Piston
4 Diaphragm
5 Outlet port
6 Outgoing liquid space
7 Piston spindle
8 Control roller

FIG. 2 ACTION OF OSCILLATING-PISTON CHAMBER

between the inlet and the outlet of the meter. Since the measuring unit contains but a single piston, without packing, the pressure difference from inlet to outlet can be predicted accurately

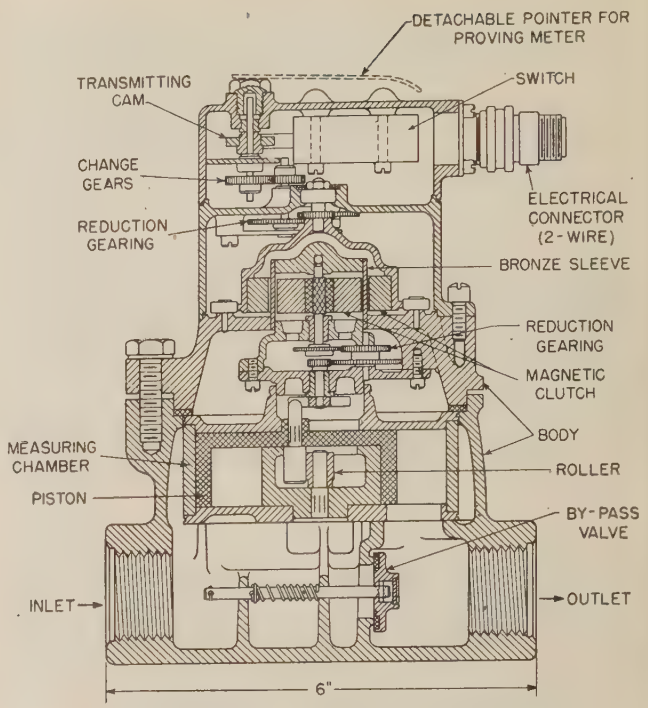

FIG. 3 CROSS SECTION OF HIGH-PRESSURE FUEL METER

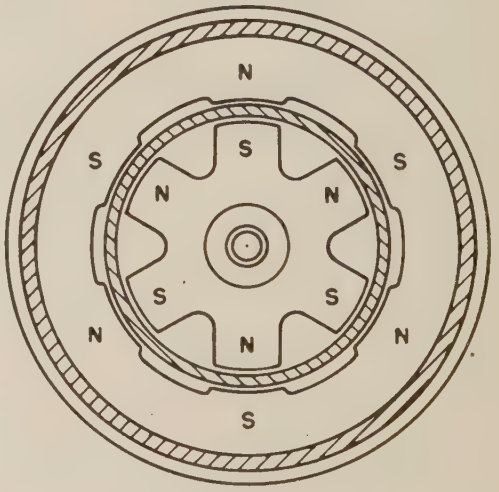

FIG. 4 MAGNETIC CLUTCH

for any maximum rate of flow. This makes it possible to set the by-pass valve to relieve at a few pounds above this maximum, without by-passing any portion of the fuel during normal running. This pressure relationship is shown in Fig. 5. As a result of the low by-passing pressure, the drop in fuel pressure, whether under normal or by-passing conditions, has a negligible effect upon the operation of the power plant.

The measuring unit used in the meters described is similar to that used in service-station gasoline pumps, and has a displacement of 5.3 cu in. per cycle. Since this displacement cannot be altered in service, the gear ratio between the chamber and the transmitting cam is varied, in order to adjust the meter. This is done by replacing the change gears, shown in Figs. 1 and 3, which are available in steps of 0.25 per cent.

ACCURACY

These meters are suitable for rates of flow between 20 and 1200 gph. Within this range, the meter will register the volumetric

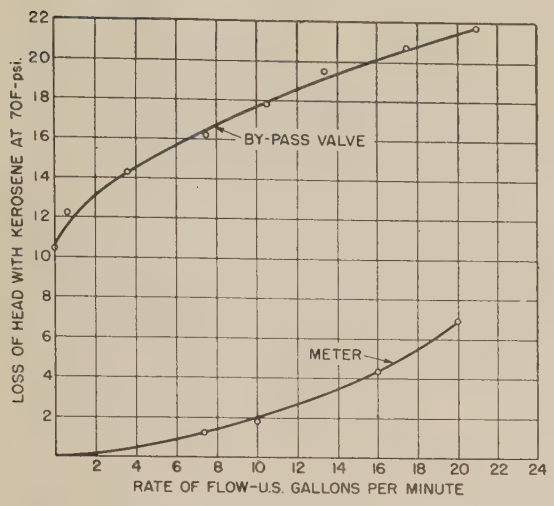

FIG. 5 PRESSURE DROP THROUGH METER AND THROUGH BY-PASS

throughput within a tolerance of ±0.2 per cent although the tolerance guaranteed is ±1 per cent under normal temperatures and pressures. This wider limit makes allowance for the following factors:

1 The difference in viscosity between the regular jet fuel (kerosene) and gasoline, either of which may be used in jet power plants. The meter will register about 0.2 per cent higher with kerosene than with gasoline. This is due to better capillary seal, and to reduction in the net volume of the measuring chamber by greater adhesion of the liquid to the walls.

2 Changes in viscosity of the fuel due to temperature changes, producing an effect similar to the foregoing.

3 Compressibility of the liquid. As shown in (7), a change in pressure of 100 psi will change the volume of gasoline 0.1 per cent.

4 The increments of adjustment of the calibrating means.

5 Residual errors in calibration.

The difficulties encountered in proving displacement meters to such close tolerances have been well analyzed by Jacobson (8), and by the ASME Fluid Meters Committee (9). In the present case, since the counter reads only to the nearest gallon, its readings are not a practical means for proving the meter. Instead, a removable pointer is installed on the cam spindle when proving. In other respects the proving procedure follows API-ASME Code 1101 (7).

The meter will operate at temperatures between 130 F and minus 60 F, indicating the volume at operating temperature. Flight experience so far has not shown a need for correcting the meter readings automatically for changes in volume of the fuel resulting from changes in its temperature during flight. These changes occur slowly, even in wing tanks, and are retarded by self-sealing liners. At worst, a change of 50 F in fuel temperature during flight would represent an average change of 25 F in the fuel as consumed, or an error of less than 2 per cent in the total. Errors due to extreme vibration, or to meter position, or to sudden accelerations of the flow are negligible, since the metering piston can move only as the liquid moves.

A peculiar effect was discovered when a rate-of-flow indicator was applied to this meter. If the metal in the piston and the diaphragm could be of zero thickness, it is easy to demonstrate that the center of the piston would travel at a constant angular rate, for a constant rate of liquid flow. The actual thickness of these parts causes a slight cyclic variation in this relationship during each cycle of the piston. This has no detectable effect on the accuracy of measurement of the meter, being absorbed in the 44:1 gear reduction; but it was found to produce a vibration of the pointer on a sensitive rate indicator. Fortunately, this can be corrected completely by the introduction of a compensating eccentricity in the connection between the piston and the gear train, resulting in an exactly linear relationship between liquid movement and piston displacement.

It is of course quite true that this method of measurement does not take account of fuel lost by leakage. It is also a fact that operating personnel would prefer to know their fuel consumption in mass units, rather than in volume units, since engine thrust is more nearly proportional to the mass of fuel consumed. Nevertheless, against the small errors arising from the use of volumetric readings must be balanced the simplicity, reliability, and lightweight of the oscillating-piston meter.

CONCLUSION

The oscillating-piston displacement meter has proved accurate and dependable for the volumetric measurement of fuel consumed by an aircraft in flight, and hence for the determination of fuel remaining.

ACKNOWLEDGMENTS

The author wishes to thank Mr. J. J. Dysart of Pan-American Airways, Mr. C. L. Johnson, Chief Research Engineer of Lockheed Aircraft Corporation, and Mr. J. A. Townsend of the Equipment Laboratory, Air Technical Service Command, Wright Field, for their collaboration in this development.

BIBLIOGRAPHY

1 "Fuel Quantity Measurement Problems," by A. J. Snyder, *Aeronautical Engineering Review*, Trans. IAS, vol. 4, October, 1945, pp. 13, 17, 19.

2 "Advances in Aircraft Fuel Gauging," by E. Kelley, *Aero Digest*, vol. 50, September, 1945, pp. 77, 120, 123.

3 "New Fuel Gauge for Aircraft," *Engineer*, London, England, vol. 181, March 1, 1946, pp. 204–205.

4 "Liquid Mass Measurement Ups Fuel Gauging Accuracy," by C. H. Odell, *Aviation*, vol. 45, June, 1946, pp. 72–73.

5 "Latest Developments in Aircraft Controls and Instrumentation," by R. A. Brown, Trans. ASME, vol. 69, 1947, pp. 109–116.

6 "Fuel Consumption Indicator," by D. W. Moore, *Electronics*, vol. 19, March, 1946, pp. 152–153.

7 "API-ASME Code for Installation, Proving and Operation of Positive-Displacement Meters in Liquid Hydrocarbon Service," API Code No. 1101, July, 1946.

8 "Some Fundamentals in the Design and Application of Displacement Meters," by E. W. Jacobson, *Oil and Gas Journal*, vol. 39, June 20, 1940, pp. 36, 39–40.

9 "Results of Tests on Volumeters for Liquid Hydrocarbons," by R. J. S. Pigott, E. E. Ambrosius, and E. W. Jacobson, Trans. ASME, vol. 65, 1943, pp. 350–352.

Discussion

R. A. BROWN.[3] Without question, there is a need for a rate meter, whether of the integrating or instantaneous type, to measure the fuel consumption in aircraft. It is the writer's opinion, however, that such devices, although adding new information, cannot be thought of as eliminating the need for the mass measurement of available fuel. The following observations are presented for the author's consideration.

1 The designing engineers anticipate, in the case of certain ultra-high-speed jet aircraft, that from 10 to 15 per cent of the available fuel will be boiled out of the tanks during the initial climb and will be lost overboard through the vent lines. Because

[3] Aeronautical Division, Minneapolis-Honeywell Regulator Company, Washington, D. C.

of the possibility of this eventuality, operating personnel will be doubly anxious to have available an accurate measurement of the remaining fuel.

2 Because fuel consumption for a given set of power conditions is a function of the mass of fuel rather than of the volume of fuel, future flying under extreme hot or cold conditions will make it more than ever necessary that a knowledge be available of the remaining fuel rather than a volumetric portrayal of that already used.

3 The observation that because the depth of the liquid in the wing tanks of an airplane is sometimes small compared to the horizontal cross-sectional area, the accuracy of measurement is limited, does not necessarily conclude that the accuracy is thus limited beyond that needed for this application. In a certain type of capacitance device, it is possible to represent an 8-in. depth of fuel on a $2^3/_4$-in. dial in 300 deg with a laboratory accuracy on the order of 0.14 per cent. The use of multiple sensing elements will of course reduce in direct proportion the maximum depth necessary to produce complete dial rotation.

4 It should also be pointed out that the use of capacitance measuring devices provides considerable flexibility of installation, for which reason the sensing elements can be located in the center of rotation of the fuel. This either eliminates, or greatly reduces, the error of indication resulting from variations of flight attitude of the aircraft.

R. G. Jewell.[4] The flowmeter described in this paper is similar to one in the development of which the writer participated between 1941 and 1943. This development was continued to the point of building and testing samples. A view of one of the samples with cover removed is shown in Fig. 6 of this comment.

It is interesting to note the similarity of the performance of the two designs with respect to pressure drop and accuracy. The pressure drop in the sample design illustrated in Fig. 6 is shown in Fig. 7. This was taken with gasoline and shows a pressure drop of 1 psi at 5 gpm compared to 0.7 for the same rate of flow given in Fig. 5 of the paper, which data were taken with kerosene.

The accuracy of the sample illustrated is shown in Fig. 8 of this discussion at room temperature, and at high and low temperature. The accuracy falls off at low rates of flow because of a higher percentage of leakage. The accuracy which the author gives is ±0.2 per cent with a guaranteed accuracy of ±1 per cent at normal temperature and pressure, and this is on the same order of magnitude as found in our work.

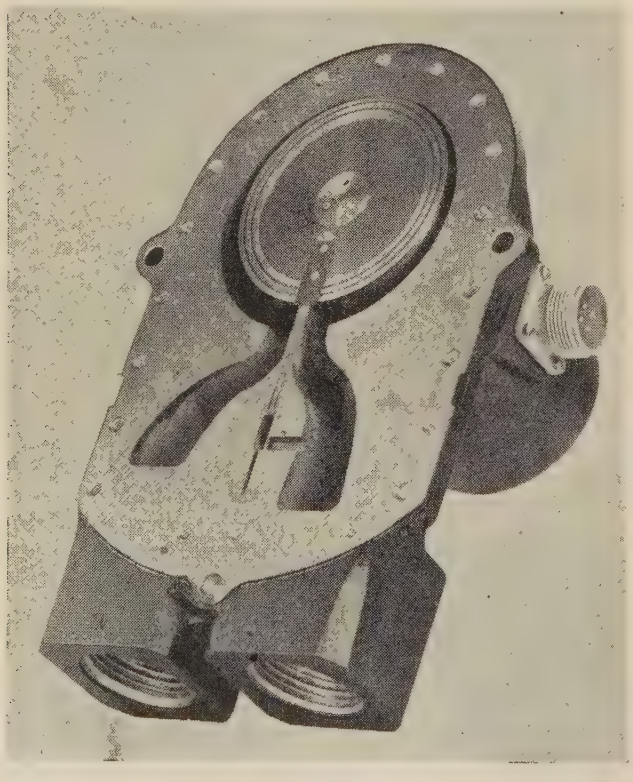

Fig. 6 Flowmeter With Cover Removed

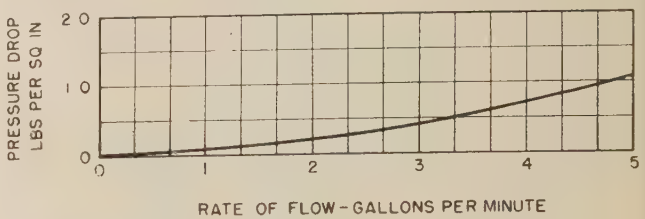

Fig. 7 Pressure Drop With 100-Octane Gasoline

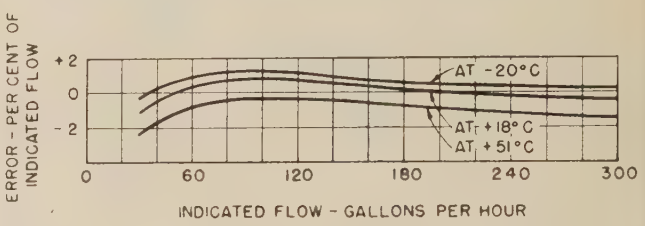

Fig. 8 Error at Room Temperature and at High and Low Temperature

The 0.0015-in. radial and 0.002-in. axial clearances which the author quotes are similar to those which our investigation showed to be necessary. This requirement presents two disadvantages, namely, difficulties in manufacturing and possible jamming due to dirt when in service.

The manufacturing difficulty is in maintaining the clearances specified. Each individual part involved must be machined to a 0.0005-in. tolerance, and while this can be done, it adds much to the cost.

Jamming due to dirt is the main difficulty with this type of meter. The close clearances used cause the meter to jam even with comparatively small particles of dirt which are encountered in fuel systems. It was found necessary to use a 100-mesh screen at the inlet to the flowmeter to overcome this difficulty. This screen must have a large area to avoid an excessive pressure drop, and should be located so that the by-pass valve will shunt the fuel around both the screen and meter. In contrast to the by-pass valve shown in Fig. 3 of the paper, this valve should be snap-acting, and once opened should remain open, definitely stopping the meter until it can be serviced, thereby avoiding the possibility of erroneous readings due to partial by-passing of the fuel.

The rate-of-flow indicator, described in a paper by Mr. Ballard,[5] was applied to this meter, and pulsation of the rate pointer was experienced as stated by the author. An eccentric coupling was also used and, while this compensated for most of the pulsation, it was necessary to increase the damping in the indicator to give

[4] General Electric Company, Lynn, Mass.

[5] "Electrical System for Aircraft Flowmeters," by R. G. Ballard; presented at the Annual Meeting, Atlantic City, N. J., December 1–5, 1947, of The American Society of Mechanical Engineers. Paper No. 47—A-67.

a steady reading. With this modification, the metering system performed satisfactorily.

Author's Closure

The data submitted by both Mr. Brown and Mr. Jewell are valuable additions to the published data on this subject.

The author was especially interested to learn of the oscillating-piston meter developed by Mr. Jewell's company. The manufacturing difficulties in mass-producing a unit requiring such close clearances are considerable, as Mr. Jewell points out. Nevertheless, measuring units of this type have been manufactured commercially by the author's company for 18 years, in capacities ranging from 15 to 600 gpm. This type of measuring unit is used for refined petroleum products at loading terminals, on tank trucks, and in retail gasoline pumps. Other types of positive-displacement meter, requiring similar close clearances, are also in widespread commercial use, and have been used in aircraft.

In all ground installations, as well as in airplanes, the meter is protected by a strainer of 80 to 100 mesh, as was found necessary by Mr. Jewell. Such a strainer provides additional protection for units downstream from the meter, such as valves, regulators, or nozzles. Apparently, the meter described by Mr. Jewell gave satisfactory results when so protected.

After this paper had gone to the printer, an article[6] appeared describing an aircraft fuel meter developed in England. This meter is of the oscillating-piston type with a manually operated by-pass valve and a solenoid counter, reading in gallons and tenths. The unit is strikingly similar to the meters described in this paper, with the addition of a built-in strainer of 120 mesh. The article states that this meter "was used in large numbers during the war in aircraft of all commands."

With regard to the points raised by Mr. Brown, the advantages of gravimetric measurement of fuel are given in detail in a recent article by J. A. Townsend.[7]

It is the author's personal opinion that the various methods of fuel measurement herein discussed supplement and verify each other; and that it has not yet been finally established whether the electrostatic tank gage, the widely used vane type rate-of-flow meter, the positive-displacement meter, or some combination of these instruments should be carried by a given type of airplane.

---

[6] "Keeping an Eye on the Fuel," *The Aeroplane*, London, England, vol. 73, August 15, 1947, p. 202.

[7] "Adoption of Gravimetric Fuel Quantity Gauges and Fuel Flowmeters for Aircraft," J. A. Townsend, U. S. Air Force, Air Technical Intelligence, *Technical Data Digest*, vol. 12, no. 7, October 1, 1947, pp. 7–12.

High-Temperature Performance of Silicone Fluids in Journal Bearings[1]

By J. E. BROPHY,[2] J. LARSON,[3] AND R. O. MILITZ[4]

This investigation covers the use of the dimethyl silicone polymer fluids and methyl phenyl copolymers at elevated temperatures. A specially designed small-bearing machine was used at bearing temperatures of 325 F to 500 F and at ambient or plate temperatures as high as 650 F. Hard chromium-plated journals were used in conjunction with bearings of 89 per cent copper, 4 per cent tin and 4 per cent lead, and 3 per cent zinc alloy. Loads up to 8500 psi were carried at 425 to 500 F, and loads up to 13,000 psi at 180 to 200 F, using the dimethyl silicone fluid. Comparisons are made of the lubricating characteristics of the two classes of silicone fluids investigated. For satisfactory operation, either a long break-in or a silicone pretreatment of the bearings is desirable. Data on safe operating temperatures and rates of increase of viscosity are presented.

Introduction

THIS investigation is part of a larger program on the lubricating properties of silicones undertaken by the Naval Research Laboratory at the request of the Bureau of Ships. As previous experience was concerned with the dimethyl silicone fluids, this investigation of high-temperature lubrication commenced using the dimethyl fluid. Since the methyl phenyl copolymers exhibited better stability in oxidation tests at elevated temperatures, the commercial fluid, DC 710, was also used in this investigation.

The dimethyl and methyl phenyl silicone fluids are included among the various silicones manufactured by both the Dow Corning Corporation and the General Electric Company and are commercially available under each supplier's trade name. At the start of this investigation only one manufacturer was in commercial production and able to supply large enough quantities of the desired fluids; hence all data given here relate to several large batches of well-reproduced fluids made by the Dow Corning Corporation. The dimethyl silicone fluid was stripped of volatiles and identified as Dow Corning fluid, DC 500, batch 369-62-69. The methyl phenyl silicone fluid was not stripped of volatiles and was identified as Dow Corning fluid, DC 710, batch 406-1-118. The viscosity-temperature characteristics of these fluids are summarized in Table 1.

Earlier reports from the manufacturers of the remarkable viscosity-temperature properties of the silicone fluids are well confirmed. A recent investigation by this laboratory of the high-temperature viscometric properties of the silicones had its origin in present interest in these fluids as high-temperature journal lubricants. The early and widespread belief that the silicones are poor lubricants is gradually being qualified as more information on their properties becomes available. This laboratory's initial work (1)[5] on journal bearings, followed by an investigation of various metal systems in silicones (2), have revealed new possibilities for them as lubricants in journal bearings.

TABLE 1 VISCOSITY-TEMPERATURE CHARACTERISTICS OF SILICONE FLUIDS USED

Temperature, deg F	Kinematic viscosity, centistokes[a] DC 500 dimethyl fluid	DC 710 methyl phenyl fluid
500	6.5	3.2
400	10.2	5.2
300	17.3	9.9
210	29.8	21.9
130	55.6	68.6
100	73.5	131.0
0	275.0	20400
—20	390.0	...
—40	600.0	...

[a] The data at temperatures above 210 F are results of another investigation (6) to be reported later.

It was also shown (1) that all the common nonferrous bearings were satisfactory when used with ground chromium-plated shafts. Even exercising the greatest possible care, the load-carrying capacity of steel on steel, or steel on cast iron, was very low in comparison with the nonferrous bearings. The necessary break-in was performed by either slowly increasing the load on the bearing during the run-in period or by suitable pretreatment of the bearings. Each method yielded satisfactory results, but the pretreating method greatly shortened the run-in period.

Tests with hydraulic pumps revealed that the Vickers piston pumps required a very small change to render satisfactory service with the silicone fluid. This change (replacement of steel knuckles in the universal joint with bronze knuckles) was necessary to avoid the action of the steel knuckles sliding on a steel seat. Similarly, Pesco gear pumps failed rapidly when the bronze bushings were replaced with cast-iron bushings. The pretreatment or lacquering process developed (1) formed a very thin organic silicon-containing film on the treated surface. This was accomplished by immersing the surface in a bath of dimethyl silicone fluid maintained at 300 F or higher. The duration of this treatment was dependent upon the temperature; however, 500 F for 24 hr was sufficient to produce the desired film on all the copper-base alloys tried. Such a film permitted a load to be placed on a new bearing almost immediately after starting the machine. The break-in time for a bearing could be reduced from a period of 16 hr as low as a few seconds. Two hours were usually devoted to the break-in when possible.

Experimental Methods

A modification of the bearing machines used in the previous work (1) was made for this study. The principal changes were the addition of heating elements above the support bearing, the relocation of the drive unit, and the necessary remounting. Thus the physical appearance of the machine differs from that of the preceding machine, but the essential features have been unchanged. Two of these machines were built. In Fig. 1 the bearing machine is shown completely assembled and loaded.

[1] Opinions or assertions contained in this paper are the authors' and are not to be construed as official or reflecting the views of the Navy Department.

[2] Mechanical Engineer, Lubrication Section, Naval Research Laboratory, Washington, D. C.

[3] Research Assistant, Lubrication Section, Naval Research Laboratory.

[4] Mechanical Engineer, R. T. French Company, Rochester, N. Y.

Contributed by the Research Committee on Lubrication and presented at the Annual Meeting, Atlantic City, N. J., December 1–5, 1947, of THE AMERICAN SOCIETY OF MECHANICAL ENGINEERS. Paper No. 47—A-114.

[5] Numbers in parentheses refer to the Bibliography at the end of the paper.

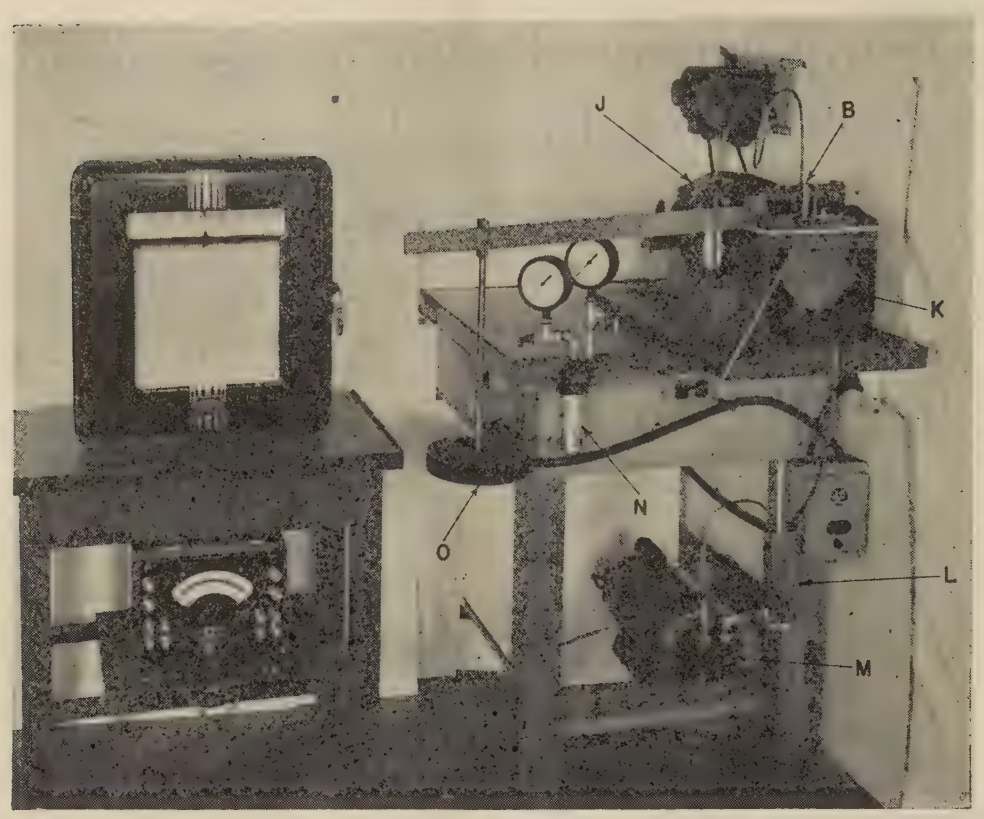

B = Test-bearing holder
J = Drive motor
K = Drain pan
L = Sump
M = Gear pump
N = Filter
O = Loading weight

FIG. 1 HIGH-TEMPERATURE BEARING MACHINE, ASSEMBLED

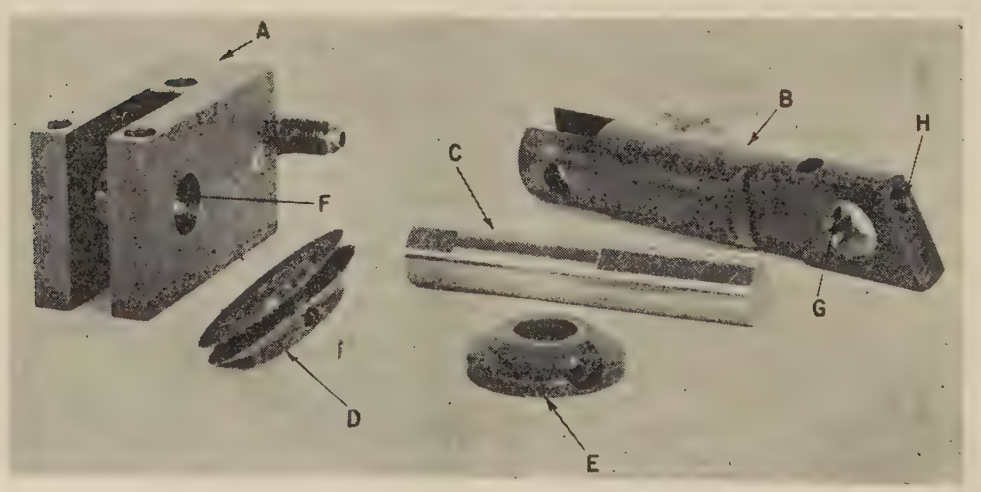

A = Support bearing block
B = Test-bearing holder
C = Journal
D = Flinger
E = Thrust collar
F, G = Fluid supply to bearings
H = Thermocouple hole

FIG. 2 TEST-BEARING COMPONENTS

Fig. 2 shows the components of the test-bearing assembly. Fig. 3 is an assembly drawing of the machine.

Available Pesco 1P-349 gear pumps were used to supply the bearings with fluid. A small reservoir was mounted directly over the gear pump, while the output of this pump was reduced by driving it with a 36-rpm motor.

The low surface tension of the DC 500 fluid, ca 20 dynes per cm, and its remarkable creeping tendencies caused leakage difficulties. The solution was found in the proper shape for the flinger guarding the opening in the drip pan.

To heat the system, a pair of concentric circular heating elements were mounted above the support bearing and test bearing. The test-bearing temperature was measured at the outer surface of the bearing through the bottom of the test-bearing holder.

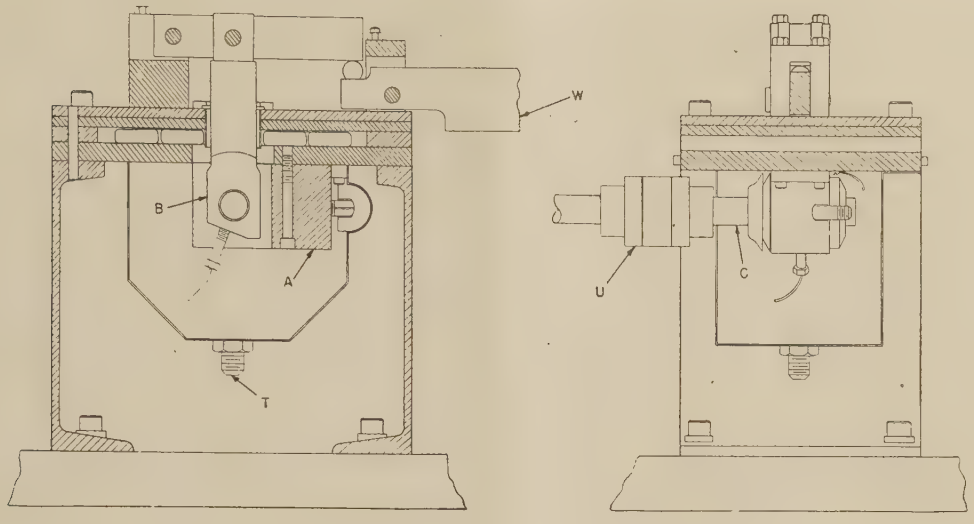

FIG. 3 ASSEMBLY DRAWING OF BEARING MACHINE

Temperatures were recorded continuously on a Tagliabue Celectray, a Leeds and Northrup Micromax, or a Brown electronic potentiometer, all of 0 to 800 F range. The Tagliabue instrument was a multiple-point recorder; the other instruments were single-point recorders. With the single-point recorder it was possible to follow the bearing-temperature changes more closely than with the multiple-point recorder. Incipient seizure was easily noted with the potentiometer as shown in Fig. 4.

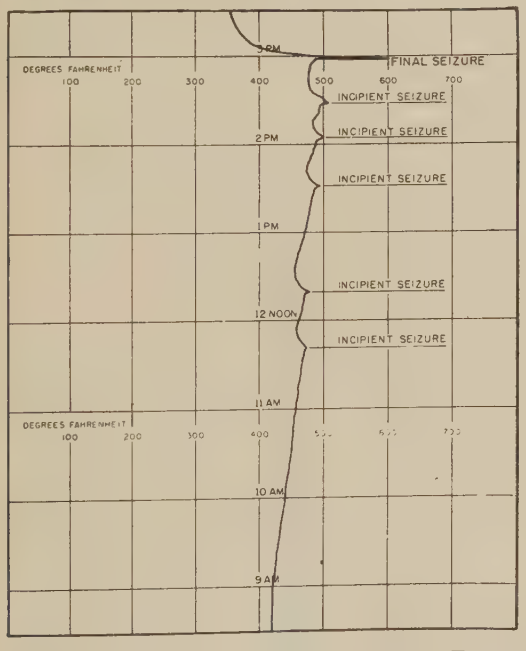

FIG. 4 EFFECTS OF INCIPIENT SEIZURES ON BEARING TEMPERATURE

Another recording potentiometer noted the temperature of the plate at the point where contact was made with the support bearing block. This "plate" temperature corresponded to the hottest part of the system. Inasmuch as the fluid came in contact with the plate, its temperature had an effect on the resulting viscosity of the fluid.

The drive motors on the two test machines were calibrated using a blocked-rotor test to determine the motor losses at varying loads. A polyphase wattmeter placed to read the input to the motor then was used to read the power demanded by the bearings. This arrangement was very sensitive to changes in the coefficient of friction in the bearing. Incipient seizures were easily noted and could be detected 2 or 3 sec before they were visible on the recording potentiometers.

Plain bearings having a wall thickness of $^1/_{32}$ in. were used in all runs. A bore of 0.687 in. and an L/D ratio of 0.73 were used. The diametral clearance (bore diameter minus journal diameter) was 0.0010 in. ± 0.0001 in. at 68 F.

Thin-wall bearings were pressed into the test-bearing holder and support block. The bearings were finish-bored in a lathe, using the special fixture previously described (1). This fixture was built to insure bearings that would be reproducible in size and finish. The analysis of the bearing used is as follows: Cu 88.92 per cent, Pb 3.79 per cent, Sn 4.01 per cent, Zn 3.28 per cent, Sb less than 0.01 per cent, Fe less than 0.01 per cent. Bearings of this composition were used as they had been successful in previous work (1), were readily obtainable from Delco, and easily finished. The journals were made of hard chrome-plated high-carbon steel since the conventional hardened journals were annealed slowly at the elevated operating temperatures.

The finish of the bearings and shafts was determined with a Brush analyzer, using a PA-2 pick-up. The finish was measured on the chrome-plated shafts before running and after running. The bearings were checked after boring, after treating with silicone fluid, and after running. Thus the visual examination of the oscillograph record from the surface analyzer and a microscopic examination could be carried out at the same time on any desired specimen. "Faxfilms" were also used to examine the bearing and journal surfaces to supplement the Brush analyzer record.

The speed of the journal was 1780 rpm ± 5 rpm, and a peripheral speed of 320 fpm. The silicone fluid was fed into the bearing opposite the loaded area at 26 psi. During these experiments, the bearing temperatures were varied from 240 F to 505 F; the sump temperatures accordingly varied from 104 F to 240 F.

The bearings were operated at no load for 2 hr, after which a 3000-psi load was placed on the bearing. After running the machine for another 2 hr, the load was increased to 6000 psi, and the heaters were turned on to increase the bearing temperature. If the bearing temperature was raised before adding the 6000-psi load, erratic behavior was obtained; the bearing would not carry the load in some instances. This condition is more fully described later. To provide the most favorable loading condi-

tions for runs with the methyl-phenyl silicone, an automatic ball-loading mechanism was used to increase the bearing load 1000 psi per hr.

Viscosity measurements were made during the runs by drawing a sample of the fluid from the sump, measuring the viscosity at 100 F, and returning the sample to the sump. At the end of the run, the viscosity of a fluid at various temperatures (300 F, 350 F, 400 F, 450 F) was determined (6). These data were obtained by other members of the laboratory in connection with a concurrent investigation of the physical properties of the various silicone fluids at high temperatures.

Before each run, all parts of the test setup were washed in unleaded gasoline and blown dry with air. To eliminate the lengthy break in time normally required for bearings lubricated with silicone, both the test bearing and support bearings were immersed in dimethyl silicone fluid at 300 F for 48 hr or longer (1). The test bearing and support bearings were drained of fluid and washed again in unleaded gasoline. The chromium-plated shaft and the bearing surfaces were wet with fluid before assembly.

Results With Dimethyl Silicones

Operation at bearing temperatures up to 505 F and ambient temperatures up to 685 F has been successful using a plain journal bearing. Runs as long as 338 hr have been made at 325–425 F bearing temperature. Summarized data are given in Table 2.

The effect of the bearing temperature on the viscosity of the dimethyl silicone is shown in Figs. 5 to 9, inclusive. The rate of increase of viscosity rises immediately upon raising the bearing temperature. This increase may be noted in runs A and C in Fig. 5. In run A the bearing temperature was increased from 325 F to 425 F after 207 hr. In run C, the bearing temperature was increased from 325 F to 400 F after 227 hr. Run K was made with dimethyl silicone of higher viscosity than the fluid used in any other runs shown in Table 2. The viscosity was increased from the original 73.5 to 86.7 centistokes by heating it in an open beaker approximately 300 hr before the run. For the first 60 hr in the bearing, the viscosity-increase rate was approximately 0.05 per cent per hr calculated as the ratio of the increment of increase to the original viscosity.

Run M was stopped after 72.5 hr and the fluid-supply lines, test-bearing holder, and support-bearing block were blown free of accumulated gel which had been restricting the passage of the silicone to the bearings. The effect may be noted in Fig. 8 by the rise in the rate of increase. As the supply pressure was constant, the amount of fluid feeding the bearings was increased by freeing the lines of gel. An increase in the plate temperature (from 570 F to 630 F) was then necessary to maintain the test-bearing temperature at 420 F. The higher plate temperature then caused a further permanent increase in the viscosity owing to oxidation. It is to be noted that both sections of run M can be superimposed on the second section of run A (plate temperature, 425 F). Moreover the rate of increase of viscosity for both sections of run M was approximately 0.11 per cent per hr. The rate of increase at the same temperature in run A was approximately 0.11 per cent per hr. The influence of the plate temperature on runs may be noted in Figs. 5 to 7, inclusive. Runs A and C had the same bearing temperature but the plate temperature was higher for run A. Therefore the resulting viscosity of the fluid was also higher. The same effect may be seen by comparing run D with runs E and F (Fig. 6), and G with H (Fig. 7). Hence among the factors influencing the increase of the viscosity of silicone fluid in a bearing are the increase of the ambient or plate temperature and the bearing temperature, as well as the decrease of the rate of flow through the bearing.

TABLE 2 RESULTS OF JOURNAL-BEARING TESTS USING DIMETHYL SILICONE FLUID

Run	Bearing temp, deg F	Plate temp, deg F	Sump temp, deg F	Bearing load, psi	Change in viscosity in entire run, per cent	Approx. viscosity increase, calc. as per cent of original viscosity per hr	$\frac{ZN}{P}$	PV	Duration of run, hr
A[a]	325/425	430/530		3000	31	0.02/0.1	10.3/6.3	16000	336
B[b]	350	470		3000	10	0.03	9.1	16000	226
C	325/400	355/500		3000	20	0.01/0.11	10.4/7.1	16000	356
D	375	460 to 525		3000	16	0.04	8.1	16000	258
E	375	400		3000	10	0.02	8.1	16000	301
F	375	400		3000	6	0.02	8.1	16000	194
G	400	645		3000	24	0.1	7.1	16000	214
H	400	470		3000	11	0.07	7.1	16000	141
J	420	620		3000	126	0.8	6.4	16000	112
K[c]	425	545		3000	65	0.5	6.3	16000	136
L	420	650		6000	61	0.5	3.2	32000	123
M[d]	420	570/630		3000	34	0.11/0.11	6.4	16000	150
1[e]	220	...	210	500			117	2600	10
2	460	550	116	2270			7.1	12000	9
3	260	...	...	3000			15.0	16000	21
4	420	670	220	3000			7.2	16000	60
5	240	...	165	6000			8.6	32000	6
6	300	390	...	6000			6.0	32000	60
7	375	580	240	6000			4.0	32000	56
8	410	524	220	6000			3.4	32000	9
9	413	538	180	6000			3.3	32000	6
10	425	450	102	6000			3.2	32000	12
11	430	575	113–177	6000			3.1	32000	44
12	440	450	116	6000			2.9	32000	36
13	455	530	130	6000			2.8	32000	29
14	475	580	104–170	6000			2.5	32000	38
15	500	660	180–240	6000			2.3	32000	27
16	505	650	211–223	6000			2.2	32000	32
17[f]	445	620	...	8480			2.0	44000	15
18	165	...	124	8100			10.9	42000	...
19	146	...	...	9740			10.6	51900	...
20	145	...	120	9740			10.6	50000	...
21[g]	178	...	120	10650			7.4	55000	...
22[h,j]	207	...	122	13610			4.7	70000	...

[a] Bearing temperature increased from 325 F to 425 F after 207 hr.
[b] Bearing temperature increased from 325 F to 400 F after 227 hr.
[c] Initial viscosity of fluid increased from 73.5 to 86.7 centistokes by heating and stripping. Approximate viscosity increase rate given for first 60 hr.
[d] Run stopped after 72.5 hr and system blown clean.
[e] No break-in, no treatment on bearings.
[f] Lower viscosity dimethyl fluid (51.9 centistokes at 100 F).
[g, h] Journal speed (640 rpm).
[j] Runs 1–22 inclusive were short runs to observe load-carrying capacity.

$\frac{ZN}{P}$ (Viscosity in centipoises) (rpm of journal)/(load in psi).

PV (Load in psi) (peripherol velocity of journal in fps).

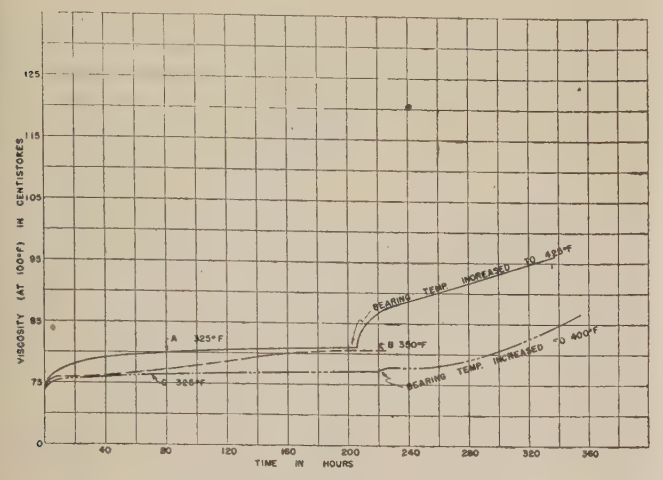

Average plate temperature of A-430 F—530 F
Average plate temperature of B-470 F
Average plate temperature of C-355 F—500 F

FIG. 5 EFFECT OF CHANGING BEARING TEMPERATURE DURING RUN

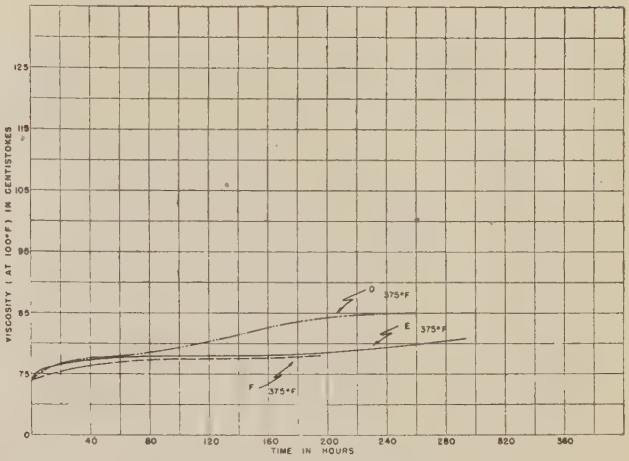

Average plate temperature of D-460 F
Average plate temperature of E-400 F
Average plate temperature of F-400 F

FIG. 6 EFFECT OF VARYING PLATE TEMPERATURE

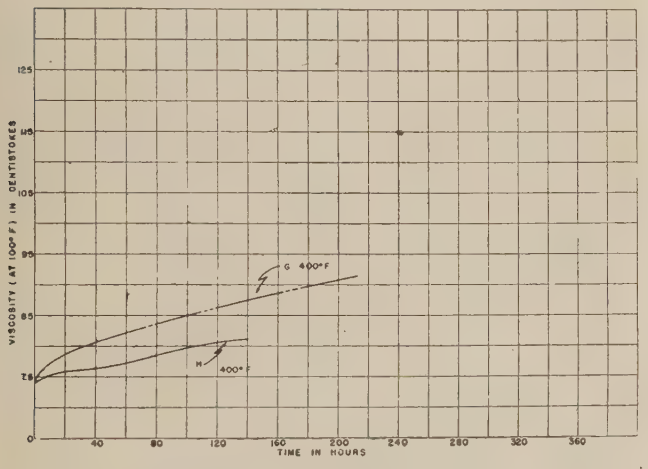

Average plate temperature of G-645 F
Average plate temperature of H-470 F

FIG. 7 EFFECT OF VARYING PLATE TEMPERATURE

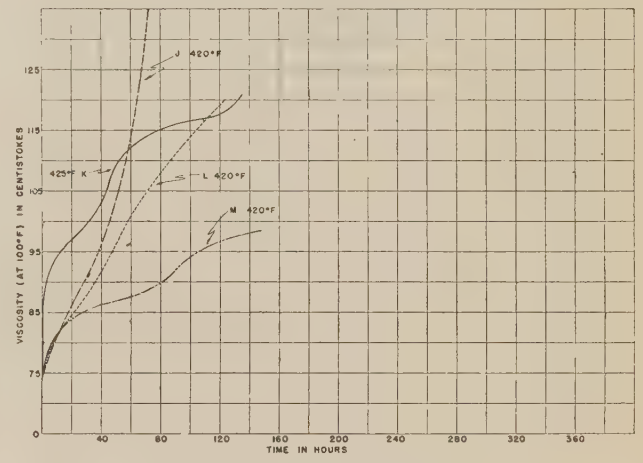

Average plate temperature of J-620 F
Average plate temperature of K-545 F
Average plate temperature of L-650 F
Average plate temperature of M-570 F—630 F

FIG. 8 EFFECT OF VARYING PLATE TEMPERATURE

A bearing temperature near 400 F permits operation with a viscosity-increase rate of approximately 0.07 to 0.10 per cent per hr. In the apparatus used, a further increase in the bearing temperature to 425 F caused such a high viscosity-increase rate (0.5 to 0.8 per cent per hr) that the life of the fluid was considerably shortened. Thus the viscosity changes noted in the bearing machine are explainable by known chemical oxidation results (3, 4).

The duration of a run could be increased by stopping the machine and cleaning all supply lines which had become heated by proximity to the bearing. The time to clean the supply lines was indicated by a rise in pressure of the fluid being supplied to the test bearing. At 400 F bearing temperature and a plate temperature of 550 to 600 F, the lines were cleaned after approximately 90 hr of operation. The initial increase in viscosity was accompanied by a decrease of the volume of the fluid in the system and was largely due to the removal of the volatile initially present in the silicone fluid. After this initial loss of volatiles, the viscosity increase was low and almost linear.

In all runs except No. 1, the bearings were treated prior to use. Satisfactory operation could be achieved without pretreating the bearings, but the break-in time was increased from 2 hr to 16 hr at bearing temperatures of approximately 400 F. The pretreatment produced a surface similar to the surface formed on the

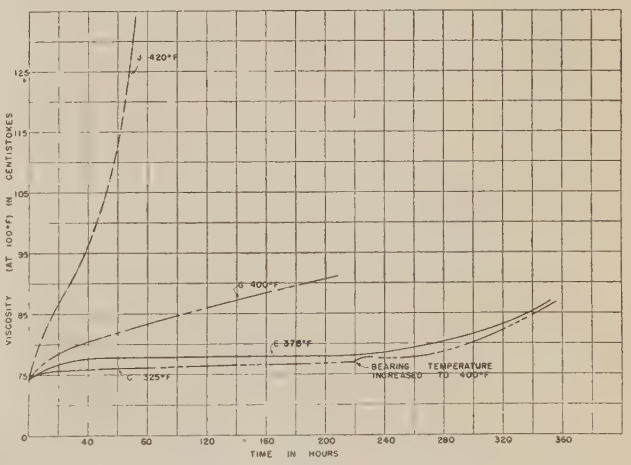

FIG. 9 EFFECT OF BEARING TEMPERATURE AND TIME ON VISCOSITY OF DIMETHYL SILICONE

bearing by a long break-in. Without the long break-in or a treatment, the bearings seized at a load of 500 psi. This fact was observed in run No. 1; previous data (1) demonstrate similar occurrences at lower temperatures (150 F to 180 F). At both low and high temperatures, the formation of a film on the bearing surface appears necessary for optimum load-carrying capacity.

A bearing which has failed by seizure could be reclaimed by treating it as if it were new, provided the surface had not been badly scored or grooved. It was necessary that the shaft be free of bearing metal. With these conditions the seized bearing was washed and heated in silicone fluid until a new film was formed on the surface. The bearing could then be placed in the machine again and the load increased as with a new bearing. The method of loading a bearing at high loads had a pronounced effect on the length of the run or the life of the bearing. If the bearing was heated before the load was applied, the run was often of short duration (see runs Nos. 2, 9, and 10). However, if the load was applied before the bearing was heated, results were much more reproducible (see runs Nos. 12, 13, 14, 15, and 16).

No deposits, such as produced by petroleum oils, were found in any runs. For those where the surface of the bearing was worn prior to seizure, a brownish-green residue was found on the flingers and sides of the test bearing. Continued operation at bearing temperatures of 425 F or above resulted in gel being formed where the fluid passed slowly over the heated surfaces.

Stalactites and stalagmites of gel were formed on the plate and the drain pan. These formations ranged from colorless to opaque white and from a soft gel at the tip to a crystalline material at the base. These products are similar in appearance to those formed by continued heating of the dimethyl silicone in an open beaker or in an oxidation cell (3). After operation, the dimethyl fluid changed from the original water-white liquid to one faintly tinged with yellow. No change in the ASTM viscosity-temperature slope was noted after running. No precipitate was visible after 48 hr storage at 0 F. At —40 F the fluid was slightly cloudy.

Results With Methyl Phenyl Silicones (DC 710)

Using the DC 710 fluid at low temperatures of from 150 to 220 F, relatively low values were found for the load-carrying capacity with a short break-in. A similar condition was encountered at a temperature of 400 F. Treatment of the bearing at 150 C for 72 hr before a run with the dimethyl fluid was of little value. A similar treatment even up to 300 hr with the methyl phenyl silicone was also unsatisfactory. No successful treatment for bearings in DC 710 has yet been worked out. Operation with the methyl phenyl fluid in a system which had previously contained a dimethyl silicone resulted in an emulsion of the two fluids. Such operation was always accompanied by rapid failure. The bearing would not carry a load of 500 psi. Therefore runs with the methyl phenyl silicone were made in a machine, all replaceable parts of which had been renewed. All other parts had been boiled in a saturated alcohol solution of potassium hydroxide or had been refinished by a surface grinder.

It has been noted that the dimethyl and methyl phenyl silicones did not form solutions with each other but formed two layers which became emulsions on stirring. These emulsions were difficult to break. No separation was noted on standing for several months and centrifuging for 4 hr at approximately 200 g was unsuccessful.

Summarized data on the runs with the methyl phenyl silicone fluid are presented in Table 3. The data in the last column show the low values of the load at incipient seizures. These are seizures which are made evident by a sudden but transient rise of the torque and of the bearing temperature. A comparison of incipient-seizure loads is considered more valuable than the relative values of the final seizure loads. Incipient seizures were recorded at loads as low as 1440 psi in run No. 27. Run No. 26 checked this with incipient seizures beginning at 1960 psi. However, the bearings used in run No. 27 were pretreated and recovered from several successive incipient seizures before finally failing at 4940 psi. Run No. 26 was not pretreated and failed at 2380 psi. Run No. 29 was given a very long break-in since an untreated bearing was used. The long break-in (48 hr at 500 psi and 209 hr to get up to the peak load, 7250 psi) was helpful in starting to form a protective coating on the surface of the bearing. The bearings for runs Nos. 24 and 25 had been treated in DC 710 fluid for 72 hr at 150 F. Incipient seizures occurred in run No. 28 at 2950 psi, 3000 psi, and 3065 psi before finally failing at 5160 psi after 10.5 hr.

In the longest test (run No. 23) lasting over 330 hr, a total increase in viscosity was found of 6 per cent. After the first 40 hr, the rate of increase was approximately 0.02 per cent per hr expressed as a per cent of the original viscosity per hour. The comparable runs (G and H) with the dimethyl fluid reveal rates of increase 3 to 5 times as large.

At the present time an extremely long break-in period (over 200 hr) is required for the methyl phenyl fluid when used at temperatures near 400 F. DC 710 fluid does not have as great a load-carrying capacity as either DC 500 or a nonadditive petroleum oil of approximately the same viscosity, Navy Symbol 3120, when used under the same conditions.

No deposits, such as seen with the dimethyl fluid, were noted in operation at 400 F. The fluid at the end of a run had changed from the pale straw color of the original fluid to a deeper color tending to become reddish. No change in the ASTM viscosity-temperature slope was noted after running. No precipitate was visible after storage at 0 F for 48 hr and at —40 F for 48 hr. The viscosities of DC 500 and DC 710 are approximately equal at 155 F. The viscosities of DC 500 and NS 3120 are approximately the same at 135 F. The viscosities of DC 710 and NS 3120 are approximately equal at 240 F.

Discussion

A factor important in determining whether or not a bearing will continue to run is the method of loading the bearing. Loading the bearing before heating is equivalent to a gentler and more

TABLE 3 RESULTS OF JOURNAL-BEARING TESTS USING METHYL PHENYL SILICONE FLUID

Run	Bearing load at seizure, psi	Bearing temp, deg F	Plate temp, deg F	Sump temp, deg F	$\frac{ZN}{P}$	PV	Duration of run, hr	Bearing load at 1st incipient seizure, psi
23[a]	500	400	425–530	...	19.7	2600	332	...
24	1740	400	550	158	5.6	9000	13	1040
25	1850	405	600	210	5.1	9600	9	...
26	2380	151	...	92	40.0	12300	96	1960
27	4940	217	...	91	7.7	26000	195	1440
28	5160	400	615	203	1.9	27000	10	2950
29	7250	162	...	96	11.0	37000	225	4460

[a] Not a seizure load, a safe load for duration of run to observe viscosity increase. Viscosity increased from 127 to 145 centistokes in 332 hr.

continuous method of loading than the sequence of heating first and loading afterward. This fact may be explained by noting the effect of the two sequences on the friction versus ZN/P curve during the period of loading the bearing. Let

Z = viscosity before heating
Z' = viscosity after heating
P_1 = initial load
P_2 = final load
N = rpm
$Z > Z'$
$P_2 > P_1$

Then

$$[1] \quad \frac{ZN}{P_1} \overset{\text{Increase of load}}{>} \frac{ZN}{P_2} \overset{\text{Increase of temp}}{>} \frac{Z'N}{P_2}$$

also

$$[2] \quad \frac{ZN}{P_1} \overset{\text{Increase of temp}}{>} \frac{Z'N}{P_1} \overset{\text{Increase of load}}{>} \frac{Z'N}{P_2}$$

However, in sequence [1] the transition of ZN/P_2 to $Z'N/P_2$ (reduction) is very smooth and continuous as the change is due to the decrease in viscosity by applied heat. In sequence [2] the transition from $Z'N/P_1$ to $Z'N/P_2$ is quite discontinuous and abrupt due to the change in load. Thus the choice of increasing the temperature (sequence 1) seems preferable in conditions in which the operation is at high loads unless the load can be changed (increased) uniformly and gradually.

Journal bearings may now be operated at higher temperatures than has been the practice with petroleum oils. The oxidation stability data obtained in these journal-bearing studies using viscosity changes are in good general agreement with the results given by Murphy and Saunders (3, 4) which were based upon chemical research. In both investigations it has been found that at up to 300–375 F the fluids may be used without significant deterioration for long periods of time, while above 400 F the rate of thickening, discoloring, and precipitation of gel increased rapidly, indicating need for periodic inspection or cleaning. The change in viscosity of the fluid at a given operating temperature is practically linear after the first 3 hr when using dimethyl fluid, and after the first 40 hr when using the methyl phenyl silicone fluid. The viscosity-increase rates given can be only rough approximations at high temperatures. At bearing temperatures of 450 to 500 F in such systems, the dimethyl silicone fluid cannot be used for more than approximately 30 hr unless the lines feeding the bearings are blown free of restrictions caused by the gelled oxidation products. Therefore, for continuous hot operation over hundred of hours or more, the bearing temperature should not exceed 400 F.

Either a long break-in period or a pretreatment of the bearings is necessary for satisfactory load-carrying capacity.

The maximum load-carrying capacity using dimethyl silicone fluid is about 9700 psi at 145 F, while about 7200 psi at 200 F was obtained using methyl-phenyl silicone fluid. However, the latter fluid necessitated a much longer and more careful break-in than the former. Using a nonadditive petroleum oil with a high viscosity index (Navy Symbol 1080) the highest load-carrying capacity obtained with the same procedure was about 2600 psi at 143 F (1).

The dimethyl silicone fluids have low pour points (from —65 F to below —100 F) in the low-viscosity grades, while the methyl-phenyl silicones have higher pour points (ca —5 F). However, the latter are the more stable to viscosity changes caused by high temperature and oxidation. Both fluids are more stable than nonadditive petroleum oils at the same temperature. The ASTM viscosity-temperature slopes of the dimethyl silicone fluids are always less than those of methyl-phenyl silicones having the same viscosities at the reference temperature. Both classes of silicone fluids have ASTM slopes less than those of comparable petroleum oils. This permits one viscosity grade of silicone fluid to be used over a wider temperature range than is permissible with a single petroleum oil. As in the earlier investigation (1), the low surface tensions and creeping properties of the silicone fluids caused greater sealing difficulties than are encountered with petroleum oils.

Published data are meager on the comparative lubricating characteristics of the methyl-phenyl and dimethyl silicone fluids. Kauppi and Pedersen (7), using a steel ball sliding on a plane, found much better wear preventative properties with the methyl-phenyl silicones. These conclusions are in apparent contradiction; however, this may be due to the considerable difference in the lubrication test methods involved. It may be due, in part, to the fact that a satisfactory method of forming a methyl-phenyl-silicone-lacquer film on a bearing surface has not yet been found.

Some of the future improvements indicated in silicone-lubricated bearing systems and in silicone fluids are increased oxidation stability and the development of other and better journal and bearing materials for high temperatures. The differences between the DC 500 and DC 710 fluids suggest an intermediate copolymer (one with a lower ratio of phenyl groups to methyl groups than found in DC 710). The early difficulties encountered (1, 2) at temperatures over 140 F in preventing leakage through packings became more serious at the high temperature used here. Necessary packings have been compounded of Hycar rubber with silicone fluid as a plasticizer. This packing material should be improved if possible for use at high temperature. At present a slight shrinkage occurs on prolonged contact with the silicones. A better pretreatment method is desirable for bearing surfaces to be used with the dimethyl fluids, and particularly the methyl-phenyl fluids. It may be possible to design totally enclosed systems for increased life at elevated temperatures.

Acknowledgments

The skillful machine work and suggestions of William Kostowicz were of considerable aid in this study. The efforts of Ralph Taylor and Ferdinand Thurman of the High Polymer Section were very helpful. The special rubber packings were developed by this group. The viscometric data on the various fluids before and after running were made available through the courtesy of J. B. Romans and Chester Cox.

BIBLIOGRAPHY

1 "Dimethyl Silicone Polymer Fluids and Their Performance Characteristics in Unilaterally Loaded Journal Bearings," by J. E. Brophy, R. O. Militz, and W. A. Zisman, Trans. ASME, vol. 68, May, 1946, pp. 355–359.

2 "Dimethyl Silicone Polymer Fluids and Their Performance Characteristics in Hydraulic Systems," by V. G. Fitzsimmons, D. L. Pickett, R. O. Militz, and W. A. Zisman, Trans. ASME, vol. 68, May, 1946, pp. 361–369.

3 "Investigation of the Thermal and Oxidation Stabilities of the Polymethyl Siloxanes," by D. C. Atkins, C. M. Murphy, Jr., and C. E. Saunders, *Industrial and Engineering Chemistry* (to be published).

4 "Investigation of the Thermal and Oxidation Stabilities of the Copolymers of the Methyl-Phenyl Siloxanes," by C. E. Saunders and C. M. Murphy, Jr. (to be published).

5 "Some Surface Active Properties of the Linear Polyorganosiloxanes," by H. W. Fox, Paula W. Taylor, and W. A. Zisman, *Industrial and Engineering Chemistry*, vol. 39, November, 1947, pp. 1401–1409.

6 "Viscosities and Densities of Synthetic and Petroleum Oils

From —40 to 700° F," by C. M. Murphy, J. B. Romans, and W. A. Zisman (to be published).

7 "Silicones as Lubricants," by T. A. Kauppi and W. W. Pedersen, *National Petroleum News*, Technical Section, vol. 37, Dec. 5, 1945, pp. r944–r948.

Discussion

C. M. Larson.[6] The authors are to be congratulated for the fine work they have done in the realm of high-temperature and high-pressure application of silicone fluids. This investigation enlarges our knowledge as to the further range of application of silicone fluids, and the need for pretreatment of bearing surfaces and the proper selection of metalworking surfaces where such conditions are met.

Previously, it was stated by the manufacturers of silicone fluids that such fluids were only for light loads. This was probably due to lack of pretreatment. The differences in the two types of silicone fluids are very interesting.

It is hoped that further work along lines of the authors' investigations will be made with silicone greases.

D. W. James.[7] The use of silicone fluids in journal bearings is something that the industry cannot afford to overlook. Although at present its use appears restricted to special problems, new applications will be found. For example, its use as a lubricant for high-temperature electric motors seems appropriate.

The low rate of viscosity increase of the silicone fluids, and the lack of deposit formation below 400 F, especially for the methyl-phenyl silicone fluid, recommend their use over mineral oils. However, these factors are not the only criteria for the selection of a lubricant. In most instances the pretreatment of the bearing material, plus handling care required for its protection would make the use of silicone fluids undesirable. Also, unusual care must be exercised to prevent leakage of the fluid in any but a totally enclosed mechanism.

In the test apparatus used it should be noted that the bearing was as free as possible from edge loading in order to maintain a uniform thickness of lubricant film across the bearing. In this way, very low ZN/P values can be obtained.

J. B. Bidwell.[8] The data of the paper clearly indicate the desirability of obtaining a film on the bearing surface before running at high load. The mechanism by which this film aids operation may well be a smoothing effect upon the bearing surface. The minimum oil-film thickness for the bearings used in these tests at $ZN/P = 10$ is about 50 microinches. Though no figures of roughness were presented in the paper, the peak-to-valley roughness of the bearings is probably of this same order. Thus some metallic contact would be expected. However, if the film produced filled the valleys, metallic contact might be prevented up to considerably higher loads.

This explanation is not complete, however, since the data of Table 3 show dependence of seizure load on bearing temperature. If the data of Table 3 are rearranged and listed in order of increasing bearing temperatures (decreasing viscosity), it will be noted that the corresponding values of ZN/P are then arranged in decreasing order with the exception of one test. Thus apparently smaller minimum film thicknesses are permissible at higher bearing temperatures. No explanation is advanced for this characteristic, but the effect of temperature suggests some surface chemical change.

The authors' statement that DC 710 does not have as high a load capacity as nonadditive petroleum oil of the same viscosity should be further qualified, since it is further stated that at 200 F the DC 710 carried a load of 7200 psi and NS 1080 at 143 F carried only 2600 psi.

Proper selection of bearing materials and finishes permits the use of petroleum oils at values of ZN/P as low as 2. The use of additives reduces deposits and allows operation at bearing temperatures of 325–350 F. These temperatures are seldom exceeded in reciprocating-engine bearings. Thus the use of silicone lubricants for this service does not appear desirable. In addition, if the silicone fluid is subjected to flame, as it may be in a reciprocating engine, on the cylinder walls, silica is formed and serious wear results. The gel formation of the DC-500 fluid at temperatures over 425 F, as pointed out in the paper, would be a serious drawback to its use in high-temperature bearings.

Authors' Closure

Silicone-grease research at the Naval Research Laboratory was started during the war and since then much further work has been done. A publication of the earlier research will be forthcoming in the near future.

No special handling or protection was found necessary after the bearings had been pretreated. No attempt has been made to study bearings under edge-loaded conditions. Roughness of the bearings was approximately 35 microinches (maximum) peak to valley. Roughness of the chromium-plated shaft was approximately 50 microinches (maximum), peak to valley.

Table 3 shows the values of ZN/P at failure. However, it is well known that failure of a bearing does not always occur at the minimum value of the ZN/P curve and in these tests the failures with the silicones usually did not occur at the minimum ZN/P. Therefore it has not been found possible to completely correlate the minimum film thickness with the highest bearing temperature.

The relative load-carrying capacity of NS 1080 and DC 710 should, in the opinion of the authors, be compared at the incipient seizure load since complete failure of the bearing can easily occur at the lower load. Moreover, the difficulty of breaking-in and running a bearing with the methyl phenyl silicone fluid should not be minimized when compared to the nonadditive petroleum oil.

The possibilities of using silicone fluid in the crankcase of a single-cylinder engine were explored by the Naval Research Laboratory late in the war. High wear on the cylinder walls was not noted but severe scoring and welding between the rings and the cylinder were observed. The hardened cam shaft and push rod were badly scored. However, changing the composition of the mating moving parts of the engine was not done. This is considered worth while.

Silicone fluid which was atomized and burned resulted in a fine, fluffy, white powder. Examination with an electron microscope revealed that the particles were spheres and ranged from 200 to 600 Å in diameter. U. S. Patent 2,432,109 entitled "Break-in-Fuel" granted to W. A. Zisman, H. R. Baker, and C. M. Murphy of the Naval Research Laboratory, dealt with the use of silicon containing compounds which form silicon dioxide when burned. The compounds were added to the fuel and were burned in the combustion chamber of engines. Silicone fluids and silicates were among the compounds acting as polishing agents during break-in if added to the fuel. The limitations of the silicone fluids due to gel formation may be minimized, in some systems, by the proper design of the system and filters.

[6] Sinclair Refining Company, New York, N. Y. Mem. ASME.

[7] Mechanical Engineer, Mechanical Engineering No. 4 Research Laboratories Division, General Motors Corporation, Detroit, Mich. Mem. ASME.

[8] Mechanical Engineering No. 5 Research Laboratories Division, General Motors Corporation, Detroit, Mich.

Problems Associated With Use of Diesel Fuels

By W. L. H. DOYLE[1] and E. W. LANDEN,[2] PEORIA, ILL.

This paper presents results of recent investigations dealing with the nature of exhaust products resulting from combustion of Diesel fuels, particularly those products composing smoke. Development of some new inspections for improved control over certain properties of Diesel fuels is suggested. New standardized tests should be developed, one whereby the relative stability of a Diesel fuel can be determined, and another whereby the "Diesel-fuel combustibility" quality can be evaluated. New additive-type lubricating oils must be made available for use in the medium- and higher-speed Diesels to combat the deleterious effects of sulphur contents in the fuels for these engines.

Introduction

In less than a decade a great number of Diesels have been produced for use in buses, trucks, tractors, locomotives, naval and other marine services, and for a wide variety of stationary power-plant requirements. The total horsepower involved is many millions, and includes about 60,000,000 hp which were produced for our own Navy. These widespread applications of the Diesel have resulted in a remarkable growth in the demand for Diesel fuels. This same period marks the development of important changes in petroleum-refining techniques, and the large-scale application of catalytic cracking. These, together with hydrogenation and other reforming processes, make it possible to produce on a wide scale practically any type of hydrocarbon fuel, starting with petroleum crude.

Economic factors, more than ever before, will have an increasing influence on the make-up of available Diesel fuels. Since combustion processes vitally influence the performance of the Diesel, it is important to consider fuel properties and their relation to Diesel combustion. Fuel properties will also be discussed in relation to existing and future fuel specifications.

Criteria for Diesel Combustion Performances

The products of incomplete combustion serve as important indexes of combustion performance. When these products are related to fuel properties, we have a sound criterion for evaluating the combustion performance of fuels. Table 1 shows the various products of combustion present in the exhaust gases and the form in which they occur.

Diesel Smoke

In general, smoke may be defined as a particular atmosphere containing suspended solid particles and minute liquid particles in various proportions. Diesel smoke is produced from liquid and gaseous hydrocarbon fuels. It may contain solid carbonaceous particles or a fog consisting of minute liquid hydrocarbon droplets and condensed water droplets.

TABLE 1 PRODUCTS OF COMBUSTION PRESENT IN DIESEL EXHAUST GASES

Products of Complete Combustion	State			Comments
	Gas	Liquid	Solid	
a) CO_2	x			Corrosive under some conditions
b) H_2O	x At temp. above dew point	x At temp. below dew point		Contributes to corrosion at film temperatures below dew point
c) N_2	x			Inert
d) O_2	x			Excess
Products of Incomplete Combustion				
a) CO	x			Odorless, toxic, formed under locally over lean or locally over rich conditions
b) H_2	x			Formed under locally over rich conditions
c) CH_4	x			Formed under locally over rich conditions
d) Unburned fuel	x At temp. above dew point	x At temp below dew point		
e) Partially Oxidized Fuel	x At temp. above dew point	x At temp. below dew point		Include: Aldehydes (odorous compounds) Organic acids (corrosive compounds) Probably formed under locally over lean conditions
f) Carbon			x	
g) Ash			x	
Other Products				
a) SO_2	x			Corrosive in presence of water
b) SO_3	x			Corrosive in presence of water
c) Nitrogen Oxides	x			Corrosive in presence of water

The minute solid particles found in Diesel smoke occur under all conditions of operation but are more evident at higher outputs, as shown in Fig. 1. To obtain these data, the exhaust products from the two engines, A and B, were passed through a surge tank, through four condensers cooled with solid carbon dioxide or "dry ice" and finally through a cloth filter. Exhaust back pressure at the engine outlet was maintained at atmospheric pressure by a vacuum pump. At the end of each test run the nongaseous products exhausted by the engine were recovered and analyzed. These included the water from combustion, unburned carbonaceous particles, and oily residues. The carbonaceous particles result from the cracking of the hydrocarbon molecules at elevated temperatures and pressures and also from incomplete chemical reactions occurring in the cylinder during the combustion cycle.

Landen (1)[3] has demonstrated that much of this cracking occurs early in the combustion cycle, since large quantities of solid particles appear in the combustion chamber shortly after initiation of combustion. Best combustion will occur only if the fuel vaporizes completely, there is sufficient oxygen, the oxygen is adequately mixed with the fuel vapors, temperatures are favora-

[1] Assistant Director of Research, Caterpillar Tractor Company. Mem. ASME.

[2] Staff Physicist, Research Department, Caterpillar Tractor Company.

Contributed by the Oil and Gas Power Division and presented at the Annual Meeting, Atlantic City, N. J., December 1–5, 1947, of The American Society of Mechanical Engineers.

[3] Numbers in parentheses refer to the Bibliography at the end of the paper.

ble, and sufficient time is allowed for completion of the chemical reactions. Under conditions of proper rating there is always an over-all excess of oxygen present in the Diesel. Air temperatures are favorable for vaporization of normal fuels when the engine is operating at reasonable loads and speeds. Inadequate mixing of oxygen with any of the fuel vapors, insufficient time for the various chemical reactions, and the cooling of the reaction products during expansion are the important factors which prevent complete combustion, and thus contribute to the production of carbonaceous particles appearing in the exhaust.

The fog type of smoke may occur when the engine is operating at reduced power outputs, when idling, or when the engine is used as a brake with incomplete fuel cutoff. This fog of minute liquid hydrocarbon particles may come from unburned fuel which has passed through the cylinder. It may also come from the various liquid hydrocarbon fractions formed from the original fuel and the lubricating oil, as the result of various cracking reactions and incompleted-combustion reactions. Fig. 2 shows measured quantities of liquid hydrocarbon products recovered simultaneously with the solid carbon products shown in the previous figure. These data show that the liquid components increase with reduction of fuel-air ratio or power output. The liquid hydrocarbon residue from combustion, as recovered from the condensing system, had an average molecular weight nearly twice that of the fuel. This indicates that some liquid fractions, particularly heavier ends, and some polymerization products are present in the exhaust. Here again best combustion requires complete vaporization, a sufficiency of oxygen, adequate mixing of oxygen and fuel vapors, favorable temperatures, and sufficient time.

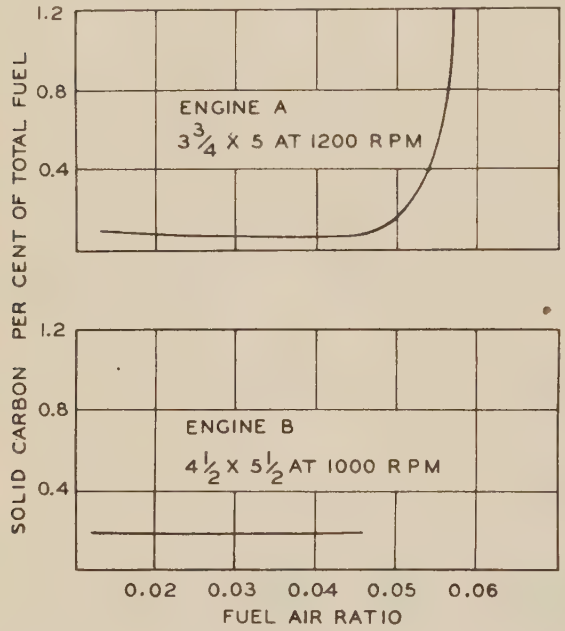

Fig. 1 Solid Carbon Content in Diesel Exhaust

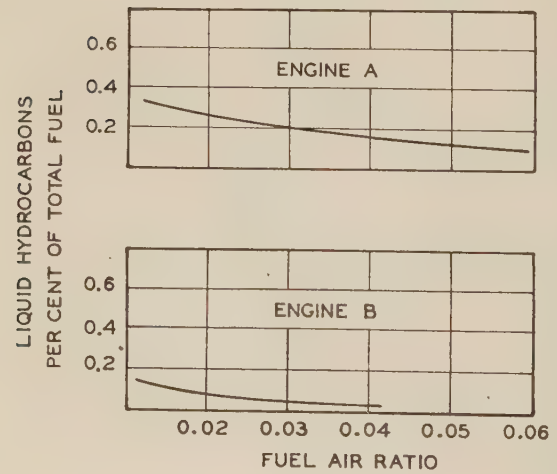

Fig. 2 Liquid Hydrocarbon Content in Diesel Exhaust

Under conditions of reduced power output and also when an engine is used as a brake with incomplete fuel cutoff, relatively small quantities of fuel are injected. Due to less favorable atomization the average fuel droplet is large, and droplet velocities are low. Air temperatures are unfavorable because of reduced compression and reduced heat-energy input, and hence more time is required for vaporization. Ample oxygen exists but the oxygen and fuel vapors tend to mix inadequately. Localized ignition and localized combustion reactions are delayed, and in addition there are also local regions in the combustion chamber where fuel-air mixtures are too lean to allow any inflammation. Thus these localized conditions may produce vapors of unburned hydrocarbons and partially oxidized hydrocarbons. The vapors of the various hydrocarbon fractions which are not completely oxidized, and any unburned fuel vapors condensed in the atmosphere will appear in the exhaust as a light bluish-gray smoke.

Water vapor results from combustion of hydrocarbons. At lower atmospheric temperatures this vapor will condense and appear as a white fog or smoke.

Thus Diesel smoke may consist of black solid carbonaceous particles, and minute droplets of fuel, various liquid hydrocarbons, partially oxidized hydrocarbons, and condensed water vapor. The general appearance of the smoke is determined by the predominating constituents.

Fuel Properties Influencing Diesel Smoke

The chemical composition and certain physical properties of the fuel are factors which influence Diesel combustion. The chemical make-up of the fuel influences its ignition quality, or cetane number as shown (1) in Fig. 3. Ordinary fuels of high paraffin content have relatively high cetane-number ratings. For normal paraffins the cetane number increases with the number of carbon atoms in the straight chain. In general, the ease of ignitibility follows the molecular configuration and reduces in the following order: Normal paraffins, olefins, naphthenes, and aromatics.

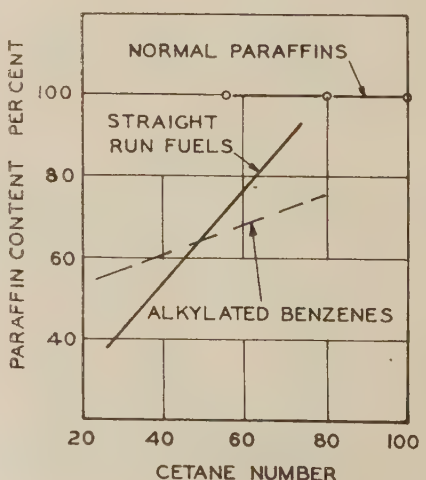

Fig. 3 Cetane Number as a Function of the Paraffin Content

The cetane number of a fuel, without additive, serves as a useful measure of its inherent ignition quality. However, the volatility of the fuel and the localized fuel-air mixture formations are factors controlling fuel combustion. High-volatility fuels with good ignition qualities tend to burn quickly and in such a manner that only a small amount of residue is exhausted from the combustion chamber.

The quantity of a given fuel injected into the combustion chamber has an influence on the relative cleanliness of combustion, and the type and quantity of exhaust smoke. A fuel of average cetane number and volatility, when consumed in a Diesel which is in good mechanical condition, presents a smoke pattern that is dependent upon engine power output and the related fuel-air ratio and is characteristic of all engines and most fuels. At idle operation, fuel-air ratios are extremely small, and the bluish-gray fog type of smoke appears at the exhaust. At increased loads and higher fuel-air ratios, in the approximate range of 0.015 to 0.05, fuel combustion is more generally complete, and hence less smoke is visible. As fuel-air ratios increase above this range, the black, or predominantly carbonaceous-particles type of smoke becomes more evident.

The cetane number and the volatility of the fuel also influence the Diesel smoke pattern. In Fig. 4, taken from Wetmiller and

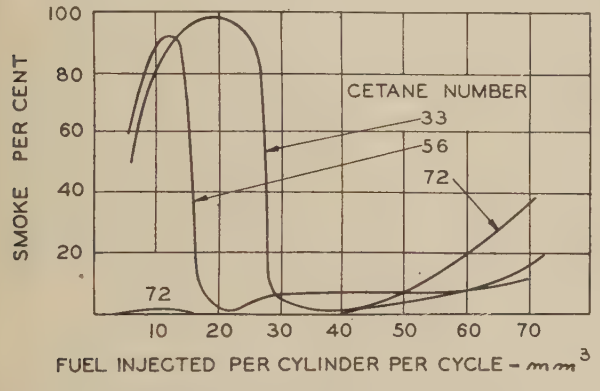

Fig. 4 Effect of Fuel Injection Rate on Exhaust Smoke at 1400 Rpm

Endsley (2), smoke is shown in relation to the quantity of fuel injected and the cetane number of the fuel. The three fuels used for these tests had essentially the same volatility characteristics. The lower cetane-number fuels produced large quantities of smoke at low fuel-air ratios, indicated by the lower fuel-injection rates. At the intermediate and higher values of fuel-air ratios, smoke was much less, indicating better combustion. The fuel having the highest cetane number produced little smoke at low and intermediate fuel-air ratios, but at high fuel-air ratios larger quantities of smoke were produced.

Landen (1) has illustrated the effects of cetane number and volatility on Diesel combustion from data obtained when using special fuels in a direct-injection engine. Fig. 5 indicates smoke measurements with fuels of different cetane numbers, having two values of volatility. The first group of highly volatile fuels, having a boiling range of 400–500 F, shows little smoke at the low brake mean effective pressure (bmep) or low fuel-air ratios. For this group as the bmep or fuel-air ratio increases, the smoke increases. At any given fuel-air ratio, the higher-cetane-number fuels produce more smoke than the lower-cetane-number fuels. This is in agreement with the data of Wetmiller and Endsley, who used fuels of comparable volatility. However, Landen's data do not cover some of the lower values of fuel-air ratios reported by Wetmiller and Endsley. These data indicate that under conditions of higher power outputs with highly volatile fuels of high

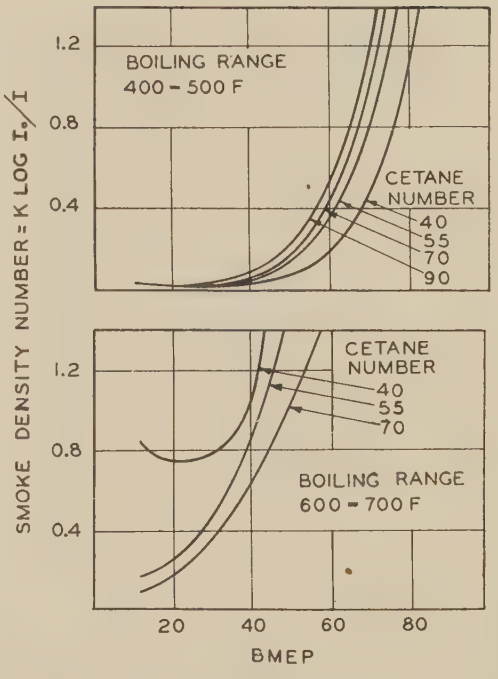

Fig. 5 Effect of Cetane Number and Boiling Range on Exhaust Smoke at 1200 Rpm

cetane number much more cracking of the fuel occurs due to thermal breakdown than with fuels of comparable volatility having lower cetane-number ratings.

Now consider the second group of less volatile fuels having a boiling range of 600 to 700 F. These fuels produce more smoke than the first group of highly volatile fuels at comparable bmep's or fuel-air ratios. For this group the low-cetane-number fuel produced more smoke than the higher-cetane-number fuels. During the ignition-delay period some fuel mixes with air in proportions which do not allow inflammation. Due to the inherent longer ignition delay, the flame boundaries for the lower-cetane-number fuels are extended, permitting existence of more local over lean fuel-air mixtures than for the shorter flame boundaries characterizing the shorter ignition delay of higher-cetane-number fuels. The larger droplets in the fuel spray may be carried beyond the flame boundaries and some may reach the combustion-chamber walls where they become chilled. This chilled fuel evaporates later in the combustion cycle. Some of it burns under unfavorable conditions and the rest is exhausted as unburned fuel. The longer ignition delay of the lower-cetane-number fuel permits more of these droplets to be carried to the walls than for the higher cetane-number fuels. Also, as the lower-cetane-number fuel evaporates from the wall, since it is more resistant to cracking, liquid hydrocarbons will predominate in the exhaust appearing as bluish-gray smoke. The higher-cetane-number fuels being less resistant to cracking will break down. Part of the cracked products will burn and part will be exhausted, mostly as solid carbonaceous particles. Thus the lower-cetane-number low-volatility fuels produce a heavier smoke for a given bmep or fuel-air ratio than for the higher-cetane-number fuels of comparable volatility.

Blends of two 40-cetane-number fuels used in operation of a direct-injection engine serve to illustrate further the effect of volatility. Fuel A had a 400–500 F boiling range and fuel B had a 600–700 F boiling range. Fig. 6 shows the smoke measurements of these fuels and the fuel blends (1). From this figure the effect of volatility on smoke is illustrated.

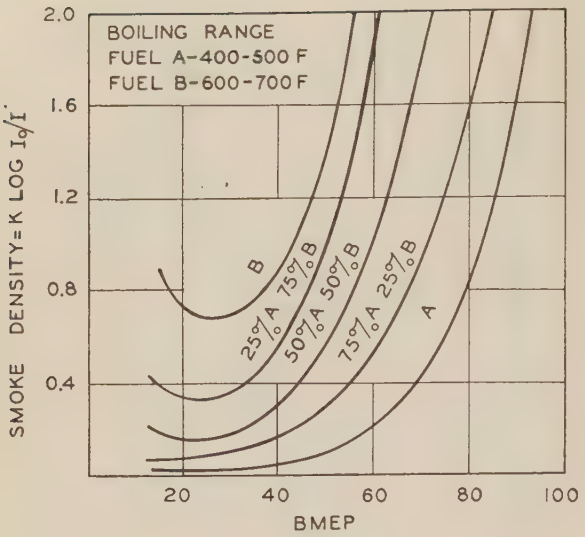

FIG. 6 EXHAUST SMOKE PRODUCED BY BLENDS OF 40-CETANE-NUMBER FUELS AT 1200 RPM

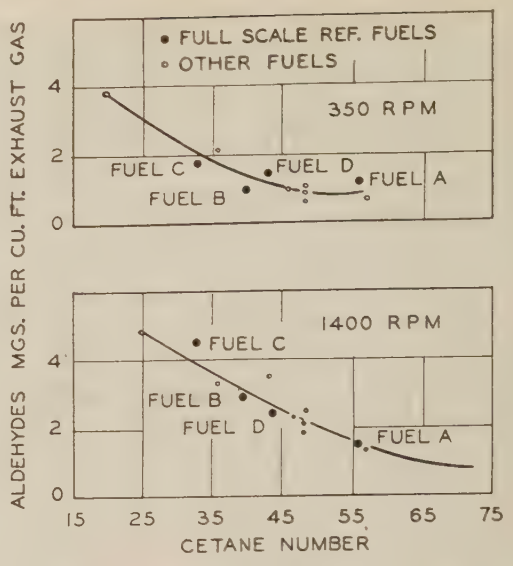

FIG. 7 ALDEHYDES IN EXHAUST AS FUNCITON OF CETANE NUMBER OF FUEL, ENGINE IDLING

Other fuel properties may be considered, such as viscosity and gravity. Obviously, the viscosity affects the mechanics of injection and is primarily related to combustion performance because of influence of engine design features. The heat content of a fuel is largely a function of the gravity and will influence the specific fuel-consumption rates.

FUEL PROPERTIES RELATING TO ODOR

Diesel exhaust may contain products having pungent odors. The exhaust odor when referred to in the literature is associated with the aldehyde content of exhaust gases. The ignition quality seems to be the one factor which influences the aldehyde content in exhaust gases. Fuels of higher cetane number minimize this aldehyde content, according to Wetmiller and Endsley (2), and Ainsley (3). In Fig. 7 Ainsley reports the effect of cetane number on aldehydes in the exhaust. These observations were obtained with an engine which was idled at two speeds. From these data it will be observed that higher-cetane-number fuels yield lowest aldehyde concentrations in the exhaust.

FUEL PROPERTIES CONTRIBUTING TO ENGINE DEPOSITS AND WEAR

Engine deposits and wear have been investigated over a period of years and data are reported in the literature. For ordinary Diesel fuels it is difficult to determine the isolated influence of any one fuel property quantitatively, since, in attempting to change one fuel property, other properties of the fuel are also altered. Lubricating oils also may be responsible for deposits in the cylinders. An exception is to be noted in the case of Diesel fuels having appreciable sulphur contents. Sulphur content in present-day fuels varies over a wide range and is tending to increase. The reactions occurring during combustion produce either sulphur dioxide or sulphur trioxide.

Cloud and Blackwood (4) have demonstrated the individual effect of sulphur trioxide on engine deposits by motoring an engine with no fuel being admitted and when supplying sulphur trioxide with the intake air. Under these conditions, pronounced oil sludging and engine deposits were observed. This indicates that sulphur trioxide combines with the lubricating oil. Fuels containing sulphur produce sulphur trioxide during combustion in the Diesel. Thus the sulphur content in the fuel is detrimental to the lubricating oil and contributes to formation of engine deposits. Blanc (5) shows that the deleterious effects of sulphur in Diesel fuels can be minimized by the use of special additive types of lubricating oils when operating under conditions of normal high jacket temperatures.

It has been demonstrated by Blanc (5), and by Broeze and Gravesteyn (6), that wear increases rapidly with increased sulphur content in the fuel. Evidence therefore points to increased operating difficulties with increased sulphur content in the fuel. The detrimental effects on engine wear and deposits when using the nonadditive types of lubricating oil are out of all proportion to the content of sulphur compounds which may be present in the Diesel fuel.

FUEL PROPERTIES INFLUENCING STARTING

The ignition quality of a fuel has a direct bearing on starting. Shoemaker and Gadebusch (7) show for a given Diesel that an 89-cetane-number fuel was required for startability at an ambient temperature of —20 F, whereas at 60 F a 36-cetane-number fuel gave good starting.

Factors affecting ignition under starting conditions include air pressure, air temperature, vaporization characteristic of the fuel, ignition delay of the fuel, and the auto-ignition temperature of the fuel. Terminal air pressures at various cranking speeds for a particular engine having a compression ratio of 17 to 1 are given by Heldt (8), as shown in Fig. 8. Corresponding values of terminal compression temperatures have been calculated for four ambient temperature conditions as shown in the figure.

The effect of the auto-ignition temperature and ignition-delay characteristics of the fuel may be indicated by considering one cranking speed, a uniform fuel vapor-air mixture and a finite time of 0.05 sec for the oxidation process of auto-ignition. Under these conditions, Tizard and Pye (9), for a cylinder having a compression ratio of 7 to 1, found that the auto-ignition temperature for a 20 to 1 heptane-air mixture is 620 F, and that for a 15 to 1 ether-air mixture is 480 F. For the same ignition delay the ether-air mixture has an auto-ignition temperature which is 140 deg below that of the heptane which is one of the more volatile hydrocarbons.

An ignition delay of 0.05 sec involves a crank angle of 90 deg at 300 rpm. On the basis of these data the lower-compression engine would not be expected to start at subnormal temperatures. However, the Diesel with its higher compression ratio using a suitable if more complex hydrocarbon fuel in the injection system, does start at temperatures well below —20 F when cranked at

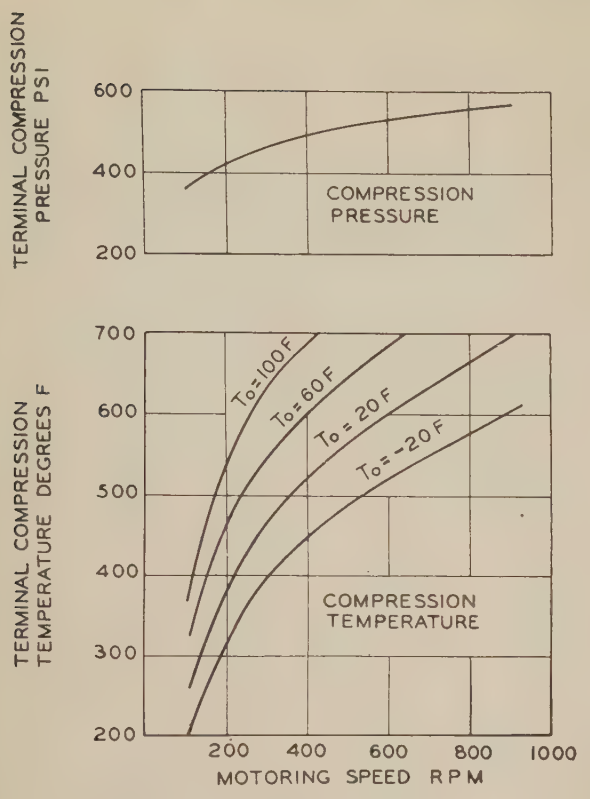

FIG. 8 COMPRESSION PRESSURES AND TEMPERATURES AS FUNCTION OF MOTORING SPEED

relatively low speeds and when diethyl-ether is atomized promiscuously into the engine air intake.

It develops that the experimenters (9) used a special commercially pure diethyl-ether, whereas for low-temperature starting, commercial, as distinguished from the commercially pure, ether is used. This has considerably greater contents of the peroxides as impurities. Being unstable even at normal temperatures, these peroxides act as ignition accelerators, starting oxidation reactions early in the compression stroke. The combined effect of the increasing compression pressures and temperatures, occurring during successive compression strokes, steps up these reactions enormously. Thus the effective localized ignition delays and auto-ignition temperatures are greatly reduced. This explains why a $5^3/_4$-in-bore engine, for instance, will start at cranking speeds below 150 rpm under ambient temperatures of less than —20 F in a matter of 6 to 9 sec when ether is atomized into the engine air intake.

FUEL ADDITIVES

There is a sound associated with Diesel ignition and combustion which is recognized as "Diesel knock." This sound may vary from zero intensity to a very high value occurring at incipient detonation. Best combustion for the Diesel occurs under conditions approaching incipient detonation because of the high rates of burning. Design features are necessarily established so as to limit combustion performances to conditions well below those approaching the incipient-detonation type of combustion.

For a fuel having a given cetane number, a given volume of fuel will enter the cylinder before inflammation starts. This volume is larger for a low-cetane-number fuel than for a high-cetane-number fuel. The rate at which energy is released by the initial combustion of the fuel is a function of the inflamed volume. Thus for the lower-cetane-number fuel, the larger volume existing in the cylinder will release energy at higher rates and will produce a more intensive knock. An ignition accelerator added to a fuel reduces the ignition delay and therefore reduces the volume available at instant of inflammation.

Field experience (10) with distillates containing certain additives indicates that additives offer possibilities as a means of converting some rough-running fuels into satisfactory fuels.

It will be of interest to determine if the intensity of knock changes with fuel composition as between fuels of equal volatility and cetane number, and the influence of ignition accelerators on the phenomenon. The effect of fuel composition on deposits should also be determined when comparing fuels of equal volatility and cetane number.

OPERATING CONDITIONS WHICH CONTRIBUTE TO SMOKE

The results of a comprehensive investigation (2), comparing performances of engines at the end of extended periods of actual service in automotive buses with performances after these same engines had been serviced and returned to good mechanical condition, are shown in Table 2. From these data it will be

TABLE 2 EFFECT OF ENGINE CONDITION ON PERFORMANCE

	Engine A	
Performance Feature	Injectors after Extensive Use in Bus Service	Same Injectors after Overhaul
Exhaust Smoke - 350 rpm Idle, %	2	0
Exhaust Smoke - 1400 rpm No Load, %	2	0
Exhaust Smoke - 1400 rpm 1/4 Load, %	8	6
Exhaust Smoke - 1400 rpm 1/2 Load, %	11	8
Exhaust Smoke - 1400 rpm 3/4 Load, %	16	14
Exhaust Smoke - 1400 rpm Full Load, %	42	37
Exhaust Smoke - 1400 rpm 3/4 Load, after 15 min at 350 rpm Idle, %	37	18
Fuel Consumption at 1400 rpm No Load - mm^3/cyl/cycle	21.2	18.0

	Engine A	
	Governor in Bad Repair	Same Governor after Overhaul
Exhaust Smoke Decelerating, %	70	0
Aldehydes - mg/ft^3 Exhaust Gas Decelerating	0.9	0

	Engine B	
	Engine after Extensive Use	Same Engine after Major Overhaul
Exhaust Smoke - 1400 rpm Full Load, %	34	20
Exhaust Smoke - 2500 rpm Full Load, %	44	16
Exhaust Smoke - Accelerating, %	38	16

observed that poor maintenance practices in many cases overshadow any beneficial effects derived from selected fuels. This observation is generally applicable to all types of Diesels in all kinds of service.

SPECIFICATIONS AND DIESEL FUELS

We have discussed the influence of certain fuel qualities on combustion performances, considered in terms of products in the exhaust, and also their influence on engine wear, deposits, and starting. Under operating conditions of normal speeds and reasonable power outputs, factors inherent in the engine construction obviously are conducive to favorable ignition and combustion. Field experience indicates that under these conditions a wide variety of fuels will give approximately equal satisfaction. At reduced loads and idling, engine factors are less favorable to combustion, and the scope of practicable fuels is

narrowed. It is important to define the permissible ranges of fuel properties so as to indicate the nature of fuels suited to the various classes of engines and the conditions under which they function. Research and mass field experience provide the data needed for establishing satisfactory specifications.

Under previous conditions with the relatively limited demands for the classes of fuels used for the medium and higher-speed Diesels and for the household burners, it was possible for the refineries to meet these demands with essentially straight-run distillate fuels. As a result of extensive experience on the part of fuel producers and users, specifications applying to those fuels have proved quite workable.

There has been a marked increase in Diesel-fuel demands accompanying the growth in application of the medium and higher-speed Diesels. The increase in household burner oil demands has been even greater. Sizable as these demands are, they are considerably overshadowed by the growing demands for gasolines. To satisfy the demands for gasolines of an improved quality, the petroleum industry is extending the use of catalytic-cracking and of course will continue to employ existing thermal-cracking facilities.

With the production of these large quantities of gasoline are also produced large quantities of catalytic-cracked distillates and some thermal-cracked distillates. These cracked distillates are produced from the material which is being recycled through the cracking processes. Thus the fuel producer can furnish straight-run distillates, catalytic-cracked distillates, thermal-cracked distillates, or blends of the cracked distillates and straight-run distillates as may be needed to meet the requirements for the various classes of Diesel fuels and burner oils. The predominating quantities of available catalytic-cracked distillates and their lower cost are factors of moment to the Diesel-fuel user. Because of their growing economic importance, it is of particular interest to consider the catalytic-cracked distillates in relation to the fuel needs of the Diesel.

The nature of the catalytic-cracked distillates is influenced by the hydrocarbon make-up of the straight-run distillates used as charging stocks and by the extent to which cracking is applied to the recycle stocks. Thus distillates from the cracked recycle stocks differ materially from the straight-run distillates in the same boiling range. The catalytic-cracked distillates tend toward increased contents of aromatics, iso-paraffins, and various unsaturates, including certain of the unstable types of hydrocarbons. While thermal-cracked distillates are roughly of the same general nature, processing conditions in catalytic-cracking make it possible to produce catalytic-cracked distillates which are superior to the thermal-cracked distillates as a source for Diesel fuels. In either case, the cracked distillate from a given recycle stock will have an ignition quality which is lower than that of the charging stock. The unstable hydrocarbons included in the untreated cracked distillates have marked gum- and lacquer-forming tendencies and must be removed to avoid sticking of injection-system elements and engine deposits from this source.

As indicated in Fig. 9, it is possible to select catalytic-cracked distillates of any desired boiling range from favorable recycle stocks. From the figure it will be evident that three general classes of fuel oils can be produced. These may be blends of catalytic-cracked distillates and straight-run distillates, or unblended catalytic-cracked distillates, with or without ignition accelerators. The make-up depends importantly upon the nature of the charging stocks and the extent of the cracking applied to the recycle stocks. As pointed out by the petroleum industry, to meet the increased demands for Diesel fuels and household burner oils, the quantities of straight-run distillates used for blending must be held to a minimum.

Growth in demand for petroleum products makes it necessary to refine larger quantities of sour crudes. At the same time the supply of domestic sweet crudes is dwindling. Sour crudes include more corrosive sulphur compounds as part of the total sulphur content than do the sweet crudes. The need for commercially applicable methods to remove the corrosive sulphur content from the crudes early in the refining operations involves problems of great importance to the petroleum industry. Pending development of commercially practicable means for reduc-

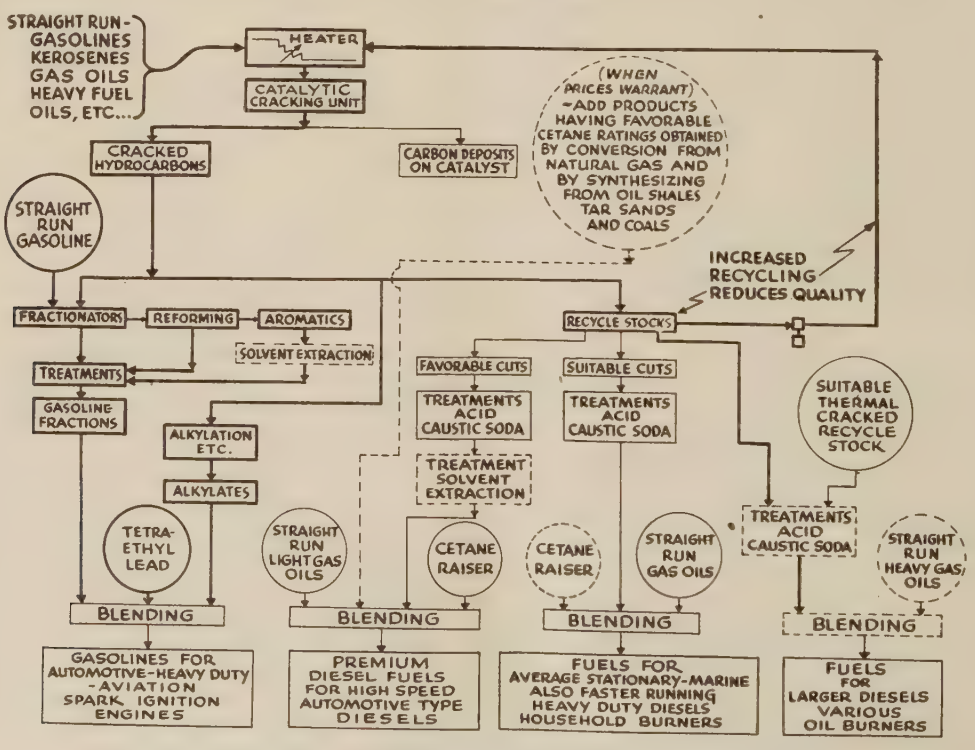

FIG. 9 PROCESSING OF LIQUID FUELS FROM CATALYTIC-CRACKING PLANTS

tion of sulphur in the initial refining stages, the various classes of distillate fuels other than gasolines may be expected to reflect an increase in sulphur content over the same classes of fuels as available under previous conditions.

Specifications for Defining Newer Types of Diesel Fuels

The changing nature of available fuels appears to warrant a comprehensive resurvey of the specifications used for defining Diesel fuels. Any reformulated Diesel-fuel specifications must define fuels which are suited to the various Diesel needs and at the same time are compatible with economic factors. The petroleum industry and the users need to co-operate closely to evaluate any recasting of the limits for currently used inspections so as to define adequately the properties of these newer fuels.

Unstable hydrocarbons contribute to certain operating difficulties and must be restricted. At present there exists no acceptable inspection. Therefore it becomes evident that a suitable inspection must be developed and practical limits established.

New inspections of Diesel fuels must consider factors involving fuel introduction, ignition, and combustion. With our present knowledge, fuels can be selected so as to insure satisfactory introduction. Knowledge of ignition phenomenon in the Diesel has been advanced but is still in need of further development. The introduction of the cetane-alpha-methylnaphthalene scale for measuring the ignition quality of a Diesel fuel constitutes one of the outstanding contributions from prewar research. Anticipated changes in the nature of the newer fuels, with and without ignition accelerators, justify additional research to clarify the relative importance of cetane-number ratings to be used in future specifications. Based upon a nation-wide survey in 1944 of the postwar Diesel-fuel situation, it was concluded among other things that there is great need for a test whereby the quality which may be termed Diesel-fuel combustibility can be evaluated, necessarily under a particular set of test conditions, much as in the case of cetane-number evaluations. At present this important quality is indicated only after having burned a given Diesel fuel under actual operating conditions for a long time. The development of a practical test for this quality, one giving reproducible results expressed on a suitable scale, would be expected to reduce the currently debatable emphasis on cetane number to a more generally acceptable basis.

In a Diesel, optimum thermal efficiencies and enduring performances are obtained with fuels which burn rapidly and when complete combustion of the fuel is approached. The chemical energy in the fuel is released at high rates throughout the inflammation phase and this is manifested by the high rates at which the temperatures and pressures of the gases in the cylinder increase. Under these conditions there are favorable exchanges of fuel energy into mechanical energy. Limiting considerations to hydrocarbon fuels, this suggests that the Diesel-fuel combustibility quality might be evaluated by comparing the temperature-time relations for a particular fuel with those obtained from certain reference fuels, these fuels being delivered into a given Diesel at a prescribed energy-supply rate, under standardized operating conditions. Instruments (1, 11) have been developed to measure instantaneous temperatures occurring during the combustion phase. The authors hope that the possibilities in this test scheme using instruments of this type will be explored thoroughly. In any event, it is hoped that this work will lead to some form of test which is suitable for evaluating this important quality in lieu of the long-time observation now required. Granting the development of a practicable test of this general nature, it is envisioned that rates of heat energy released under prescribed test conditions could, as a result of laboratory and field observations, be correlated so as to define satisfactorily the usable ranges in this Diesel-fuel combustibility quality.

Conclusions

The liquid fuel used for operation of the Diesel plays a vital part in determining its over-all success. Engine power outputs, reliability, and durability are significantly influenced by the fuel used for operating the engine.

Due to the changing make-up of generally available fuels, there appears to be a need for a resurvey of the specification means used for defining practicable Diesel fuels.

It is suggested that new standardized tests be developed, one whereby the relative stability of a Diesel fuel can be determined, and another whereby the Diesel-fuel combustibility quality can be evaluated. Suitable inspection limits used in connection with these tests would serve as additional useful means for specifying Diesel fuels properly.

Specifications for these newer fuels must comprehend the widest range in fuel properties or qualities compatible with the economic factors involved in engine reliability and durability on the one hand and, on the other hand, with those involved in fuel availabilities, fuel costs, engine-maintenance costs, and lubrication costs. Research and mass field experience must provide the data needed for the development of these specifications.

New additive-type lubricating oils must be made available for use in the medium- and higher-speed Diesels to combat the deleterious effects of sulphur contents in the fuels for these engines.

BIBLIOGRAPHY

1 "Combustion Studies of the Diesel Engine," by E. W. Landen Trans., *SAE Journal*, vol. 54, 1936, p. 270.

2 "Effect of Diesel Fuel on Exhaust Smoke and Odor," by R. S. Wetmiller and L. E. Endsley, Jr., Trans., *SAE Journal*, vol. 50, 1932, p. 509.

3 "Evaluation of Diesel Fuels in Full Scale Engines," by W. G. Ainsley, Report of the Cooperative Fuel Research Committee, Trans., *SAE Journal*, vol. 49, 1941, p. 4481.

4 "The Influence of Diesel Fuel Properties on Engine Deposits and Wear," by G. H. Cloud and A. J. Blackwood, Trans., *SAE Journal*, vol. 51, 1943, p. 408.

5 "The Effects of Diesel Fuel Characteristics on Engine Deposits and Wear," by L. A. Blanc, presented at the National Fuels and Lubricants Meeting SAE at Tulsa, Okla., Nov. 6–7, 1947; summary of paper appeared under the title, "Sulphur in Fuel Seen Shortening Diesel Life," *SAE Journal*, vol. 56, March, 1948, pp. 43–44.

6 "Fuel and Wear in Diesel Engines," by J. J. Broeze and J. J. Gravesteyn, *British Motor Ship*, vol. 19, September, 1938, p. 216.

7 "Effect of Fuel Properties on Diesel Engine Performance," by F. G. Shoemaker and H. M. Gadebusch, Trans., *SAE Journal*, vol. 54, 1946, pp. 339–346.

8 "High Speed Diesel Engines," by P. M. Heldt, third edition, P. M. Heldt, Nyack, N. Y., 1940.

9 "Experiments on the Ignition of Gases by Sudden Compression," by H. T. Tizard and D. R. Pye, *Philosophical Magazine*, series 6, 1944, p. 79.

10 "Diesel Fuel Additives Create New Concepts," by C. M. Larson, preprint of paper presented at National Fuels and Lubricants Meeting of SAE at Tulsa, Okla., Nov. 6–7, 1945.

11 "Flame-Temperature Measurements in Internal-Combustion Engines," by O. A. Uyehara, P. S. Myers, K. M. Watson, and L. A. Wilson, Trans. ASME, vol. 68, 1946, p. 17.

Discussion

C. C. Moore.[4] The writer would like to propose a new scale for use with such papers as the present one. This scale is based upon the "irritation number," and this number is the result of the writer's inability to answer many of the questions and problems that are raised. Diesel engines do run and operate very

[4] Research Department, Union Oil Company of California, Wilmington, Calif.

satisfactorily, and this is in no way connected with the fact that we thoroughly understand their combustion mechanism. It should be stated that they operate in spite of our lack of knowledge of why and how!

If the Diesel engine could operate without hydrocarbon fuels, things would be much simpler. As is pointed out in the paper, a fuel that is heated to a certain point starts to "crack," which means that it starts to change into other kinds of hydrocarbons. If we have oxygen present, additional chemical compounds are formed. Some of this fuel is burned to carbon dioxide and water vapor, and during the process supplies heat that eventually is transmitted into ton-miles or brake horsepower-hours. Some of the fuel, however, does not complete this cycle, and the result is a smoky exhaust, a fouled engine, and sometimes stuck piston rings.

It is shown in the paper that fuel residues were recovered from the exhaust which had an average molecular weight nearly twice that of the original fuel. This means simply that for a portion of the fuel, cracking and polymerization have taken place rather than combustion. When it is considered that this has taken place in the presence of 50 per cent or more of excess air, it is evident that there is still much work to be done in perfecting the combustion process of a Diesel engine. Part of this work undoubtedly lies in what might be called the strictly mechanical field, but it is our opinion that there is also much improvement possible in the chemical field. We have available certain types of chemicals, such as the organic peroxides, that cause self-ignition to start quicker, or at a lower temperature, but there seems to be evidence that such materials do not appreciably affect the end point of the combustion. Of interest would be research directed toward the development of a combustion catalyst, such that combustion once started would continue to the end products of carbon dioxide and water.

It is stated in the paper that best combustion will occur when: (*a*) the fuel vaporizes completely; (*b*) adequate mixing with the oxygen is obtained; and (*c*) sufficient time is allowed for completion of the chemical reactions. As opposed to these desirable conditions there seems to be a general tendency to increase engine speeds and thereby reduce the time allowed for the combustion to complete itself. An equally definite tendency is the growing reluctance of petroleum refiners to make available a low-boiling-range straight-run fuel, for such material is the favorite diet of the new catalytic crackers that turn out high-anti-knock-value gasoline. By simple elimination, the only remaining field of improvement is the better mixing of the fuel charge with the oxygen, and possibly the better or more complete burning of this mixture by means of some catalytic aid.

The authors discuss the need for a test whereby the "Diesel-fuel combustibility" can be evaluated. Certainly the cetane number of a Diesel fuel is not a good criterion of its performance, nor is the distillation range, of itself, of much value in forecasting engine performance. The temperature-time relations suggested by the authors, in comparison with those of some standard reference fuels, might be of considerable interest, and especially so if they could correlate the results with some less difficult test to run. It would seem as though there should be some formula wherein distillation range, viscosity, and gravity, and some paraffinicity or aromaticity factor could be combined to give the Diesel-fuel combustibility or "x-number" of a fuel.

The research work of the authors in developing their temperature-time concept of combustibility may serve a very good economic purpose in opening new compositions for Diesel fuels. For example, there is a general reluctance to use cracked or blends of cracked and straight-run products in Diesel fuel. It may be that certain cracked fractions are satisfactory for use, or that blending with some material, such as a Fischer-Tropsch fuel, might give the desired temperature-time relationship. There is certainly much room for speculation and research along these lines.

The writer wishes to compliment the authors on the high irritation number of their paper, for such irritation causes interest and thinking, and it is only by the realization of our inadequate knowledge that real progress can be hoped for in the field of combustion research.

H. F. Bryan.[5] It is refreshing to note that the authors have broken down Diesel smoke into its various constituents rather than attempting to evaluate it by a smokemeter. In this way the products of combustion can be made to tell the real story of what is going on inside the combustion chamber.

Combustion in the Diesel engine is such a heterogeneous process that one may have a high percentage of carbon, some hydrocarbons of varying chemical composition, water vapor, and under certain conditions, some very corrosive compounds all masquerading under the one term, "smoke."

We agree with the statement that much of the cracking of the hydrocarbon molecules which produces carbonaceous particles in smoke occurs early in the combustion cycle and is due to poor preparation and distribution of the fuel in the combustion chamber.

It is interesting to note that "cetane number" is now becoming a more specific term to indicate the inherent ignition quality but not necessarily the burning quality of a fuel. More attention is now being given to the influence of volatility on the burning of the fuel and the influence of viscosity on the mechanical preparation of the fuel for burning.

We are in accord with the authors on the influence of sulphur on engine deposits and cylinder wear. High-sulphur fuels definitely increase engine deposits and, under certain conditions of operation, produce excessive wear. We have found the high gum content found in some of the burner fuel oils will also produce excessive deposits under certain conditions.

On the broad subject of Diesel-fuel specifications from the present available distillates, we are still "too close to the woods to see the trees." Whether we like them or not, we will have certain types of distillates available for Diesel-engine and burner use. The burner-fuel demand, being the greatest, will influence the over-all specifications. Therefore it is the job of the Diesel-engine manufacturers and burner makers to improve their respective products so that similar fuel specifications can be used. Otherwise premium fuels for Diesel engines will be required.

A tremendous amount of research and field experimentation together with a fine spirit of co-operation will be necessary to reach this desirable goal. Considerable progress has been made in the past 2 years, and with the present unanimity of thought a solution of the problem is possible.

P. H. Schweitzer.[6] The writer was interested in Figs. 1 and 2 of the paper and considers them a valuable addition to our knowledge of Diesel combustion. Fig. 1 shows that solid carbon in the exhaust increases rapidly in the full-load and overload region. Fig. 2 shows that liquid fuel in the exhaust decreases with load. The obvious reason for the increased per cent carbon in the exhaust is overrich or locally overrich mixture, hot smoke. The obvious reason for the decreased liquid fuel in the exhaust at heavy load is the higher temperature and more complete ignition of the fuel, cold smoke.

The authors have analyzed the exhaust products as they should

[5] Research Engineer, Mechanical Research and Development Division, International Harvester Company, Chicago, Ill.

[6] Professor, Engineering Research, Pennsylvania State College, State College, Pa. Mem. ASME.

be analyzed by collecting the solids and the liquid in a condensing system. Those who try to apply a conventional gas analysis to Diesel exhaust get disappointing results. In a Diesel engine, the products of incomplete combustion are largely solids and liquids which cannot be caught by gas analysis. The percentage of CO_2 and CO in the exhaust is not a measure of the combustion.

It would have been helpful if in Figs. 1 and 2 the corresponding smokemeter readings had also been indicated, but they can be inferred from the fuel-air ratios. Anyhow, it is notable that it does not take much carbon or liquid fuel to cause bad smoke, only a fraction of a per cent. In so far as the smokemeter is concerned, an innocent white smoke resulting from condensed water vapor can obscure the light rays and cause as high a smokemeter reading as a very black smoke.

The writer disagrees with the authors' interpretation of the observation that high-cetane fuels frequently increase the exhaust smoke. They say that with high-cetane fuels "much more cracking" occurs due to thermal breakdown than with fuels having lower cetane number. The paper points out earlier that such cracking occurs early in the combustion cycle. However, smoke is more affected by what occurs late in the combustion cycle. High-cetane fuels behave in the indicated manner in the high-volatility range but, curiously, reverse themselves in the low-volatility range (Fig. 5).

His preferred explanation is that extra-short ignition lags are conducive to smoke, irrespective of whether they are caused by high cetane number or by other factors, and suggested reasons for this are mentioned in a recent paper[7] on the subject.

In a paper on Diesel combustion temperatures by Uyehara, et al,[8] is shown the effect of inlet-air pressure on the beginning and end of combustion (radiation). When the air pressure was reduced by 8 in. Hg, the ignition lag increased from 5 to 20 deg, but the shorter the ignition lag became the longer the combustion stretched out. When radiation began at 10 deg BTC (5 deg ignition lag) it ended at 82 deg ATC. When it began at 13 deg ATC, it was over at 59 deg ATC. A decrease in air pressure accelerated the combustion ignition. How do the authors explain this by their thermal cracking theory?

The deciding factor probably is not how much cracking takes place but rather how late it occurs during the expansion stroke. With very short ignition lag, part of the fuel burns too late.

R. J. Greenshields[9] and L. S. Echols.[9] The authors mention the work of Tizard and Pye in connection with ignition quality. Since no discussion of Diesel fuels would be complete without an effort to present the whole picture in one piece, we show in Fig. 10 of this discussion an effort that we have made to do this. The plot of log (the ignition delay) versus the absolute temperature of the compressed mixture of fuel and air prior to self-ignition indicates by the straight dashed lines relations of the type observed by Tizard and Pye, and also by Jost and Teichmann. The lines have been drawn for 0- and 100-cetane fuel on the basis of compression temperatures for various compression ratios for three conditions; steady running, starting at 32 F inlet temperature, and —40 F inlet temperature. It should be stated that the relations shown are simply "best guesses," rather than rigorous experimental data.

The heavy solid lines represent ignition delays of fuel sprays in bombs (at the lower temperatures) and in Diesel-engine combustion chambers. They are shown displaced from the prevaporized

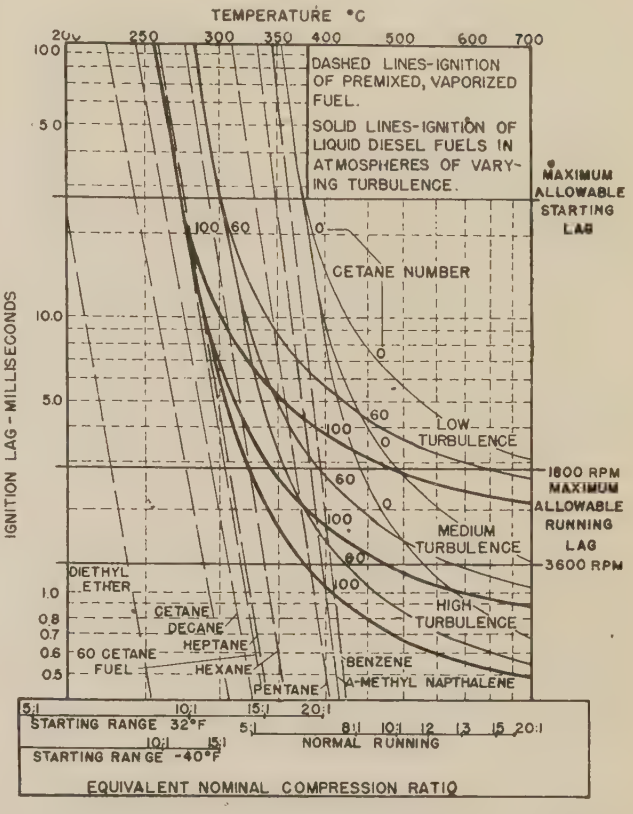

Fig. 10 Relation of Ignition Delay, Cetane Number, and Engine-Operating Factors

fuels (dashed lines) toward higher temperatures by an amount necessary to correct for the heat of vaporization. Notable is the result, coming from studies at short delay periods, such as those of Rose and Wilson, that at delays below 1 millisec the deviations from the prevaporized fuel lines are very great. Indeed the slope of the heavy lines is such as to indicate that the ignition delay is controlled by rate of vaporization rather than cetane number in this region of time and temperature. Notable also is the position of the line for diethyl ether, indicating its superiority for low-temperature starting. It is believed that these relations, although approximate, are conducive to a clearer view of the whole problem and point the way to interesting future work.

With reference to present trends in fuel-oil composition, it does appear that higher sulphur crudes and catalytic cracking may have their effect. The trend is certainly not toward a "chemically pure" fuel of the type of the 100-cetane fuel we prepared some years ago. Diesel engines will continue to use, or possibly require, a "technical grade" product.

As a matter of general interest, the effect of a catalytic-cracking operation on the hydrocarbon types present in a fuel oil is shown in Table 3 of this comment. Noteworthy is the fact that the paraffin content and sulphur content are little affected, while the naphthene content is diminished, and the aromatic content increases by roughly 15 per cent. This apparent selectivity for naphthenes appears to be rather general. In other respects it is dangerous to generalize regarding the effect of catalytic cracking, as shown by the data in Table 4, where the results of several different catalytic-cracking operations on a single charging stock are shown.

Finally, it can be said that we cannot at present recognize the existence of a characteristic of a fuel which can be called "com-

[7] "Must Diesel Engines Smoke?" by P. H. Schweitzer, SAE Quarterly Transactions, vol. 1, July, 1947, pp. 476–487.

[8] "Diesel Combustion Temperatures—The Influence of Operating Variables," by O. A. Uyehara, P. S. Myers, K. M. Watson, and L. A. Wilson, Trans. ASME, vol. 69, 1947, pp. 465–477.

[9] Research Laboratories, Shell Oil Company, Inc., Wood River, Ill.

TABLE 3 EFFECT OF CATALYTIC-CRACKING FUEL OIL

	Full range SR gas oil	Catalytic-cracked product
Gravity, API	33	26.5
Refractive index	1.477	1.514
Aniline point, deg C	67	50.1
Bromine no.	6	12
Sulphur, per cent (weight)	0.96	0.99
Aromatics, per cent (weight)	13	28
Naphthenes, per cent (weight)	40	29
Paraffins, per cent (weight)	47	43
Pour point, deg F	+5	−10
Viscosity SSU at 100 F	40	38
Molecular weight	224	208
Boiling range, deg F	464–623	478–640

TABLE 4 RESULTS OF SEVERAL CATALYTIC-CRACKING OPERATIONS ON SINGLE CHARGING STOCK

	SR gas oil	Product			
Gravity, API	36.2	32.9	31.7	30.0	33.6
Aniline point, deg C	....	60.2	55.5	51.3	67
Sulphur, per cent (weight)	0.62	0.37	0.43	0.55	0.44
Pour point, deg F	+15	+5	+5	0	0
Viscosity at 100 F, SSU	49.1	37.4	35	33.8	36.3
Boiling range, deg F	377–694	454–580	460–620	460–560	460–640
Diesel index	....	46.2	41.8	37.3	51.3

bustibility." Combustibility, if anything, is a joint (fuel-engine-operating condition) phenomenon, and its problems continue to be joint problems of the refiner, the equipment manufacturer, and the engine operator. The fact that the combustion of present-day fuel oils, earlier forecasted as a difficult problem, appears to have been solved in the domestic-burner field by suitable adjustments and minor design changes, is at least an indication of the importance of the equipment manufacturer as a factor in determining the combustibility of a fuel.

L. C. Lichty.[10] The authors have done a good job in summarizing the problems associated with the use of Diesel fuels, and particularly in focusing attention on the desirability of a combustibility rating or a test procedure to determine the combustibility of Diesel fuels. It is interesting to note that numerous factors are mentioned affecting the combustibility of the fuel which might be classed as engine variables, such as the following:

1 Engine output.
2 Mixture formation.
3 Air temperature and density.
4 Time for combustion.

Items 1 and 2 involve the fuel-injection system and the combustion-chamber size and design, which includes the turbulence built into the engine. Item 3 depends principally upon the compression ratio and ambient conditions. Item 4 depends upon engine speed. It is true that some of the fuel properties are involved in the effect of all of these variables, but, since one fuel performs better than another in a given engine, it is not necessarily true that a change in engine or fuel-injection system design would not improve the performance of the poorer fuel as determined in the given engine.

It would appear that a test for combustibility of fuels in any engine would introduce the limitations of the various engine variables associated with that particular design, and the net result might merely indicate which fuel best suits that engine. Hence would it not be desirable to rate the combustibility of fuels in a test device which would not introduce the limitations of the various engine variables? Then, if one understands the effect of the various engine variables in restricting or promoting the mixing and combustion of the various types of fuels, would it not be possible for the engine designer to modify his engine so that it would utilize efficiently the most available fuel even though it might rate lower than others on a truly comparative combustibility scale?

[10] Professor of Mechanical Engineering, School of Engineering, Yale University, New Haven, Conn. Mem. ASME.

Obviously, engine tests must also be run and perhaps this is the best way to rate the combustibility of fuels. However, if engine tests were run with fuels of varying combustibility, determined by some truly comparative method, it is thought that the tests should indicate whether the engine or the fuel is responsible for poor performance. This should point the way to better utilization of an available fuel.

R. B. Rice.[11] The authors' fine paper would tend to emphasize certain phenomena which have been studied by engineers for many years with but a very small degree of success. Their conclusions still tend to indicate the inadequacy of the Diesel engine as it is now designed and built in this country.

In this paper the authors show clearly the results of smoke as correlated with bmep and/or air-fuel ratios. Most of the test data submitted apparently deal with the high-speed Diesel engine. Assuming a rotative speed of 2000 rpm, the entire combustion process, involving timing, injection of the fuel, breaking up of the fuel into a fine spray or mist, mixing of that fuel with oxygen (air), ignition of the mixture and the process of combustion, is expected to take place in a matter of $^1/_{600}$ sec, as for example:

High-speed Diesel 0.0016 sec	1 Injection 2 Spray 3 Mixing 4 Ignition 5 Combustion	Low-speed Diesel 0.01 sec

For most discussions at this time involving the Diesel engine approximately one half of the air in the combustion chamber is involved in the combustion process regardless of the type of fuel employed. It is doubtful that the petroleum industry can ever overcome this inherent weakness of the Diesel by any of the means discussed in this paper

F/A = for actual Diesel's = 0.020 to 0.045
F/A = for theoretical Diesels = 0.066

While it is granted that it would be highly desirable were the Diesel engineer able to procure from the oil refineries a better fuel, or if we had better test standards for our present fuels, there is need for a better knowledge as a result of more and better study of the fundamental combustion process.

Engine designers and fuel engineers need to meet on a common ground: (*a*) to understand better the economics of the petroleum industry from the standpoint of the fuels which are and will be available; and (*b*) to encourage builders to devote more study and research to the subject of combustion-chamber design as well as to the design of their entire fuel system.

At present there appears to be a situation wherein the engine manufacturers build engines, combustion chambers, and fuel systems and then hope that the oil companies can give them a satisfactory fuel. The outcome is rather apparent in the resulting bmep, air-fuel ratios, smoke limitation, and other factors as discussed so ably by the authors.

It is now beginning to look as though the supply of fuel oil will always be limited. If the Diesel is to survive, then it must be designed around those fuels which are already available.

Smoke has always been a factor contributory to the Diesel's unpopularity. While this paper shows only too clearly the influence of fuel constituents on smoke, it might be well for scientists and engineers to study the other side of the problem, that is, the merits and virtues of combustion-chamber designs in terms of fuel characteristics.

In Fig. 6 of the paper (for example at 60 bmep) is indicated a wide range of smoke conditions from 0.2 to 2.0 using two widely

[11] Head, Diesel School, North Carolina State College, Raleigh, N. C. Mem. ASME.

different fuels in, it would be presumed, a given standard engine with apparently the same fuel system and combustion chamber for both fuels. It is evidently on the basis of smoke and incomplete combustion that less than one half of the air in the combustion chamber is being consumed even in the case of A, the most desirable fuel. On the other hand, it is conceivable that a combustion chamber and fuel system could be designed around fuel B so that a resulting bmep in excess of 100 could be achieved without undue smoke.

This contention is not too hypothetical if we analyze the basic Diesel cycle, using atmospheric intake and a compression ratio of 15 wherein the values are derived as given in Table 5.

TABLE 5 FUNDAMENTAL DIESEL DATA

(For 100 per cent air, 15 compression ratio, and atmospheric air intake)

Fuel-air ratio	$= F/A$	= 0.006
Ideal mep	$= P_m$	= 200 psi
Ideal indicated mep	$= P_{mi}$	= 170 psi
Ideal brake mep	$= P_{mb}$	= 144 psi

Concerning the starting of Diesels, and especially high-speed Diesel engines which operate on variable atmospheric conditions, due regard for this function must be observed by the engine manufacturers as well as the petroleum industry.

The writer is certain the petroleum industry would receive the unlimited blessing of the engine designers and manufacturers if it could provide at crude-oil prices a fuel oil which would enable prompt starting at low ambient temperature and operate with high fuel-air ratio without smoke, with a resulting high bmep, and with the absence of shock-loading due to too rapid pressure rise during the combustion period of any engine regardless of its combustion chamber or other peculiarities of design.

On the other hand the petroleum industry can do better in providing fuels for the Diesel engine even if, for the time being at least, it concentrates on the removal of the sulphur, which tests indicate is a most undesirable constituent and most harmful to the lubricant and bearings of the engine.

F. T. Ward.[12] Others like the writer, who are in the Diesel bus transportation field, are well aware of the problems associated with Diesel fuels and Diesel engines and, being obviously confirmed optimists, we scan every word on these subjects with a hope that sometimes seems to be more than human.

It would seem that discussion of a paper such as this should be guided by three requirements: (*a*) are the conclusions based upon accurate data that are representative of field as well as laboratory conditions; (*b*) do the data and conclusions have what is called "practical" value; (*c*) do the conclusions cover all alternatives? If these three conditions are not met, then, while the paper may have great intrinsic worth, it falls short of reaching the ultimate goal of contributing to the better and more economical operation of Diesel engines—a goal that still seems quite distant.

It is believed that the authors have fairly met two of these requirements in their paper. Their data certainly represent what those of us in the field observe, and their analyses of the data appear to be sound. Their comments on specifications are certainly of genuine practical value to the engine operator.

If there is any room for criticism of their efforts, it would appear to be in what they have left unsaid. It would have helped their paper had they stated somewhere that their data were based on tests made with conventional engines in which the fuel-injecting system was kept in as nearly perfect operating condition as it could be. One may say "but this is of course taken for granted." It should not be so assumed (and perhaps is not in view of Table 1 of the paper), for the reason that regardless of all that is known and all that has been disclosed in this paper, the task of maintaining injection systems in prime condition is one of the major problems associated with the use of Diesel fuels. The least neglect can largely vitiate any improvement in fuels or lubricating oils, no matter how great.

For the same reason, it is felt that the conclusions should have included a section on engine and fuel-injection equipment improvement. All of the conclusions have merit. The fifth, for example, calls for improvements in lubricating oils to offset the deleterious effects of sulphur. Should there not have been a sixth and alternative conclusion, especially in view of past history (wherein lubricating oil has been developed to be the "whipping boy" for many unsolved problems of engine design), requiring that improvement in engine design must be equally accelerated to the end that the high-speed Diesel may be made to operate reliably and cleanly whether or not new and more comprehensive standardized tests, or new and better fuel-oil specifications, or new and better fuel oils and lubricating oils are developed.

H. M. Gadebusch.[13] Every phase of technical development contains a period during which the empirical information is collected which, at some later date, may enable a qualified mathematician to evolve an exact formula containing all pertinent factors in their true proportions.

The excellent presentation of a number of Diesel-fuel problems which the authors have given in their paper, may be taken as an indication that our understanding of the combustion phenomena in Diesel engines is approaching this final stage.

All these seemingly unrelated problems we know to stem from a common source, e.g., incomplete fuel oxidation, and while the formula by which they may be reduced to this common denominator is still unknown, a survey of our present standing with regard to each individual problem fulfills the purpose of bringing us one step closer to the ultimate solution.

Analysis of the exhaust products as an indicator of proper fuel combustion has been used by the heat-generating industries for a long time.

If the combustion occurs under controllable conditions, such an analysis and the measures to correct combustion faults are relatively simple routine procedures. If, however, fuel oxidation must take place under the adverse conditions prevailing in fuel-injection engines, a multitude of intermediate as well as end products may be formed which defy most methods of analysis.

Varying depth of fuel penetration into the air charge, stratification of the resulting mixture, chilling and incomplete vaporization of some fuel, varying ignition delay, and cooling of burning mixture with subsequent soot formation are but a few of the handicaps which we know liquid fuels to be faced with in the combustion chambers of an engine.

By the time we can recondense the intermediate combustion products from the exhaust gases, many of them will have changed their state to such an extent that any attempt to conclude what they might have been in the combustion chambers would be mere speculation.

It is probably for these reasons that the authors have limited themselves to the analysis of three main groups of offenders, namely, solid carbon, unburned hydrocarbons, and aldehydes.

Better knowledge of the effects of these three groups is badly needed. Besides producing the obviously noticed exhaust smoke and odor, some of these by-products of incomplete combustion also contribute a good share to the deposits found on engine parts and thereby to a shortening of the operational life.

Smoke in any form, whether it be of the whitish-blue variety which Professor Schweitzer has so significantly christened "cold

[12] Surface Transportation Company, New York, N. Y.

[13] Engineering Department, Detroit Diesel Engine Division, General Motors Corporation, Detroit, Mich.

smoke," or of the gray-black kind associated with solid carbon particles, is but an outward manifestation of the same engine ailments which produce worn cylinder liners, broken compression rings, sticking exhaust valves, and many related engine troubles.

Too little attention has been paid in the past to this phase of the fuel problem.

Under adverse conditions, unburned or partially burned fuel may be noticed visually in the form of smoke but even in the normal load range where the exhaust is apparently clean, fuels of different chemical composition have been found to possess widely varying deposit-formation characteristics.

The amount of fuel which is not completely converted into heat is very small and amounts usually to less than 0.1 per cent of the total fuel consumed.

Incomplete combustion of this magnitude, therefore, does not show up as excessive fuel consumption and cannot be discovered in indicator diagrams.

Observation of fuel deposits has thus become a time-consuming and costly project which is commonly moved from the laboratory to some field operation.

With recondensation of the exhaust products, the authors deserve full credit for the development of a new and unique method which may enable us to bring tests of this type back into the laboratory where they belong. Particularly interesting among the results reported is the clearly noticeable reverse tendency of solid carbon formation versus unburned hydrocarbon shown in Figs. 1 and 2 of the paper.

While the latter increase with decreased load or low fuel/air ratios, carbon soot formation rises rapidly as the load is increased beyond a certain point.

If the authors had amplified these data by showing the corresponding results at both low and high speeds, the prevalence of unburned hydrocarbons at low-load low-speed operation and that of solid carbon at the opposite end of the operating range would have become still more obvious.

The adverse effect of soot due to engine overloading on smoke and deposit formation is well known by most operators but the insidious part which unburned hydrocarbon fractions play with regard to deposits formed at light loads is generally still underrated.

The tests conducted with fuels of different boiling ranges and cetane rating are another real contribution of this paper.

On the basis of field experience, particularly with western "stove fuels," we have advised our customers for many years to employ lower boiling fuels wherever satisfactory ignition quality could not be obtained.

This purely empirical recommendation could not be more plainly illustrated than with the laboratory data shown by the authors in Figs. 5 and 6. This information will go a long way toward changing the thinking of quite a few people in the petroleum industry.

Keeping in mind that the smoke scale is but another expression of engine deposits and operational life, it would appear from these curves that if we have to live with a minimum cetane rating of 40, suitable fuels for high-speed Diesel engines will have to be limited to a final boiling point of around 600 F.

If, on the other side, our customers are to have the advantage of the inherently better economy of the heavier fuel grades, the ignition quality should not be dropped below about 50 cetane.

As the authors have pointed out in their conclusions, Diesel-fuel specifications so far have been limited to a number of properties which experience had proved to be of some influence.

The chemical side of the fuel and particularly its combustibility have been sadly neglected, simply because the related industries did not know much about it.

Flame-temperature measurements and condensation of exhaust products will be of great help to further our combustion knowledge.

Availability of these new tools and further pursuit of the information given in this paper may soon enable us to write Diesel-fuel specifications containing all factors important for Diesel-engine operation.

Authors' Closure

The authors agree with Mr. Moore's general observation that development of mechanical features of engines aimed toward improved mixing of fuel and oxygen is of importance. However, it should be pointed out that there is a practical limit, for each engine, beyond which improved mixing may become harmful because of excessive rates of combustion, such as those occurring under conditions approaching incipient detonation. Development in this direction must therefore include an accompanying improvement in mechanical features for controlling and limiting the rates of fuel introduction so that combustion rates are held to suitable values.

Mr. Bryan affirms the need for developing Diesels suited for operation on less favorable fuels than those which have been more generally available in the past. This indicates an important challenge to Diesel manufacturers. Improvements in this direction are to be expected with time. It should also be noted that since the Diesel provides power services of important economic value to mankind, there is a still broader challenge to both the Diesel builders and Diesel-fuel producers to co-operatively develop sound economic Diesel mechanisms and the newer fuels suitable for operating these engines. The fine spirit of co-operation now existing holds promise of favorable developments.

Professor Schweitzer asks how we would explain results of Uyehara, et al, on the basis of thermal cracking. Values taken from the original paper are listed in the following table:

	Normal intake pressure	8" Hg vacuum
Injection begins	15° BTC	15° BTC
Radiation begins	5° BTC	14° ATC
Injection ends	15° ATC	13° ATC
Radiation ends	82° ATC	59° ATC
Ignition delay	10°	29°
Duration of injection	30°	28°
Fuel injected before ignition	1/3	All
Flame duration	87°	45°

From this table we can see that at normal intake pressure two thirds of the fuel is injected into a burning mixture; hence it would be subjected to much thermal cracking early in the combustion cycle and there would be large quantities of soot produced. It takes a long time to burn this soot as indicated by the end of radiation at 82 deg ATC. At reduced pressure all the fuel is in the combustion chamber before it ignites. In this case, better mixing of the fuel and air causes a greater part of the fuel to burn directly with less thermal cracking. This fuel-air mixture burns in a shorter time as indicated by the end of radiation. The rate of burning in the latter case is higher, and much more combustion sound is associated with this type of burning.

Messrs. R. J. Greenshields and L. S. Echols affirm the general conclusion that ignition quality of the fuel, as indicated by the cetane number, has played an important part in helping to explain combustion phenomena. Since the cetane number of the fuel is obtained under carefully prescribed inspection test conditions, such ratings are applicable only under the particular conditions used as basis of test. Paralleling this, the authors are proposing that a carefully prescribed set of inspection test conditions be developed for determining what may be called the "Diesel-fuel combustibility characteristic." The ratings obtained in such a manner would be useful in helping more intelligently to classify ranges of fuels for the different engines under various service conditions.

Comments by Messrs. Greenshields and Echols present data

which contribute valuable information on initiation of combustion, and the authors hope that this will be expanded and presented in the form of a technical paper. In this event it is suggested that the data on the graph be reformulated on several graphs to emphasize more fully this important information.

The comments given to the discussion of Messrs. Greenshields and Echols also apply to the discussion presented by Dr. Lichty. The development and use of the "Diesel fuel combustibility characteristic" as obtained by a particular set of test conditions is much the same as the development and use of the cetane number as a measure of ignition quality. Once the combustibility rating of a given fuel is determined by a prescribed set of test conditions the fuel can be operated in the field and in this manner the combustibility in a particular engine would be evaluated. It would then be possible to use this combustibility index in the future engine designs.

A point brought out by Mr. Rice is one which many of us may minimize. This is the time factor allowed for combustion in the Diesel engine. Effective combustion may end 60 deg after top center, but there are remnants which continue to burn for a longer time. Conditions of afterburning contribute to smoke.

Mr. Ward inquires as to the mechanical condition of the engine used for our tests. Laboratory engines were used for our tests. These engines are kept in good mechanical condition. Single-cylinder engines, such as used for our tests, have operating characteristics consistent with conventional multicylinder engines of the same cylinder size. Small-bore engines were used in these tests as a matter of convenience. It is to be expected that the fundamentals apply to all engine sizes and all types of combustion chambers.

Mr. Gadebusch desires a mathematical formula for evaluating Diesel combustion. We are in accord with this view and hope for developments in this direction. This would be expected to help us to alter engine design to meet requirements of fuels of various compositions.

Knowledge of the relationships between fuel and lubricating-oil characteristics and engine deposits is not very well developed. When such relationships are well formulated we will have made a great step forward in the direction of advantageous interrelation of fuel oil, lubricating oil, and engine. Development of the "Diesel fuel combustibility characteristic" advocated by the authors would be expected to be an important step in this direction.

It seems that there is a need for a measure of the Diesel fuel combustibility characteristic just as there was a need for a measure of ignition quality. The cetane-number method of ignition rating has proved to be a most useful measurement. Similarly, if a Diesel fuel combustibility characteristic were made available, it could be used to advantage in Diesel fuel evaluation.

The authors are particularly pleased with the stimulating discussions presented and they hope that an experimental procedure for measuring the "Diesel fuel combustibility characteristic" will soon be in the offing.

A Method of Correlating Axial-Flow-Compressor Cascade Data

By HUNT DAVIS,[1] JEANNETTE, PA.

This paper describes a method of correlating wind-tunnel tests on axial-flow-compressor cascades. The use and construction of two charts for the NACA four-digit airfoil series are described. The charts relate the three cascade quantities; camber, solidity, and stagger angle with two flow angles; the entrance angle, and the turning angle, for low Mach numbers. When four of these five variables are given, the fifth is determined. A simple computation procedure to correct the solution for a high subsonic Mach number is given. The profile drag does not enter the correlation scheme directly but an approximate guide is indicated on the charts.

Nomenclature

A FEW airfoils in cascade are shown schematically in Fig. 1, in which the nomenclature is defined. The nomenclature is also given as follows:

α_1 = entrance angle of flow, deg
α_2 = discharge angle of flow, deg
$\Delta\alpha$ = turning angle, or deflection of flow, deg
γ = stagger angle of cascade, deg
c = chord of airfoil, in.
δ = deviation angle of flow, deg
i = incidence angle of flow, deg
M_1 = entrance Mach number
M_2 = discharge Mach number
σ = solidity of cascade, c/t
θ = camber angle of airfoil, deg
t = pitch of cascade, in.
Π, λ, μ = cascade parameters

Subscripts:

0 = at low Mach number, $M < 0.4$
m = at Mach number, $M > 0.4$
1 = entrance conditions
2 = discharge conditions

Introduction

In the stage-by-stage design of an axial-flow compressor, the designer continually faces the problem of selecting appropriate airfoil cascades to match a set of predetermined velocity diagrams. He may use any of several approaches:

1 The calculation of a cascade design using perfect fluid theory modified by "experience factors," such as the Eckert-Weinig method.[2]

2 The application of data obtained from stationary cascade tests, modified to include accumulative three-dimensional effects.

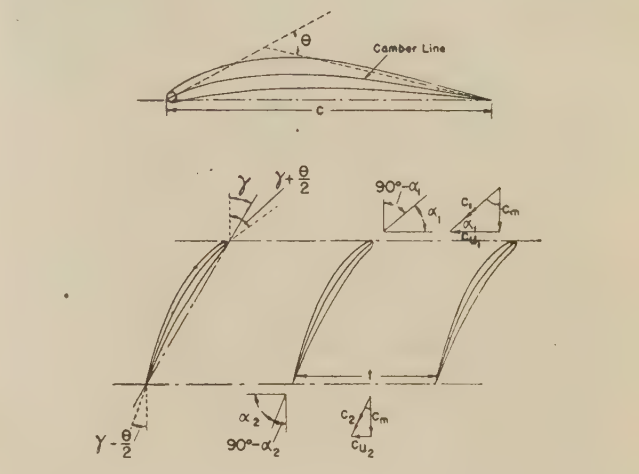

Fig. 1 Profile and Cascade Nomenclature for Axial-Flow-Compressor Cascades; Two-Dimensional

3 The application of data obtained from rotating-cascade tests, modified to include accumulative three-dimensional effects.

All three of these approaches have been used successfully by various designers at one time or another. Method (1) has the advantage of simplicity, and the major weakness of applying an "experience factor" that is expected to cover a multitude of errors. Method (3) undoubtedly gives the most accurate and most directly applicable data with respect to the design of a rotating machine. However, the data are obtained slowly and usually at great cost. The instrumentation problems involved with a rotating-cascade test-rig program are much more exasperating than for the corresponding stationary-cascade type. Method (2) has been at a disadvantage because of the lack of correlation methods between the variables involved. The design data therefore have been voluminous and many different cascades have had to be tested individually.

This paper describes a method whereby two charts are used to determine the "incidence angle versus turning angle" curve for any cascade using airfoils of one particular family. Such a chart obviously reduces the need of testing great numbers of different cascades because it has continuity in all the variables; and a limited number of tests covering the range of all variables serves to construct the chart.

In applying the results of any stationary-cascade tests to the design of a compressor, the designer must remember that the flow pattern in a stationary cascade is essentially two-dimensional; whereas in the machine, there are important three-dimensional effects. These arise directly from the centrifugal accelerations involved, and take the form of radial displacements and

[1] Division Engineer, Elliott Company. Jun. ASME.

[2] "Berechnung und Auslegung des Laders zum Motor 9–900 VI, (Motor D)," by B. Eckert, FKFS Stuttgart, 1945.

Contributed by the Gas Turbine Power Division and presented at the Annual Meeting, Atlantic City, N. J., December 1–5, 1947, of The American Society of Mechanical Engineers.

Note: Statements and opinions advanced in papers are to be understood as individual expressions of their authors, and not those of the Society. Paper No. 48—A-81.

vortexes due to boundary-layer formations. These secondary-flow phenomena are difficult to analyze, either experimentally or analytically, and many designers choose to lump all such extraneous effects into a correction factor, which is applied to a design method based fundamentally upon stationary-cascade tests.

The purpose of this paper is to present a new method for correlating the characteristics of airfoil cascades. Two charts are developed which relate the camber, solidity, and stagger of the cascade, and the entrance angle and turning angle of the flow. When four of these variables are given, the fifth may be quickly found from the charts. These charts were made from tests on about forty different cascades at low Mach numbers, with a Reynolds number of about 2 times 10^5.

The use of the chart can be extended to apply for any subsonic Mach number by Prandtl's correction, as used by Eckert.[2]

Use of Correlation Chart

The charts have been constructed for airfoil profiles belonging to the NACA four-digit series,[3] and may be used directly for Mach numbers less than 0.4. For greater subsonic Mach numbers, some slight corrections will be made.

In the stage-by-stage design of a compressor, the blade-setting problem is usually either of the following:

(*a*) Given entrance and turning angles, solidity, and camber; to find the stagger.

(*b*) Given entrance and turning angles, solidity, and stagger; to find the camber.

If the Mach numbers are low, the process is: for (*a*); locate the point X on Fig. 2, from the entrance angle and turning angle. Find the Π value associated with the camber and solidity of the cascade from Fig. 3. Select the correct Π line on the right-hand set of lines in Fig. 2. By trial and error, find a straight line that passes through X and intersects the correct Π line at the same stagger value as the intersection of the straight line with the extreme left-hand stagger curve.

For example: Given $\alpha_1 = 38$ deg, $\Delta\alpha = 28$ deg, $\theta = 34$ deg, $\sigma = 1.0$.

Point X, Fig. 2, is located by α_1 and $\Delta\alpha$. From Fig. 3 we get $\Pi = 2.25$. The straight line through X, giving the solution, is that which at Z reads $\Pi = 2.25$, $\gamma_0 = 30$ deg, and at Y reads $\gamma_0 = 30$ deg. Hence the correct stagger to satisfy the required conditions is 30 deg.

[3] "The Characteristics of 78 Related Airfoil Sections From Tests in the Variable Density Wind Tunnel," by E. N. Jacobs, K. E. Ward, and R. M. Pinkerton, NACA Technical Report no. 460, 1933.

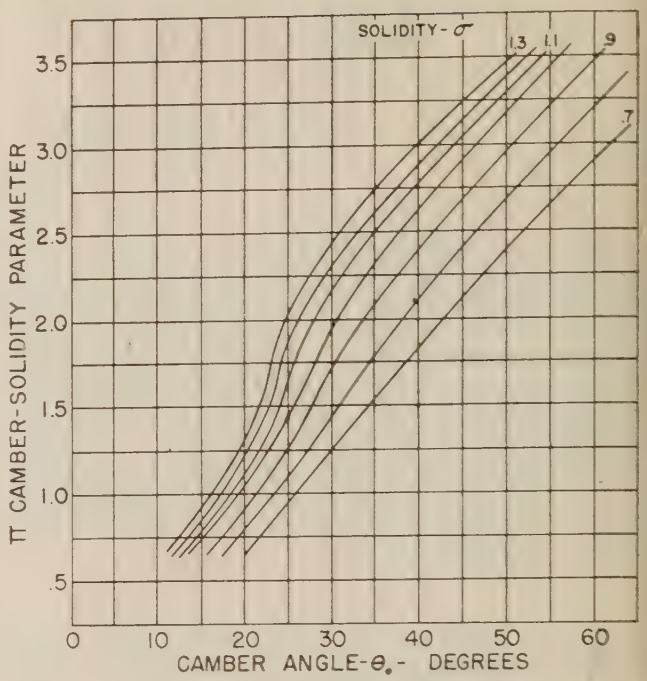

Fig. 3 Cascade Parameter Π Versus Camber and Solidity (NACA "four-digit" family of profiles.)

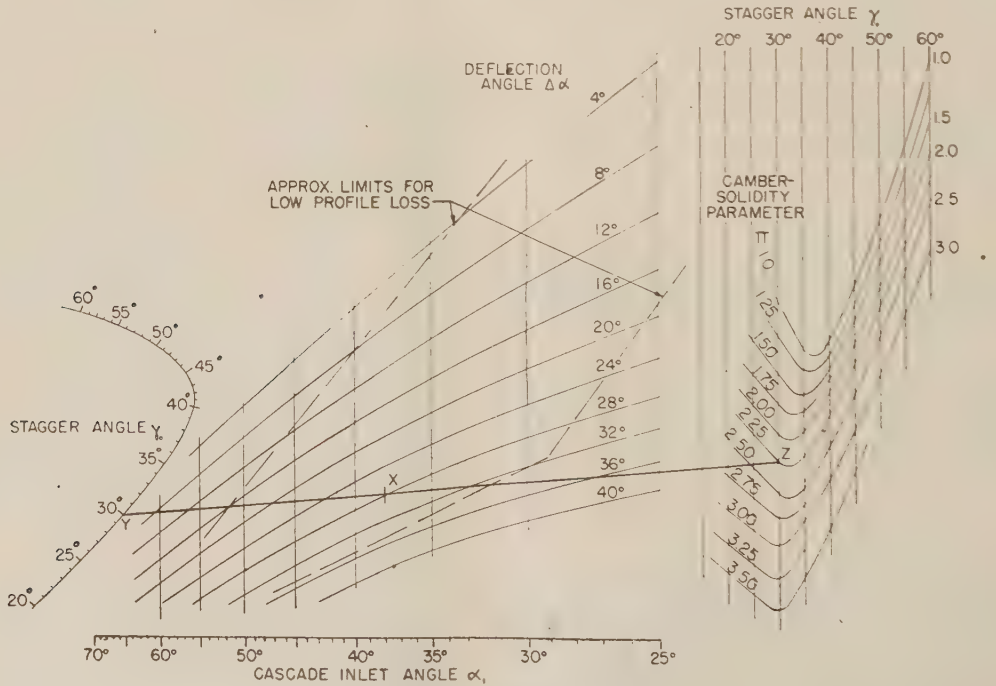

Fig. 2 Cascade Correlation Chart (NACA "four-digit" family of profiles.)

For conditions (*b*), the process is similar except that the straight line is determined by X and Y, Fig. 2, and the correct II value is read from the Z-intersection with the 30-deg stagger line. The correct camber is then found from the curves in Fig. 3.

The path of the XYZ line through the central field in Fig. 2 represents the turning angle versus entrance angle characteristic of the particular cascade.

If the Mach number entering the cascade is greater than 0.4, the following sequence of calculations is used:

Let us assume that the following values are known: α_1 = inlet angle, $\Delta\alpha$ = turning angle, θ_m = camber angle, σ = solidity, M_1, M_2 = Mach numbers.

For $M_1 > 0.4$ a correction factor $\sqrt{1 - M_1^2}$ is multiplied with i_0 to give the correct incidence, i_m. In other words

$$i_m = i_0 \sqrt{1 - M_1^2} \quad \ldots\ldots [1]$$

Similarly, the deviation is

$$\delta_m = \delta_0 \sqrt{1 - M_2^2} \quad \ldots\ldots [2]$$

For a reasonable approximation, we can assume that $(\delta_0 - i_0) \approx 8$ deg, which leads to

$$\theta_0 - \theta_m = 8(1 - \sqrt{1 - M_1 M_2}), \text{ deg} \quad \ldots\ldots [3]$$

which is the small correction necessary for camber angles.

The problem is to find the appropriate stagger angle γ_m.

θ_0 is determined from Equation [3]. With this value of θ_0, and knowing σ, a II value is found from Fig. 3. We now use the chart in Fig. 2 to determine the stagger value γ_0, associated with θ_0 and $M = 0$. From θ_0 and γ_0, we calculate

$$i_0 = 90 - \alpha_1 - \frac{\theta_0}{2} - \gamma_0$$

$$i_m = i_0 \sqrt{1 - M_1^2}$$

$$\gamma_m = 90 - i_m - \alpha_1 - \frac{\theta_m}{2}$$

This method of correcting the incidence and deviation for Mach number is due to Eckert.[2]

Discussion of Theory of Correlation-Chart Construction

The correlation chart, Fig. 2, is based on the premise that for any one cascade (camber, solidity, stagger all given), there is a linear relation between the cotangents of α_1 and α_2, as the entrance angle varies. This is exactly true for incompressible perfect fluids, as shown in the Appendix.

With this principle in mind, the results of tests on many cascades at low Mach numbers were plotted with cot α_1, as a function of cot α_2.

In Fig. 4 are shown some of the straight lines obtained by these tests. A few characteristic test points are shown to illustrate the agreement with linearity.

It is to be noted that all the lines representing tests made at one stagger, regardless of camber and solidity, pass through one point on the left side of Fig. 4.

On the other hand, one camber and one solidity, tested at different staggers, produced the lines A, B, and C in Fig. 4.

In order to define the slope of a particular line, a function of camber and solidity must be used.

From the test data it was seen that there are sets of camber and solidity values which have the same aerodynamic characteristics for the same stagger. Hence the curve A, Fig. 4, does not define uniquely one camber-solidity combination. For example, for any one stagger in the working range, the combination $\theta_0 = 30$ deg, $\sigma = 1.0$, and the combination $\theta_0 = 35$ deg, $\sigma = 0.86$ are identical with regard to their turning angle versus entrance angle curve. This means that a parameter II can be invented and defined to be identical numerically for such pairs of camber and solidity values.

Referring back to the A, B, and C-lines, we can lay out a stagger scale on the right side of Fig. 4, and note the respective intersections, a, b, and c. These points must now all be on one II line, by the definition of the II parameter. All the pairs of camber and solidity values which perform similarly to the A, B, and C-lines, are plotted in Fig. 3 on one constant II line.

The complete chart in Fig. 2 was constructed from turning angle versus entrance angle test data covering the following ranges:

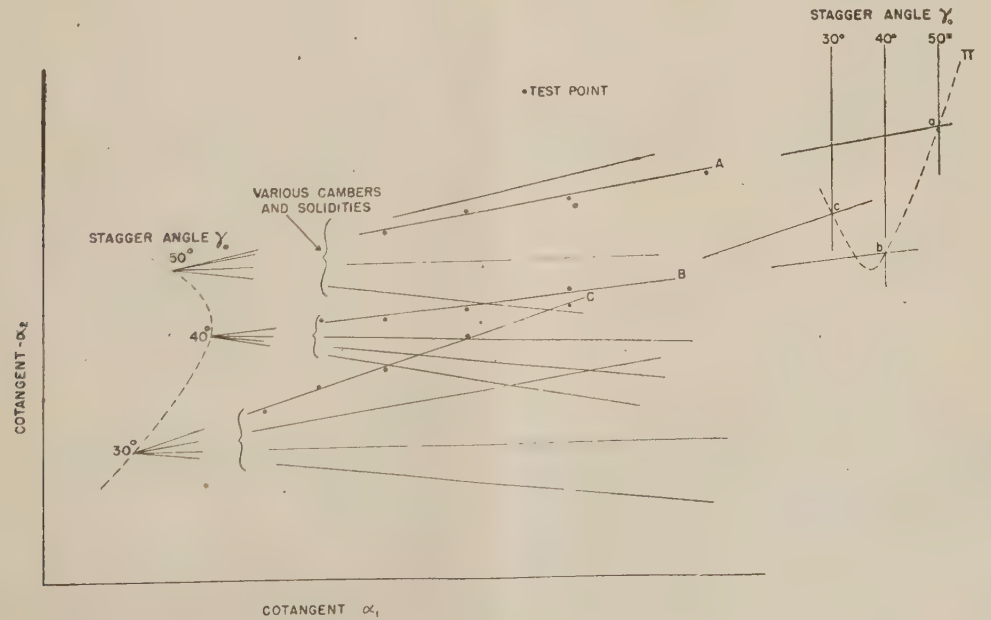

Fig. 4 Construction of Correlation Chart From Cascade Test Data

Camber—27 to 62 deg
Solidity—0.7 to 1.4
Stagger—22 to 51 deg

These test data were checked against calculated cascade performance,[3] and the agreement generally was good. Hence the range in Fig. 2 was extended beyond the test-data range by the calculation methods given by Eckert.[3] The camber range was extended down to 20 deg, and the stagger range up to 60 deg.

One question that must be considered in using these charts is the relation between the turning angle and profile drag. Naturally, it is desirable to keep the profile drag as low as possible.

By examining the test data on loss coefficients, it was seen that a region could be mapped in Fig. 4, inside of which the profile drag was less than approximately twice its minimum value. This region is shown in Fig. 2. Values of α_1, and $\Delta\alpha$ lying inside this region are associated with cascades having low profile drag coefficients. This low drag area concept is not rigorous, but seems to work satisfactorily in predicting the regions of low profile loss for the combinations of camber and stagger likely to occur in practice. For many cascades there is a degree of correlation between the profile loss and the incidence angle. This could be explored further.

Conclusion

In conclusion it should be pointed out that the correlation chart would be more useful if the stagger range were increased. It would also be of interest to attempt to make such a chart for profile families other than the NACA four-digit series. The author has been unable to explain the observed formation of intersections along the left-hand stagger curve in Figs. 2 and 4, which is one major key to the simplification produced by this correlation method.

Appendix

Proof is given for incompressible perfect fluids, which shows that for a given cascade, as the entrance angle of the flow is changed, there is a linear relationship between cot α_1 and cot α_2.

Consider the cascade shown in Fig. 5. For a purely axial entering velocity of unit magnitude, the discharge velocity will have an axial component of unit magnitude and a tangential component of magnitude λ, Fig. 5(a). For a purely tangential entering velocity of unit magnitude, the discharge velocity will be purely tangential, of magnitude μ, Fig. 5(b). By superimposing unit axial velocity and k times unit tangential velocity, as in Fig. 5(c), the discharge velocity will be as shown, with unit axial component, and $(k\mu + \lambda)$ for the tangential component. We now have, for Fig. 5(c)

$$\text{Cot } \alpha_1 = k$$
$$\text{Cot } \alpha_2 = k\mu + \lambda = \mu \cot \alpha_1 + \lambda$$

in which μ and λ are constants identified with the cascade.[4]

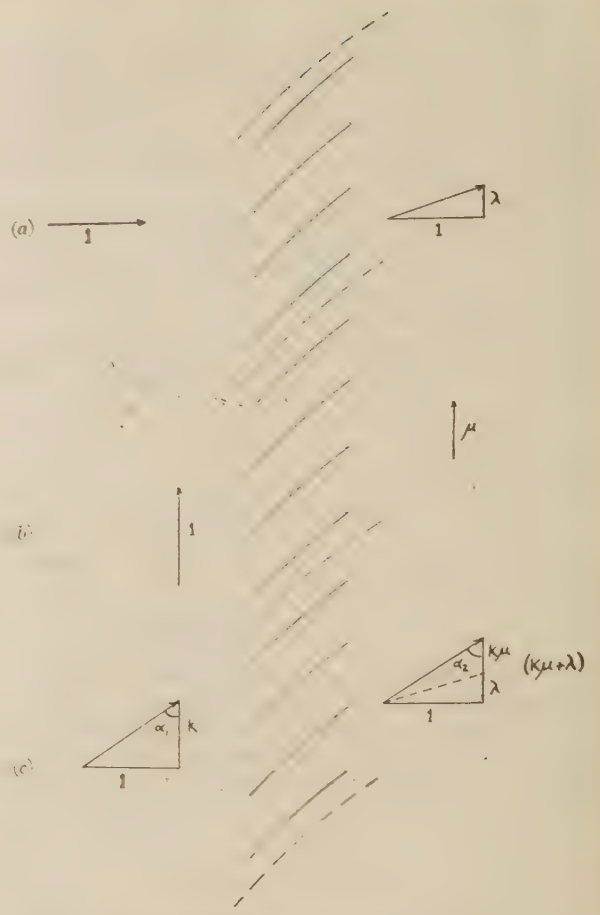

Fig. 5 Diagram for Proof of Cot $\alpha_2 = \mu$ Cot $\alpha_1 + \lambda$

Discussion

J. R. Bressman.[5] This paper is an empirical approach to the problem of determining the proper relationships for axial-flow-compressor blade cascades. When compared with theoretical investigations dealing with this problem, it is unique in that only purely physical quantities are considered rather than such mathematical tools as the mean streamline, equivalent vortex, source-and-sink strengths and distributions, and the resulting incidence and deviation angles. However, care must be taken when it is desired to systematize and simplify the solution of such a complex problem as the flow in an axial-flow compressor.

Obviously, it is the goal of every axial-flow-compressor design to perform the compression required in the most efficient manner or with a minimum of losses. In this case it is impossible to choose arbitrarily the four quantities, entrance and turning angles, solidity, and camber. For fixed quantities of the two independent variables, entrance and turning angles, there is an optimum value for the solidity, camber, and stagger, each of the latter group being related for maximum efficiency. It is true that when a designer is limited by economic considerations such as the necessity of having all stages of a design with the same type of blades, the camber also becomes an independent variable. However, it must be expected under these circumstances, that all stages will not work at equal efficiency. With the proper emphasis on compressor efficiency, the importance of the lines in Fig. 2 of the paper, showing the limits of low profile loss, can be recognized.

With regard to Fig. 2, the limit line on the left indicates that for an inlet angle of 45 deg, deflection angles of 4 deg to approximately 12 deg can be accomplished only with high profile drag coefficients. There is no apparent reason why this condition necessarily exists.

It might also be pointed out that the definition of incidence and deviation angles given in Fig. 1 of the paper, is limited to the case of a circular arc or other symmetrical camber line in which the inlet and outlet blade angle equals one half the camber angle.

[4] This proof was advanced by Dr. A. Vazsonyi, formerly of the Elliott Company.

[5] Research Engineer, Aircraft Gas Turbine Division, De Laval Steam Turbine Company, Trenton, N. J.

Author's Closure

Mr. Bressman is entirely correct in emphasizing the importance of profile drag in applying cascade data to compressor design, and his remarks about the optimum solidity, camber, and stagger are pertinent. However, the author knows of no correlation system that defines the optimum cascade for a given application.

The method described in the paper supplies all the information for design except the profile drag. This means that several trials of camber, solidity, and stagger may be necessary to find one with satisfactorily low drag losses. But, even so, the method proposed offers a rapid means of selecting values of camber, solidity, and stagger that will match the velocity diagram.

In addition, we have a convenient means of calculating off-design characteristics by using the straight line Y-X-Z, Fig. 2, to represent the cascade performance with varying inlet angle.

Fluid Devolatilization of Coal for Power-Plant Practice[1]

By ALAMJIT D. SINGH[2] AND LESLIE J. KANE,[3] CHICAGO, ILL.

A brief review on the desirability of burning char in central power stations and the technical as well as economic factors which prevented the development of a satisfactory process in previous years for the production of char, are given. Application of the fluidization process to devolatilization of coking bituminous coal is described, and specific results are presented on Kincaid coal from seam No. 6, Christian County, central Illinois. Composition, yield, and physical characteristics of the important products obtained in fluid devolatilization of Kincaid coal are given to facilitate technical and, to a certain degree, economic evaluation of the process. Reference is made to other recent developments which are expected to play an important role in the successful application of this process in steam and power-generating stations.

THE direct combustion of high-volatile coal for the production of heat energy has long been regarded as subject to certain drawbacks. Principal objections to direct combustion have been (*a*) atmospheric pollution in large industrial areas; (*b*) loss of valuable products of industrial importance through the combustion process; (*c*) low rates of heat release per unit volume of furnace; and (*d*) the loss of latent heat of water vapor resulting from the combustion of hydrogen in coal.

During the decade following World War I, considerable engineering talent and funds were spent on the attempted development of a satisfactory process for the production of power char from agglutinating bituminous coals. Gentry (1)[4] in summarizing the work of several investigators in low-temperature coal carbonization concluded that power char possessed certain distinct advantages over raw coal as a fuel. The advantages cited by Gentry are as follows:

1 Power char is spongy and easily friable. In comparison to coal, in the pulverization step the power requirement would be 20 per cent less and maintenance generally lower due to decreased abrasion.

2 Higher rates of combustion with a considerably shorter flame, resulting in increased furnace capacity.

3 Saving of 4 to 5 per cent in fuel due to appreciably lower hydrogen content of the char and reduced surface moisture.

4 Char is considerably more free-flowing compared to coal in pulverized form, thus simplifying the handling problem.

5 Danger of spontaneous combustion is almost entirely eliminated.

Soule (2) studied the economics of pulverized-coal carbonization in power plants and concluded that both from a standpoint of initial investment and net savings, it offered interesting possibilities. For instance, this authority gave $1000 per net ton of raw coal per day as the investment cost for the carbonizing plant and indicated that after making due allowance for by-products, the net cost per ton of power char would be $2.85, as compared with $4.50 per net ton of raw coal. These estimates were based upon price levels prevailing in 1928. Similar conclusions were drawn by other investigators, and before engineering conservatism had the opportunity to raise a note of caution, the "gold rush" was on. As a result, several costly experiments on a large scale ended in complete failures. In general, the reasons for such failures were twofold; (*a*) technological and (*b*) economic.

The equipment used in low-temperature carbonization was usually cumbersome and owing to a small temperature gradient between the heated walls of the carbonizing chamber and the coal charge, the production rate was low in comparison with high-temperature carbonization. This was especially true where a lump semicoke was the desired product. In order to overcome the disadvantage of low heat-transfer rates, attempts were made to carbonize pulverized coal for power-plant use by dropping it down vertical retorts countercurrent to the ascending gases and vapors. Systems involving both indirect and direct heat transfer were employed. In each case, no improvement in heat transfer was noted, however, because of the insulating gas film surrounding each tiny coal particle. Actually, the heat-transfer rates were found to be less than in systems used for producing lump semicoke. Still another difficulty encountered was the inability to keep gas off-take systems from plugging due to deposits formed by coal particles and condensing tar vapors.

It was hoped by the proponents of low-temperature carbonization that smokeless semicoke would compete with raw coal on the market, with the gas and tar by-products absorbing all the operating costs and yielding a certain margin of profit. Actually, this hope was not realized because the yield of gas was relatively low, and there were no existing markets for the low-temperature tar.

Changed economic aspects of coal in relation to other competitive fuels and certain recent developments in engineering techniques have again revived interest in the problem of power char production. With increasing production costs of coal, it has become necessary to consider some method of processing it which would yield by-products absorbable on the existing markets and produce a power char costing less than raw coal to generate a kilowatthour of electrical energy. Increasing public demand for cleaner air in urban areas is another factor responsible for current interest in rendering coal smokeless prior to its combustion.

Several new engineering developments, which have either been applied successfully on a commercial scale or show a good promise of practical application are expected to have an important bearing on the problem of char production and utilization. One of these developments is the fluidization process used extensively by the petroleum-refining industry in the production of high-octane gasoline, and which has been studied at The Institute of Gas Technology (3) for application to devolatilization of bituminous coal.

---

[1] This paper is based on the work done for the Illinois Coal Products Commission, Springfield, Ill.

[2] President, Singh Company, Chicago, Ill.; formerly Research Engineer, Institute of Gas Technology. Mem. ASME.

[3] Chemical Engineer, Bureau of Mines, Morgantown, W. Va.; formerly Associate Chemical Engineer, Institute of Gas Technology.

[4] Numbers in parentheses refer to the Bibliography at the end of the paper.

Contributed by the Fuels Division and presented at the Semi-Annual Meeting, Chicago, Ill., June 16–19, 1947, of THE AMERICAN SOCIETY OF MECHANICAL ENGINEERS.

Another development which has been studied at The Institute of Gas Technology is the flash pulverization of coal and other solid substances (4). The flash-pulverizer system has been modified to incorporate a "cyclonizer" chamber, of which the pulverizing nozzle is an integral part. By introducing hot combustion gases into the cyclonizer, char may be flash-pulverized so that about 80 per cent of the product will pass a 325-mesh screen. Hence this method shows promise for utilizing char in existing pulverized fuel installations.

In addition to the foregoing developments, the successful application of the cyclone-type furnace (5) at the Calumet Station of the Commonwealth Edison Company in Chicago, is considered highly significant with respect to the possibilities in the burning of hot char coming from the fluid devolatilization of coal.

Originally the object of the fluid devolatilization of bituminous coal, as carried out at The Institute of Gas Technology, was to produce a char as a substitute for low-volatile Pocahontas coal used in the production of metallurgical coke. Recently this study has been extended further to explore the possibilities of power char production, the results of which are described in this paper.

Experimental Equipment and Procedure

Partial devolatilization studies on Kincaid coal from central Illinois were carried out in the fluid char maker and the by-product recovery train shown in Fig. 1. The retort consisted of a stainless clad steel cylinder, 6 in. in diam and approximately 6 ft high. An electric furnace equipped with a power-input control system to maintain uniform temperatures, was used to transfer heat through the retort walls to the fluid bed of char. At the bottom of the retort a connection was provided for blowing in the raw coal and steam continuously. A side arm near the upper end of the retort formed an outlet for the char and gaseous products, and was connected to two electrically heated cyclones in series for separating the char from the tar vapors and other gases at high temperatures. Following the second cyclone were two tubular surface condensers in series, with a tar receiver under each condenser. For final cooling of gas and condensing of tar vapor, a water-spray condenser was provided. A packed column was installed after the second surface condenser to remove entrained mist of water and tar, and a dry meter was used for measuring the volume of gas liberated during devolatilization of coal.

When making char, the feed consisted of a 50-50 mixture of coal and char, crushed to pass a 20-mesh U.S.S. sieve and superheated steam was used as the fluidizing medium. Temperature measurements were taken on the retort wall, at various levels in the fluid bed, on the walls of the cyclones and char receivers, and at a point immediately before the dry meter. Pressure taps were located at the bottom and top of the retort, after each of the two cyclones and at a point just before the dry meter. By observing carefully the pressures at the various points indicated, it was possible to ascertain whether or not the operation was proceeding smoothly.

The coal used in this entire investigation was obtained from the Peabody Coal Company Mine No. 9 in central Illinois. Its average composition is shown in Table 1.

TABLE 1 PROXIMATE ANALYSIS OF KINCAID COAL SAMPLE AS RECEIVED

Moisture, per cent	6.86
Volatile matter, per cent	33.68
Fixed carbon, per cent	45.00
Ash, per cent	14.46
Sulphur, per cent	3.33
Btu per lb (dry basis)	11330

Production of Char. Fluid-devolatilization studies on this coal were carried out in a temperature range of 752–1472 F (400–800 C). A 50-50 mixture of crushed coal and char (—20 U.S.S. sieve) was successfully used up to a temperature of 932 F (500 C), but above this temperature operating difficulties due to agglomeration of coal particles were encountered. In order to extend the temperature range beyond 932 F (500 C), it was found that a partial reduction in the agglomerating property of raw coal was desirable before admitting it to the fluid bed for devolatilization. Fluidization of raw coal with air at 536 F (280 C) for short periods gave a satisfactory reduction in its agglutination. The coal sample so oxidized was then successfully devolatilized in admixture with an equal weight of char up to a maximum operating temperature of 1472 F (800 C). At this temperature volatile

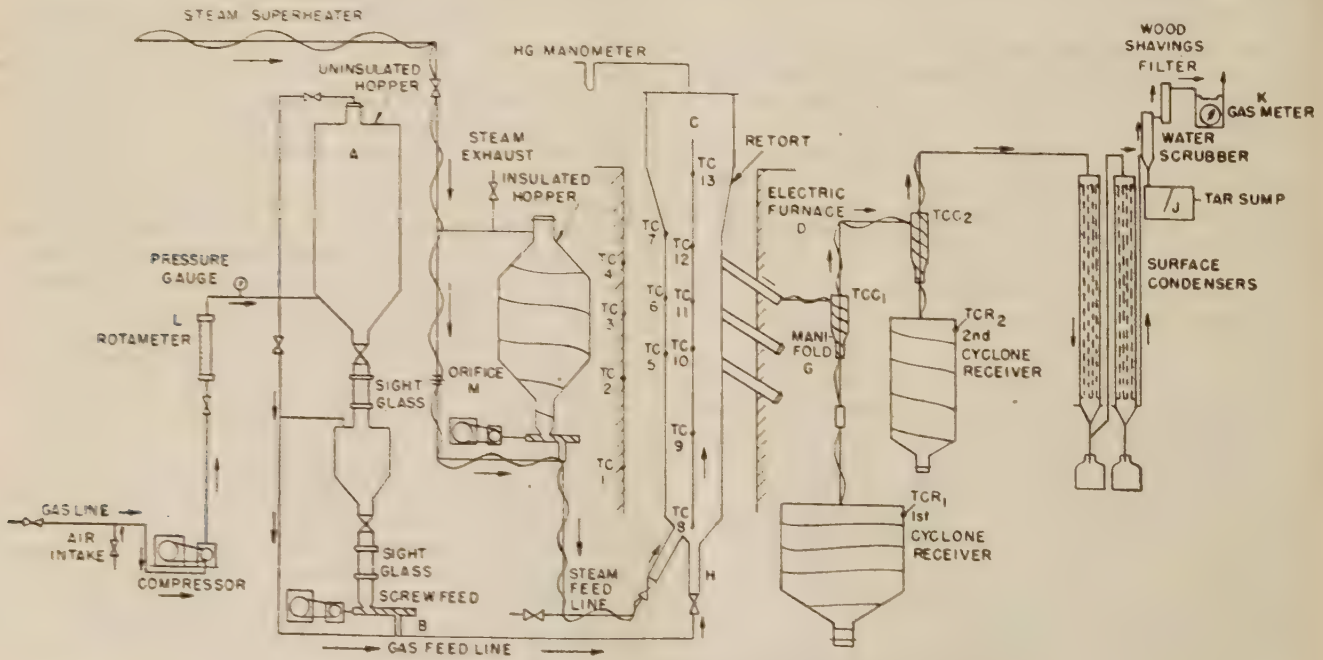

Fig. 1 Flow Diagram of Apparatus for Fluid Devolatilization of Coal

matter of the char product was less than 2 per cent. A summary of results in the afore-mentioned two temperature ranges is given in Tables 2 and 3.

The char product at 932 F (500 C), contained approximately 12 per cent volatile matter, 15 per cent ash, 2.88 per cent sulphur, and slightly over 1 per cent moisture. The heating value of this char was 11,740 Btu per lb, compared to 11,560 Btu per lb, of the raw coal from which the char was made. The coal on "as shipped" basis, with about 15 per cent moisture, had a heating value of about 10,000 Btu per lb. It is interesting to note that the ash content of the char, on a dry basis, remained practically unchanged, while the volatile matter, on a similar basis, decreased from 38.2 per cent in raw coal to 10.29 per cent in the char. This is considered significant since it points to a possibility of rendering high-ash Illinois coals into a smokeless char without raising unduly the ash content of the final product. Mechanical separation of high-ash-bearing fractions of coal fines and of ash particles in the fluidizer probably was a primary contributing factor in reducing the ash content of the char product, with the ash finally being entrapped by the condensing tar in the surface condensers. Another important improvement noted in the char produced was that its sulphur content was 2.88 per cent compared to almost 4 per cent in the raw coal on a dry basis.

Raw coal crushed to pass a 20-mesh sieve, after an oxidizing treatment with air as the fluidizing medium at 536 F (280 C), subsequently was devolatilized successfully at all temperatures from 932–1472 F (500–800 C). At 1472 F (800 C), the char produced had less than 2 per cent volatile matter, 17.35 per cent ash, and 2.98 per cent sulphur. The heating value of the char was 12,100 Btu per lb, compared to 11,740 Btu per lb of the raw coal, both expressed on a dry basis. Again, the ash content of the char product in a temperature range of 932–1472 F (500–800 C) did not increase proportionately to volatile-matter reduction, and was only about 2 per cent higher compared to the ash content of the untreated dry raw coal. Total reduction in the volatile-matter content during the foregoing temperature range was from 38.2 per cent in the dry raw coal to 16.5 per cent in the 932 F (500 C) char, 9.95 per cent in 1292 F (700 C) char, and less than 2 per cent in the 1472 F (800 C) char. Sulphur content of the char made at temperatures above 932 F (500 C) was substantially unchanged from the residual sulphur obtained at 932 F (500 C). Graphical representation of the volatile-matter content and yields of the various chars made from raw as well as oxidized-coal samples is shown in Figs. 2 and 3.

The maintenance of a satisfactory fluid bed of char in the devolatilizing retort is dependent to an appreciable extent on the average particle-size distribution in the material involved. Furthermore, if ultimate combustion of such char is contemplated in a cyclone furnace, it is important to know the particle-size range in the char product. Typical screen analyses on the coal, char mixed with coal for feed purpose, and the char product are given in Table 4.

The particle-size range shown for the various materials in Table 4 does not represent a definite limit within which the fluidization operation must be carried out. Materials, which may be either coarser or finer than those shown, can be handled, dependent on the velocity of the fluidizing medium through the retort.

Production of Gas From Raw Coal. The volume of gas produced steadily increased with temperature and at 932 F (500 C) the gas yield amounted to an average of 2500 cu ft per ton of dry raw coal or about 2100 cu ft per ton of coal with 15 per cent moisture. An increase in operating temperature resulted not only in a greater volume of gas evolved, but also in a lower percentage of carbon dioxide in the gas made. The actual volume of carbon dioxide produced increased with temperature, but

TABLE 2 SUMMARY OF OPERATING RESULTS IN FLUID CHAR MAKER USING RAW OR UNOXIDIZED COAL

	Temperature: deg F	752	842	932	932
	deg C	400	450	500	500
1	Coal analysis as charged:				
	Moisture, per cent	6.86	7.64	7.64	8.54
	Volatile matter, per cent	33.68	34.32	34.32	33.06
	Fixed carbon, per cent	45.00	45.24	45.24	44.20
	Ash, per cent	14.46	12.80	12.80	14.20
	Total, per cent	100.00	100.00	100.00	100.00
	Sulphur, per cent	3.33	3.66	3.66	3.27
	Volatile matter (ash and moisture free), per cent	42.8	43.2	43.2	42.8
	Heating value, dry basis, Btu per lb	11330	11560	11560	11550
2A	Yield, per ton of coal as shipped:[a]				
	Char, per cent	77.7	69.0	56.8	...
	Gas, cu ft	332	865	2050	2150
	Gas, therms	2.05	6.30	11.80	...
	Tar, lb. dry basis	168	230	354	310
2B	Yield, per ton of dry coal:				
	Char, per cent	91.5	81.2	66.8	...
	Gas, cu ft	390	1080	2410	2530
	Gas, therms	2.41	7.40	13.9	...
	Tar, lb. dry basis	197	271	417	366
3	Char composition:				
	Moisture, per cent	0.0	0.50	1.59	...
	Volatile matter, per cent	30.6	26.4	10.29	...
	Fixed carbon, per cent	52.5	57.0	73.07	...
	Ash, per cent	16.9	16.1	15.05	...
	Total, per cent	100.0	100.0	100.00	...
	Sulphur, per cent	...	2.89	2.88	...
	Heating value, per lb dry basis, Btu	11310	11500	11740	11780
4	Gas made:				
	Analysis (raw gas):				
	CO_2, per cent	19.5	28.0	15.9	16.2
	Unsaturates, per cent	6.5	7.6	4.1	5.0
	O_2, per cent	2.3	0.0	2.5	1.2
	H_2, per cent	3.0	5.5	20.3	12.7
	CO, per cent	13.7	13.7	11.9	12.5
	Saturates, per cent	27.1	35.9	32.1	37.8
	N_2, per cent	24.5	4.9	4.5	7.2
	H_2S, per cent	3.4	4.4	8.7	7.4
	Specific gravity of raw gas	0.986	0.963	0.849	0.836
	Heating value of H_2S free gas, Btu per cu ft	639	718	630	...
	Analysis of H_2S and CO_2 free gas:				
	Unsaturated, per cent	8.4	11.1	5.4	6.5
	O_2, per cent	3.0	0.0	3.3	1.6
	H_2, per cent	3.9	8.1	26.9	16.6
	CO, per cent	17.8	20.2	15.8	16.4
	Saturates, per cent	35.2	53.3	42.7	49.5
	N_2, per cent	31.7	7.3	5.9	9.4
	Specific gravity of H_2S and CO_2 free gas	0.953	0.851	0.664	0.720
	Heating value of H_2S and CO_2 free gas, Btu per cu ft	802	1014	878	
5	Tar made:				
	Moisture, per cent	13.1	26.8	26.0	9.39
	Free carbon, per cent	9.24	10.51	14.89	21.87

[a] Based on moisture content of 15 per cent in coal as shipped.

at a slower rate than the production of other gas constituents. The major portion of carbon dioxide may be attributed to the reaction

$$H_2O + CO = H_2 + CO_2$$

With an enormous surface area due to pulverized coal, the rate of carbon-dioxide production would be increased, since the reaction is assumed to take place in the gas film surrounding each carbon particle.

The heating value of the gas produced generally decreased with increasing fluid-bed temperature except at 400 C, when the indicated heating value was lower than anticipated due to the dilution with nitrogen. At 752 F (400 C), substantially all the nitrogen occluded in the surface of the coal particles is driven off and the decomposition of the nitrogenous compounds in coal results in the evolution of additional quantities of nitrogen as such instead of its conversion into ammonia due to lack of sufficient hydrogen. Since the volume of gas given off from the carbonization of coal at 752 F (400 C) is relatively small, the effect of dilution with nitrogen from various sources becomes large.

Production of Gas From Oxidized Coal. The volume of gas evolved from coal previously dried and oxidized with air at 536 F (280 C) rose rapidly in a temperature range of 932–1472 F (500–800 C). At 1472 F (800 C), the gas production amounted to 14,800 cu ft per ton of dry coal or 12,700 cu ft per ton of coal with a 15 per cent moisture content. The heating value of the raw gas was 578 Btu per cu ft.

TABLE 3 SUMMARY OF OPERATING RESULTS IN FLUID CHAR MAKER, USING OXIDIZED COAL

	Temperature: deg F	932	1022	1050		1112	1202	1292	1472
	deg C	500	550	566		600	650	700	800
1	Coal analysis as charged:								
	Moisture, per cent	1.35	1.09	1.00	1.09	1.09	1.03	1.09	1.65
	Volatile matter, per cent	29.93	31.04	34.50	31.04	31.04	30.67	31.04	34.25
	Fixed carbon, per cent	54.33	55.42	51.30	55.42	55.42	55.92	55.42	51.00
	Ash, per cent	14.39	12.45	13.20	12.45	12.45	12.38	12.45	13.10
	Total, per cent	100.0	100.0	100.00	100.00	100.00	100.00	100.00	100.00
	Sulphur, per cent	4.11	4.00	3.67	4.00	4.00	3.99	4.00	3.65
	Volatile, matter (ash and moisture free), per cent	35.1	35.9	40.2	35.9	35.9	35.4	35.9	39.7
	Heating value, dry basis, Btu per lb	11200	11460	11600	11460	11460	11400	11460	11600
2A	Yield, per ton of coal as shipped:[a]								
	Char, per cent	61.0	60.7	...		56.0	55.0	56.4	52.5
	Gas, cu ft	2045	2230	2570		3480	5150	7050	12700
	Gas, therms	9.2	11.2	15.0		16.4	23.7	33.7	71.7
	Tar, lb dry basis	236	163	179		169	159	115	83
2B	Yield, per ton of dry coal:								
	Char, per cent	71.8	71.5	...		66.0	64.8	66.4	61.5
	Gas, cu ft	2405	2625	3020		4080	6060	8300	14800
	Gas, therms	10.8	13.2	17.6		19.3	27.9	39.4	84.3
	Tar, lb dry basis	278	192	211		199	187	135	97
3	Char composition:								
	Moisture, per cent	0.80	0.60	...		0.59	0.27	0.38	0.61
	Volatile matter, per cent	16.50	16.60	...		9.02	10.70	9.95	1.77
	Fixed carbon, per cent	65.60	67.70	...		73.91	71.51	73.68	80.27
	Ash, per cent	17.10	15.10	...		16.48	17.52	15.99	17.35
	Total, per cent	100.00	100.00			100.00	100.00	100.00	100.00
	Sulphur, per cent	3.47	...	2.80		2.49	3.05	2.93	2.98
	Heating value, dry basis, Btu per lb	11770	11400	...		12140	12250	12180	12100
4	Gas made:								
	Analysis (raw gas):								
	CO_2, per cent	29.70	19.49	25.60		19.35	15.32	14.3	10.8
	Unsaturates, per cent	4.00	2.70	4.70		3.00	3.60	4.3	4.5
	O_2, per cent	0.00	1.90	0.90		1.00	1.30	1.3	1.4
	H_2, per cent	10.30	24.10	14.33		24.70	32.20	34.4	41.0
	CO, per cent	18.90	16.40	18.20		16.30	15.80	17.9	18.2
	Saturates, per cent	28.40	25.90	26.80		19.30	18.30	19.6	14.2
	N_2, per cent	1.00	5.10	1.40		10.20	8.50	3.9	7.9
	H_2S, per cent	7.70	4.41	8.10		6.15	4.98	4.3	2.0
	Specific gravity of raw gas	0.909	1.06	1.09		0.953	0.773	0.764	0.739
	Heating value of H_2S free raw gas, Btu per cu ft	484	527	632		503	483	495	578
	Analysis of H_2S-CO_2 free gas:								
	Unsaturates, per cent	6.4	3.5	7.1		4.0	4.5	5.3	5.15
	O_2, per cent	0.0	2.5	1.3		1.3	1.6	1.6	1.60
	H_2, per cent	16.5	31.8	21.8		33.2	40.5	42.2	47.00
	CO, per cent	30.2	21.8	27.8		21.9	19.7	22.0	20.90
	Saturates, per cent	45.3	34.0	40.8		25.9	23.0	24.1	16.30
	N_2, per cent	1.6	6.4	2.1		13.7	10.7	4.8	9.05
	Specific gravity of H_2S-CO_2 free gas	0.5627	0.5734	0.7292		0.4788	0.4692	0.5508	0.5408
	Heating value of H_2S-CO_2 free gas, Btu per cu ft	714	662	891		634	576	582	649
5	Tar made:								
	Moisture, per cent	7.52	21.6	16.9	24.2[c]	27.90	14.47	... 8.8[b]	37.7[c]
	Free carbon, per cent	15.10	24.4	30.2	19.5	30.80	29.68	22.08 69.6	12.6

[a] Based on moisture content of 15 per cent in coal as shipped.
[b] From first condenser.
[c] From second condenser.

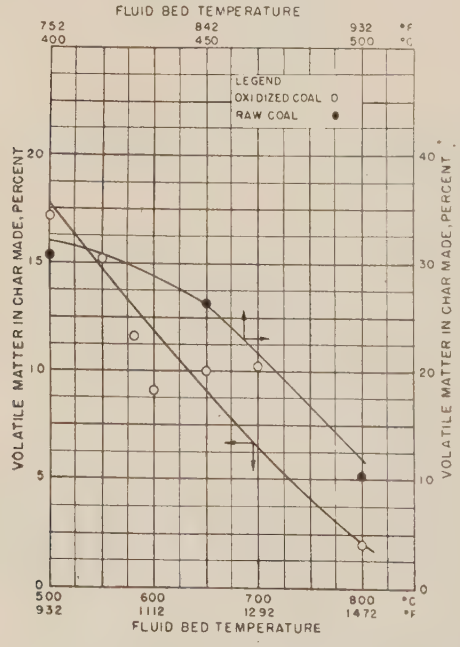

FIG. 2 EFFECT OF FLUID-BED TEMPERATURE ON VOLATILE-MATTER CONTENT OF CHAR MADE

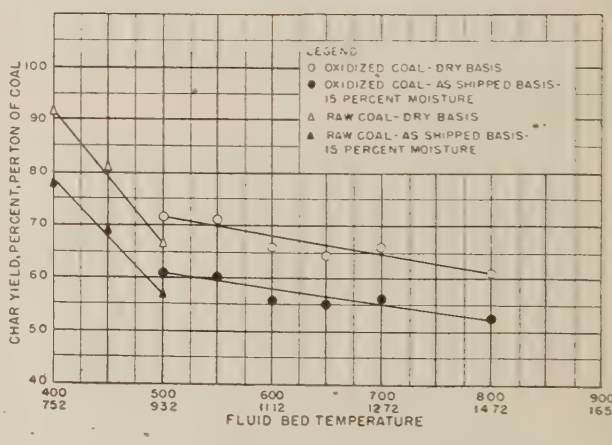

FIG. 3 EFFECT OF FLUID-BED TEMPERATURE ON CHAR PRODUCTION

The concentration of carbon dioxide in the gas produced from oxidized coal decreased with increasing temperature by virtue of the large yield of gas at the higher temperature. The actual volume of carbon dioxide produced, however, increased with increasing temperature. At 932 F (500 C), the production of carbon dioxide was 715 cu ft per ton of dry oxidized coal, and at 1472 F (800 C), this rose to 1610 cu ft.

TABLE 4 SCREEN ANALYSIS OF CHAR AND COAL MATERIALS USED IN FLUIDIZATION TESTS

Fluid-bed temperature, Deg F	Fluid-bed temperature, Deg C	Material	Weight per cent retained on U. S. S. sieves: 8	16	30	50	100	200	—200
1022	550	Coal	0.0	0.0	12.8	31.3	23.3	13.6	18.7
		Char in feed	0.0	0.0	10.9	31.2	23.3	15.2	19.4
		Char product	0.0	1.1	14.9	26.7	21.7	14.9	20.6
1051	566	Coal	0.0	0.0	12.8	31.3	23.3	13.6	18.7
		Char in feed	0.0	0.0	13.5	31.1	24.4	14.7	16.5
		Char product	0.0	0.8	13.4	26.0	22.3	15.3	22.0
1112	600	Coal	0.0	0.0	12.8	31.3	23.3	13.6	18.7
		Char in feed	0.0	0.0	8.8	27.0	22.8	17.4	23.9
		Char product	0.0	1.6	14.8	25.7	21.3	15.6	21.5
1292	700	Coal	0.0	0.0	12.8	31.3	23.3	13.6	18.7
		Char in feed	...	...	...	...	...	...	...
		Char product	0.2	0.7	8.9	24.2	23.3	18.3	24.4
1472	800	Coal	0.0	0.0	12.8	31.3	23.3	13.6	18.7
		Char in feed	0.0	0.0	10.3	31.3	29.8	14.8	13.8
		Char product	0.0	0.6	16.6	28.6	24.1	13.9	15.5

From the analyses of raw gas in Table 2 it will be noted that at 932 F (500 C) the ratio of hydrogen to carbon monoxide is about 0.5, and at 1472 F (800 C) this ratio rises to almost 2.5. A part of the excess hydrogen is believed to have resulted from the increased cracking of the paraffinic hydrocarbons, which the analyses show have decreased from 28.4 per cent at 932 F (500 C) to 14.2 per cent at 1472 F (800 C).

Since the normal concentration of carbon monoxide in ordinary coke-oven gas is of the order of 4 to 10 per cent, its concentration of almost 20 per cent in the gas from fluid devolatilization of coal (together with the high hydrogen content) would indicate that the reactions

$$2\,H_2O + C = 2\,H_2 + CO_2$$

$$CO_2 + C = 2\,CO$$

did occur to an appreciable extent at 1472 F (800 C).

The yield of gas by the fluidization process was noted to be about 25 per cent higher than is usually obtained in commercial coking practice from premium-quality coking coals.

The effect of fluid-bed temperature on the production of gas from raw and oxidized-coal samples is shown in Fig. 4. In Fig. 5 the effect of fluid-bed temperature on the gas therms produced is plotted, since the value of any gas made is determined not by its volume alone, but by its heating value as well.

Production of Tar. Using unoxidized raw coal as feed material, the yield of tar increased with temperature, and a maximum production of 417 lb (about 46 gal) of tar per ton of dry coal was obtained at 932 F (500 C). This is probably the highest yield of low-temperature tar obtained in any process reported to date.

Using coal previously dried and oxidized at 536 F (280 C), by fluidization with air, the production of tar declined to 278 lb per ton of dry coal at 932 F (500 C). A similar effect of coal oxidation on tar yield has been noted previously by other investigators (1). In a temperature range of 932 to 1472 F (500 to 800 C), the yield of tar from oxidized coal steadily decreased, and at 1472 F (800 C), it amounted to only 97 lb per ton of dry coal. A decrease in tar production was accompanied by an increase in gas production due to thermal cracking of the tar. This behavior points to the possibility that the fluidization process may be operated to produce power char and high Btu gas as the main products with tar as a minor by-product. Fig. 6 shows the effect of fluid-bed temperature on the production of tar.

Sulphur Removal. Snow (6) in investigating the elimination of sulphur from coal in streams of various gases reported that 27 to 84 per cent of original sulphur in coal could be removed in the presence of steam at temperatures of 752–1472 F (400–800 C). During the present study, however, Snow's results were not entirely confirmed both with respect to sulphur elimination and loss in weight of coal. It was further noted that desulphurization in the fluid state takes place at a considerably faster rate compared to the static-bed method used by Snow. Results on desulphurization of coal with steam as a fluidizing medium at different temperatures are shown in Table 5.

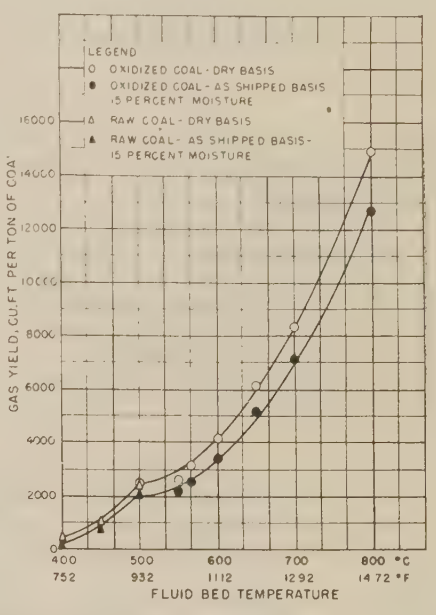

FIG. 4 EFFECT OF FLUID-BED TEMPERATURE ON GAS PRODUCTION

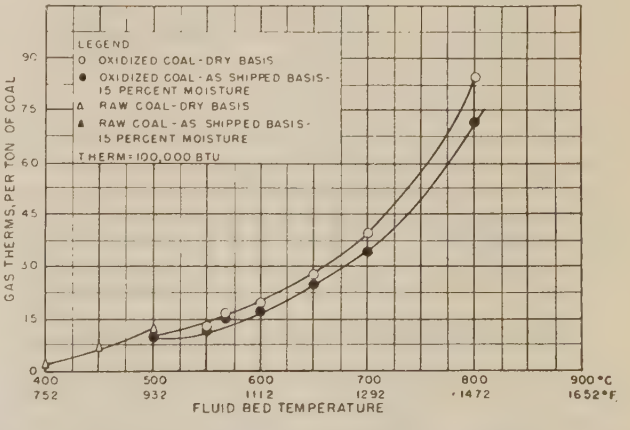

FIG. 5 EFFECT OF FLUID-BED TEMPERATURE ON THERMS IN GAS MADE H_2S FREE

From the results given in Table 5 it appears that both for raw and oxidized coal, elimination of sulphur increases steadily up to 1112 F (600 C), approaching a maximum of about 76.5 per cent. Above this temperature increasing amounts of sulphur seem to be retained by the char and at 1472 F (800 C), the removal of sulphur drops to 38.5 per cent. This last behavior is substan-

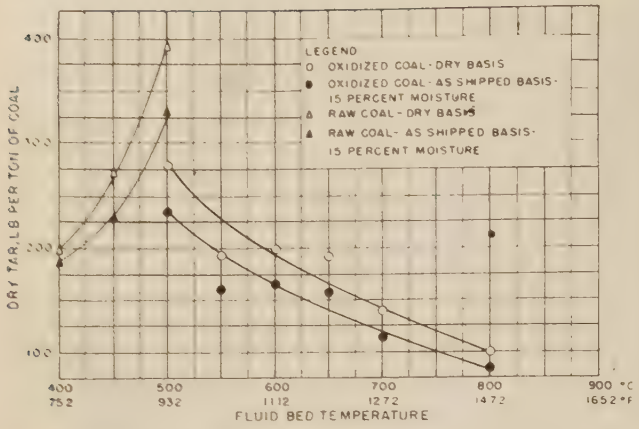

FIG. 6 EFFECT OF FLUID-BED TEMPERATURE ON TAR PRODUCTION

tiated by high-temperature coking results in commercial ovens in which the coke retains between 60 and 70 per cent of sulphur originally present in the coal.

Sulphur elimination from coal occurs in this process mostly in the form of H_2S gas evolution. Several commercial processes exist that can be employed to remove H_2S from the gas made. After its concentration, H_2S may be burned into SO_2 and converted into commercial grades of sulphuric acid or changed into elemental sulphur by its partial combustion into SO_2 and then reacting H_2S and SO_2 to form sulphur and water. This last method has been used recently in Germany on a commercial scale.

TABLE 5 REMOVAL OF SULPHUR FROM KINCAID COAL DURING FLUID DEVOLATILIZATION WITH STEAM

Type of coal sample	Temperature, Deg F	Temperature, Deg C	Sulphur removed, per cent
Oxidized	932	500	33.50
Oxidized	1050.8	566	63.60
Oxidized	1112	600	77.00
Oxidized	1202	650	47.00
Oxidized	1292	700	44.50
Oxidized	1472	800	38.50
Raw	752	400	7.50
Raw	842	450	44.50
Raw	932	500	51.50
Raw	1112	600	76.00

Material Balance. The material balances have been calculated for the tests conducted on oxidized coal in the temperature range of 932–1472 F (500–800 C) on two separate bases. In the first case, the weight of the dry coal fed has been compared with the total combined weights of char, gas, and tar produced. These are shown in Table 6. It will be noted that for the temperature range of 932–1202 F (500–650 C), there is a loss in weight of 5.7

TABLE 6 WEIGHT BALANCE ON COAL CHARGED AND CHAR, GAS, AND TAR PRODUCED. BASIS: 1 TON DRY COAL

Temperature, Deg C	Temperature, Deg F	Weight recovered, lb: Char	Gas	Tar	Total	Weight, per cent: Gain	Loss
500	932	1436	172	278	1886	...	5.7
550	1022	1430	213	192	1835	...	8.3
600	1112	1320	298	199	1817	...	9.2
650	1202	1296	358	187	1841	...	8.0
700	1292	1328	485	135	1948	...	2.6
800	1472	1230	840	97	2167	8.4	...

per cent to slightly over 8 per cent in the various products recovered. Since the oxygen content of Kincaid coal is about 7.9 per cent on a dry basis, the weight loss noted in products may be logically attributed, aside from experimental deviations, to the formation of liquor during the devolatilization step. For 1292 F (700 C), the weight loss due to liquor formation decreases, because of the accelerated reaction between carbon and oxygen to form CO and CO_2. At 1472 F (800 C), there is actually a gain in weight of products, amounting to 8.4 per cent, which may be attributed to the various reactions between carbon and steam. In the second case, a carbon balance has been worked out between the carbon content in the coal fed and the carbon found in the various products. These results are shown in Table 7. Considering the fact that multiplying factors of 20 to 50 were employed in changing the experimental data to express yields of various products on a basis of per ton of dry coal, any experimental errors were unduly magnified.

TABLE 7 WEIGHT BALANCE ON CARBON IN COAL CHARGED AND CARBON IN CHAR, GAS, AND TAR RECOVERED. BASIS: 1 TON DRY COAL—1360 LB CARBON

Temperature, Deg C	Temperature, Deg F	Lb of carbon recovered in: Char	Gas	Tar	Total	Deviation-weight, per cent: Gain	Lo
600	1112	1137	78	180	1395	2.44	...
650	1202	1117	108	168	1383	2.42	...
700	1292	1158	158	125	1441	5.95	...
800	1472	1020	238	87	1335	...	1.1

Application of Fluid Devolatilization of Coal in Power Plants. The results on the fluid devolatilization of a bituminous coal just presented offer some interesting possibilities in power-plant practice. For a combined gas and electric utility enterprise, the process should be particularly attractive from a standpoint of handling the two main products, i.e., char and gas. Unless there is a profitable market for tar, its complete disposal may be achieved through gasification. Thus it should be possible to obtain power char, with gas suitable for utility distribution, as the only other product. The requisite of developing special markets for tar obtained in low-temperature distillation of coal can thus be completely eliminated.

Technologically, the prospects are definitely encouraging. In previous investigations, two serious difficulties were encountered in the production of power char from pulverized bituminous coal. These difficulties as discussed before are as follows:

1 Plugging of cyclones with fine sticky plastic coal particles. In some earlier attempts the products of distillation were withdrawn countercurrent to the crushed-coal feed, and a portion of the falling coal particles was entrained in the off gas and was deposited with the condensing tar vapors, resulting in the plugging of gas line.

2 Low rates of heat transfer to the finely divided coal particles, in both external and internal heating systems, due to an insulating gas film surrounding each particle.

Both of these difficulties have been eliminated successfully in the fluidization process. Of the several systems attempted, the one involving an overhead draw-off for char, gas, and tar vapors into heated cyclones has proved to be most satisfactory. By maintaining the cyclones at substantially the fluid-bed temperature, condensation of tar vapors is reduced to a degree where it no longer interferes with the cyclone efficiency. The scouring action of the coarser fractions of the char product effectively prevents any "build-up" from fine sticky coal particles passing through the plastic zone.

The rate of heat transfer in the fluid bed has been found to be four to sixfold, compared to conventional coking methods. This has been made possible due to effective scrubbing action on the gas film surrounding each coal particle in the fluid bed.

The successful development of the cyclone-type furnace on a commercial scale has opened an ideal possibility to burn the hot char as it leaves the fluidizer. The char product at temperatures ranging from 1292–1472 F (700–800 C) in the form of hollow crude spheres, should be an excellent fuel for the cyclone furnace. It is expected that the combustion of highly preheated

and activated char will result in heat releases greater than 15,000 to 22,000 Btu per cu ft of total combustion volume per hr for pulverized-coal burners and 30,000 to 40,000 Btu for cyclone-type installations.

If it is desired to save high-Btu gas and tar as valuable by-products in the production of char for pulverized-fuel installations, a combination of fluid-devolatilization system and the flash pulverizer-cyclonizer system may be employed. The char produced in the fluidizer may be separated from gaseous by-products at high temperatures and subsequently flash-pulverized for pulverized-fuel burners.

In the burning of char, heat economy of 4 to 6 per cent may be made possible due to its lower hydrogen content. The desulphurization of the coal in the fluidizer will reduce sulphur emission from stacks to the extent of 25 to 35 per cent.

Other advantages from the burning of char will be in the form of eliminating soot deposits on tubes permitting higher furnace temperatures, faster rates of combustion, and a comparatively less visible stack discharge. The decrease in visibility of the stack discharge is due to two effects; first, the fuel has been rendered smokeless prior to its combustion; and second, the reduction in the hydrogen and surface moisture results in appreciably less water vapor in the flue gases. The water vapor normally present in the flue gas from coal combustion is objectionable when rendered visible by cold weather.

As previously mentioned, the char is relatively less abrasive and more easily pulverized than raw coal. Combustion of char in pulverized-fuel installations therefore should be feasible and this, in fact, has been confirmed by actual tests on a boiler with a steam capacity of 40,000 to 50,000 lb per hr (7). A further advantage in using char would be that its finely divided particles will not form agglomerates as do the coal particles, thus resulting in rapid and more complete combustion. Eastern coals, which coke more easily compared to the high-oxygen coals, will be considerably improved in their burning qualities in pulverized form on being converted into a char first. The high-oxygen coals will be improved in calorific value due to removal of oxygen in the devolatilization step.

The over-all economy obtainable from a combination of fluid devolatilization of coal and burning of the char will depend upon conditions in individual localities. The data presented so far can be used to a certain degree, to calculate the possible economy for a given location. For plants burning Kincaid coal, preliminary calculations have indicated that a substantial over-all economy may be possible by the use of power char system.

Conclusions

1 Kincaid coal has been successfully made into a char by the fluid-devolatilization process. At 1292 F (700 C), the yield of char amounted to 1328 lb per ton of dry coal. The char contained 10 per cent volatile matter and showed a heating value of 12,180 Btu compared to 11,460 Btu per lb of raw coal on a dry basis.

2 The gas yield was 8300 cu ft at 1292 F (700 C) and 14,800 cu ft at 1472 F (800 C) per ton of dry coal. In terms of heat units, the gas amounted to 40 therms at 1292 F (700 C), and 84 therms at 1472 F (800 C).

3 The tar yield was 15 gal per ton of dry coal at 1292 F (700 C), and 11 gal at 1472 F (800 C).

4 The ash content of the char is 2 to 3 per cent higher than in coal when the process is operated at 1292–1472 F (700 to 800 C). At temperatures below 1022 F (550 C), the increase in ash content of char is insignificant. Reduction in ash content of char made in a temperature range of 752–1472 F (400 to 800 C) is believed to be due to mechanical separation of the high-ash-bearing fractions of coal and ash particles in the fluidizer.

5 Substantial desulphurization of coal is effected with steam during the devolatilization process, ranging from 38.5 per cent at 1472 F (800 C) to as high as 76 per cent at 1112 F (600 C).

6 The char produced consists of hollow spheres and is in an activated condition. It is believed to be ideally suited for a cyclone-type furnace.

7 The char has been found to be more pulverizable than raw coal and therefore is considered applicable in pulverized-fuel-burner installations.

8 Heat economy of 4 to 6 per cent should be possible due to lower hydrogen losses, as well as due to sensible heat that may be carried into the furnace by the char.

9 The technological difficulties, which prevented the successful production of power char from finely crushed coal in previous investigations, have been overcome effectively by the application of the fluid technique and other improvements.

10 The process seems to offer excellent opportunity for combined gas and electric utility systems.

Acknowledgment

The laboratory studies described here were carried out at the Institute of Gas Technology, Chicago, Ill., under the sponsorship of the Illinois Coal Products Commission. The authors are indebted to Mr. John C. Foster for his assistance in the experimental work, and to Messrs. E. S. Pettyjohn and V. G. Leach for helpful criticism in the preparation of this manuscript.

BIBLIOGRAPHY

1 "The Technology of Low Temperature Carbonization," by F. M. Gentry, The Williams and Wilkins Company, Baltimore, Md., 1928, pp. 156 and 314–347.

2 "The Economics of Carbonization at Central Electric Stations," by R. P. Soule, *Combustion*, vol. 5, no. 18, 1928, pp. 237–243 and 260.

3 "Partial Devolatilization of Coal by the Fluidization Process," by A. D. Singh, American Gas Association, Technical Section Joint Production and Chemical Committee Conference, New York, N. Y., June 3–5, 1946.

4 "Coal Atomizer: New Method for Pulverizing and Drying Coal," by J. I. Yellott and A. D. Singh, *Power Plant Engineering*, vol. 49, no. 12, 1945, pp. 82–86.

5 "The Horizontal Cyclone Burner," by A. E. Grunert, L. Skog, and L. S. Wilcoxson, Trans. ASME, vol. 69, 1947, pp. 613–627.

6 "C nversion of Coal Sulfur to Volatile Sulfur Compounds During Carbonization in Streams of Gases," by R. D. Snow, *Industrial and Engineering Chemistry*, vol. 24, no. 7, 1932, pp. 903–910.

7 "The Use of Pulverized Smokeless Fuel in Boiler Firing," *Engineering*, vol. 122, Dec. 10, 1926, p. 720.

Discussion

R. A. Sherman.[5] The authors hold out considerable hope that the fluidization technique, as reported in their paper, will solve the many problems relating to the preparation of low-temperature coke which have prevented successful operation of processes previously proposed. All will hope that the predictions of the authors will be realized because a successful method of low-temperature carbonization of coal has long been sought.

The success of this or any other method of low-temperature carbonization depends upon the economics and, despite the considerable amount of data included in the authors' paper, the data required to judge the economics of the process are lacking. For example, no information is presented in the paper on the throughput of coal. This is most important as it is the rock upon which practically all other processes have been wrecked. Still further information that could be desired by an engineer or an economist looking at the process is the amount of steam used per pound of coal.

[5] Assistant Director, Battelle Memorial Institute, Columbus, Ohio. Mem. ASME.

A complete material balance is not given in the paper. The tables show, in general, a deficiency of 2 to 8 per cent in the weight of the product below the weight of the coal used, but if the steam were included, the deficiency would be of greater amount.

A heat balance should also have been included in the paper. It is not to be expected that the heat balance on a large plant would be the same as that on a pilot-scale plant such as the authors used, but it would have been indicative of what was to be expected. A rough approximation has been made by the writer on one run of oxidized coal at 800 C, which gives results as follows: There were recovered per ton of coal approximately 8,000,000 Btu in the form of gas, 14,400,000 Btu in the form of char, and about 2,000,000 Btu in the form of tar, if we assume that the tar has a heating value of about 20,000 Btu per lb. This totals 24,400,000 Btu per ton, whereas the heating value of the original coal was 23,200,000 Btu per ton. The additional heat obviously came from the steam and from the heat put in, in the form of electrical energy, to heat the retort. No figures are given on the amount of electrical energy put in and thus the efficiency cannot be determined.

The large yields of gas are particularly cited by the authors. These are interesting, but not surprising as they must come from the water-gas reaction between the steam and the coal or char, and the heat energy required comes from an electrical-energy input.

The authors call attention to the lack of increase in the ash content of the char as compared to that of the coal. This is indeed noteworthy and is ascribed by the authors to the fact that there is a separation of ash in the fluidized bed. The question arises, however, as to what eventually becomes of this ash. It must at some time be removed from the system.

The suggestion that the char be used in a cyclone furnace and pass directly from the carbonizers to the furnace without loss of the sensible heat is most interesting. It may be a difficult problem to handle this high-temperature char, and there is a question as to how it is to be introduced into the furnace without ignition. The present system of introducing the coal into the cyclone furnace is in suspension in a part of the air required for combustion.

The authors also suggest the use of the char in pulverized form and predict that it would have a high reactivity and a high grindability. A number of years ago at Battelle, the White process of carbonization, in which particles of crushed coal were dropped through an externally heated refractory retort, was quite thoroughly investigated, and the writer conducted tests on the combustion of the char made by this process in pulverized form. The results are reported in the Proceedings of the American Gas Association for 1931. The chars produced in that process were varied as desired in volatile content from 10 to 16 per cent. It was possible to burn them in pulverized form, but the time required for combustion was greater than that for high-volatile bituminous coal as was to be expected. No steam was used in that process and the char was possibly less reactive than the char produced in the process described by the authors.

The writer hopes that the authors have the complete answers to the questions that he has raised about the process and that the indications will be so favorable to a continued research on this process that it can be pushed forward to get all the answers. Finally, it is hoped that the process will work as well as the authors have predicted.

Ball-Bearing Slides

By CONRAD JOBST,[1] TOLEDO, OHIO

From personal experience the author gives examples of progress made in reducing friction in sliding movements to a minimum, with the addition of preloading of the slide mechanism, so that higher operating speeds, greater precision of product, and longer life at lower cost are possible. Such preloading produces high stability in a slide because operating loads merely modify the total load, either increasing or decreasing it, in contrast with conventional slides in which the live load changes from no load to full load, and usually with no reversal of load permissible. Actually, from the standpoint of mechanics, preloaded slides constitute the introduction of couples into the system which are available to resist other couples such as those due to eccentric loads.

DESIGNERS of machines and apparatus, during the last 30 years, have applied annular ball bearings to spindles and shafts. Relatively recently, preloaded ball bearings were developed for machines when extremely accurate and lasting performance was essential.

For straight-line movements, friction slides are still common, and in a few cases V-type roller bearings are applied to machines such as thread grinders, etc. However, on larger machine tools, friction slides are universally used.

As a background for comparison, Figs. 1, 2, 3, and 4 show conventional slides which must be provided with adjustments for wear and oil clearance. All loads must be arranged near to the center of the slide if cocking and binding are to be prevented. The slides are necessarily loose in the conventional sense in order to permit free motion, and if any additional load is applied, a certain amount of instability must be exhibited, that is, instability in the realm of extremely accurate motions. For those not familiar with such accuracy, an example would be the change in location of a cutting tool due to change in thickness of the oil film in the slide. The simplest procedure to provide stability in a mechanism is to preload the entire assembly. This has been accomplished by designing a rolling contact between two slide members, with the initial preload so large that subsequent load are small by comparison.

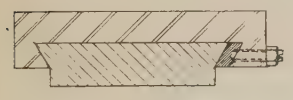

Fig. 1

Fig. 2

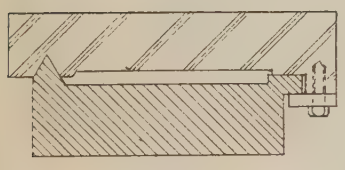

Fig. 3

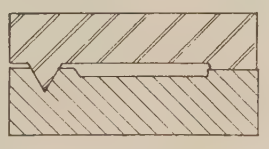

Fig. 4

To overcome these serious objections of instability in motions supposedly accurately controlled, the author replaced the sliding surfaces with preloaded ball-bearing tracks as shown in Fig. 5.

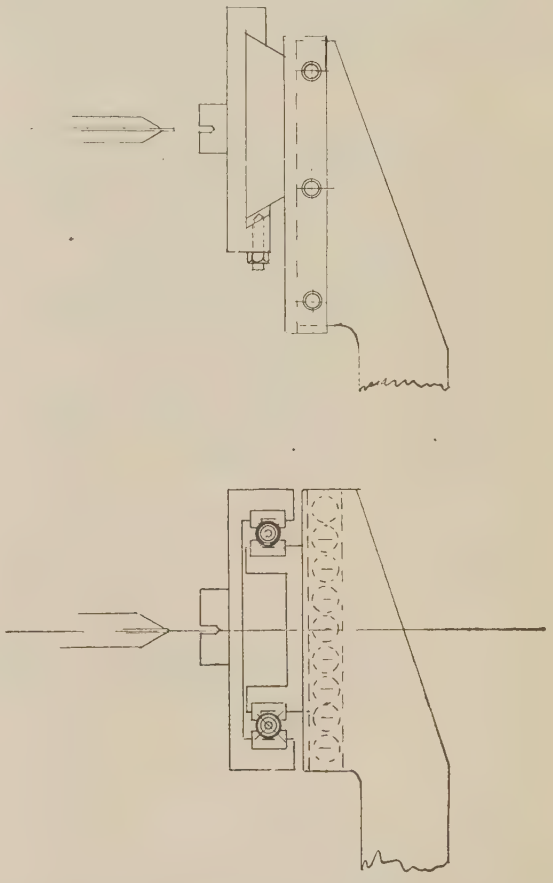

Fig. 5

Preloading is produced in the desired amount by the tolerances of the slide members prior to assembly. Manual adjustment subsequent to assembly was omitted purposely. This particular mechanism illustrated is the cross slide on a machine in which the alignment between two-positioned operations must be kept perfect in order to make a high-grade product. It was found that this accurate alignment, due to the preload principle, has actually been maintained for over 20 years of operation, and the original machine is still in operation.

Fig. 6 shows the complete unit which is composed of two tracks, 1 and 2, and spacer 3, with steel balls 4. Dimensions *A* and *B* may be kept standard for interchangeability. There are many methods of dirt protection for such slides which depend greatly on the location of the slide. The position of such a slide in a design may be chosen for convenience, because any eccentric or off-center load does not impair its precise movement, and cocking of the ball-bearing slide, in the sense of cocking of a conventional slide, is impossible.

---

[1] Consulting Engineer, Owens Brush Company.

Contributed by the Machine Design Division and presented at the Annual Meeting, Atlantic City, N. J., December 1–5, 1947, of The American Society of Mechanical Engineers.

Note: Statements and opinions advanced in papers are to be understood as individual expressions of their authors and not those of the Society. Paper No. 47—A-42.

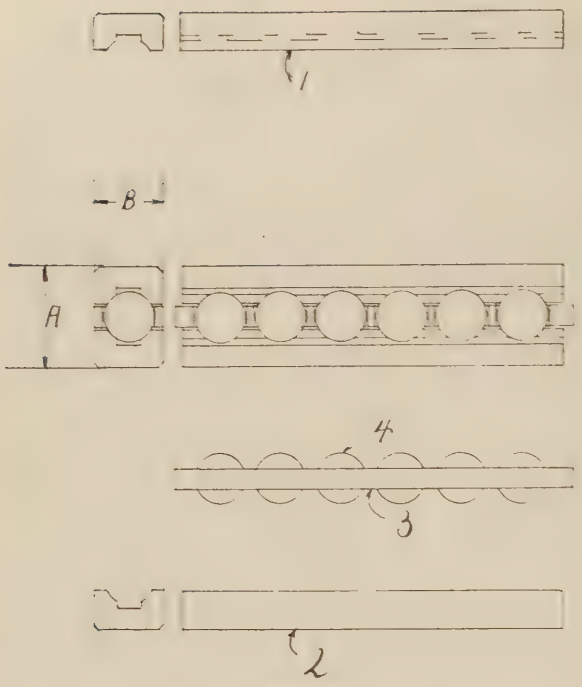

FIG. 6

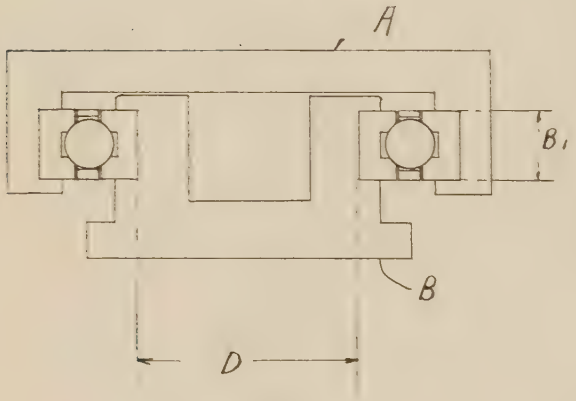

FIG. 7

Fig. 7 shows the assembled slide unit; B is the male, and A is the female slide. Dimension D is made oversize, and therefore establishes the preload, or prestress, desired. From a practical standpoint, dimension B_1 for both slides should permit a press fit for the tracks.

V-TYPE STRAIGHT-LINE ROLLER BEARING VERSUS STRAIGHT-LINE BALL BEARING

Fig. 8 is a comparison between a V-type straight-line roller bearing used in the latest precision machines, and the preloaded ball straight-line bearings which have been in operation for many years.

V-type straight-line roller bearings must be provided with adjustments because they are cylindrical in shape, and the running surfaces must be parallel with each other. On the other hand, in the straight-line ball bearing, no parallelism of the balls exists; therefore a lateral springing or yield in the frame members does not alter the relation of the tracks to each other. In such a bearing, the spherical contacts are precisely the same regardless of the movement in the parts, whereas such movements would be detrimental to long life in roller bearings. Proper compensation would be necessary for roller bearings in the form of a self-aligning mechanism which would be, after all, partly spherical. Since the ball will always keep perfect contact with its track, an angular movement does not impair its precision. The movement rotates on the ball. Adjustments are not necessary in straight-line ball-bearing slides if properly preloaded.

GREAT PRODUCTION COST SAVINGS

During the recent war, in making aluminum and zinc shell noses and fuse parts for the 20 to 47-mm sizes, the production

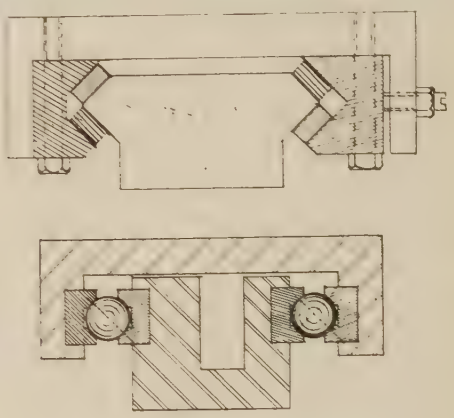

FIG. 8

requirements ran into the billions of pieces. Prior to the author's investigation of the problem, threads were cast in the die or mold for these noses, making complicated molds necessary. In spite of careful workmanship, there was always a flash on the threads which necessitated complicated cleaning, trimming, and inspection operations. Dimensional stability was very poor and production costly. It was suggested that straight-line ball slide units be installed to support an acorn die to chase the threads after a form-tool operation. A cross slide of the same construction as shown in Fig. 9 was used and there was no cock in the slide, nor was there any lateral drag on the chaser. The result was a very smooth thread, because the sharp edges of the chasers were not held back by drag and could not cut into the sides of the thread in spite of the softness of the material. The smooth thread was particularly significant in the soft metal because spindle speed

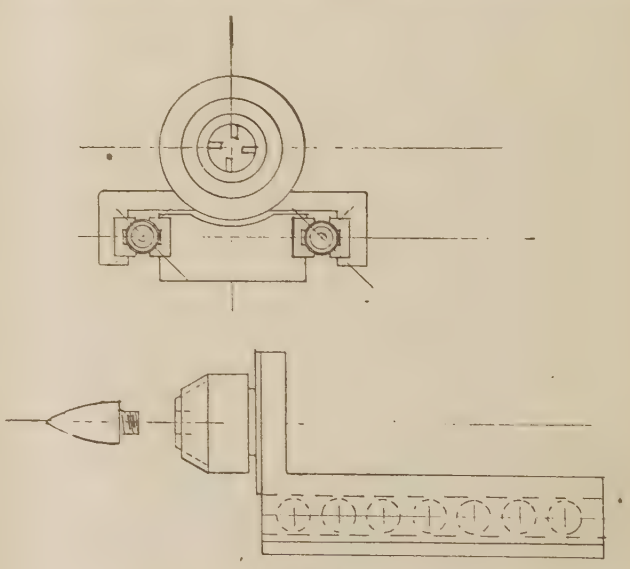

FIG. 9

was 500 rpm. Thereafter the die castings were made in a mold without threads in the cavity and the first cost of the molds was thereby reduced greatly. Maintenance of molds was small in comparison with the former method, and costs were reduced still more. A total of 2000 pieces of 47-mm parts was made per hour, and 300,000 pieces per grind of the dies was common practice. The final cost of the part was only a fraction of the original.

Universal Application

There are innumerable designs and mechanical constructions where the installation of straight-line ball bearings is essential if lasting precision results are important. This includes all special machines for the duplication of parts with dimensions of high tolerance, many machine tools, boring mills, and most important of all, instruments of inspection. Old machines with friction slides can be made up to date by machining space for the ball unit of proper size into the now-existing friction slide. It will make the old machine better than it was when new, as shown in Fig. 10. Great economy can be obtained and the machine itself

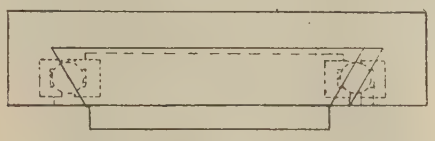

Fig. 10

will be more efficient than it was before. Since there are no adjustments, incompetent maintenance men or laymen cannot change or tamper with the original precision established by the builder.

Heavy Machinery With Supersensitivity

An example of heavy machine design is shown in Fig. 11, which is a mold-clamping device with 1,000,000 lb clamping pressure, but having a sensitivity which makes complete mold protection possible. It takes only 150 lb, spring pressure to move the carriage which weighs 5000 lb, including the die. The preload on all the balls, 18, is approximately 50 tons. The meeting of the die or mold faces is extremely accurate and does not depend upon pin and bushing, in fact, no pins are used at all. Because of the absolutely parallel meeting of the die faces, and because of the free movement in the slide, mold-protection possibilities suggested themselves.

If foreign matter thicker than 0.001 in. lodges between the die faces, particularly parts left over by flashes of the plastic material, or, if the whole molded piece is left in the mold, the carriage cannot complete the entire stroke, so that safety microswitch 60 would not be opened, and springs 50 would compress, owing to the forward motion and actuate switch 54 to reverse the motor and prevent pressure being applied to the die faces. It would prevent closing switch 49 which controls the torque-unit gear motor. This torque-gear mechanism applies 500 tons pressure to the mold faces, and that pressure would never be created if the mold faces are separated more than 0.001 in.

Such precision is not possible with conventional slides. It has been found that a cigarette placed between the mold faces has sufficient compressive strength to actuate spring 50 without

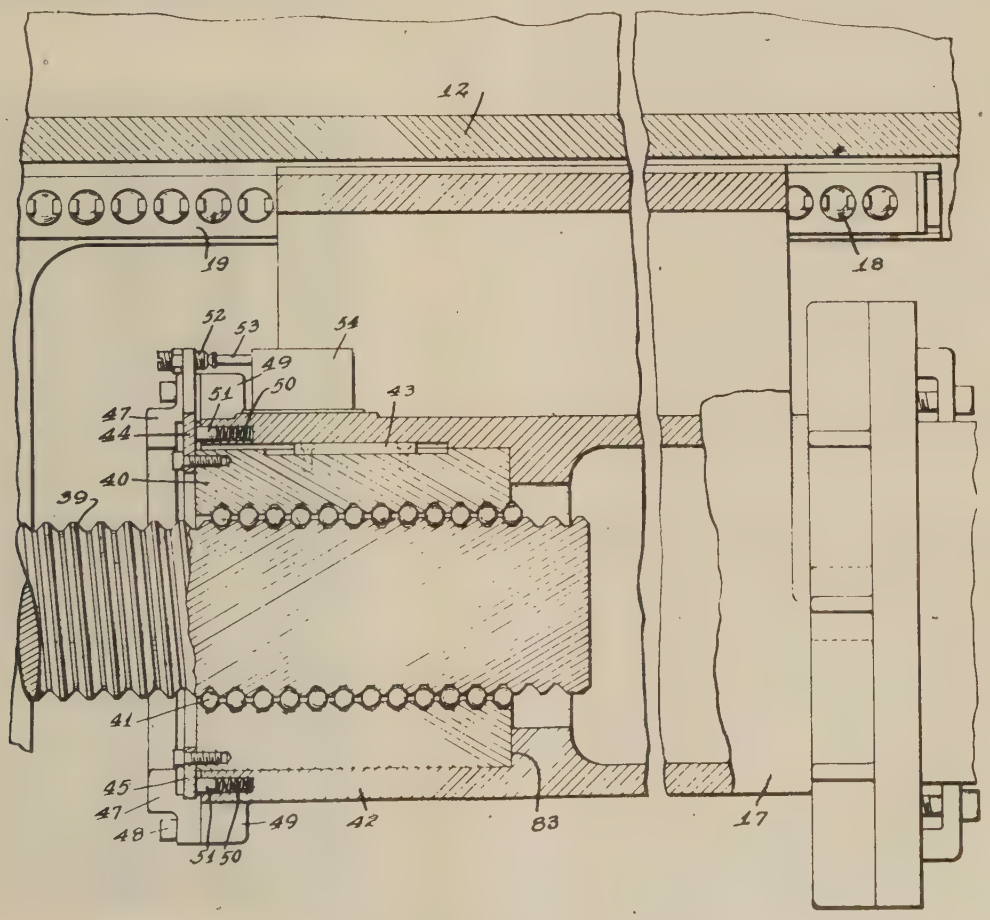

Fig. 11

breaking the paper. The cigarette did not resist the whole 150 lb required to move the carriage, but it did build up sufficient resistance to produce thrust against the forward movement, which, being free, would yield and actuate a microswitch.

The placing of a 0.001-in. shim or tissue paper at any part of the mold face over a 20-in-square area would actuate the microswitch, proving that the lateral movement of the carriage is negligible. This particular molding machine has been in operation for $3^1/_2$ years. A test revealed that it took the same twisting force against the platen to show deflection reading after $3^1/_2$ years as it did after it was 3 months old. This comparison was made after the initial 3 months, rather than when new, to permit plastic flow, or "cold flow," to become negligible.

Greatest Pressure per Square Inch With Smallest Equipment

The principles of the straight-line preloaded ball bearing can be applied to the helix, and thereby obtain similar results in rotary motions.

To provide power for the closing of a mold and injection of the plastic material into the mold, a helical ball bearing was used which creates pressure by rotation (a screw).

To illustrate application to the screw, Fig. 12 is a short male element, Fig. 13 is a long male element, Fig. 14 is an outer race only, and Fig. 15 is a bearing assembly.

In operating these two units (the screw and the slide) for molding thermoplastic resins, it was found that the cost of electric current for the 10-hp motor to operate them was less than the cost of cooling the oil for the hydraulic machine of the same capacity which required a 35-hp motor.

Motors of surprisingly small horsepowers are fixed to either or both rotating members, which, with proper electrical controllers, can be cycled automatically, or by manual control, for continuous production. A surprising sensitivity is obtained. The pressure output is many times greater than for a hydraulic system, and this higher pressure is obtained by the short-time overload which the motors can withstand and will provide. In a hydraulic system, oil pressure can be no greater than that for which the pumps were designed, not even for short intervals.

Fig. 12 is the injection element used on a plastic injection machine. This element is stopped by a limit switch, actuated by a spring-loaded plunger which extends into the runner cavity. As the pressure builds up in this distributor cavity, a spring will deflect to actuate a switch to cut off power prior to the completion of the full stroke. All during the injection time for molding, the speed of the plunger, unlike that of a hydraulic system, is constant, and the heated plastic material therefore will lose no appreciable heat. Loss of heat produces laminated plastics which are undesirable.

It should be noted that the work of final filling of the cavity is done by the inertia of the element. This accounts for the small use of power. The element, Fig. 13, remains stationary, much the same as a nut once tightened requires no pressure to hold it locked. The functions of these parts are quite different from those of a hydraulic system which require continuous pumping against the pressure induced in molding.

This pressure by ball-bearing screw can be applied to any type of press. The general over-all dimensions of such a machine would be small in comparison to an hydraulic machine of the same power.

Perfection of Spherical Bodies

All experience shows that the spherical shape of the ball permits it to withstand terrific loads with minimum wear, which will stabilize the motion of any part or parts when built into the mechanism. No one can appreciate the mechanical excellence

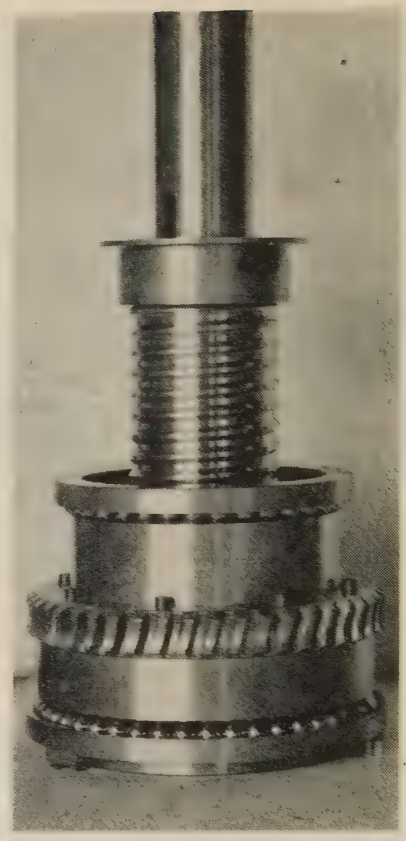

Fig. 12

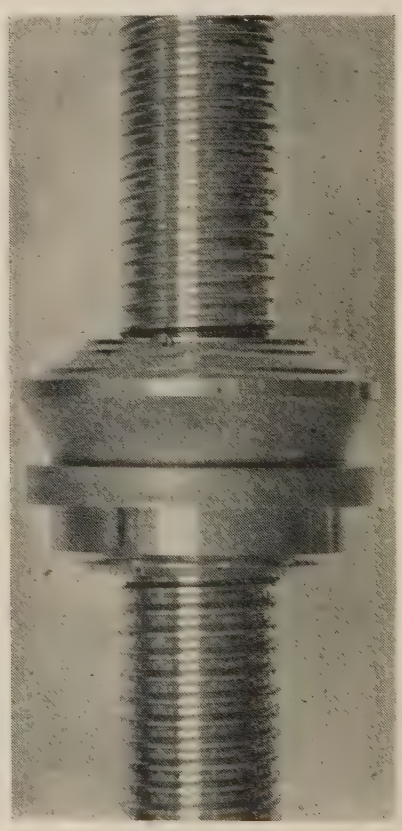

Fig. 13

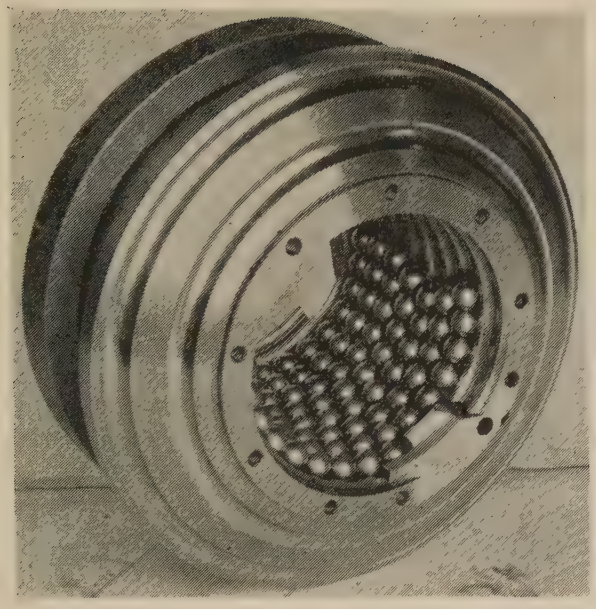

FIG. 14

of such a movement until he can visualize a preloaded annular precision bearing converted into straight-line motion.

PRELOAD IS FUNCTIONAL

There is always a deformation of metal under stress and if this deformation is controlled in mechanisms, nominally fixed positioning of component parts is obtained. If use is made of the deformation of metal (apart from dead load) to produce stability, such use may be called preload. If, for example, the preload is 1000 lb, and the functional load is 200 lb, precise positioning of the component parts will be the normal outcome. Preload represents potential energy, which can be used to resist working stresses.

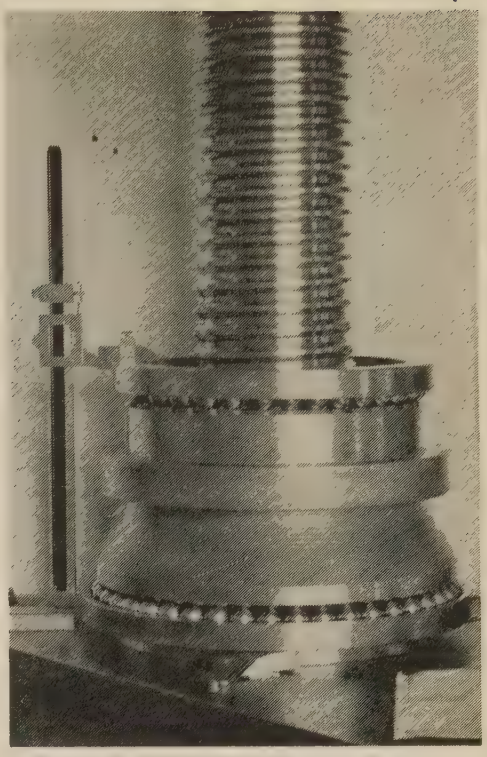

FIG. 15

In the mechanism described, no conventional sliding surfaces were used, the movements were extremely free, and the motion was as precise as the precision of the ball itself, for which dimensional stability of $^{1}/_{10,000}$ in. is common practice.

Analysis of Heat Transfer Over a Small Cylinder in Icing Conditions on Mount Washington

By MYRON TRIBUS,[1] G. B. W. YOUNG,[2] and L. M. K. BOELTER[3]

The data reported by Schaefer (1)[4] for the heat required to maintain a heated rod (Calrod) dry and with a small trace of ice are compared to the heat requirements determined analytically. Satisfactory agreement (within the limits of the simplifying assumptions) was obtained for the first case only. Discrepancies between experimental and computed results are discussed. A new design for the heated cylinder is proposed as a possible means of measuring liquid-water content and drop size in flight through clouds.

Nomenclature

The following nomenclature is used in the paper:

$A = \pi D$ = area per unit span, sq ft
a = droplet radius, ft
$b = \dfrac{\beta_0 U W_l}{h_c}$
B = barometric pressure, in. Hg
C_1, C_2 = constants
C_{pw}, C_{pi} = specific heat of water, ice, Btu/(lb) (deg F)
D = cylinder diameter, ft
E_M = percentage catch for cylinder, dimensionless
h_c = unit thermal conductance for convection, Btu/(hr) (sq ft) (deg F)
h_r = equivalent unit conductance for radiation, Btu/(hr) (sq ft) (deg F)
h_m = unit conductance for mass transfer, lb/(hr) (sq ft)
H_s, H_∞ = absolute humidity at surface, in free stream, lb/lb
k = thermal conductivity of the Calrod material, Btu/(hr) (sq ft) (deg F/ft)
L = heat of vaporization (or of fusion) of water, Btu per lb
P_s, P_∞ = vapor pressure of saturated water at t_s, τ_∞, in. Hg
q_c, q_r, q_e, q_w, q_i, q_u = heat (or energy) exchange due to convection, radiation, evaporation, sensible heating of liquid water, sensible heating of liquid water and ice, Btu/(hr) (ft) span
R_w = rate of water catch, lb per hr, ft span
$\mathbf{R}$ = Reynolds modulus of droplet
$\mathbf{R} = \dfrac{2a\,\gamma_a U}{g\mu}$, dimensionless
s' = humid heat of air, Btu/(lb) (deg F)
T_w, T_s, T_f = absolute temperature of free stream, surface, average of free stream and surface, deg R
t_s = temperature of surface, deg F
t_∞ = temperature of free stream, deg F
U_∞ = free stream velocity, fps
W_l = liquid-water content of cloud surrounding cylinder, lb per cu ft (1 g per cu m = 62.4×10^{-6} lb per cu ft)
ψ = scale modulus, $\psi = \dfrac{9}{2}\dfrac{D\gamma_a}{a\gamma_s}$
γ_a = weight density of air, lb per cu ft
γ_s = weight density of droplet, lb per cu ft
σ = Stefan-Boltzmann constant, 0.173×10^{-8} Btu/(hr) (sq ft) (deg R^4)
ϵ = emissivity of Calrod, (= approx 1.0)
$(\,)_o$ = subscript o, designates property at stagnation point
β_o = limiting value of percentage catch over small area at stagnation region, dimensionless
μ = viscosity, lb-sec/sq ft

Introduction

The problem of the measurement of the characteristics of icing conditions has received a great deal of attention in the last few years. A summary of some of these investigations is contained in references (5) and (9). One of the objectives of the current research and development is the design of a simple device for measuring the liquid-water content and droplet sizes in an icing condition. It has also been the hope of some investigators that a simple device might be used as an interim "yardstick" of icing intensity; some type of comparing device which would indicate the relative icing intensity between two storms, for use until an adequate instrument to measure liquid-water content and drop size is available. One such comparing device is the G. E. Calrod unit for anti-icing studies. This unit was investigated experimentally by Schaefer (1) and is the object of analysis of this paper. This unit is shown in Fig. 1. The dimensions of the Calrod itself are 0.81 cm diam × 40.5 cm long.

With the Calrod unit mounted transverse to the wind, data were taken on the electrical power input regulated to produce surface conditions that were visually found to be: (*a*) without any moisture; (*b*) with a slight trace of moisture; (*c*) with a very wet surface; and (*d*) with a trace of ice during exposure to icing conditions. Reported with each set of power input data was the following information: Liquid-water content, effective particle size, air speed, air temperature, snow intensity, and rate of deposition on cylinders.

It is the purpose of this paper to explain how the power required for these conditions varies with the droplet size, liquid-water content of the cloud, air density, air velocity, air tempera-

---

[1] Research Engineer, Department of Engineering, University of California. Jun. ASME.

[2] Department of Engineering, University of California.

[3] Dean, College of Engineering, University of California, Los Angeles, Calif. Mem. ASME.

[4] Numbers in parentheses refer to the Bibliography at the end of the paper.

Contributed by the Heat Transfer Division and presented at an Aviation Meeting, University of California, Los Angeles, Calif., May 26–29, 1947, of The American Society of Mechanical Engineers.

ture, cylinder diameter, and thermal conductivity of the Calrod. An analysis is given taking into account these variables and then a comparison to the experimental results is made.

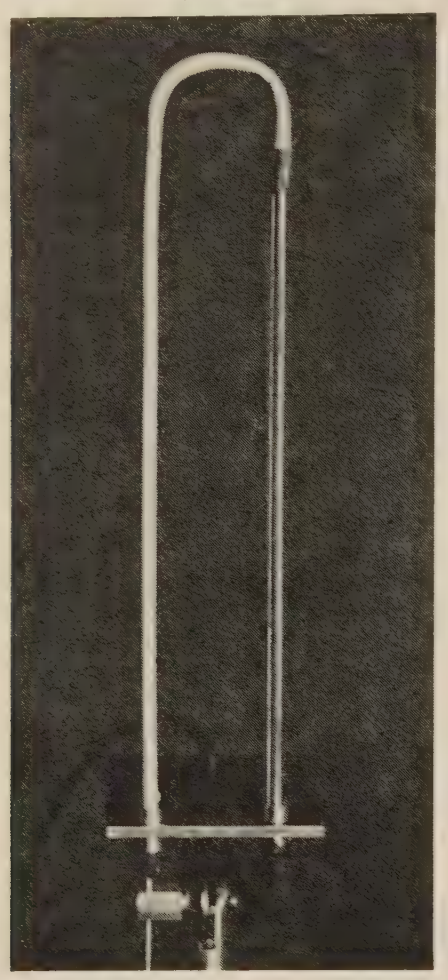

FIG. 1 GENERAL ELECTRIC CALROD UNIT FOR ANTI-ICING STUDIES (Mt. Washington Observatory, General Electric Research Laboratory.)

ANALYSIS

The power requirement for the two surface conditions (*a*) surface kept dry, and (*b*) surface with a trace of ice are analyzed and are predicted analytically herein.

When the surface is kept dry, a heated cylinder, exposed to an air stream containing small suspended drops of supercooled water, is subjected to four types of cooling: (*a*) cooling due to the forced convection by the air stream; (*b*) cooling due to the evaporation of the impinging moisture; (*c*) cooling due to radiation to the surrounding objects; and (*d*) cooling due to the sensible heating of the impinging moisture.

For the surface with a trace of ice, the heated cylinder may undergo one other form of heat transfer. Under the postulate that the surface is just at the freezing temperature, heat is added to the cylinder by the formation of ice from supercooled water. It was not included in the "dry-surface" analysis since any ice formed was considered as remelted.

The total convective heat transfer from a circular cylinder is

$$q_c = \pi D h_c (t_s - \tau_a) \quad [1]$$

where h_c, the average unit thermal conductance over a cylinder exposed to an airstream flowing at right angles to the cylinder axis (2, 3) is given by

$$h_c = 0.211\ T_f^{0.45} \frac{(U_\infty \gamma_\alpha)^{0.6}}{D^{0.4}} \quad [2]$$

For the case of a surface kept dry, the moisture impinging upon the surface must be evaporated as quickly as it arrives. The total energy lost by evaporation is therefore

$$q_e = R_w L. \quad [3]$$

The rate of water catch R_w, is a function of the liquid-water content of the cloud, the percentage catch (E_M), the cloud velocity, and the diameter of the cylinder. The relation is

$$R_w = 3600\ E_M W_l U_\infty D$$

The percentage catch E_M, is determined by the parameters

$$\mathsf{R} = \frac{2aU_\infty \gamma_a}{ug}$$

and

$$\psi = \frac{9}{2} \frac{D\gamma_a}{a\gamma_s}$$

These two parameters,[5] R and ψ, permit one to enter the charts of references (4, 5, 10) and determine the percentage catch defined by

$$E_M = \frac{R_w}{3600\ U_\infty D W_l} = f(\mathsf{R}, \psi) \quad [4]$$

The heat loss by radiation is of lesser magnitude. It is computed from the Stefan-Boltzmann equation

$$q_r = \pi D \sigma (T_s^4 - T_\infty^4) \epsilon \quad [5]$$

The heat loss due to sensible heating of the moisture is also of lesser magnitude

$$q_w = R_w C_{pw} (t_s - t_\infty) \quad [6]$$

The heat liberated by the formation of ice from supercooled water is

$$q_i = R_w [144 - C_{pw}(32 - t_\infty) - C_{pi}(32 - t_s)] \quad [7]$$

Equation [7] represents an enthalpy balance in going from supercooled water at t deg F to ice at t_s. It is independent of the path. (This equation is valid only for $t_s < 32$).

The power required to keep the surface of the heated cylinder dry is that which will balance the total heat loss

$$q = q_c + q_r + q_w + q_r \quad [8]$$

The values of q_c, q_r, and q_w as shown in Equations [1], [5], and [6], contain the unknown average surface temperature t_s, which is computed approximately in the manner given in Appendix 1.

In the case of the surface with a trace of ice, a heat balance is made at the stagnation region. The equation of balance is

$$q_0 = q_{c,0} + q_{e,0} + q_{r,0} - q_{i,0} \quad [9]$$

$$\frac{q_0}{A} = h_{c,0}(t_s - \tau_\infty) + \frac{h_{c,0}L}{s^t}(H_s - H_\infty) + h_r(t_s - t_\infty) - \beta_0 U_\infty W_l [144 - 32 + t_\infty - 0.5(32 - t_s)] \quad [10]$$

Now let

$$b = \frac{\beta_0 U_\infty (W_l)}{h_{c,0}} \quad [11]$$

[5] The parameters used in references (4, 5) are $K = \mathsf{R}/\psi$, and $\Phi = \mathsf{R}\psi$.

and

$$H_s - H_\infty = 0.62 \frac{P_s - P_\infty}{B} \quad [12]$$

and the radiation term be small, then

$$\frac{q_0}{Ah_{c,0}} = t_s - \tau_\infty + \frac{0.62(P_s - P_\infty)L}{s'B} - b(96 + t_\infty - 0.5t_s) \quad [13]$$

If the surface temperature t_s is above 32 F, Equation [13] is invalid and Equation [14] is used

$$\frac{q_0}{Ah_{c,0}} = (t_s - t_\infty) + \frac{0.62L(P_s - P_0)}{s'B} + b(t_s - t_\infty) \quad [14]$$

Appendix 2 gives the variation of $\frac{q}{Ah_{c,0}}$ versus t_s for varying values of b, above and below freezing.

Discussion

Reference (1) gives data on the heat required to maintain a heated cylinder (Calrod) dry, moist, wet, and with a trace of ice. The first two data should bracket the computed value for the heat required to just evaporate the moisture as rapidly as it impinges. Table 1 compares these data to the computed values. In Table 1 the values of t_s, computed as shown in Appendix 1, were used as the average temperature of the cylinder surface.

Of the 22 runs under consideration, 13 sets of data show acceptable agreement between the computed and measured data. Of the remaining 9 sets, one, run No. 17, obviously is in error since the quoted heat requirements appear to be reversed.

The fact that the snow catch was not included in the computation makes it difficult to understand why the agreement noted was attained. The runs in which agreement was not obtained showed no consistent variation with snow conditions as estimated.

In addition to the data given in the Schaefer report (1), 96 more sets of data were sent by Schaefer to the authors of this paper and were analyzed as noted herein. Of the 96 runs, all but approximately 10 per cent of the observations were within 30 per cent of the calculated heat requirements. Most were within 15 per cent.

Conclusion

A simple meter for measuring the liquid water content of a cloud through which an airplane is flying can be designed, based upon the heat required to run the instrument "dry." The instrument should be designed as shown in Fig. 2 to eliminate the necessity for making some of the assumptions used in the foregoing analysis. The copper tube will assure a uniform circumferential temperature and the thermocouple will permit calibration in dry and wet air. The heat required should follow the equation

$$q = \pi D\, 0.211\, T_f^{0.43} \frac{(U_\infty \gamma_a)^{0.6}}{D^{0.4}} [t_s - t_\infty - 7.1 \times 10^{-5} U_\infty^2] + E_M D U_\infty (W_l) L \quad [15]$$

The equation can be rewritten as

$$q = C_1 (U_\infty \gamma_a)^{0.6} [t_s - t_\infty - 7.1 \times 10^{-5} U_\infty^2] + C_2 U_\infty E_M W_l \quad [16]$$

where the constants C_1 and C_2 can be measured or computed. Having obtained C_1 and C_2 over the desired range of flight speeds and altitudes for several sized cylinders, it is necessary to fly into a cloud and measure simultaneously the cylinder temperatures, heat input, air temperature, density, and velocity. From the calibration curves of each cylinder the terms $(E_M \times W_l)$ for each cylinder can be rapidly computed. If these terms $(E_M \times W_l)$ be plotted against cylinder radius on log-log co-ordinate paper and superimposed on curves 23*a* to 23*f* of reference (1), the separate values of (E_M) and (W_l) can be computed by noting the vertical and horizontal displacement required to match the data to the curves. This technique of matching these points to the data of reference (1) has been in use with ice-coated rotating cylinders for 3 years and has given excellent results (11).

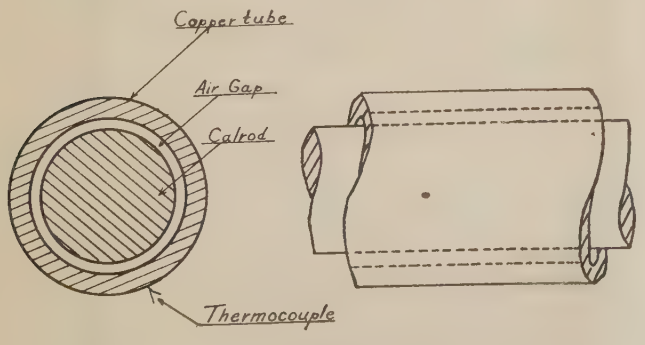

Fig. 2

Acknowledgment

The authors wish to acknowledge the kindness of Mr. Vincent Schaefer, of the General Electric Company, for forwarding complete sets of data and advance copies of his report. Also, they desire to pay sincere tribute to Sergeant Victor F. Clarke of the Mount Washington Observatory, who is responsible for the gathering of these data and without whose enthusiastic assistance it is believed these correlations could not have been obtained. This work was originally carried out with the financial assistance of the Equipment Laboratory, AAF Air Materiel Command, Wright Field, Ohio.

BIBLIOGRAPHY

1 "Heat Requirements for Instruments and Airfoils During Icing Storms on Mt. Washington," by Vincent J. Schaefer, General Electric Company, Research Laboratory Report, April, 1946.

2 "An Investigation of Aircraft Heaters—XVIII—A Design Manual for Exhaust Gas and Air Heat Exchangers," by L. M. K. Boelter, R. C. Martinelli, F. E. Romie, and E. H. Morrin, NACA ARR, August, 1945.

3 "Heat Transmission," by W. H. McAdams, McGraw-Hill Book Company, Inc., New York, N. Y., second edition, 1942, p. 222.

4 "A Mathematical Investigation of Water Droplet Trajectories," by I. Langmuir and K. Blodgett, AAF Technical Report 5418, February, 1946.

5 "Report on the Development and Application of Heated Wings," by M. Tribus and J. R. Tessman, Add. I, AAF Technical Report 4972, Add. I, January, 1946.

6 "Heat Transfer Over the Circumference of a Heated Cylinder in Transverse Flow," by E. Schmidt and K. Wenner, NACA TM No. 1050, 1943.

7 "General Electric Standards," General Electric Company, Schenectady, N. Y.

8 "Numerical Solution of the Boundary Layer Problem for the Potential Equation by Means of Punched Cards," by M. Kormes, *Review of Scientific Instruments*, vol. 14, August, 1943, pp. 248–250.

9 "Instruments for Measuring Atmospheric Factors Related to the Formation on Airplanes," by B. Vonnegut, R. M. Cunningham, and R. E. Katz, Massachusetts Institute of Technology, Department of Meteorology, April, 1946.

10 "Final Report—Icing Studies," by L. M. K. Boelter, Contract W-33-038 ac-13489 (15396), University of California, Los Angeles, Calif., August, 1946.

11 Mount Washington Observatory Bulletins, issued monthly, Mount Washington, Gorham, N. H.

TABLE 1 COMPARISON OF EXPERIMENTS AND COMPUTED DATA

	MEASURED						COMPUTED										
												Heat Loss / Frontal Area, Btu/hr ft^2					
Run	Drop Diam. Micron	Liq.Wat. Content g/m^3	Air Temp °F	Air Speed mph	Heat Loss Dry	Heat Loss Moist	E_m	β_o	$h_{c,o}$	t_s °F	$h_{c,av}$	Convect.	Evap'n	Radiant	Sensible	Total Watts/cm^2	COMMENT
1	5.8	0.29	7	41	1.7	1.3	0.14	0.70	50.0	60	27.4	4570	577	167	28	1.68	Light snow
2	6.6	0.38	7	64	2.2	1.9	0.30	0.48	62.2	62	36.1	6350	2450	176	137	2.86	Very light snow
3	6.9	0.31	-2	62	2.8	2.2	0.33	0.51	61.2	57	35.6	6600	2170	185	121	2.91	Light snow
4	7.6	0.37	-2	56	3.1	2.8	0.36	0.53	58.2	63	33.1	6760	2590	204	166	3.05	Very light snow
5	7.6	0.37	-6	59	3.3	3.0	0.36	0.55	60.0	64	34.4	7570	2690	220	178	3.34	Very light snow
6	8.2	0.38	3	70	3.7	3.2	0.44	0.60	65.1	70	38.0	8010	4020	211	255	3.92	Trace of snow
7	8.2	0.39	8.5	60	3.2	2.6	0.41	0.57	60.2	66	34.8	6290	3340	180	182	3.14	Light to moderate snow
8	8.6	0.28	-6	77	3.3	2.8	0.47	0.62	68.5	64	40.4	9050	3520	220	246	4.10	Light snow
9	8.9	0.25	-0	64	3.1	2.3	0.44	0.60	62.2	56	36.2	6360	2450	176	130	2.87	Heavy snow
10	10.2	0.38	3	64	4.0	3.4	0.52	0.66	62.2	71	36.2	7740	4350	214	280	3.94	Trace of snow
11	10.2	0.44	1	67	4.6	3.9	0.53	0.66	63.6	76	37.1	8750	5390	236	383	4.64	Light snow
12	12.7	0.13	0	56	4.7	4.1	0.60	0.72	58.2	43	33.4	4620	1520	284	67	2.03	Moderate snow
13	8.3	0.32	3	80	5.5	5.2	0.47	0.62	69.9	68	41.3	8560	4180	208	280	4.18	Very light snow
14	9.0	0.50	14	61	5.4	5.0	0.45	0.60	61.1	76	35.2	6960	4770	198	290	3.85	Heavy snow
15	9.6	0.42	7	76	7.5	4.3	0.53	0.66	68.0	77	40.1	8810	5880	219	390	4.80	Very light snow
16	11.7	0.62	12	80	7.0	6.9	0.62	0.74	69.8	93	41.3	10500	10700	279	820	7.00	Light to moderate snow
17	15.0	0.43	1	88	5.8	6.5	0.73	0.83	73.1	89	43.6	11900	9700	273	850	7.14	No snow
18	17.1	0.75	12	57	5.2	4.5	0.72	0.82	58.8	98	33.7	9000	10700	267	910	6.55	Light snow
19	16.3	0.65	30	62	5.8	5.1	0.71	0.81	61.2	94	35.6	7160	9940	201	572	5.60	Light snow
20	17.7	1.12	25	48	5.6	5.1	0.71	0.81	54.0	109	30.4	7650	13200	251	1050	6.95	No snow
21	5.7	0.12	28	71	0.7	0.4	0.24	0.43	65.8	43	38.6	2170	710	57	30	0.93	No snow
22	6.8	0.10	-18	75	3.6	2.1	0.26	0.77	67.5	40	39.8	7250	677	182	37	2.55	Light snow
					Watt/Cm^2								Btu/hr, ft^2			$\frac{\text{Watt}}{\text{cm}^2}$	

12 "Principles of Chemical Engineering," by W. H. Walker, W. K. Lewis, W. H. McAdams, and E. R. Gilliland, third edition, McGraw-Hill Book Company, Inc., New York, N. Y., 1937.
"Modern Developments in Fluid Dynamics," by S. Goldstein, Clarendon Press, Oxford, England; Oxford University Press, New York, N. Y., 1938.

Appendix 1

If the cylinder is heated so that its surface temperature is just sufficient to evaporate the moisture as rapidly as it impinges, it is possible to calculate this minimum surface temperature from the analogy between heat and mass transfer. The greatest evaporation requirement occurs at the stagnation line of the cylinder. If attention is confined to the area in this region, the following mass balance can be applied:

Rate of water impingement = evaporation rate or

$$\beta_0 U(W_l) = h_{m,0}(H_s - H_\infty) \quad [17]$$

The mass-transfer conductance can be calculated from the analogy by (12)

$$h_{m,0} = \frac{h_{c,0}}{s'} \quad [18]$$

The local unit thermal conductance at the stagnation point is computed from the data of references (2) or (6)

$$h_{c,0} = 0.194\ T_f^{0.49} \left(\frac{U_\infty \gamma_a}{D}\right)^{0.5} \quad [19]$$

The percentage catch β_0, for the stagnation area is computed from the trajectory data, references (3, 4)

$$\beta_0 = F_2(R, \psi)$$

The value of t_s obtained in this manner applies only to the stagnation region. Because of the low thermal conductivity of the Calrod material, $k = 1.5$ Btu/(hr) (sq ft) (deg F/ft), reference (7), the surface temperature will not be uniform. As a matter of fact, the stagnation region is a "cold spot." Thus if the convective losses are computed on the basis of a temperature derived from Equations [17, 18, 19, 20], the results will be low. For a detailed analysis of the effect of variation of t_s about the Calrod see reference (10), where a solution to the heat-transfer equations for the Calrod were carried out using IBM punched-card equipment in a manner similar to that described in reference (8).

Appendix 2

For typical Mount Washington conditions, $t_\infty = 15$ F, $B = 620$ mm Hg, $s' = 0.24$ Btu/(11) (deg F), and $L = 1056$ for water (above 32 F), and 1200 for ice (below 32 F), Equations [13] and [14] were solved. The curve in Fig. 3 presents the values of $\frac{q}{Ah_{c,0}}$ versus t_s for varying values of b, above and below freezing.

For example, if $h_{c,0} = 69.8$ Btu/(hr)(sq ft)(deg F), $\beta_0 = 0.74$, $(W_l) = 0.62 \times 62.4 \times 10^{-6} = 3.86 \times 10^{-5}$ lb per cu ft, $U_\infty = 89 \times 5200 = 422{,}000$ ft per hr, then

$$b = \frac{\beta_0 U_\infty W_l}{h_{c,0}} = 0.173 \text{ (lb) (deg F)/Btu}$$

From Fig. 3 the possible variations in heat-flow rate at the

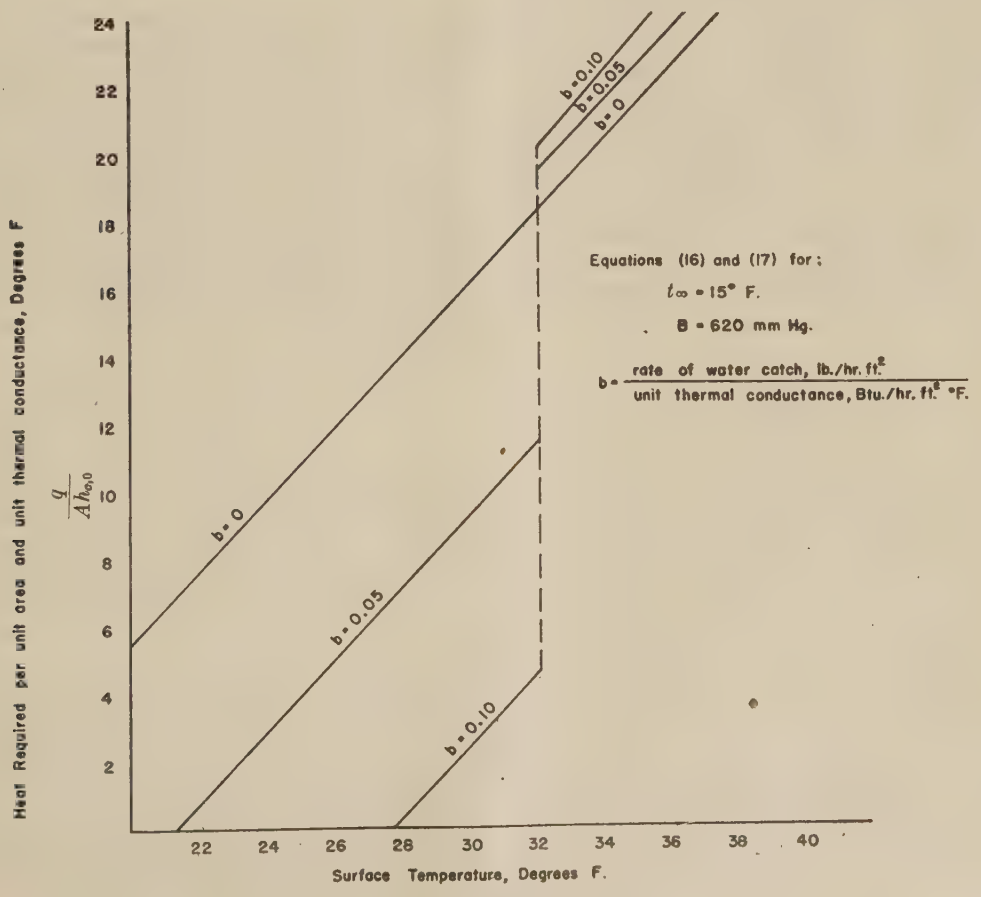

FIG. 3

stagnation line to produce a 32 F surface temperature are almost 5 to 1. Proceeding along the surface away from the stagnation line, the values of b decrease to zero at 72 F. Thus it is shown that for the region of the Calrod ± 72 deg F from the stagnation region, the heat required is indeterminate by a fairly large percentage.

Discussion

R. N. Noyes.[6] The authors present a method for determining the liquid water content W_l of an airstream based on an analysis of the heat-transfer processes which take place when a heated rod is placed in an airstream which contains liquid water droplets at temperatures below the freezing point. They conclude, by comparing their results with test data, that for the majority of cases they can predict within 15 per cent the heat input to the rod that would be necessary to keep its surface moisture-free.

A method of determining the W_l is proposed which consists of determining the heat loss due to evaporation $E_M D U_\infty$, by subtracting the computed heat loss due to convection from the measured total heat required to keep the rod moisture free. Table 1 of the paper shows that the heat loss due to convection may be as much as 10 times as great as the heat loss due to evaporation; for the majority of cases, it was at least 2 times as great. Thus an error in the determination of the convective heat-transfer coefficient will be appreciably magnified in computing W_l.

An additional error arises in the determination of the free stream static temperature t_∞. This temperature must be inferred from a wet temperature reading; at present a considerable uncertainty is involved in this measurement. For example, suppose t_∞ were in error by 5 deg, the correct difference in $(T_s - t_\infty)$ were 50 deg, and the heat loss due to convection was 3 times as great as the heat loss by evaporation. Then an error of 30 per cent would arise in the determination of W_l. Reduction of convective heat losses by reducing T_s will not reduce the error in W_l. Suppose, for the same heat input, heat-transfer coefficient and same error in τ_∞ as in the previous example, the convective heat loss were to be made equal to the heat loss by evaporation. The temperature difference $(T_s - \tau_\infty)$ would now be approximately 17 deg, resulting in an error in both convective and evaporating heat losses of $^5/_{17}$ or approximately 30 per cent.

[6] Aeronautical Research Scientist, Flight Propulsion Research Laboratory, National Advisory Committee for Aeronautics, Cleveland, Ohio.

Authors' Closure

Mr. Noyes suggests that our proposed icing meter may not yield accurate data on liquid water content because of difficulties in estimating the heat loss by forced convection. These errors, according to Noyes, should occur mainly due to errors in determining the free stream temperature. Mr. Noyes points out that the data of Table 1 show that the evaporative loss is sometimes as low as 10 per cent of the total energy loss and therefore a small error in computed convective loss should lead to large errors in water content.

These criticisms are very much to the point, and it must be admitted that at low liquid water contents, the accuracy of the proposed meter is least. However, the use of such a device may not be as bad as one would infer from Mr. Noyes's comments. For one thing the Calrod data on Mount Washington is for a surface run "dry." If the surface were permitted to run moist on the front half, the convective losses would decrease, while the evaporative loss would be maintained. Also, at higher speeds the ratio of evaporative to convective energy losses becomes more favorable, as shown in Table 2, herewith, which is considered typical for aircraft speeds (surface run dry).

TABLE 2

Cylinder diameter, in.	1/4	1/2	1	2	4
Loss by convection, Btu/(hr) (ft)	320	550	905	1510	2230
Loss by evaporation, Btu/(hr) (ft)	462	835	1262	1985	2180

Altitude: 10,000 ft — True airspeed: 200 mph — Droplet diam: 15 micron
Air temperature: 20 F — Liquid water: 0.4 g/m³

It is believed that the error in determining free air temperature should be less than 5 deg F. At 200 mph the maximum error is 7.2 deg F if one does not correct the indicated temperature for aerodynamic heating and wet-bulb depression. Applying these corrections, the uncertainty should certainly be less than 5 deg F. Mr. Carr B. Neel, in presenting a recent paper,[7] stated that the NACA at Moffett Field had satisfactorily used this technique on a P-38 at very high speeds in cloud while a slowly moving blimp took simultaneous measurements of the cloud temperature.

[7] "The Calculation of the Heat Required for Wing Thermal Ice Prevention in Specified Icing Conditions," by C. B. Neel, presented before SAE, Los Angeles, Calif., Oct. 2, 1947.

Limitations and Mathematical Basis for Predicting Aircraft Icing Characteristics From Scale-Model Studies

By MYRON TRIBUS,[1] G. B. W. YOUNG,[2] AND L. M. K. BOELTER[3]

The equations governing the motions of a water droplet impinging on an aerodynamic shape are discussed in detail and lead to two dimensionless moduli, one the Reynolds modulus of the droplet and the other a scale modulus. The data of Langmuir and Blodgett are shown replotted according to these parameters. The application of these equations to the problem of model studies atop Mount Washington indicates that scale models should be 3 to 4 times larger than the prototype if dimensional similarity is to be retained. The application to wind-tunnel studies indicates the importance of having the spray apparatus sufficiently far upstream and also of having the model well back in the throat of the tunnel, downstream from the venturi inlet.

Nomenclature

The following nomenclature is used in the paper:

a = drop radius, ft
C = a characteristic length of body, ft
C_D = drag coefficient, dimensionless
E_M = percentage catch, dimensionless
f_1, f_2, f_3 = functions defined by Equation [1]
F = function defined by Equation [6]
g = gravitational constant, ft/(sec²)
$\frac{g_1, g_2, g_3}{g_1^v, g_2^v, g_3^v}$ = functions defined by respective equations
G, G' = functions defined by respective equations
P = velocity vector difference between air and droplet, fps
S = function defined by respective equation
t = time, sec
U = free air stream velocity, fps
u_a, v_a, w_a = components of air velocity, fps
u_d, v_d, w_d = components of droplet velocity, fps
x, y, z = Cartesian co-ordinates, ft
x_0, y_0, z_0 = initial position of droplet trajectories, ft
β_0 = percentage catch at stagnation point, dimensionless
γ_a = mass density of air, lb per cu ft
γ_d = mass density of droplet, lb per cu ft
μ = absolute viscosity of air, lb-sec/sq ft

Dimensionless ratios·

$\mathbf{R}_p$ = Reynolds modulus, defined by $\frac{2a\,P\,\gamma_a}{\mu g}$

$\mathbf{R}_U$ = Reynolds modulus, defined by $\frac{2a\,U\,\gamma_a}{\mu g}$

ψ = scale modulus, defined by $\frac{9C\,\gamma_a}{a\,\gamma_d}$

K = modulus, defined by $\mathbf{R}_{U/\psi}$
ϕ = modulus, defined by $\mathbf{R}_{U\cdot\psi}$

Introduction

It has become increasingly apparent that the trajectories of the droplets about a streamlined body in an icing condition play a large part in determining the heat requirements for the anti-icing of that body. It has been demonstrated that the trajectories of droplets ahead of cylinders (1, 2, 3),[4] spheres (4), and ribbons (4), can be computed accurately by use of solutions to certain differential equations. For objects of a more complex shape, the solutions become more and more tedious to obtain, even using differential analyzers and other computing devices. The solutions to these differential equations, however, can be obtained experimentally by the use of models, and application of the principles of dimensional similarity. Thus it is possible to expose a scale model of an airplane to an icing condition, measuring the icing rates and the meteorological conditions, and then predict the icing characteristics of the prototype.

Mathematical Analysis

The field of flow about any streamlined body, considering incompressible potential flow, is a function of the shape of the body and its orientation in the air stream, that is

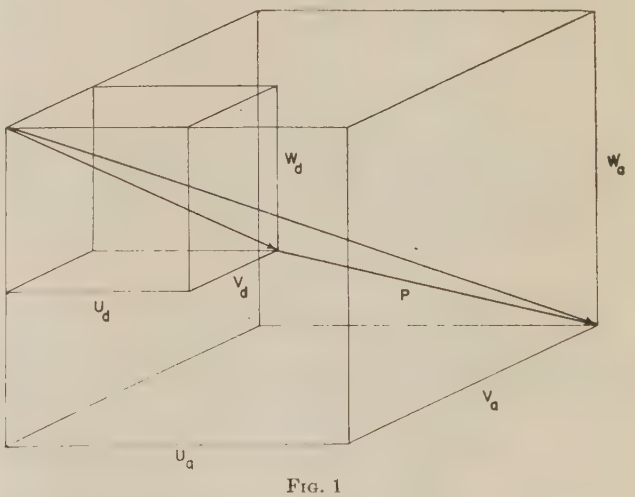

Fig. 1

[1] Research Engineer, University of California. Jun. ASME.
[2] Department of Engineering, University of California, Jun. ASME.
[3] Dean, Department of Engineering, University of California, Los Angeles, Calif. Mem. ASME.
Contributed by the Heat Transfer Division and presented at the Aviation Meeting, Los Angeles, Calif., May 26–29, 1947, of The American Society of Mechanical Engineers.
Note: Statements and opinions advanced in papers are to be understood as individual expressions of their authors and not those of the Society.

[4] Numbers in parentheses refer to the Bibliography at the end of the paper.

$$\left.\begin{aligned}\frac{u_a}{U} &= f_1\left(\frac{x}{C}, \frac{y}{C}, \frac{z}{C}\right)\\ \frac{v_a}{U} &= f_2\left(\frac{x}{C}, \frac{y}{C}, \frac{z}{C}\right)\\ \frac{w_a}{U} &= f_3\left(\frac{x}{C}, \frac{y}{C}, \frac{z}{C}\right)\end{aligned}\right\} \quad \ldots\ldots\ldots\ldots [1]$$

Spherical water droplets in this velocity-field region will not follow the air streamlines, but due to their inertia will travel trajectories somewhat less curved. At any point, then, the velocity vectors of the air and droplet will differ by a vector P, shown in Fig. 1.

The components of the drag-resistance force on the droplet are

$$\left.\begin{aligned}&-C_D\frac{1}{2}\pi a^2\,\gamma_a P(u_a - u_d)\\ &-C_D\frac{1}{2}\pi a^2\,\gamma_a P(v_a - v_d)\\ &-C_D\frac{1}{2}\pi a^2\,\gamma_a P(w_a - w_d)\end{aligned}\right\} \quad \ldots\ldots\ldots\ldots [2]$$

The Newtonian equations of motion of the drop are

$$\left.\begin{aligned}-\frac{4}{3}\pi a^3\,\gamma_d\frac{du_d}{dt} &= -\frac{4}{3}\pi a^3\,\gamma_d u_d\frac{du_d}{dx}\\ -\frac{4}{3}\pi a^3\,\gamma_d\frac{dv_d}{dt} &= -\frac{4}{3}\pi a^3\,\gamma_d v_d\frac{dv_d}{dy}\\ -\frac{4}{3}\pi a^3\,\gamma_d\frac{dw_d}{dt} &= -\frac{4}{3}\pi a^3\,\gamma_d w_d\frac{dw_d}{dz}\end{aligned}\right\} \quad \ldots\ldots [3]$$

Equating these forces and transposing to form dimensionless ratios

$$d\left(\frac{x}{C}\right) = \frac{1}{\psi}\frac{24}{C_D}\frac{U}{P}\frac{u_d}{u_a - u_d}\,d\left(\frac{u_d}{U}\right) \quad \ldots\ldots\ldots [4a]$$

$$d\left(\frac{y}{C}\right) = \frac{1}{\psi}\frac{24}{C_D}\frac{U}{P}\frac{v_d}{v_a - v_d}\,d\left(\frac{v_d}{U}\right) \quad \ldots\ldots\ldots [4b]$$

$$d\left(\frac{z}{C}\right) = \frac{1}{\psi}\frac{24}{C_D}\frac{U}{P}\frac{w_d}{w_a - w_d}\,d\left(\frac{w_d}{U}\right) \quad \ldots\ldots\ldots [4c]$$

where $\psi = (9C\gamma_a)/(a\gamma_d)$, a dimensionless modulus, hereinafter referred to as the "scale modulus."

The relation between the vector P and the components of the air and droplet velocities is

$$\left(\frac{P}{U}\right)^2 = \left(\frac{u_a}{U} - \frac{u_d}{U}\right)^2 + \left(\frac{v_a}{U} - \frac{v_d}{U}\right)^2 + \left(\frac{w_a}{U} - \frac{w_d}{U}\right)^2 \ldots [5]$$

The variable drag coefficient C_D is a function of the local Reynolds modulus ($\mathbf{R}_p$) of the droplet, that is

$$C_D = F(\mathbf{R}_p) = F\left(\frac{2a\,\gamma_a P}{\mu g}\right) = F\left(\frac{2a\,\gamma_a U}{\mu g}\cdot\frac{U}{P}\right) \ldots [6]$$

By definition

$$\mathbf{R}_U = \frac{2a\,\gamma_a U}{g\mu}$$

then

$$C_D = F\left(\mathbf{R}_U\cdot\frac{P}{U}\right) \quad \ldots\ldots\ldots\ldots [7]$$

The Reynolds modulus, $\mathbf{R}_U$, is that which the droplet would have if it traveled in still air at the velocity, U.

The simultaneous integration of Equations [4a, b, c], after substituting for the values of P/U, u_a/U, v_a/U, w_a/U, and C_D from Equations [5], [1], and [7], yields as a solution an equation (Equation [9]) which represents a family of lines that are the trajectories of the droplets starting at some position x_0, y_0, and z_0 and having the initial velocity components $u_d = U$, $v_d = 0$, and $w_d = 0$.

$$\frac{x - x_0}{C} = \frac{1}{\psi}\int_1^{\frac{u_d}{U}}\frac{24}{F\left(\mathbf{R}_U\cdot\frac{P}{U}\right)}\frac{U}{P}\frac{u_d}{(u_a - u_d)}\,d\left(\frac{u_d}{U}\right)$$

$$\frac{y - y_0}{C} = \frac{1}{\psi}\int_0^{\frac{v_d}{U}}\frac{24}{F\left(\mathbf{R}_U\cdot\frac{P}{U}\right)}\frac{U}{P}\frac{v_d}{(v_a - v_d)}\,d\left(\frac{v_d}{U}\right) \ldots [8]$$

$$\frac{z - z_0}{C} = \frac{1}{\psi}\int_0^{\frac{w_d}{U}}\frac{24}{F\left(\mathbf{R}_U\cdot\frac{P}{U}\right)}\frac{U}{P}\frac{w_d}{(w_a - w_d)}\,d\left(\frac{w_d}{U}\right)$$

or

$$\left.\begin{aligned}\frac{x}{C} &= g_1\left(\psi, \mathbf{R}_U, \frac{x_0}{C}, \frac{y_0}{C}, \frac{z_0}{C}, f_1, f_2, f_3, \frac{P}{U}\right)\\ \frac{y}{C} &= g_2\left(\psi, \mathbf{R}_U, \frac{x_0}{C}, \frac{y_0}{C}, \frac{z_0}{C}, f_1, f_2, f_3, \frac{P}{U}\right)\\ \frac{z}{C} &= g_3\left(\psi, \mathbf{R}_U, \frac{x_0}{C}, \frac{y_0}{C}, \frac{z_0}{C}, f_1, f_2, f_3, \frac{P}{U}\right)\end{aligned}\right\} \quad \ldots [9]$$

In order to find the relationship between the position (x/C, y/C, z/C) of any droplet in its trajectory and its corresponding initial position (y_0/C, z_0/C), Equation [9] is transposed to give

$$\left.\begin{aligned}\frac{x_0}{C} &= g_1'\left(\psi, \mathbf{R}_U, \frac{x}{C}, \frac{y}{C}, \frac{z}{C}, f_1, f_2, f_3, \frac{P}{U}\right)\\ \frac{y_0}{C} &= g_2'\left(\psi, \mathbf{R}_U, \frac{x}{C}, \frac{y}{C}, \frac{z}{C}, f_1, f_2, f_3, \frac{P}{U}\right)\\ \frac{z_0}{C} &= g_3'\left(\psi, \mathbf{R}_U, \frac{x}{C}, \frac{y}{C}, \frac{z}{C}, f_1, f_2, f_3, \frac{P}{U}\right)\end{aligned}\right\} \quad \ldots [10]$$

Eliminating P/U, Equation [10] becomes

$$\left.\begin{aligned}\frac{y_0}{C} &= g_2''\left(\psi, \mathbf{R}_U, \frac{x}{C}, \frac{y}{C}, \frac{z}{C}, f_1, f_2, f_3, \frac{x_0}{C}\right)\\ \frac{z_0}{C} &= g_3''\left(\psi, \mathbf{R}_U, \frac{x}{C}, \frac{y}{C}, \frac{z}{C}, f_1, f_2, f_3, \frac{x_0}{C}\right)\end{aligned}\right\} \quad \ldots [11]$$

If x_0/C is chosen far enough ahead in the free air stream, the values of y_0/C and z_0/C are independent of x_0/C; then

$$\left.\begin{aligned}\frac{y_0}{C} &= g_2'''\left(\psi, \mathbf{R}_U, \frac{x}{C}, \frac{y}{C}, \frac{z}{C}, f_1, f_2, f_3\right)\\ \frac{z_0}{C} &= g_3'''\left(\psi, \mathbf{R}_U, \frac{x}{C}, \frac{y}{C}, \frac{z}{C}, f_1, f_2, f_3\right)\end{aligned}\right\} \quad \ldots [12]$$

For any one streamlined shape and orientation of the body, the functions f_1, f_2, and f_3 are nonvariant and Equation [12] becomes

$$\left.\begin{aligned}\frac{y_0}{C} &= g_2^{iv}\left(\psi, \mathbf{R}_U, \frac{x}{C}, \frac{y}{C}, \frac{z}{C}\right)\\ \frac{z_0}{C} &= g_3^{iv}\left(\psi, \mathbf{R}_U, \frac{x}{C}, \frac{y}{C}, \frac{z}{C}\right)\end{aligned}\right\} \quad \ldots\ldots [13]$$

Given some surface, $S(x/C, y/C, z/C) = 0$, on the streamlined body upon which the problem of anti-icing is centered, the values of x/C, y/C, and z/C in Equation [13] are fixed and

$$\left.\begin{aligned}\frac{y_0}{C} &= g_2^{v}(\mathbf{R}_U, \psi)\\ \frac{z_0}{C} &= g_3^{v}(\mathbf{R}_U, \psi)\end{aligned}\right\} \quad \ldots\ldots [14]$$

Equation [14] states that the initial values of y_0/C and z_0/C for a droplet striking the model at the position x/C, y/C, and z/C depend only on the moduli ψ and $\mathbf{R}_U$. The limitations are (*a*) the position x_0/C of the water droplet is far enough ahead in the air stream so that it does not affect the values of y_0/C and z_0/C, and (*b*) the streamline shape and the orientation of the model are constant. Thus the limiting trajectories (those which just graze the model), the percentage of the droplets ahead of the model and located inside the frontal area of the surface under investigation and the velocity of impact are functions of the moduli ψ and $\mathbf{R}_U$ only under the same limitations. For example the percentage catch E_M, is

$$E_M = \frac{\displaystyle\int\int_{S\left(\frac{x}{C}\frac{y}{C}\frac{z}{C}\right)} d\left(\frac{y_0}{C}\right) d\left(\frac{z_0}{Q}\right)}{\displaystyle\int\int_{S\left(\frac{x}{C}\frac{y}{C}\frac{z}{C}\right)} d\left(\frac{y}{C}\right) d\left(\frac{z}{C}\right)} = G(\mathbf{R}_U, \psi) \quad \ldots\ldots [15]$$

and

$$\beta_0 = \lim E_M = G'(\mathbf{R}_U, \psi) \quad \ldots\ldots [16]$$

as

$$\frac{y}{C}, \frac{x}{C} \rightarrow 0$$

Returning to Equation [8], the term

$$\frac{24}{F'\left(\mathbf{R}_U \cdot \frac{P}{U}\right)} \frac{U}{P}$$

under the integral sign can be rewritten, if Stokes's law (valid for $\mathbf{R}_U \leq 1$) holds, as follows

$$\frac{24}{F\left(\mathbf{R}_U \cdot \frac{P}{U}\right)} \frac{U}{P} = \frac{24}{C_D} \frac{\mathbf{R}_U}{\mathbf{R}_P} = \mathbf{R}_U \quad \ldots\ldots [17]$$

This modulus is not a function of the droplet velocity and can be brought outside of the integral sign. Likewise, Equations [13] and [14] can be reduced to a one-parameter family of curves for $\mathbf{R}_U \leq 1$

$$\left.\begin{aligned}\frac{y_0}{C} &= g_2^{iv}\left(\frac{\mathbf{R}_U}{\psi}, \frac{x}{C}, \frac{y}{C}, \frac{z}{C}\right)\\ \frac{y_0}{C} &= g_3^{iv}\left(\frac{\mathbf{R}_U}{\psi}, \frac{x}{C}, \frac{y}{C}, \frac{z}{C}\right)\end{aligned}\right\} \quad \ldots\ldots [18]$$

and

$$\left.\begin{aligned}\frac{y_0}{C} &= g_2^{v}\left(\frac{\mathbf{R}_U}{\psi}\right)\\ \frac{z_0}{C} &= g_3^{v}\left(\frac{\mathbf{R}_U}{\psi}\right)\end{aligned}\right\} \quad \ldots\ldots [19]$$

References (1, 2, 3, 4, 5, and 6) used the ratio $\mathbf{R}_U/\psi$, represented by the symbol K and reference (3) introduced another ratio $\phi = \mathbf{R}_U\psi$ to correlate the quantities E_M, β_0, and θ_M about cylinders, spheres, and ribbons (θ_M is the angle measured from the stagnation line to the point beyond which no droplet impingement occurs). For most important icing cases, however, the Reynolds modulus is well beyond the range of Stokes's law ($\mathbf{R}_U \leq 1$) and the trajectories, likewise the quantities, E_M, β_0, and θ_M, depend fundamentally upon the two parameters $\mathbf{R}_U$ and ψ. Thus the data for cylinders of reference (3) have been replotted in Figs. 2 to 7, inclusive. These graphs, like those given in reference (3), are for uniform drop-size distribution. For other forms of droplet distribution, the averaging method given in references (1, 2) or (3) is to be used.

The most startling observation, resulting from the replotted curves, is from Fig. 2. This figure shows that for any droplet size the maximum or asymptotic value of the percentage catch E_M, is not equal to 1 as the velocity or $\mathbf{R}_U$ increases. Large cylinders, even at extremely high velocities, do not yield high values of E_M.

Applications to Model Studies

It is evident from a study of Figs. 2 to 7 that the trajectories are equally sensitive functions of $\mathbf{R}_U$ and ψ. Thus in any model study it can be said that if similarity is to be preserved, the values for $\mathbf{R}_U$ and ψ must be the same for both model and prototype.

Assume, for example, it is desired to make tests in a wind tunnel where the droplets are oversized by a factor of 10. In order to preserve the value of ψ, it will be necessary to increase the model size tenfold. Meanwhile, to preserve the value of $\mathbf{R}_U$, the velocity must be decreased tenfold.

Again, assume it is desired to make model tests atop Mount Washington, Gorham, N. H. Here the droplet sizes are of the same size as in the anticipated icing conditions, but the velocities are only of the order of one-third to one-fourth modern flying speeds. If the usual size drops are used, ψ will have its correct value when a full-scale model is used. However, $\mathbf{R}_U$ will be too small by $^1/_3$ or $^1/_4$. If the large drops, say, 3 to 4 times normal are used, $\mathbf{R}_U$ will be correct, but now a model of 3 to 4 times the size of the prototype should be used to give ψ its proper value. This is no handicap in testing such devices as helicopters or small wings, but may render the testing of large aircraft components impractical.

For large aircraft components, data from both wind-tunnel tests and tests atop Mount Washington can be reduced simultaneously to yield valuable information via sensible extrapolation. For example, a small model is tested in a wind tunnel over a wide range of $\mathbf{R}_U$ at some value of ψ, and a large model is tested atop Mount Washington, over a limited range of $\mathbf{R}_U$ at the working value of ψ. By comparing the two curves, the information obtained with the large model may be extrapolated, but with caution, beyond the experimental range of $\mathbf{R}_U$.

Returning for a moment to Equation [8], it will be noted that the limits of integration therein imply that the droplet start at some position (x_0/C, y_0/C, z_0/C) where their velocity components (u_d/U, v_d/U, w_d/U) are (1, 0, 0), that is, there is no relative motion between the drops and the air. However, in a wind tunnel

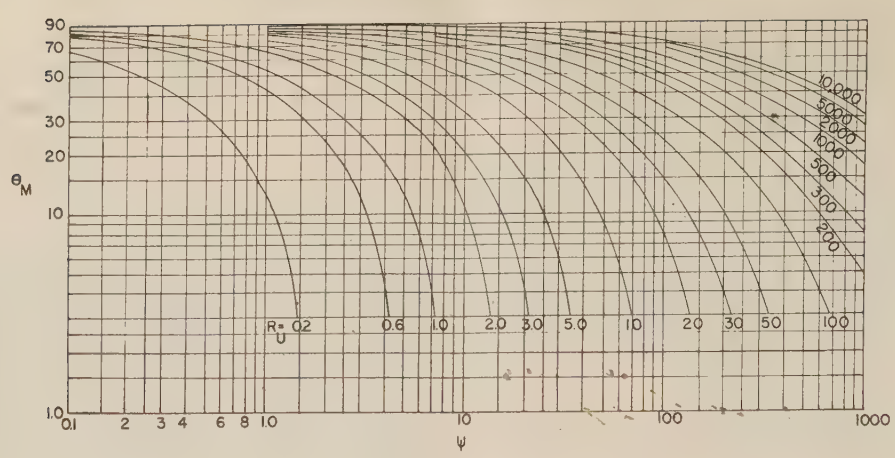

FIG. 2

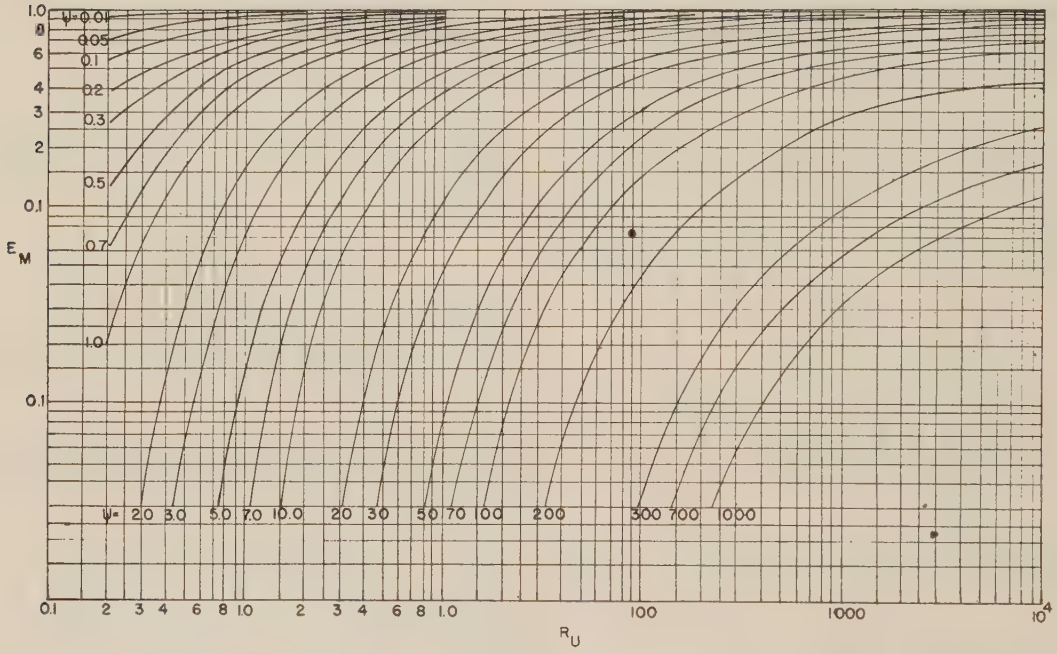

FIG. 3

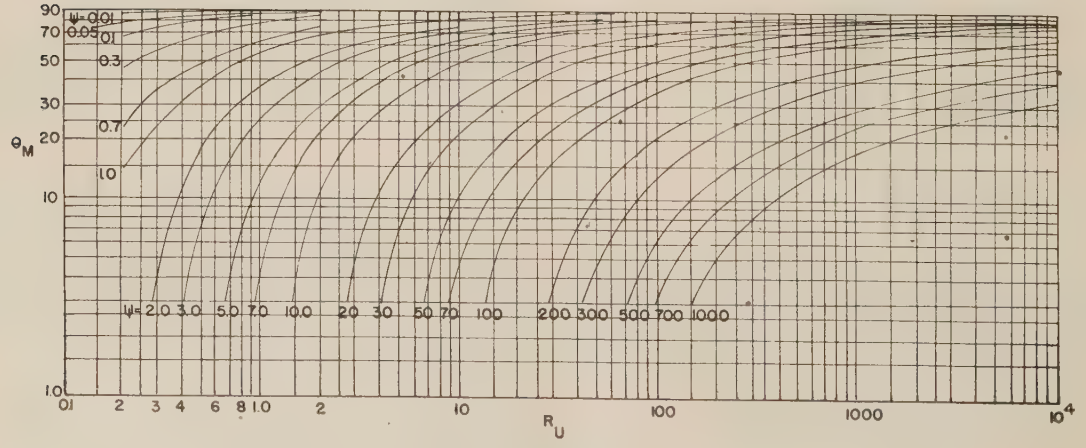

FIG. 4

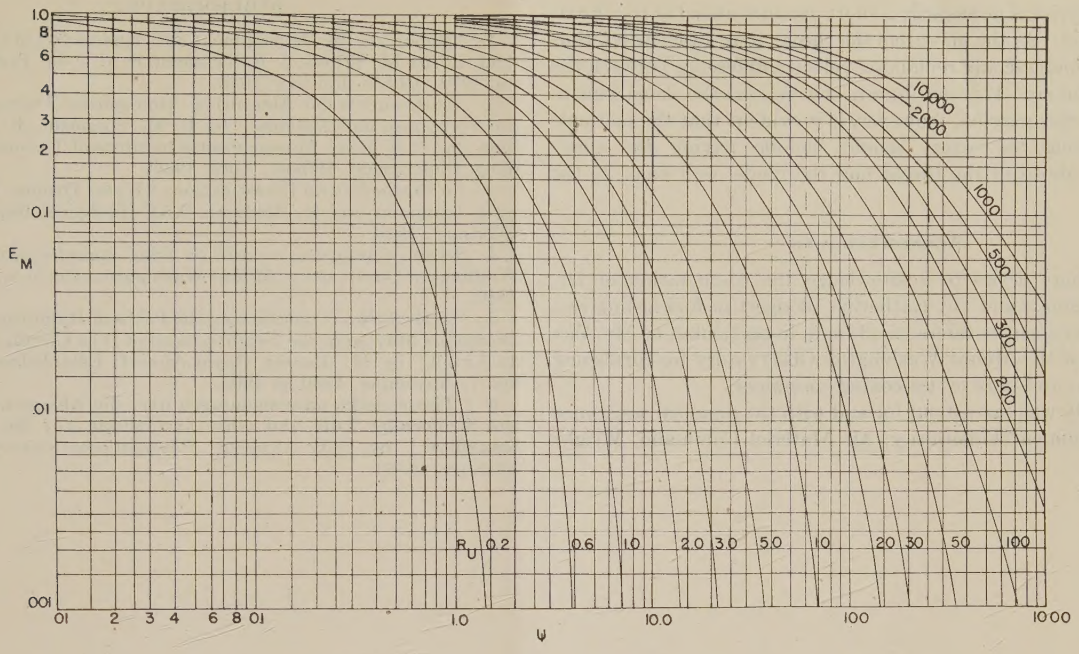

FIG. 5

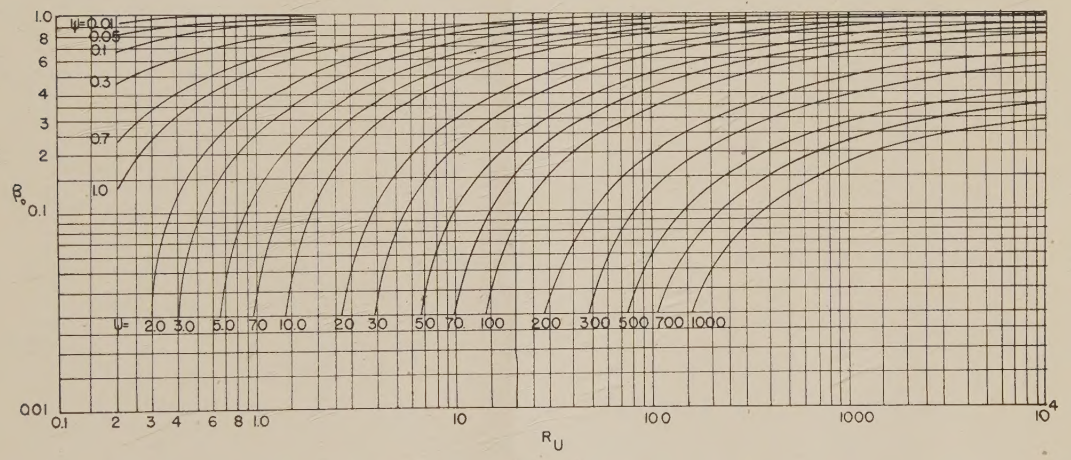

FIG. 6

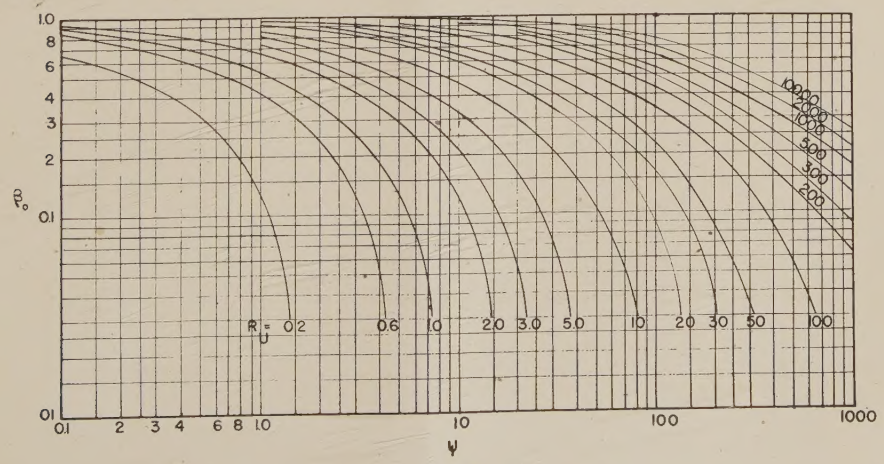

FIG. 7

the spray device is necessarily a short distance ahead of the throat of the tunnel. As the air enters the throat it is accelerated, thus tending to increase any remaining velocity difference between the drop and the air. It is not known how serious the deviations in the trajectories may be; however, it is evident that the methods of minimizing the errors should include having the spray device far ahead of the throat and the model well back in the throat.

Acknowledgment

The authors desire to acknowledge the co-operation of Dr. Irving Langmuir and Dr. Katherine Blodgett in forwarding certain data pertinent to reference (3) and, in particular, to Mr. Victor Clarke of the Mount Washington Observatory for furnishing photographs and data on ice-coated specimens.

This study was carried out for and with the financial assistance of the Equipment Laboratory, Air Materiel Command, Wright Field, Ohio.

BIBLIOGRAPHY

1 "Report on the Development and Application of Heated Wings, Add. I," by M. Tribus, J. R. Tessman, et al, AAF Technical Report no. 4972, Add. I, January, 1946.

2 "Instruments for Measuring Atmospheric Factors Related to Ice Formation on Airplanes," by B. M. Vonnegut, R. M. Cunningham, and R. E. Katz, Massachusetts Institute of Technology, Meteorology Department, Report, April, 1946.

3 "A Mathematical Investigation of Water Droplet Trajectories," by I. Langmuir and K. Blodgett, AAF Technical Report no. 5418, February, 1946.

4 Series of informal reports on icing measurements by Mount Washington Observatory, Mount Washington, Gorham, N. H., 1944–1946.

5 "A Method of Constructing the Paths of Raindrops of Different Diameters Moving in the Neighborhood of (1) a Circular Cylinder (2) an Airfoil," by M. Glauert, Royal Aircraft Establishment, D.W.T., vol. 7, November, 1940, p. 4805.

6 "Theoretische untersuchungen über die Ablagerung von Staub aus Strömender Luft und eihre anwendung auf die Theorie der Staubfilter," by Fritz Albrecht, *Physikalische Zeitschrift*, vol. 32, 1931, pp. 48–56.

NOTICE TO AUTHORS on the Preparation of Manuscripts

THE most satisfactory and economical results in publishing technical papers are obtained with the most carefully prepared manuscripts. Observance of the few simple rules which follow will help to assure correctly printed papers at minimum cost.

Length: Be brief. Eliminate unnecessary words, descriptions, data, drawings, charts, illustrations, tables, mathematics. Papers requiring more than eight pages when printed are likely to be returned for condensation or rejected. Solid type runs 1200 words per page. Allow extra for the title, footnotes, bibliography, illustrations, and mathematics.

Manuscripts: Typewrite, double or triple space, on one side of standard-size paper. Leave ample margins. Cut captions, on a separate sheet, illustrations, and tables should accompany manuscript.

Bibliography: Footnotes and bibliographical references must be complete and thoroughly checked for accuracy. Do not abbreviate. Put in A.S.M.E. style: Title, author, name of periodical, volume and number, date, page. If a book: Title, author, publisher, place of publication, date, page referred to.

Mathematics: Check carefully. Write symbols clearly. Distinguish between capital and lower case letters. Mark zero to avoid confusion with letter O; numeral 1 with the letter "el" (l) or prime (′); Greek letters (alpha with a, kappa with k). Mark subscripts and exponents clearly. Avoid dots and bars over letters.

Illustrations: Good halftones are made from good photographs. Send black and white photographic prints, not blueprints or other halftones. Make drawings, graphs, and diagrams as simple as possible. Put explanatory notes in captions rather than on the graphs. Use black ink and white paper, or preferably tracing cloth. Letter in black ink sufficiently large to reduce average drawing to $3^1/_4$ inches for column cut. Check thoroughly as changes cannot be made on the cuts.

Check Everything: Delay, expense, and errors in printed papers can be avoided only by careful and repeated checking. Changes in proof are unnecessary if manuscripts are thoroughly checked and are carefully and clearly prepared.

Help the Society to do a better publishing job at less expense by observing these simple rules when you prepare a manuscript.

A.S.M.E. Publications Committee